

THE UNIVERSITY OF HULL

**Robust model-based fault estimation and fault-tolerant
control: Towards an integration**

being a thesis submitted for the degree of Doctor of Philosophy
in the University of Hull

by

JIANGLIN LAN

MSc in Control Theory and Control Engineering (SCUT, China)

BEng in Automation (SCAU, China)

May, 2017

Acknowledgements

This work is carried out at the Control and Intelligent Systems Engineering Group (C&ISE), University of Hull, supported by a joint scholarship from the Chinese Scholarship Council and the University of Hull.

Looking back to my three years PhD study, many people have given me support and encouragement. It is, therefore, my great pleasure to take this opportunity to appreciate all of them.

First of all, I would like to express my deepest gratitude to my first supervisor Prof. Ron J. Patton. He has always been very patient, supportive, and encouraging. His guidance and support allows the outcome of several high quality works that we have published together. I am truly grateful to have my PhD studies with him. I would also like to thank my second supervisor Dr. Ming Hou for his helpful advice given during the thesis advisory meetings.

Thanks for my thesis examiners, Dr. Tim Scott and Prof. Christopher Edwards, who give me valuable comments and constructive suggestions which help to improve the quality of this thesis.

During my three years at Hull I have been very lucky to meet the colleagues: Zhihuo Wang, Bingyong Guo, Siya Jin, Yanhua Liu, Mustafa Abdelrahman, and Shuo Shi, as well as several other PhD students. Thank you to all my friends. We have shared countless enriching and cheerful moments, which makes my life in Hull unforgettable.

Finally, my special gratitude goes to my family and my beloved Xianxian Zhao, for their understanding and support.

Abstract

To maintain robustly acceptable system performance, fault estimation (FE) is adopted to reconstruct fault signals and a fault-tolerant control (FTC) controller is employed to compensate for the fault effects. The inevitably existing system and estimation uncertainties result in the so-called *bi-directional robustness interactions* defined in this work between the FE and FTC functions, which gives rise to an important and challenging yet open integrated FE/FTC design problem concerned in this thesis. An example of fault-tolerant wind turbine pitch control is provided as a practical motivation for integrated FE/FTC design.

To achieve the integrated FE/FTC design for linear systems, two strategies are proposed. A H_∞ optimization based approach is first proposed for linear systems with differentiable matched faults, using augmented state unknown input observer FE and adaptive sliding mode FTC. The integrated design is converted into an observer-based robust control problem solved via a single-step linear matrix inequality formulation.

With the purpose of an integrated design with more freedom and also applicable for a range of general fault scenarios, a decoupling approach is further proposed. This approach can estimate and compensate unmatched non-differentiable faults and perturbations by combined adaptive sliding mode augmented state unknown input observer and backstepping FTC controller. The observer structure renders a recovery of the Separation Principle and allows great freedom for the FE/FTC designs.

Integrated FE/FTC design strategies are also developed for Takagi-Sugeno fuzzy modelling nonlinear systems, Lipschitz nonlinear systems, and large-scale interconnected systems, based on extensions of the H_∞ optimization approach for linear systems.

Tutorial examples are used to illustrate the design strategies for each approach. Physical systems, a 3-DOF (degree-of-freedom) helicopter and a 3-machine power system, are used to provide further evaluation of the proposed integrated FE/FTC strategies. Future research on this subject is also outlined.

Table of contents

List of abbreviations and symbols	ix
List of figures	xi
List of tables	xv
List of publications	xvi
1 Introduction	1
1.1 Background	1
1.2 Basic concepts of FTC systems	2
1.2.1 Definitions	2
1.2.2 Architectures and classifications	5
1.3 Challenges in AFTC systems design	8
1.4 Outline of the thesis	9
2 Literature review of FTC systems	12
2.1 Introduction	12
2.2 Current developments of FTC systems	12
2.3 Integration of fault diagnosis and FTC	17
2.3.1 Integrated design of FDI/control	17
2.3.2 Integrated design of FDI/FTC	19
2.4 Summary	24

3	Practical and theoretical motivations of integrated FE/FTC design	25
3.1	Introduction	25
3.2	Fault-tolerant wind turbine pitch control: a practical motivation	26
3.2.1	Problem statement	28
3.2.2	Adaptive step-by-step SMO-based FE design	32
3.2.3	FTC design	36
3.2.4	Simulation results	38
3.3	Mathematical analysis: a theoretical motivation	50
3.4	Concluding discussion	52
I	Integrated FE/FTC design for uncertain linear systems	53
4	Integrated FE/FTC design: H_∞ optimization approach	54
4.1	Introduction	54
4.2	Problem formulation	56
4.3	Integrated FE/FTC design: state feedback	58
4.3.1	Reduced-order ASUIO-based FE design	58
4.3.2	State feedback sliding mode FTC design	63
4.3.3	Integrated synthesis	65
4.4	Integrated FE/FTC design: output feedback	69
4.4.1	Full-order ASUIO-based FE design	69
4.4.2	Output feedback sliding mode FTC design	70
4.4.3	Integrated synthesis	72
4.5	Integrated FE/FTC design: multiplicative faults	74
4.6	A tutorial example	76
4.6.1	Integrated FE/FTC design with additive faults	77
4.6.2	Integrated FE/FTC design with multiplicative faults	80
4.7	Summary and discussion	82

5	Integrated FE/FTC design: decoupling approach	84
5.1	Introduction	84
5.2	Problem formulation	86
5.3	Basic idea of the decoupling approach	87
5.4	Adaptive sliding mode ASUIO design	90
5.4.1	Observer design	90
5.4.2	Estimation performance analysis	91
5.4.3	Observer parameters determination	94
5.5	FTC design	99
5.5.1	System reformulation	99
5.5.2	Adaptive backstepping FTC controller design	99
5.6	A tutorial example	104
5.6.1	Differentiable fault case	106
5.6.2	Non-differentiable fault case	108
5.7	Summary and discussion	110
II	Integrated FE/FTC design for uncertain nonlinear systems	112
6	Integrated FE/FTC for nonlinear systems using T-S fuzzy modelling	113
6.1	Introduction	113
6.2	Problem statement	115
6.3	ASUIO-based FE	117
6.4	FTC controller	119
6.5	FE and FTC synthesis	120
6.5.1	Separated designs of FE/FTC	120
6.5.2	Integrated design of FE/FTC	123
6.5.3	Computational complexity analysis	128
6.6	A tutorial example	130

6.6.1	Comparison of linear FTC and T-S fuzzy integrated FTC . . .	132
6.6.2	Comparison of integrated and separated FE/FTC designs . . .	133
6.7	Conclusion	139
7	Integrated FE/FTC for a Lipschitz nonlinear 3-DOF helicopter system with actuator faults and saturation	140
7.1	Introduction	140
7.2	Problem formulation	144
7.3	FE observer design	147
7.3.1	Differentiable approximation of the composite actuator fault .	147
7.3.2	Observer design	148
7.4	FTC controller design	150
7.5	Synthesis of the FE observer and FTC controller	152
7.5.1	Traditional separated approach	153
7.5.2	Integrated approach	155
7.6	Simulation results	158
7.6.1	Case 1: fault-free	160
7.6.2	Case 2: single actuator fault	160
7.6.3	Case 3: multiple actuator faults	161
7.7	Conclusion	165
III	Integrated FE/FTC design for large-scale interconnected systems	166
8	Integrated FE/FTC for large-scale interconnected systems with application to a 3-machine power system	167
8.1	Introduction	167
8.2	Problem statement and preliminaries	169
8.3	Integration of decentralized FE/FTC with actuator faults	171

8.3.1	Decentralized FE observer design	171
8.3.2	Decentralized FTC controller design	172
8.3.3	Integrated synthesis of FE/FTC	173
8.4	Extension to sensor fault case	177
8.5	Application to a 3-machine power system	181
8.5.1	Actuator fault case	183
8.5.2	Sensor fault case	187
8.6	Conclusion	191
9	Summary and future research	192
9.1	Summary	192
9.2	Future research	193
	Appendix A Lemmas used frequently in the thesis	195
A.1	Bounded Real Lemma (Anderson and Vongpanitlerd, 1973)	195
A.2	Schur complement (Boyd et al., 1994)	195
A.3	Pole placement lemma (Chilali and Gahinet, 1996)	196
A.4	Young inequality (Boyd et al., 1994)	196
	Appendix B Notes on the Separation Principle	197
	References	200

List of abbreviations and symbols

Abbreviations

AFTC	Active fault-tolerant control
ASO	Augmented state observer
ASUIO	Augmented state unknown input observer
BMI	Bilinear matrix inequality
FDI	Fault detection and isolation
FE	Fault estimation
FTC	Fault-tolerant control
LMI	Linear matrix inequality
PFTC	Passive fault-tolerant control
SMC	Sliding mode control
SMO	Sliding mode observer
T-S	Takagi-Sugeno
UIO	Unknown input observer

Symbols

$\exp(\cdot)$	The exponential function.
$\kappa_{m \times n}$	A $m \times n$ matrix with elements all equal to a constant κ .
$ \cdot $	The absolute value of a scalar.

$\ \cdot\ _p$	The p -norm in the Euclidean space. $\ \cdot\ $ and $\ \cdot\ _\infty$ represent the 2-norm and ∞ -norm, respectively.
\mathbb{C}	The set of all complex numbers.
\mathbb{R}	The set of all real numbers.
\mathbb{R}^n	The set of n -dimensional real vectors.
$\text{diag}(X_1, X_2)$	A diagonal matrix $\begin{bmatrix} X_1 & 0 \\ 0 & X_2 \end{bmatrix}$.
$\text{He}(X)$	The sum of a matrix X and its transpose, $\text{He}(X) = X + X^\top$.
$\text{Re}(\lambda)$	The real component of the eigenvalue λ .
$\text{sat}(\cdot)$	The saturation function.
$\text{sign}(\omega)$	The signum function of a variable ω . If $\omega \neq 0$, $\text{sign}(\omega) = \frac{\omega}{\ \omega\ }$; If $\omega = 0$, $\text{sign}(\omega) = 0$.
\star	The transpose of the element on its symmetric position in a matrix.
I_p	An identity matrix with dimension $p \times p$.
X^\dagger	The pseudo inverse of the matrix X .
X^\top	The transpose of the matrix X .
X^{-1}	The inverse of the matrix X .

List of figures

1.1	A control system with actuator, process and sensor faults (Patton, 2015).	2
1.2	General FTC system schemes (Blanke et al., 2003).	5
1.3	A classification of FTC methods.	6
1.4	General fault hiding FTC systems diagram (Lunze and Richter, 2008).	7
1.5	Structure of the thesis.	10
2.1	A general scheme of closed-loop FDI systems.	17
2.2	Unidirectional robustness interaction between FDI and control.	19
2.3	A general scheme of FDI-based FTC systems.	20
2.4	Bi-directional robustness interactions between FDI and FTC.	23
3.1	A general scheme of FE-based FTC systems.	25
3.2	The 4.8 MW benchmark wind turbine structure (Molina and Alvarez, 2011).	29
3.3	The 4.8 MW benchmark wind turbine control system.	29
3.4	Nominal pitch system control scheme.	30
3.5	Step response of a pitch system under different fault conditions.	31
3.6	Fault-tolerant pitch system control scheme.	32
3.7	Effective wind speed.	39
3.8	Fault estimation: pitch 3, Case 1.	40
3.9	Pitch rate: pitch 3, Case 1.	40
3.10	Pitch angle: pitch 3, Case 1.	40

3.11 Pitch angle: pitch 1, Case 1.	41
3.12 Pitch angle: pitch 2, Case 1.	41
3.13 Generator speed: Case 1.	41
3.14 Generator power: Case 1.	42
3.15 Fault estimation: pitch 1, Case 2.	42
3.16 Fault estimation: pitch 2, Case 2.	43
3.17 Fault estimation: pitch 3, Case 2.	43
3.18 Pitch rate: pitch 1, Case 2.	43
3.19 Pitch rate: pitch 2, Case 2.	44
3.20 Pitch rate: pitch 3, Case 2.	44
3.21 Pitch angle: pitch 1, Case 2.	44
3.22 Pitch angle: pitch 2, Case 2.	45
3.23 Pitch angle: pitch 3, Case 2.	45
3.24 Generator speed: Case 2.	45
3.25 Generator power: Case 2.	46
3.26 Fault estimation: Case 3.	48
3.27 Pitch angle: Case 3.	48
3.28 Pitch rate: Case 3.	48
3.29 Generator speed: Case 3.	49
3.30 Generator power: Case 3.	49
3.31 The separated FE/FTC system scheme.	50
3.32 Bi-directional robustness interactions between FE and FTC functions.	52
4.1 The integrated FE/FTC system scheme.	54
4.2 Integrated FE/FTC design: state feedback case.	66
4.3 Integrated FE/FTC design: output feedback case.	73
4.4 FE performance: state feedback case.	78
4.5 FTC performance: state feedback case.	78

4.6	FE performance: output feedback case.	79
4.7	FTC performance: output feedback case.	80
4.8	Fictitious fault estimation performance.	81
4.9	FTC performance of i_a : multiplicative fault case.	81
4.10	FTC performance of w : multiplicative fault case.	82
5.1	Robustness interactions within (a) integrated and (b) decoupling FE/FTC.	84
5.2	Robustness interactions within (a) integrated and (b) decoupling FE/FTC.	89
5.3	Angular velocity: differentiable fault case.	106
5.4	Control effort: differentiable fault case.	107
5.5	Fault estimation: differentiable fault case.	107
5.6	Perturbation estimation: differentiable fault case.	108
5.7	Angular velocity: non-differentiable fault case.	109
5.8	Control effort: non-differentiable fault case.	109
5.9	Fault estimation: non-differentiable fault case.	110
5.10	Perturbation estimation: non-differentiable fault case.	110
6.1	Angle response using linear and T-S fuzzy integrated FTC.	133
6.2	Actuator fault estimation with different initial angles: <i>Case 1</i>	134
6.3	Angle response with different initial angles: <i>Case 1</i>	134
6.4	Sensor fault estimation with different initial angles: <i>Case 2</i>	135
6.5	Angle response with different initial angles: <i>Case 2</i>	135
6.6	Actuator fault estimation with different initial angles: <i>Case 3</i>	135
6.7	Sensor fault estimation with different initial angles: <i>Case 3</i>	136
6.8	Angle response with different initial angles: <i>Case 3</i>	136
6.9	Actuator fault estimation with different uncertainties: <i>Case 1</i>	137
6.10	Angle response with different uncertainties: <i>Case 1</i>	137
6.11	Sensor fault estimation with different uncertainties: <i>Case 2</i>	137
6.12	Angle response with different uncertainties: <i>Case 2</i>	138

6.13	Actuator fault estimation with different uncertainties: <i>Case 3</i>	138
6.14	Sensor fault estimation with different uncertainties: <i>Case 3</i>	138
6.15	Angle response with different uncertainties: <i>Case 3</i>	139
7.1	The Quanser 3-DOF helicopter free body diagram (Zheng and Zhong, 2011).	144
7.2	The actuator model with both fault and saturation.	145
7.3	The proposed FE-based FTC 3-DOF helicopter system.	153
7.4	Angle response: Case 1.	160
7.5	Control effort: Case 1.	161
7.6	Fault estimation performance: Case 2.	162
7.7	Angle response: Case 2.	162
7.8	Control effort: Case 2.	163
7.9	Fault estimation performance: Case 3.	163
7.10	Angle response: Case 3.	164
7.11	Control effort: Case 3.	164
8.1	Decentralized large-scale control systems.	167
8.2	Decentralized integrated FE/FTC design for large-scale systems.	171
8.3	A 3-machine power system.	182
8.4	Actuator faults (black dash) and their estimates (red solid).	186
8.5	States with (red solid) or without FTC (black dash) for machine 1.	186
8.6	States with (red solid) or without FTC (black dash) for machine 2.	186
8.7	States with (red solid) or without FTC (black dash) for machine 3.	187
8.8	Sensor fault estimation performance.	189
8.9	Outputs with (red solid) or without FTC (black dash) for machine 1.	190
8.10	Outputs with (red solid) or without FTC (black dash) for machine 2.	190
8.11	Outputs with (red solid) or without FTC (black dash) for machine 3.	190

List of tables

3.1	Design parameters of the observers.	38
6.1	H_∞ attenuation level and consuming time.	131
6.2	Maximum initial angle $ x_1(0) $ of the pendulum.	133
7.1	Definitions of the physical parameters.	144
7.2	3-DOF helicopter parameters.	158
8.1	Definitions of the physical parameters.	183

List of publications

Book chapter

1. Huang, Z., Patton, R. J., and **Lan, J.**, (2016). Sliding mode state and fault estimation for decentralized systems. In *Variable-Structure Approaches* (pp. 243–281). Springer.

Journal papers

1. **Lan J.**, Patton R. J., (2016). A decoupling approach to integrated fault-tolerant control for linear systems with non-differentiable faults. *Automatica*, submitted. (Materials for Chapter 5)
2. **Lan J.**, Patton R. J., and Zhu X., (2017). Integrated fault-tolerant control for a 3-DOF helicopter with actuator faults and saturation. *IET Control Theory & Applications*, DOI: 10.1049/iet-cta.2016.1602. (Materials for Chapter 7)
3. **Lan, J.**, Patton, R. J., and Zhu, X., (2016). Fault-tolerant wind turbine pitch control using adaptive sliding mode estimation. *Renewable Energy*, DOI: 10.1016/j.renene.2016.12.005. (Materials for Chapter 3)
4. **Lan, J.** and Patton, R. J., (2016). Integrated fault estimation and fault-tolerant control for uncertain Lipschitz nonlinear systems. *International Journal of Robust and Nonlinear Control*, 27(5): 761-780. (Materials for Chapter 7)
5. **Lan J.** and Patton R. J., (2016). Integrated design of fault-tolerant control for nonlinear systems based on fault estimation and T-S fuzzy modelling. *IEEE Transactions on Fuzzy Systems*, DOI: 10.1109/TFUZZ.2016.2598849. (Materials for Chapter 6)
6. **Lan J.** and Patton, R. J., (2016). A new strategy for integration of fault estimation within fault-tolerant control. *Automatica*, 69: 48-59. (Materials for Chapter 4)

Conference papers

1. **Lan J.**, Patton R. J., and Punta E., (2017). Fault-Tolerant Tracking Control for A 3-DOF Helicopter with Actuator Faults and Saturation. *IFAC World Congress 2017*, 9-14 July, Toulouse, France, accepted.
2. **Lan J.** and Patton, R. J., (2016). Decentralized fault estimation and fault-tolerant control for large-scale interconnected systems: an integrated design approach. In *Proceedings of the UKACC 11th International Conference on Control*, pp. 1-6. IEEE. (Materials for Chapter 8)
3. **Lan J.** and Patton, R. J., (2016). Integrated fault estimation and fault-tolerant control design for large-scale interconnected systems. In *Proceedings of the 3rd International Conference on Control and Fault-Tolerant Systems*, pp. 263-268. IEEE. (Materials for Chapter 8)
4. Guo B., Patton, R. J., Abdelrahman M. and **Lan J.**, (2016). A continuous control approach to point absorber wave energy conversion. In *Proceedings of the UKACC 11th International Conference on Control*, pp. 1-6. IEEE
5. Abdelrahman M., Patton, R. J., Guo B. and **Lan J.**, (2016). Estimation of wave excitation force for wave energy converters. In *Proceedings of the 3rd International Conference on Control and Fault-Tolerant Systems*, pp. 654-659. IEEE.
6. **Lan J.** and Patton, R. J., (2015). Integrated design of robust fault estimation and fault-tolerant control for linear systems. In *Proceedings of the IEEE 54th Annual Conference on Decision and Control*, pp. 5105-5110. IEEE.
7. **Lan J.** and Patton, R. J., (2015). Robust fault-tolerant control based on a functional observer for linear descriptor systems. In *Proceedings of the 8th IFAC Symposium on Robust Control Design*, 48 (14): 138–143. IFAC-PapersOnLine.

Chapter 1: Introduction

1.1 Background

In real operations of modern engineering systems there exist system faults that may lead to performance degradation or instability, or even trigger a chain of failing subsystems and cause major catastrophes in large-scale interconnected systems. This gives rise to strong demands for enhanced control system reliability and safety in the presence of system faults. It is crucial to not only determine the onset and development of faults before they become serious, but also adaptively compensate the fault effects within the closed-loop system or replace faulty components by fault-free alternatives (hardware redundancy). The procedure of accounting for faults acting within a control system to render the closed-loop system insensitive to the faults is known as “fault-tolerant control (FTC)”, of which the fault estimation and compensation control is one approach (Blanke et al., 2003; Patton, 1997, 2015).

In 1985, Eterno et al. (1985) developed a reconfigurable flight control system, in which the title “failure tolerant control” was first used to define the meaning of control system tolerance to failures or faults. The word “failure” is used when a fault leads to the situation that the system function concerned fails to operate (Isermann, 2006). FTC began to develop in the early 1990s and for the last 25 years a significant number of methods have been established, which can be found in the bibliographical reviews Zhang and Jiang (2008) and Yu and Jiang (2015). Now FTC has become a standard technique in the literature (Blanke et al., 2003; Patton, 1997, 2015; Yu and Jiang, 2015; Zhang and Jiang, 2008), based on the aerospace subject of reconfigurable flight control making use of redundant actuators and sensors (Edwards et al., 2010; Steinberg, 2005).

FTC has been applied to many areas in the past 25 years. A comprehensive survey for the applications before 2008 can be found in Zhang and Jiang (2008), while the main applications since 2008 include, but not limited to, the following areas:

- **Flight and vehicle control systems.** (1) Aircraft: Ducard (2009), Edwards et al. (2010), Amoozgar et al. (2013), Hajjiev and Caliskan (2013), Zolghadri et al. (2014), Balague and Hajjiev (2016); (2) Spacecraft: Jiang et al. (2010), Shen et al. (2012), Xiao et al. (2012); (3) Vehicles: Soylyu et al. (2008), Yang et al. (2010a), Wang and Wang (2011), Wang et al. (2015); (4) Friction compensation: Patton et al. (2010).
- **Electric and power systems.** (1) Electric drive systems: Campos-Delgado et al. (2008), Isermann (2011), Akrad et al. (2011), Song and Wang (2013), Bourogaoui et al. (2016); (2) Power system: Benghea et al. (2015), Bianchi et al. (2015), Pedersen et al. (2016); (3) Wind turbine control systems: Amirat et al. (2009), Yin et al. (2014b), Sloth et al. (2011), Odgaard et al. (2013), Sami and Patton (2013), Shi and Patton (2015a), Badihi et al. (2015).
- **Distributed network systems.** (1) Water networks: Eliades and Polycarpou (2010), Quevedo et al. (2010), Robles et al. (2016); (2) Wireless networks: Chen et al. (2011), Ding et al. (2013), Xu et al. (2017).

1.2 Basic concepts of FTC systems

1.2.1 Definitions

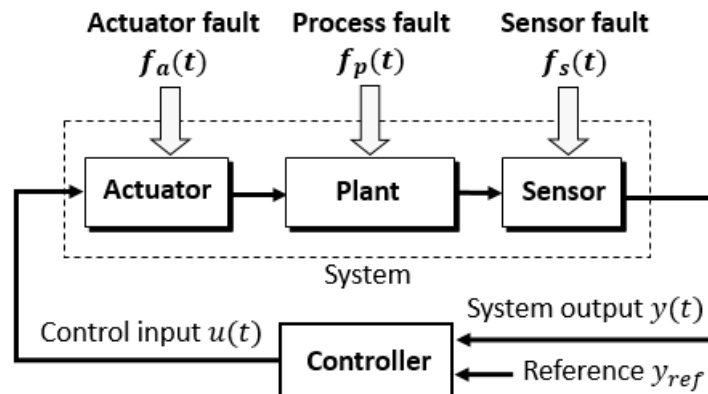


Fig. 1.1 A control system with actuator, process and sensor faults (Patton, 2015).

A *fault* is defined as an unpermitted deviation of at least one characteristic property or parameter of the system from the acceptable condition (van Schrick, 1997). It is important to determine how a fault should be detected, isolated, estimated, and

compensated. The faults outlined in Fig. 1.1 acting at different system locations are defined as follows (Blanke et al., 2003; Chen and Patton, 1999; Isermann, 2006):

- *Actuator fault.* An actuator fault ($f_a(t)$) is defined as variations of the control input $u(t)$ applied to the controlled plant, which can be either completely or partially. In the presence of total loss of effectiveness, an actuator can no longer produce any actuation regardless of the applied input. This can be caused by breakage, burn out of wiring, or stuck at a position. It cannot be directly compensated through control action and is out of the scope of this thesis. A partial loss of effectiveness means that the actuator becomes less effective, e.g., has degradation in the actuator gain due to a clogged or rusty valve. Another kind of actuator faults are called offset actuator faults, e.g., oscillatory or drift faults in flight control systems (Goupil, 2010), which corresponds to deviations of the actuator action from its nominal situation due to some parameter changes or unknown disturbances.

- *Sensor fault.* A sensor fault ($f_s(t)$) implies that incorrect measurements are taken from the system, either completely or partially. Sensor faults can be caused by poor calibration, bias, scaling error, or sensor dynamic change.

- *Process fault.* A process fault ($f_p(t)$) directly affects the physical system parameters and subsequently the system input and output properties. Process faults are also often called component faults, arising as variations from the structure or parameters used during system modelling. As such it can cover a wide class of potential faults, e.g., change of mass, damping constant, aerodynamic coefficients, and etc.

In some literature faults are also classified as *additive fault* or *multiplicative fault*, according to the ways in which they are modelled (Isermann, 2006):

- *Additive fault.* A fault affects the system signal by adding an extra fault signal to it. Offset actuator and sensor faults can be considered as forms of additive fault.

- *Multiplicative fault.* A fault affects the signal by multiplying an extra fault signal. Parametric faults can be a form of multiplicative fault.

Moreover, with respect to the control input signal, faults are divided as follows:

- *Matched fault.* A fault that is inside the range space spanned by the control input. If the matching condition $\text{rank}(B, F) = \text{rank}(B)$, where B and F are distribution matrices of the control and fault, respectively, is satisfied, then this fault is matched and can be directly compensated through control actions.

- *Unmatched fault.* A fault that is outside the range space spanned by the control input.

In this thesis, faults are also divided into *differentiable* and *non-differentiable* faults, based on whether they are differentiable or not with respect to time. Some examples for non-differentiable faults are: random jumps due to environmental changes or system component failures (Willsky and Jones, 1974), and random faults widely existing in networked control systems as a result of the randomly occurring phenomena (Dong et al., 2013).

The above different fault classifications are not independent but have some overlaps, e.g., a certain fault can be viewed as more than one type of fault. Throughout this thesis, different classifications will be discussed under particular scenarios.

Fault-tolerant control is a control strategy and design to ensure that a closed-loop system can continue acceptable operation in the presence of either single or multiple fault actions. When prescribed stability and closed-loop performance indices are maintained despite the action of faults the system is said to be “fault-tolerant” and the control scheme that ensures the fault tolerance is the fault tolerant controller (Blanke et al., 2003; Patton, 1997, 2015).

Within an FTC system, another important concept is **fault diagnosis**, defined as a procedure to obtain fault information (fault location, time occurrence, and/or magnitude) used for fault compensation design and the scheduled system maintenance. In the past three decades, fault detection and isolation (FDI), also called fault detection and diagnosis (FDD), and fault estimation (FE) have been developed as mainstream approaches to achieve fault diagnosis (Chen and Patton, 1999; Gertler, 1998; Patton et al., 2013).

The FDI approach for the diagnosis of faults involves standard procedures of fault detection and fault isolation, while FE is used to estimate the actual fault signals based on system observer methodologies. Since FDI does not provide fault estimation, some investigators use FDI followed by FE to estimate the faults. However, if only detection and isolation are required, the FDI approach is then not necessary here. It is also important to note that the FE procedure actually includes both detection and isolation in some sense, since the accurate estimation of the faults implies detection and isolation. Thus, FE can totally replace FDI in some situations. For example, **in this thesis FE totally replaces the FDI functions in the context of fault estimation combined with fault compensation within FTC.**

1.2.2 Architectures and classifications

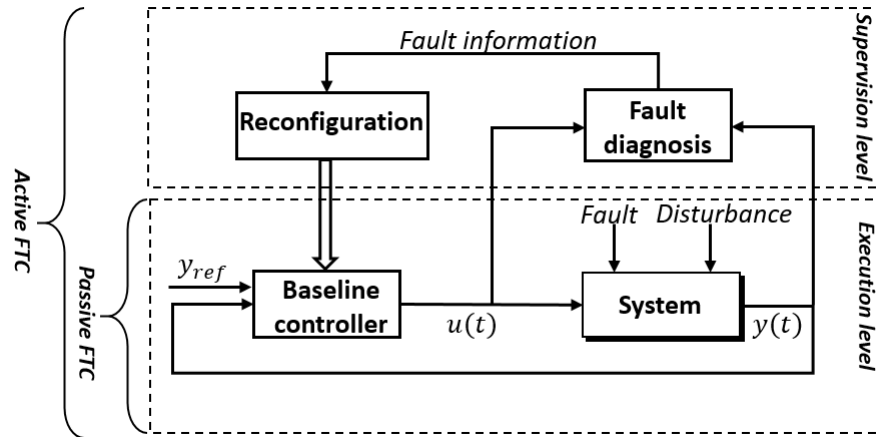


Fig. 1.2 General FTC system schemes (Blanke et al., 2003).

FTC methods can be classified according to whether they are “passive” or “active”, using fixed or reconfigurable control strategies (Eterno et al., 1985). Fig. 1.2 shows the general system schemes of *active* and *passive* FTC (AFTC and PFTC) methods in which a distinction is made between the “execution” and “supervision” levels. Their essential differences and requirements are also illustrated.

PFTC is based solely on the use of robust control in which potential faults are treated as uncertain signals (uncertainties or external disturbances) acting on the system dynamics. This can be related to the concept of reliable control (Veillette et al., 1992; Yang et al., 2001; Yang and Ye, 2010). PFTC does not require either on-line fault information from the fault diagnosis (FDI/FE) function or control reconfiguration (Patton, 1997; Šiljak, 1980). Several PFTC methods have been developed based on robust control theories, e.g., multi-objectives optimization, quantitative feedback theory method, H_∞ optimization, absolute stability theory, nonlinear regulation theory, and etc. More details for this can be found in the survey papers Benosman (2009) and Yu and Jiang (2015). Since a PFTC system uses a controller designed off-line based on certain *a priori* knowledge of the faults, it is considered to be able to handle very limited fault scenarios.

AFTC provides a system with fault tolerant capability by including the following two conceptual steps (Blanke et al., 2003; Patton, 2015; Yu and Jiang, 2015; Zhang and Jiang, 2008):

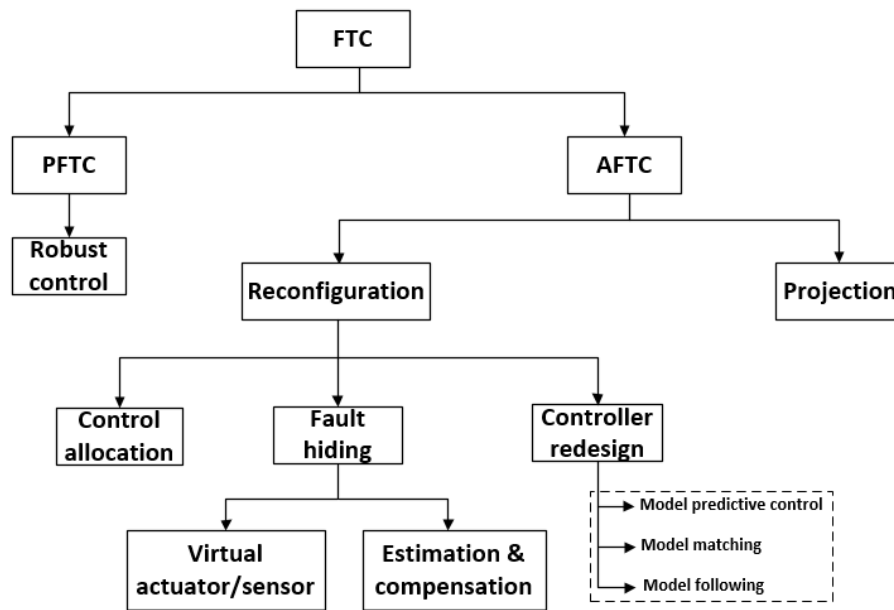


Fig. 1.3 A classification of FTC methods.

1) Equip the system with a diagnosis mechanism to diagnose the faults and select the required remedial action to maintain acceptable post-fault closed-loop performance. In the absence of faults a “Baseline Controller” is used to ensure good stability and tracking performances. (Supervision level)

2) Make use of the supervision level information and adapt or reconfigure/restructure the controller to achieve the required remedial activity. (Execution level)

Compared with PFTC, AFTC is applicable for a broader range of areas and thus has been the major concern of the FTC community, which is also the main focus of this research.

A classification of the PFTC and AFTC methods is given in Fig. 1.3. The AFTC approaches are further classified as: projection and reconfiguration methods.

- The **projection method** diagnoses the fault occurrence through FDI and compensates the fault effect by using a switching mechanism to select an appropriate control action from the pre-computed controller set. In this method, the potential fault modes of the controlled plant are *a priori* known and an associated controller is designed to achieve desired system performance under each fault situation. Thus, this method is also called multiple model approach in the literature (Maybeck and Stevens, 1991; Rauch, 1995; Zhang and Jiang, 2001). More discussion on this method is provided in Section 2.3.2.

- The **reconfiguration method** mainly includes three types of approaches: control allocation, controller redesign, and fault hiding.

The control allocation approach re-allocates the required control actions from the faulty actuators to the healthy redundant ones, according to the fault diagnosis results (Buffington et al., 1999). It is an approach for actuator redundancy management and useful for over-actuated control systems, such as flight systems. However, the requirement of physical redundancy makes the control allocation approach expensive and somehow limited in application.

Controller redesign involves the calculation of new controller parameters following control impairment using, e.g., model predictive control (Maciejowski, 1999) and model matching or following (Staroswiecki, 2005).

The “fault hiding” approach aims to “hide” the fault from the baseline controller by adding an extra reconfiguration block between the faulty plant and the baseline (nominal) controller (Steffen, 2005). A general diagram of FTC systems using the fault hiding method is given in Fig. 1.4.

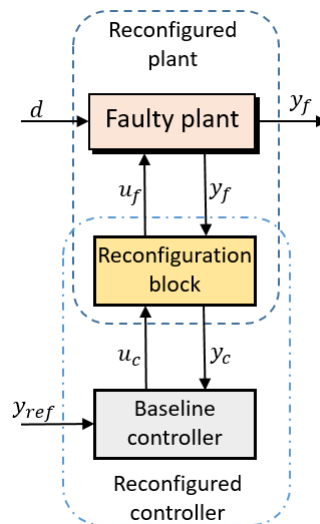


Fig. 1.4 General fault hiding FTC systems diagram (Lunze and Richter, 2008).

Currently, two main types of methods have been proposed to achieve fault hiding: virtual actuator/sensor, and estimation & compensation. The virtual actuator/sensor method to FTC design includes three separate steps: 1) Design a baseline controller for the healthy plant; 2) Design a fault diagnosis block to diagnose the faults and determine the system dynamics of the faulty plant; 3) Design a reconfiguration control signal such that the faulty plant behaves like the original healthy one.

Similarly, the estimation & compensation method uses on-line fault compensation based on fault diagnosis of the unanticipated faults. However, compared to the virtual actuator/sensor method, the estimation & compensation method has the following new properties: 1) The FTC controller consists of a baseline control component and a fault compensation component, which are designed together; 2) The FE function is embedded with the controller, automatically estimating the actual fault signals and forwarding the estimates to the FTC controller.

According to the above background, the estimation & compensation method is considered to be a good alternative to achieve robust AFTC strategy. It also offers an opportunity to avoid the control and diagnosis uncertainties and time delays brought by the multiple-step designs in the virtual actuator/sensor method. Considering this background, **this thesis focuses on the estimation & compensation method for AFTC systems design.**

1.3 Challenges in AFTC systems design

As a result of imperfect system modelling there inevitably exist uncertainties in the mathematical system models that are used for control designs. It has long been known that system uncertainty has negative effects on the control performance. Moreover, since both uncertainty and faults can lead to system dynamic changes, it is usually difficult or impossible to distinguish between their effects. Therefore, there are mainly two challenges in AFTC system design:

- How to extract the required fault information from the dynamic changes in the presence of system uncertainty?
- How to design a closed-loop FTC system with admissible fault-tolerant performance and good robustness to uncertainty?

The first challenge is fundamental to an AFTC system, since accurate fault information is a prerequisite. Moreover, fault diagnosis depends on the mathematical system model explicitly. Hence, it has been known for some time that within a closed-loop system the fault diagnosis performance is affected by the control system uncertainty (Patton, 1997). Initiated by Nett et al. (1988), many works have been published on the integration of control and FDI by combining their designs into a joint robustness problem to achieve good robust control and acceptable FDI properties, as shown in the review paper Ding (2009).

When combining the functions of fault diagnosis with FTC into an AFTC system, the diagnosis uncertainties (false alarm, time delay, diagnosis error, and etc.) also affect the closed-loop system performance. Therefore, there exist mutual interactions between the fault diagnosis and FTC system functions. If these functions are designed separately without taking into account the mutual effects, they may not fit with each other when assembled together (Zhang and Jiang, 2006). This will lead to an FTC system with degraded performance and robustness. Therefore, a necessary consideration is to synthesise the fault diagnosis and FTC functions from a holistic perspective so as to achieve a robust closed-loop FTC system. This is the the problem of integrated design of fault diagnosis and FTC defined in this thesis as follows.

Definition 1.1 Integrated design of fault diagnosis and FTC is a system synthesis procedure for co-design of the fault diagnosis and FTC functions, by taking into account their mutual interactions, to achieve a robust closed-loop FTC system with admissible performance.

A detailed mathematical analysis of the necessity, importance, and challenges of integrated design of fault diagnosis and FTC is provided in Chapters 2 and 3. As mentioned before, the estimation & compensation method based on FE (instead of FDI) function is the focus of this thesis. Hence, the integrated design problem concerned in this research is the integration of FE and FTC.

1.4 Outline of the thesis

This thesis has the challenge of presenting a novel approach to FTC. The fundamental contribution of this work is that the presence of uncertainty in state and fault estimation along with the uncertainty associated with control leads to a new concept called **integrated FE and FTC design**. The thesis describes a number of approaches to achieve this integration, considering various types of linear and nonlinear systems problems.

The structure of the thesis is outlined in Fig. 1.5 and described in detail as follows.

Chapter 1 tells a brief history of FTC systems and introduces the related definitions, architectures and classifications along with design challenges. The thesis structure is also outlined.

Chapter 2 gives an overview of the current development of FTC systems, and a mathematical analysis and review of integrated design of fault diagnosis and FTC.

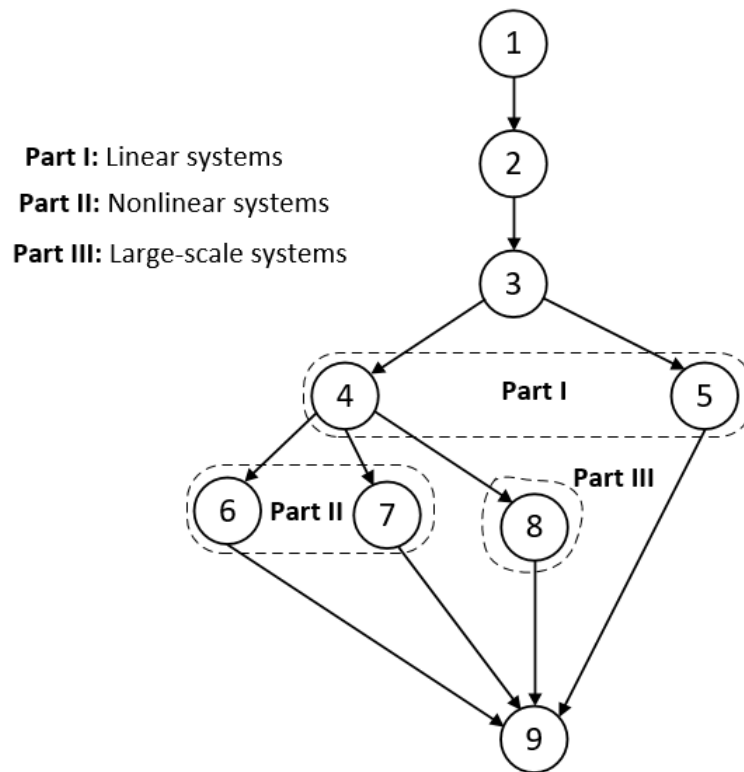


Fig. 1.5 Structure of the thesis.

Chapter 3 provides practical and theoretical motivations of integrated FE/FTC design. A fault-tolerant wind turbine pitch control example gives a simple guide for FE-based FTC systems design and, more importantly, serves as a practical motivation of integrated FE/FTC design.

Several strategies have been developed in Chapters 4 - 8 for integrated FE/FTC design.

- **Part I:** Integrated FE/FTC design strategies for uncertain linear systems

Chapter 4 proposes a H_∞ optimization approach to realize the integrated FE/FTC design. The basic idea is to formulate the integrated design as an observer-based robust control problem and solve it using a single-step linear matrix inequality (LMI) formulation. An uncertain linear system with matched differentiable actuator and sensor faults along with external disturbances is considered. A new augmented state unknown input observer (ASUIO) is proposed for the simultaneous estimation of faults and system state. Both the cases of state and output feedback controls are studied, using reduced-/full-order ASUIOs, respectively. An FTC design in the case of multiplicative faults is also included as a new contribution.

Chapter 5 addresses the integrated FE/FTC design by proposing a decoupling approach, which can handle both differentiable and non-differentiable, matched and unmatched faults. Moreover, the decoupling recovers the well-known Separation Principle (see Appendix B) for the designs of FE and FTC functions, which offers great design freedom. This approach estimates and compensates the uncertainty and disturbance to achieve a more robust FTC system.

- **Part II:** Integrated FE/FTC design strategies for uncertain nonlinear systems

Chapter 6 describes an extension of the H_∞ optimization approach in Chapter 4 to address the integrated FE/FTC design for nonlinear systems, which are modelled using the Takagi-Sugeno (T-S) fuzzy method, subject to uncertainty, disturbance, and actuator and sensor faults.

Chapter 7 further extends the H_∞ optimization approach for Lipschitz nonlinear systems. It also demonstrates the capability of applying the proposed strategy to a 3-DOF helicopter system with both actuator faults and input saturation constraints.

- **Part III:** Integrated FE/FTC design strategies for large-scale systems

Chapter 8 studies the integrated FE/FTC for large-scale interconnected systems subject to uncertain interconnections and with actuator or sensor faults. A decentralized integrated FE/FTC strategy is proposed based on the H_∞ optimization approach used in Chapters 4 - 7 for small scale systems. Its capability of industrial applications is also demonstrated through the study of the stabilization of a 3-machine power system.

Chapter 9 summarizes the thesis highlighting the main contributions and providing a statement of likely ideas for future research.

Chapter 2: Literature review of FTC systems

2.1 Introduction

Chapter 1 introduces briefly the history of FTC systems, including the basic definitions, architectures, classification, and the existing problem of integrated design of fault diagnosis and FTC. The purpose of this chapter is to give an overview of the current developments of FTC systems, and a mathematical analysis and review of the integrated design of fault diagnosis and FTC.

The rest of the chapter is organized as follows. Section 2.2 gives a literature review of FTC systems. Section 2.3 provides mathematical analysis and a review of integrated fault diagnosis and FTC, including integrated FDI/control design and integrated FDI/FTC design. Section 2.4 summarises the chapter.

2.2 Current developments of FTC systems

(1) Analysis tools

The capability of a system to tolerate faults through control design, using either PFTC or AFTC approaches, is essentially a structural property of the system itself. A system with inadequate (control relevant) redundancy cannot be made effectively tolerant to faults regardless of the FTC strategy used. Therefore, a tool is needed to check the fault-tolerance capability before designing the FTC system or be a guide to design a plant with high fault-tolerance capability.

The concept of control reconfigurability was first developed by Wu et al. (2000) for linear time-invariant systems. It is a measure of the capability of a system to allow

restoration of performance in the presence of faults through the application of some FTC strategy. Later, the concept of coverage of FTC was developed in Wu (2004) for analyzing the reliability of an FTC system design.

These two concepts have been further developed and used by many researchers as analysis and design tools for FTC systems. The concept of control reconfigurability has been extended to bilinear systems by Shaker (2013) and switched systems by Yang et al. (2012). Huang and Wu (2013) propose a fault-tolerant placement strategy for phasor measurement units based on control reconfigurability. Yang et al. (2015) study the fault recoverability and FTC for interconnected nonlinear systems.

(2) Fault diagnosis

Since the beginning of 1970s, a large number of fault diagnosis techniques have been developed. The current fault diagnosis approaches mainly make use of the basic principle of residual generation and are mainly divided into two categories: mode-based and data-driven methods. The former method depends on the mathematical system model and uses approaches such as state observer, parity space, and parameter estimation. The latter uses historical data of the systems, based on approaches such as statistical, neural networks, expert systems. A comprehensive review of FDI methods can be found in Gao et al. (2015a,b); Hwang et al. (2010); Qin (2012); Venkatasubramanian et al. (2003a,b,c); Yin et al. (2014b).

The main drawback of the observer-based FDI methods is its dependence on explicit mathematical system models. This limits their applications for systems with unknown structure. To overcome this, data-driven methods without explicit requirement of mathematical system models have attracted increasing attention in the last few years, see the review papers Qin (2012) and Yin et al. (2014a). However, they require a preprocessing step for extracting useful information from the historical data which involves high online computational cost. Therefore, there is also a trend of developing hybrid approaches for FDI by using a combination of the model-based and data-driven methods to achieve a more robust FDI with low computational cost (Tidriri et al., 2016).

As a powerful alternative to using the FDI approach in FTC systems, it is attractive to consider a direct reconstruction of the fault signal through FE once it occurs. The FE function intrinsically includes the fault detection and isolation roles and the more complex FDI role is thus obviated. In this approach the reconstructed (or estimated) fault signals are used directly in the control system to compensate for the fault effects. Several approaches to FE designs have been proposed, based on: adaptive observers (Jiang et al., 2006; Kabore and Wang, 2001), SMO (Edwards and Tan, 2006), augmented

state observer (ASO) (Gao and Ding, 2007), UIOs (Odgaard and Stoustrup, 2012; Tan et al., 2015), and moving horizon estimation (Feng and Patton, 2014). A combination of SMO and ASO is also proposed in Shi et al. (2015).

(3) AFTC approaches

- Control allocation approach

It was first used for FTC in Buffington et al. (1999). An extensive study of fault-tolerant drive-by-wire systems using control allocation is provided in Isermann et al. (2002). Recently, several interesting FDI or FE based FTC approaches have been developed and verified using sliding mode method for on-line control allocation to achieve robust FTC performance, see for example, Alwi and Edwards (2008); Hamayun et al. (2012); Ríos et al. (2015).

- Model predictive control approach

Model predictive control uses on-line computed control redesign for fault accommodation. The representation of actuator faults in model predictive control is relatively natural and straightforward, since actuator faults like jams and slew-rate reductions can be represented by changing the optimization constraints. Thus, model predictive control has good fault-tolerant ability under some state and input constraints even if the faults are not detected, as first claimed by Maciejowski (1999). Since on-line fault information is not required, model predictive control is an interesting method for flight control reconfiguration as demonstrated by Maciejowski and Jones in the GARTEUR AG 16 project on fault tolerant flight control (Edwards et al., 2010).

Moreover, the fault tolerance of model predictive control can be improved by including fault knowledge in the internal model (Maciejowski and Jones, 2003), e.g., using FDI approaches (Mhaskar, 2006; Ocampo-Martinez and Puig Cayuela, 2009; Patwardhan et al., 2006; Yetendje et al., 2013).

- Model-matching/-following approach

This is a controller redesign AFTC method that makes use of the concept of model-matching or model-following. It aims at finding a new controller that can assign the reconfigured closed-loop system the same behaviour as the nominal closed-loop system. A comprehensive review of this approach is provided in Lunze and Richter (2008). This kind of approach has the following challenges: 1) guarantee of closed-loop stability of the reconfigured system, and 2) minimization of the time required to approach the acceptable matching.

Since exact model-matching may be too demanding, extensions of this approach have been made by using alternative approximate (norm-based) model-matching through computation of the required model-following gains. To further relax the matching condition, Staroswiecki (2005) proposes an admissible model-matching approach, which is extended by Tornil-Sin et al. (2010) using \mathcal{D} -region pole assignment and by Puig (2016) using LPV representation.

- Virtual actuator/sensor approach

This approach is studied extensively in the books Blanke et al. (2003); Steffen (2005) for linear time-invariant systems. It has been extended to a range of nonlinear systems, e.g., linear parameter varying systems (Rotondo et al., 2014), T-S fuzzy systems (Dziekan et al., 2011), piecewise affine systems (Richter, 2011), and Lipschitz nonlinear systems (Khosrowjerdi and Barzegary, 2014). The above actuator/sensor reconfiguration designs usually assume that accurate fault diagnosis is fully available. Further considering FDI time delay and possible actuator saturation effects, a virtual approach for FTC for unstable linear systems is studied in (Rotondo et al., 2015b). A virtual actuator strategy for model reference FTC using set-membership FE is also proposed in Rotondo et al. (2015a). Niemann and Stoustrup (2003) describe another control reconfiguration approach that also has the function of virtual actuator/sensor, by using the loop transfer recovery method.

- Estimation & compensation approach

The estimation & compensation approach uses explicitly the fault information obtained through fault diagnosis using the FE method. The FTC controller design can be achieved by using classical control methodologies, e.g., adaptive control, robust control and sliding mode control (SMC). Many works have been published on FE-based FTC systems using state observers, e.g., adaptive observers (Jiang et al., 2006; Kabore and Wang, 2001), SMO (Edwards and Tan, 2006), ASO (Gao and Ding, 2007), UIOs (Odgaard and Stoustrup, 2012; Tan et al., 2015), moving horizon estimation (Feng and Patton, 2014), and combined SMO and ASO (Shi et al., 2015).

- Adaptive FTC approach

In this approach faults are treated as a form of system uncertainty and they are compensated via automatic changes of the control parameter based on the mature adaptive control technique. Many papers have been published under this framework, among which are works based on adaptive update laws (Jin, 2016; Tao et al., 2013, 2001; Wang and Wen, 2010), or neural network approximation (Panagi and Polycarpou, 2011a,b; Polycarpou, 2001). Adaptive FTC schemes with fault diagnosis have also been devel-

oped in many works, based on, e.g., information-based FDI (Zhang et al., 2004, 2010b), or observer-based FE (Ye and Yang, 2006).

(4) FTC for complex systems

Nowadays there is a rapid increase in the complexity of industrial, process, banking and IT systems, since modern technology makes more and more use of interconnected, embedded, networked and distributed architectures. Potential faults may lead to performance degradation or even trigger a chain of failing subsystems and cause major catastrophes. Therefore, more effective and robust fault diagnosis and FTC designs are required.

FDI for large-scale interconnected systems has attracted great attention in the last decade, using, e.g., artificial intelligent based approach (Korbicz et al., 2012) and distributed approaches (Boem et al., 2017; Dong et al., 2014; Keliris et al., 2015; Yang et al., 2016; Zhao et al., 2005). Lots of research has also been carried out on FTC for complex systems, e.g., hybrid systems (Yang et al., 2010b), large-scale interconnected systems (Panagi and Polycarpou, 2011b; Riverso et al., 2016; Yang et al., 2016), stochastic systems (Liu et al., 2013a), discrete-event systems (Moor, 2016; Nooruldeen and Schmidt, 2015; Paoli et al., 2011; Wen et al., 2008).

As one important type of complex systems, network control systems (NCSs) are defined as spatially distributed systems in which the communication between actuators, sensors, and controllers is realized through shared networks (Hespanha et al., 2007). With numerous advantages such as low cost, flexible architectures and easy diagnosis, the last few years have witnessed a rapid development of NCSs in a variety of applications including, but not limited to, smart building, automotive vehicles, and electric power grids. Fault diagnosis and FTC designs are more challenging for NCSs than conventional control systems, due to the integration of communication networks (especially wireless networks) that are always subject to various constraints, e.g., time-delay, packet loss, and bandwidth limits (Patton et al., 2007).

A large number of works have been published on fault diagnosis for NCSs, which can be classified as follows: 1) Fault detection for NCSs with measurement packet dropout and communication time delay (Gu et al., 2010; He et al., 2008; Wang and Xiong, 2016; Zhang et al., 2011; Zong et al., 2012) and with limited access to the communication networks (Long and Yang, 2015). 2) FE. Menon and Edwards (2014) describe FE for multi-agent networks using only the relative information. Li et al. (2014) and Song et al. (2016) propose recursive FE approaches over packet losses. An ASO-based FE

for nonlinear networked systems with incomplete measurements is presented in Jiang and Fang (2014).

2.3 Integration of fault diagnosis and FTC

2.3.1 Integrated design of FDI/control

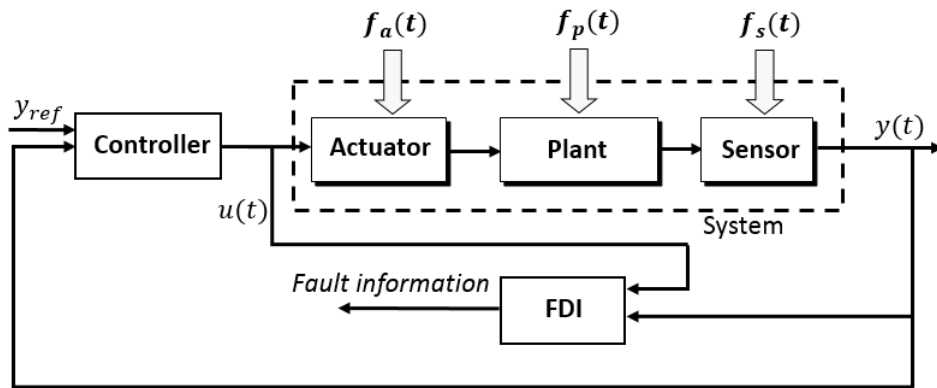


Fig. 2.1 A general scheme of closed-loop FDI systems.

It has been known for some time that the FDI performance within closed-loop systems (Fig. 2.1) is affected by system uncertainty (Ding, 2009; Nett et al., 1988; Patton, 1997; Zhang and Jiang, 2006). To illustrate this influence, a simple example of model-based FDI using a residual generator described in Patton (1997) is given as follows.

Consider an uncertain linear system with actuator faults represented by

$$\begin{aligned}\dot{x}(t) &= Ax(t) + Bu(t) + Ff(t) + \Delta(x, u, t), \\ y(t) &= Cx(t),\end{aligned}\tag{2.1}$$

where $x(t) \in \mathbb{R}^n$, $u(t) \in \mathbb{R}^m$, and $y(t) \in \mathbb{R}^p$ are the state, control input, and system output vectors, respectively. $f(t) \in \mathbb{R}^q$ denotes the actuator fault. $\Delta(x, u, t) \in \mathbb{R}^n$ denotes the lumped uncertainty including system uncertainty (parametric uncertainties on A and B) and external disturbances. A , B , F , and C are known constant matrices of compatible dimensions. It is assumed that the pair (A, C) is observable.

A state observer based residual generator design is given by

$$\begin{aligned}\hat{x}(t) &= A\hat{x}(t) + Bu(t) + L(y(t) - \hat{y}(t)), \\ \hat{y}(t) &= C\hat{x}(t), \\ r(t) &= y(t) - \hat{y}(t),\end{aligned}\tag{2.2}$$

where $\hat{x}(t)$ is the estimate of $x(t)$, $\hat{y}(t)$ is the estimate of $y(t)$, $r(t)$ is the residual signal, and L is a design matrix of compatible dimension.

Define the state estimation error as $e(t) = x(t) - \hat{x}(t)$. It follows from (2.1) and (2.2) that the error system is

$$\begin{aligned}\dot{e}(t) &= (A - LC)e(t) + Ff(t) + \Delta(x, u, t), \\ r(t) &= Ce(t),\end{aligned}\tag{2.3}$$

where $r(t)$ is the residual signal which reflects the discrepancy between the real and analytic outputs. The observer gain L is designed such that $(A - LC)$ is Hurwitz (stable). According to (2.3), the time response of the residual signal $r(t)$ (Chen, 1995) is represented by

$$r(t) = Ce^{(A-LC)t}e(0) + C \int_0^t e^{(A-LC)(t-\tau)} [Ff(\tau) + \Delta(x, u, \tau)] d\tau.\tag{2.4}$$

The principle of residual generation for fault diagnosis is to make $r(t)$ sensitive to the fault $f(t)$. However, it can be seen from (2.4) that it is sensitive to both the fault and the lumped uncertainty $\Delta(x, u, t)$. Hence, *the subsequently designed FDI function is also affected by the uncertainty $\Delta(x, u, t)$.*

Since the existing FDI methods all use explicitly either the mathematical system model or process data, their performances are always affected by system uncertainty. Therefore, it can be concluded that, in the presence of system uncertainty and external disturbance, there always exists a *unidirectional robustness interaction* between the control system and FDI unit, as shown in Fig. 2.2.

In order to achieve robust FDI in the presence of system uncertainty and unknown external disturbance, the H_-/H_∞ optimization method was first developed in Hou and Patton (1996) for robust residual generation, with the purpose of minimizing the disturbance effect and meanwhile maximizing the fault sensitivity. This method

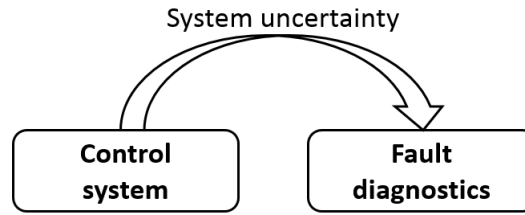


Fig. 2.2 Unidirectional robustness interaction between FDI and control.

has been further developed using LMI formulation for a linear time-invariant system (Wang et al., 2007) and a linear time-varying system (Li and Zhou, 2009). A H_-/H_∞ optimization method using matrix factorization has been proposed in Jaimoukha et al. (2006); Zhang and Ding (2008). Combined H_-/H_∞ optimization with LPV (Chen et al., 2016b; Grenaille et al., 2008) or T-S fuzzy modellings (Chadli et al., 2013) have also been used to design FDI for uncertain nonlinear systems. However, the above FDI methods merely focus on the robust design of FDI.

In 1998, Nett et al. (1988) first defined the concept of “integrated design” for combining the control and FDI designs into a joint robustness problem to achieve good robust control and acceptable FDI properties. They also proposed a four-parameter controller for integrated FDI/control design. Following this direction, numerous works have been published for linear and nonlinear systems, see for example, the review paper Ding (2009) and some recent papers Davoodi et al. (2014, 2016, 2011); Du et al. (2016); Weng et al. (2008); Zhai et al. (2016); Zhong and Yang (2015). Nevertheless, all these studies focus on the integration of FDI/control without considering FTC system design.

2.3.2 Integrated design of FDI/FTC

A general scheme of FDI-based FTC systems is provided in Fig. 2.3. Within this scheme, it is assumed that the plant has N potential fault situations which are known *a priori*. Thus the plant has N different operating modes. For each of the operating modes an associated controller is pre-computed to achieve desired system performance. Meanwhile, a bank of estimators are used for FDI purpose to identify the current operating mode with the help of the “Supervisor”. Once a certain mode is identified by the Supervisor, a switching signal is sent to the “Switching mechanism” to select the corresponding controller from the pre-computed controller set.

Without loss of generality, the following simple example is used to provide a mathematical analysis of the basic idea and design challenges of the FDI-based FTC systems.

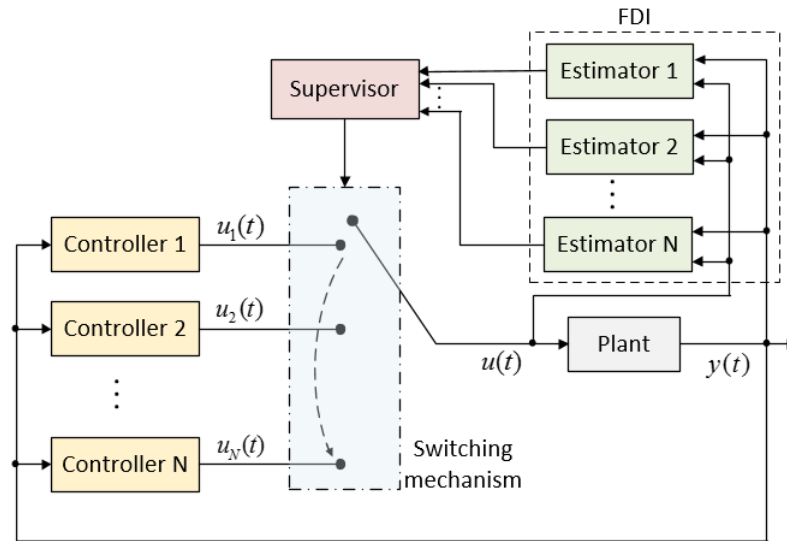


Fig. 2.3 A general scheme of FDI-based FTC systems.

Representative FTC controllers and FDI estimators will be described, following the approaches developed in the literature, e.g., Yang et al. (2009) and Cieslak et al. (2015).

Consider an uncertain linear system represented by

$$\begin{aligned}\dot{x}(t) &= Ax(t) + Bu(t) + \Delta(x, u, t), \\ y(t) &= Cx(t),\end{aligned}\tag{2.5}$$

where $x(t) \in \mathbb{R}^n$, $u(t) \in \mathbb{R}^m$, and $y(t) \in \mathbb{R}^p$ are the state, control input, and system output vectors, respectively. $\Delta(x, u, t) \in \mathbb{R}^n$ denotes the lumped uncertainty including system uncertainty and external disturbance, as defined in (2.1). A , B , and C are known constant matrices of compatible dimensions.

Assume that the system (2.5) has N operating modes (one for fault-free case and $N - 1$ for fault situations). The i -th operating mode is represented by

$$\begin{aligned}\dot{x}(t) &= A_i x(t) + B_i u(t) + \Delta_i(t), \\ y(t) &= Cx(t),\end{aligned}\tag{2.6}$$

where A_i , B_i and $\Delta_i(t)$ are the system matrices and uncertainty under the i -th faulty mode. It is assumed that the pairs (A_i, C) and (A_i, B_i) are observable and controllable, respectively.

A controller to stabilize the system (2.6) can be designed as

$$u_i(t) = -K_i y(t), \quad (2.7)$$

where K_i is the design parameter.

Substituting (2.7) into (2.6) gives the closed-loop system

$$\dot{x}(t) = (A_i - B_i K_i C) x(t) + \Delta_i(t), \quad (2.8)$$

where K_i is designed such that $(A_i - B_i K_i C)$ is Hurwitz (stable).

In order to identify the i -th operating mode (2.6), an estimator is given by

$$\begin{aligned} \dot{z}_i(t) &= A_i z_i(t) + B_i u(t) + L_i (y(t) - C z_i(t)), \\ r_i(t) &= y(t) - C z_i(t), \end{aligned} \quad (2.9)$$

where $z_i(t)$ is the estimate of $x(t)$, L_i is a design matrix, and $r_i(t)$ is a residual signal which reflects the discrepancy between the real plant output $y(t)$ and the i -th operating mode output $C z_i(t)$.

Define the estimation error as $e_i(t) = x(t) - z_i(t)$. It follows from (2.6) and (2.9) that

$$\begin{aligned} \dot{e}_i(t) &= (A_i - L_i C) e_i(t) + \Delta_i(x, u, t), \\ r_i(t) &= C e_i(t), \end{aligned} \quad (2.10)$$

where the observer gain L_i is designed such that $(A_i - L_i C)$ is Hurwitz (stable).

(1) Ideal case: $\Delta(x, u, t) = 0$ and $\Delta_i(x, u, t) = 0$

In this case, if currently the plant is working at the i -th operating mode, then $r_i(t) = 0$ and all other $r_j(t)$, $j \neq i$, $j = 1, 2, \dots, N$, are non-zero. Thus, the Supervisor is able to identify the current operating mode of the plant by collecting and comparing all the residual signals $r_i(t)$, $i = 1, 2, \dots, N$, from the estimators.

After the i -th operating mode has been identified, the control signal $u(t)$ is set as $u(t) = u_i(t)$. Substituting (2.7) into (2.5), the closed-loop system is

$$\dot{x}(t) = (A - B K_i C) x(t). \quad (2.11)$$

Since the system is working at the i -th operating mode, $A = A_i$ and $B = B_i$. Hence, (2.11) is equal to

$$\dot{x}(t) = (A_i - B_i K_i C)x(t). \quad (2.12)$$

According to (2.8), $(A_i - B_i K_i C)$ is stable, so the closed-loop system (2.11) is stable.

(2) Uncertain case: $\Delta(x, u, t) \neq 0$ and $\Delta_i(x, u, t) \neq 0$

In this case, it follows from (2.10) that

$$r_i(t) = C e^{(A_i - L_i C)t} e_i(0) + C \int_0^t e^{(A_i - L_i C)(t-\tau)} \Delta_i(x, u, \tau) d\tau. \quad (2.13)$$

Obviously, *all the residual signals $r_i(t)$, $i = 1, 2, \dots, N$, are affected by the system uncertainty $\Delta_i(x, u, t)$. So $r_i(t) \neq 0$, even if the plant is working at the i -th operating mode. This leads to a challenge of identifying the actual operating mode.*

For example, if the actual operating mode is i , but it is wrongly identified as j by the Supervisor. Then the controller $u(t)$ is chosen as $u(t) = u_j(t)$ and the resulting closed-loop control system is

$$\dot{x}(t) = (A - B K_j C)x(t) + \Delta(x, u, t). \quad (2.14)$$

Since $A = A_i$ and $B = B_i$, (2.14) is equal to

$$\begin{aligned} \dot{x}(t) &= (A_i - B_i K_j C)x(t) + \Delta(x, u, t) \\ &= (A_j - B_j K_j C)x(t) + (\Delta A_{ij} - \Delta B_{ij} K_j C)x(t) + \Delta(x, u, t), \end{aligned} \quad (2.15)$$

where $\Delta A_{ij} = A_i - A_j$ and $\Delta B_{ij} = B_i - B_j$.

Although K_j is designed such that $(A_j - B_j K_j C)$ is stable, *the stability of the FTC control system (2.15) is affected by both the system uncertainty $\Delta(x, u, t)$ and the identification (FDI) uncertainty $(\Delta A_{ij} - \Delta B_{ij} K_j C)x(t)$.*

Summing up the mathematical analysis presented above, when applying the FDI approach to an FTC system design (see Fig. 2.3), the (fault) operating mode identification directly affects the control actions applied to the plant. In the presence of system uncertainty, the FDI is affected by the uncertainty, referred as the *unidirectional robustness interaction* described in Section 2.3.1. Moreover, the closed-loop FDI-based

FTC system performance is affected by not only the system uncertainty, but also the diagnosis uncertainties. This results in *bi-directional robustness interactions* between the FDI and FTC functions, as shown in Fig. 2.4.

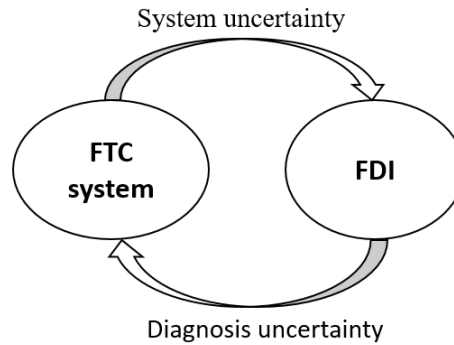


Fig. 2.4 Bi-directional robustness interactions between FDI and FTC.

Within the closed-loop FDI-based FTC system the diagnosis and control functions may not fit with each other, if they are designed well separately without taking into account the *bi-directional robustness interactions*. Therefore, it is necessary to consider the mutual interactions by integrating the designs of FDI/FTC into a simultaneous procedure (Zhang and Jiang, 2006).

The integration of FDI/FTC discussed here is a hard challenge, since the reconfiguration and FDI roles have a bi-directional uncertainty which is more complex when compared with the integration of FDI/control. The complexity arises from the joint multi-objectives of robust closed-loop stability, robust residual performance (requiring optimal fault detection thresholds), and robust fault tolerance with stable reconfiguration, generally operating in the presence of various time delays and uncertainties.

Integrated FDI/FTC designs have been considered in several works (Cieslak et al., 2015; Mhaskar et al., 2006; Yang et al., 2009). However, the true integration defined in this thesis as a single procedure to obtain the FDI and FTC parameters simultaneously (see Definition 1.1) has not been achieved. **It is very difficult or impossible to achieve the true integration using the FDI approach**, since it involves: 1) discrete-event structure with complex decision, 2) variable and unknown time delay, and 3) a control reconfiguration that is very complex.

Therefore, the FDI approach to FTC can be one of the most difficult problems of adaptive control and in general is not suitable for achieving true integration of fault diagnosis and FTC as well as practical application. In a word, the true integration of fault diagnosis and FTC still remains an open problem.

2.4 Summary

The purpose of this chapter is to provide a literature review for FTC systems and the integrated design of fault diagnosis and FTC. In the presence of system uncertainty, the concepts of *unidirectional robustness interaction* and *bi-directional robustness interactions* are defined for the FDI/control and the fault diagnosis/FTC systems, respectively. The existence of bi-directional interactions gives rise to a consideration of integrating the fault diagnosis and FTC functions, which is an important subject for FTC systems but remains open. Although the FDI-based FTC approach can be an alternative way to achieve the integration, it is complex in design and implementation due to the requirements of robust residual generation, reconfiguration mechanism, and the associated time delay and uncertainties. It is thus considered in this research a more realistic and effective FE-based FTC approach to realize the true integration. A motivation for this is given in detail in Chapter 3.

Chapter 3: Practical and theoretical motivations of integrated FE/FTC design

3.1 Introduction

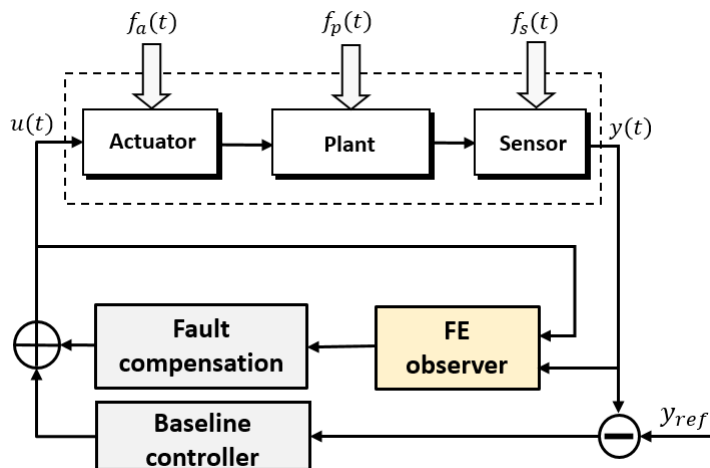


Fig. 3.1 A general scheme of FE-based FTC systems.

The literature review of FTC systems provided in Chapter 2 implies that the integration of fault diagnosis and FTC remains a very open problem. The FDI-based FTC under the framework shown in Fig. 2.3 can be an alternative way to achieve robust FTC performance, but its design is necessarily a big challenge due to the requirements of robust residual generation and reconfiguration mechanism (see the discussion in Section 2.3.2).

As also reviewed in Chapter 2, the past decade has seen more and more interest in utilizing the observer-based FE approach to obtain a direct reconstruction of a fault. Since the FE function intrinsically includes the fault detection and isolation roles, the

more complex FDI role is thus obviated. In the FE-based FTC approach (as shown in Fig. 3.1) the reconstructed (or estimated) fault signals are used directly in the control system to compensate for the fault effects. This direct use of FE for FTC without the need of a reconfiguration mechanism brings significant convenience and application potential to the subject of FTC system design. This approach can also facilitate the development of robust methods for a true integration of fault diagnosis and FTC.

This chapter aims to provide a tutorial guide for FE-based FTC systems design and an intuitive motivation for integrated FE/FTC design with mathematical analysis.

The remainder of this chapter is organized as follows. A fault-tolerant wind turbine pitch system based on FE is presented in Section 3.2 as an illustrative example for FE-based FTC systems and serves as a practical motivation of integrated FE/FTC. Section 3.3 gives a more detailed mathematical analysis for the necessity and importance of integrated FE/FTC design. Finally, conclusive discussions are present in Section 3.4.

3.2 Fault-tolerant wind turbine pitch control: a practical motivation

This section provides a tutorial example of fault-tolerant wind turbine pitch control to show the power and also challenges of FE-based FTC systems. It uses an observer-based FE and FTC design in which their functions are designed separately. The FE/FTC performance in the cases of system uncertainties is also investigated.

Nowadays wind turbines contribute to large parts of the world's power production. Meanwhile, there is a strong demand on enhanced reliability of the wind turbine control system to guarantee power generation and reduce operation and maintenance cost (Cheng and Zhu, 2014; Kaldellis and Zafirakis, 2011). Within a wind turbine system hydraulic pitch control subsystems play a critical role, because pitch actuation is important for limiting power capture under high wind situations (in operation region 3 with effective wind speeds of 12.5 m/s – 25 m/s), mitigating operational load, stalling, and aerodynamic braking (Burton et al., 2011). At lower wind speeds (in operation region 2 with effective wind speeds of 3 m/s – 12.5 m/s), the pitch actuation system is not involved and the turbine conversion efficiency is regulated by rotor speed control.

Wind turbine pitch control has attracted significant research attention and on which numerous strategies have been developed under a collective control scheme, using PID control (Boukhezzar et al., 2007; Burton et al., 2011; Gao and Gao, 2016; Hand, 1999),

linear quadratic Gaussian control (Novak et al., 1995; Stol and Fingersh, 2004), robust control (Geng and Yang, 2010), gain scheduling (Bianchi et al., 2005), disturbance accommodating control (Stol and Balas, 2003), fuzzy logic control (Mohamed et al., 2001), and LPV control (Shi and Patton, 2015a; Sloth et al., 2011), all of which take on the form of baseline control as a definition in this work.

However, in real operations pitch systems may have actuator faults. The pitch actuator faults may be caused by a drop in pressure in the hydraulic supply system or high air content in the oil, and lead to slow pitch action, which makes it impossible for the pitch control to maintain the rotor at rated speed, and thus cause fluctuations on the generator speed and power and degrade wind turbine system stability (Odgaard et al., 2013; Ribrant and Bertling, 2007). This study considers a low pressure pitch actuator fault, which is faster and more severe than the high air content fault. In the presence of low pressure actuator faults, the existing baseline control alone cannot maintain desired pitch action, which gives rise to the research of FTC for pitch systems. FTC can be used to achieve baseline control system performance in fault free cases, and also compensate fault effects to maintain robust system performance when faults occur (Patton, 2015). Moreover, the FTC strategy can also be used to provide fault information for effective use in subsequent maintenance schedules by incorporating a fault diagnostic module (Gao et al., 2015a,b).

A projection-based FTC design is proposed in Jain et al. (2013) for pitch systems without explicit use of fault information (detection or estimation). An FTC pitch system is developed in Sloth et al. (2011) based on FDI. However, it is difficult or impossible for this FDI strategy to get the pitch actuator fault magnitude. A pitch actuator is in principle a piston servo modelled by a second-order system. As described in Esbensen and Sloth (2009), the parametric low pressure pitch actuator fault can be modelled as a convex function of the nominal values of natural frequency and damping factor together with low pressure values, combined by a fault indicator function in a form of additive fault. With this model the actuator fault can be known if the fault indicator function is known. Therefore, instead of using the FDI approach it is possible to develop a more direct and effective method to reconstruct the fault indicator function.

Observer-based FE approaches have been applied to replace the FDI approach to reconstruct the pitch actuator fault (Chen et al., 2013b; Shi and Patton, 2015a) based on the fault model described by Esbensen and Sloth (2009). In Chen et al. (2013b) fault shapes are attained using an adaptive observer whose gains are solved via LMIs dependent on the fault indicator with solution requiring a linear parameter varying strategy. Recently, a reconfigurable FTC design based on linear parameter varying system modelling of the

wind turbine system is proposed in Shi and Patton (2015a), using a descriptor form of extended state observer. Although their FTC design framework is proved to be effective, a fictitious actuator fault is reconstructed, instead of the real fault indicator function, this is seen to be a disadvantage.

It will be shown in Section 3.2.1 that the distribution function of the fault indicator is nonlinear, this makes it difficult or impossible to achieve FE using the existing observers. In Georg and Schulte (2014) a T-S SMO is proposed for estimating pitch actuator parameter faults of the NREL 5 MW wind turbine with verification on the aero-elastic code FAST. In their work the pitch actuator is modelled as a first order delay system and the SMO depends on a regular form of the system model involving coordinate transformation.

In this section an adaptive step-by-step (hierarchical) SMO adapted from Floquet et al. (2004) is used to estimate the real fault indicator function. Compared with the FE observers in Chen et al. (2013b); Shi and Patton (2015a) and others in the literature, the proposed SMO has a simpler form with design parameters that are easy to determine to facilitate the real-time implementation. Following a similar FTC framework used in Shi and Patton (2015a), an FE-based FTC strategy for wind turbine pitch systems is proposed to recover admissible pitch dynamics in the presence of low pressure actuator faults.

3.2.1 Problem statement

A sketch of the 4.8 MW benchmark wind turbine is shown in Fig. 3.2. As outlined in Fig. 3.3, the 4.8 MW benchmark wind turbine closed-loop system comprises five subsystems: aerodynamics, pitch system, drive train, generator unit, and pitch and generator control (Odgaard et al., 2013). The variables in the system are defined as follows: v_w is the wind speed acting on the turbine blades, β is the pitch angle, T_r is the rotor torque, ω_r is the rotation speed of the rotor, T_g is the generator torque, ω_g is the rotation speed of the generator, P_g is the generator power, $T_{g,r}$ is the torque reference to the generator, P_r is the power reference to the wind turbine, and β_r is the angle reference to the pitch actuator system. It is assumed throughout in this work that the yaw control has normal operation with no yaw misalignment.

The control subsystem includes both pitch and generator speed control, used to generate the angle reference β_r and the torque reference $T_{g,r}$, respectively. At wind speeds below rated value (< 12.5 m/s), the pitch control signal β_r is set zero and the generator control

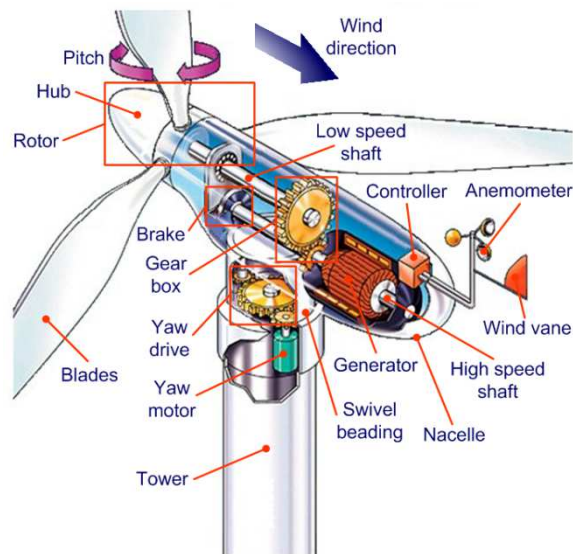


Fig. 3.2 The 4.8 MW benchmark wind turbine structure (Molina and Alvarez, 2011).

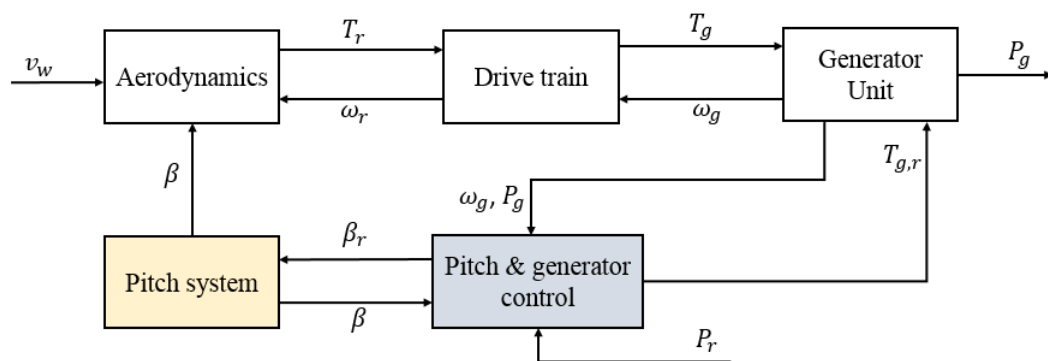


Fig. 3.3 The 4.8 MW benchmark wind turbine control system.

is used to adjust the rotor speed to maximize power capture. In Region 3, pitch control is required to keep the rotor at rated speed (Muljadi and Butterfield, 2001). Therefore, this work considers the pitch control design in Region 3 and it is assumed that there are no stuck actuator faults, so that the proposed control can also work well in Region 2.

In the benchmark model the three pitch systems each has an individual pitch actuator and the three individual actuators are assumed to have the same dynamic structure. All the pitch systems have the same control input (i.e., collective pitch control). For the sake of simplicity, in the design procedure a single pitch system is considered and in

principle it is a piston servo modelled by a second-order system (Odgaard et al., 2013)

$$\begin{aligned}\dot{x}_1 &= x_2, \\ \dot{x}_2 &= -\omega_n^2 x_1 - 2\xi\omega_n x_2 + \omega_n^2 u, \\ y &= x_1,\end{aligned}\tag{3.1}$$

where $[x_1 \ x_2]^\top = [\beta \ \dot{\beta}]^\top$ are the system states and $u = \beta_r$ is the pitch command input. y is the output angle. β and $\dot{\beta}$ are the pitch angle and angular velocity, respectively. ω_n and ξ are the natural frequency and damping factor, respectively.

The collective pitch control scheme used here has a single command input β_r acting on the three pitch systems to actuate a common desired angle β , as outlined in Fig. 3.4. In the scheme, $\omega_{g_nominal}$ and ω_g are the nominal (rated) and real speeds of the generator, respectively. β_r is the pitch angle command input and β is the pitch angle output. Due to physical constraints of each actuator system, a magnitude and rate limiter is implemented in the benchmark.

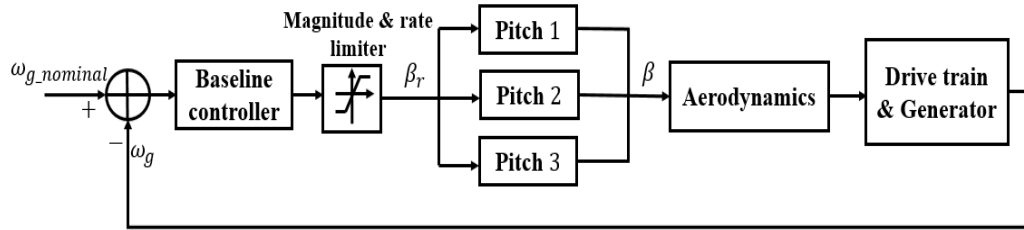


Fig. 3.4 Nominal pitch system control scheme.

Each pitch system may have faults resulting from dynamical changes (variations of the values of ω_n and ξ), due to a drop in hydraulic pressure (Esbensen and Sloth, 2009). Under this low pressure fault, the parameters ω_n^2 and $\xi\omega_n$ in the pitch system (3.1) can be modelled as convex combinations of their values at nominal and low pressure situations in a form of

$$\begin{aligned}\omega_n^2 &= \omega_{n_0}^2 + (\omega_{n_f}^2 - \omega_{n_0}^2)f, \\ \xi\omega_n &= \xi_0\omega_{n_0} + (\xi_f\omega_{n_f} - \xi_0\omega_{n_0})f,\end{aligned}\tag{3.2}$$

where ω_{n_0} and ξ_0 are the nominal values of ω_n and ξ , while ω_{n_f} and ξ_f are their values at low pressure. The unknown function $f \in [0, 1]$ is a fault indicator. $f = 0$ corresponds to the normal pressure with $\omega_{n_0} = 11.11$ rad/s and $\xi_0 = 0.6$ rad/s, and

$f = 1$ corresponds to the low pressure with $\omega_{n_f} = 3.42$ rad/s and $\xi_f = 0.9$ rad/s. Assume that $\|f\| \leq \bar{f}_0 < \infty$ for some unknown constant \bar{f}_0 .

Using the convex model (3.2) of the pitch actuator faults, the original parametric faults are converted into a form of additive faults. By (3.2), the pitch system (3.1) with actuator faults is represented by

$$\begin{aligned} \dot{x}_1 &= x_2, \\ \dot{x}_2 &= G_0(x) + B_0 u + F(x)f, \\ y &= x_1, \end{aligned} \tag{3.3}$$

where $x = [x_1 \ x_2]^\top$, $G_0(x) = -\omega_{n_0}^2 x_1 - 2\xi_0 \omega_{n_0} x_2$, $B_0 = \omega_{n_0}^2$, and the fault distribution matrix is $F(x) = (\omega_{n_0}^2 - \omega_{n_f}^2)(x_1 - u) + 2(\xi_0 \omega_{n_0} - \xi_f \omega_{n_f})x_2$.

Unit step responses of a pitch system with different values of f are shown in Fig. 3.5. It can be seen that the pressure drop slows down the pitch actuator dynamics. Therefore, when suffering from low pressure fault, the pitch actuator dynamics become slow and degrade the pitching performance. To recover the pitch action an ideal solution is to compensate the fault by implicitly changing the dynamic characteristics of the actuator.

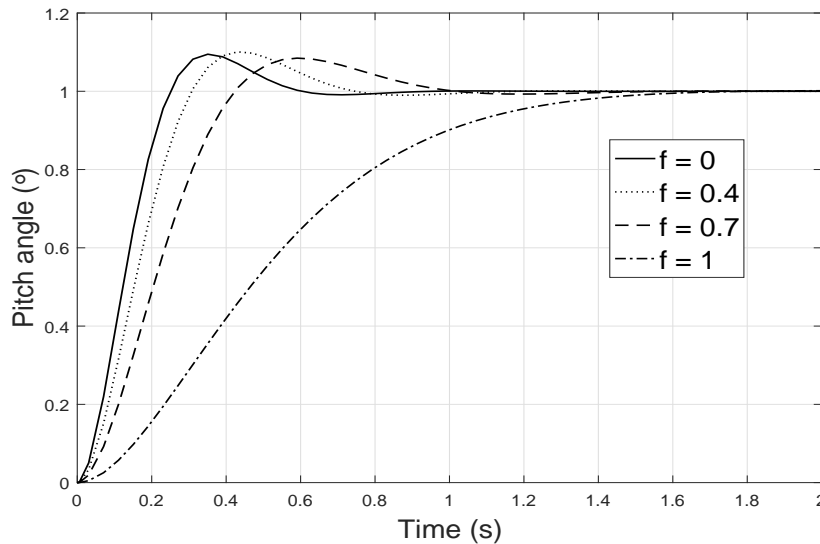


Fig. 3.5 Step response of a pitch system under different fault conditions.

This work aims to design an FTC pitch system based on FE to maintain pitching action despite actuator faults. The FTC pitch system schematic (see Fig. 3.6) involves: 1) a baseline controller, 2) observers for estimating the states and faults, and 3) reconfigurable controllers for fault compensation. Besides, the gains k_i , $i = 1, 2, 3$, are also to

be designed. In the presence of the considered actuator faults the three pitch systems have the same baseline controller of the fault-free case in Fig. 3.4. It should also be noted that in the fault-free case the proposed FTC system reverts to a baseline system.

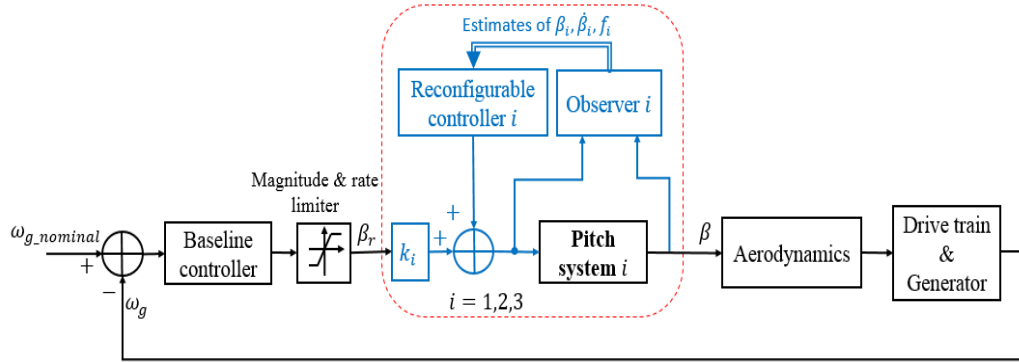


Fig. 3.6 Fault-tolerant pitch system control scheme.

3.2.2 Adaptive step-by-step SMO-based FE design

A step-by-step SMO is proposed in Floquet et al. (2004) for fault detection (not estimation) for nonlinear system. This SMO is modified here to estimate the states and the fault of the system (3.3) with time-varying distribution function $F(x)$ with a form (3.4). Moreover, an adaptive approach is incorporated with the SMO, thus *a priori* knowledge of the bounds of estimation errors and first-order derivative of f is not required.

$$\begin{aligned}\hat{\dot{x}}_1 &= \hat{x}_2 + v_1, \\ \hat{\dot{x}}_2 &= G_0(\hat{x}) + B_0 u + F(\hat{x})\hat{f} + v_2, \\ \hat{\dot{f}} &= \eta_f \text{sign}(e_f),\end{aligned}\tag{3.4}$$

where $\hat{x} = [\hat{x}_1 \ \hat{x}_2]^\top$ are the state estimates. \hat{f} is the estimate of f . Define the estimation errors of the states and fault as $e_{x_1} = x_1 - \hat{x}_1$, $e_{x_2} = x_2 - \hat{x}_2$, and $e_f = f - \hat{f}$, respectively. The SMO switching functions are defined by

$$v_1 = \eta_{v_1} \text{sign}(e_{x_1}), \quad v_2 = \eta_{v_2} \text{sign}(\tilde{x}_2 - \hat{x}_2),\tag{3.5}$$

where $\tilde{x}_2 = \hat{x}_2 + v_1$, and η_{v_1} , η_{v_2} and η_f are design parameters.

Now it is necessary to show the existence of the observer (3.4) and to determine the stability conditions.

Theorem 3.1 (FE action) For the pitch system (3.3), there exists an adaptive step-by-step SMO (3.4) to achieve asymptotic state and fault estimations.

Proof: (1) Step 1

Denote $\tilde{G}_0 = G_0(x) - G_0(\hat{x})$ and $\tilde{F} = F(x) - F(\hat{x})$, then $F(x)f - F(\hat{x})\hat{f} = \tilde{F}f + F(\hat{x})e_f$. It follows from (3.3) and (3.4) that the estimation error system is

$$\dot{e}_{x_1} = e_{x_2} - v_1, \quad (3.6)$$

$$\dot{e}_{x_2} = \tilde{G}_0 + \tilde{F}f + F(\hat{x})e_f - v_2, \quad (3.7)$$

$$\dot{e}_f = \dot{\hat{f}} - \eta_f \text{sign}(e_f). \quad (3.8)$$

A Lyapunov function for the subsystem (3.6) is given as

$$V_1 = \frac{1}{2}e_{x_1}^2.$$

It follows from (3.5) and (3.6) that

$$\begin{aligned} \dot{V}_1 &= e_{x_1}(e_{x_2} - v_1) \\ &\leq (\|e_{x_2}\| - \eta_{v_1})\|e_{x_1}\|. \end{aligned} \quad (3.9)$$

Since all the signals in (3.7) are bounded in finite time, so e_{x_2} is also bounded in finite time and there exists a positive scalar satisfying $\rho_{v_1} \geq \|e_{x_2}\|$. Hence, in order to compensate the effect of the unknown estimation error e_{x_2} , designing $\eta_{v_1} = \rho_{v_1} + \varepsilon_{v_1}$, where ε_{v_1} is a positive constant. Substituting η_{v_1} into (3.9) yields

$$\dot{V}_1 \leq -\varepsilon_{v_1}\|e_{x_1}\|. \quad (3.10)$$

From (3.10), it can be obtained that $\dot{V}_1 \leq -\alpha_1\sqrt{V_1}$, where $\alpha_1 = \sqrt{2}\varepsilon_{v_1}$. Hence, (3.10) satisfies the standard reachability condition (Edwards and Spurgeon, 1998) and the sliding surface $s_1 = e_{x_1} = 0$ is reached in finite time $t_r \leq 2\sqrt{V(0)}/\alpha_1$.

(2) Step 2

According to (3.6) and the proof in Step 1, the dynamics of e_{x_1} reach the sliding surface $s_1 = 0$ in finite time t_r and remain on it thereafter. After t_r , by using the equivalent

output injection concept (Edwards et al., 2000), the subsystem (3.6) is reduced to be

$$\mathbf{0} = e_{x_2} - v_{eq,1},$$

where $v_{eq,1}$ is the equivalent output injection signal and $v_{eq,1} = e_{x_2}$. Thus, after a finite time t_r , $\tilde{x}_2 = \hat{x}_2 + e_{x_2}$ and $v_2 = \eta_{v_2} \text{sign}(e_{x_2})$.

A Lyapunov function for the subsystems (3.7) and (3.8) is given as

$$\dot{V}_{20} = \frac{1}{2}e_{x_2}^2 + \frac{1}{2}e_f^2. \quad (3.11)$$

It is derived that

$$\begin{aligned} \dot{V}_{20} &= e_{x_2} [\tilde{G}_0 + \tilde{F}f + F(\hat{x})e_f - v_2] + e_f (\dot{f} - \eta_f \text{sign}(e_f)) \\ &\leq [\|\tilde{G}_0\| + \|\tilde{F}f\| + \|F(\hat{x})e_f\| - \eta_{v_2}] \|e_{x_2}\| + (\rho_f - \eta_f) \|e_f\| \\ &\leq (\rho_{v_2} - \eta_{v_2}) \|e_{x_2}\| + (\rho_f - \eta_f) \|e_f\|, \end{aligned} \quad (3.12)$$

where $\rho_{v_2} \geq \|\tilde{G}_0\| + \|\tilde{F}f\| + \|F(\hat{x})e_f\|$ and $\rho_f \geq \|\dot{f}\|$.

Using $\hat{\rho}_{v_2}$ and $\hat{\rho}_f$ to estimate ρ_{v_2} and ρ_f , respectively, with update laws

$$\dot{\hat{\rho}}_{v_2} = \sigma_{v_2} \|e_{x_2}\|, \quad \dot{\hat{\rho}}_f = \sigma_f \|e_f\|, \quad (3.13)$$

where σ_{v_2} and σ_f are positive design constants.

Design $\eta_{v_2} = \hat{\rho}_{v_2} + \varepsilon_{v_2}$ and $\eta_f = \hat{\rho}_f + \varepsilon_f$ with positive design constants ε_{v_2} and ε_f . Define the estimation errors of ρ_{v_2} and ρ_f as $\tilde{\rho}_{v_2} = \rho_{v_2} - \hat{\rho}_{v_2}$ and $\tilde{\rho}_f = \rho_f - \hat{\rho}_f$, respectively. A Lyapunov function for the augmented estimation error system (including e_{x_2} , e_f , $\tilde{\rho}_{v_2}$, and $\tilde{\rho}_f$) is given as

$$V_2 = V_{20} + \frac{1}{2\sigma_{v_2}} \tilde{\rho}_{v_2}^2 + \frac{1}{2\sigma_f} \tilde{\rho}_f^2.$$

From (3.12) and (3.13),

$$\begin{aligned}
\dot{V}_2 &= \dot{V}_{20} + \frac{1}{\sigma_{v_2}}(-\tilde{\rho}_{v_2}\dot{\rho}_{v_2}) + \frac{1}{\sigma_f}(-\tilde{\rho}_f\dot{\rho}_f) \\
&\leq (\rho_{v_2} - \tilde{\rho}_{v_2} - \eta_{v_2})\|e_{x_2}\| + (\rho_f - \tilde{\rho}_f - \eta_f)\|e_f\| \\
&\leq -\varepsilon_{v_2}\|e_{x_2}\| - \varepsilon_f\|e_f\| \\
&\leq 0.
\end{aligned} \tag{3.14}$$

It follows from (3.14) and the Barbalat's lemma (Slotine et al., 1991) that $\lim_{t \rightarrow \infty} V_2(t) = 0$. Therefore, $V_2(t) \leq V_2(0)$ and e_{x_2} , e_f , $\tilde{\rho}_{v_2}$, and $\tilde{\rho}_f$ are bounded. Furthermore, $|e_{x_2}(t)| \leq \sqrt{2V_2(0)}$ and $|e_f(t)| \leq \sqrt{2V_2(0)}$. Under zero initial condition $V_2(0) = 0$ (i.e., $e_{x_2}(0) = e_f(0) = \tilde{\rho}_{v_2}(0) = \tilde{\rho}_f(0) = 0$), then it holds that $\lim_{t \rightarrow \infty} e_{x_2}(t) = 0$ and $\lim_{t \rightarrow \infty} e_f(t) = 0$.

It is concluded here that for the pitch system (3.3), by ensuring satisfaction of the zero initial conditions, then there exist parameters η_{v_1} , η_{v_2} , and η_f such that the observer (3.4) can estimate the system states and fault accurately. \square

Remark 3.1 Although e_f is not available in practice, it can be obtained using the equivalent output injection concept. Design a sliding surface as $s_2 = e_{x_2} = 0$. Since the SMO switching functions v_1 and v_2 can ensure the reachability of s_2 , i.e., $s_2 = \dot{s}_2 = 0$, then the equivalent output injection signal of v_2 is

$$v_{eq,2} = F(\hat{x})e_f.$$

Thus, $e_f = v_{eq,2}/F(\hat{x})$. $v_{eq,2}$ is attained by applying v_2 to a low-pass filter, i.e.,

$$v_{eq,2} \cong \frac{1}{1 + \tau_1 s} v_2,$$

where τ_1 is a time constant.

In order to avoid singularity when $F(x) = 0$, $e_f = v_{eq,2}/F(\hat{x})$ is approximated by the following function in real-time implementation,

$$e_f = \frac{F(\hat{x})}{F(\hat{x})^2 + \varepsilon} v_{eq,2}$$

with a small enough positive scalar ε .

Moreover, since the fault indicator function is known to be $f \in [0, 1]$, a magnitude limiter is used to ensure $\hat{f} \in [0, 1]$.

Remark 3.2 For the pitch system (3.3), the observer design parameters are ε_{v_1} , σ_{v_1} , ε_{v_2} , σ_{v_2} , ε_f , σ_f , and τ_1 . These offline design parameters should all be positive constants, whilst ε_{v_1} , ε_{v_2} , ε_f , and τ_1 are of small values and should be tuned by trial and error.

3.2.3 FTC design

The pitch actuator system (3.3) can be rearranged into

$$\begin{aligned}\dot{x}_1 &= x_2, \\ \dot{x}_2 &= G_0(x) + \omega_n^2 u + F_1(x)f,\end{aligned}\tag{3.15}$$

where $F_1(x) = (\omega_{n_0}^2 - \omega_{n_f}^2)x_1 + 2(\xi_0\omega_{n_0} - \xi_f\omega_{n_f})x_2$.

An FTC controller for the pitch system (3.3) comprises a baseline controller and a reconfigurable controller (see Fig. 3.6), designed as

$$u = k_1\beta_r + u_f,\tag{3.16}$$

where β_r is the baseline controller to achieve pitch angle control under fault-free case, and u_f is the reconfigurable controller to compensate the fault effect. The design parameter k_1 is used to modify the baseline controller and the designs of β_r , k_1 and u_f are given below.

(1) Baseline controller design

Proportional-Integral (PI) baseline controllers have been used effectively in wind turbine pitch control in academic research (Boukhezzar et al., 2007; Gao and Gao, 2016; Hand, 1999) and industrial implementation (Burton et al., 2011) due to its facilitation and robustness. Therefore, in this study the baseline controller β_r for the three pitch systems is chosen as a PI controller given by

$$\beta_r(t) = K_P e_{w-g}(t) + K_I \int_0^t e_{w-g}(\tau) d\tau,\tag{3.17}$$

where e_{w_g} is the tracking error of the generator speed, defined as $e_{w_g} = w_g - w_{g_nominal}$. K_P and K_I are the proportional and integral gains, respectively.

The modification parameter k_1 is given by

$$k_1 = \frac{\omega_{n_0}^2}{\hat{\omega}_n^2},$$

where $\hat{\omega}_n^2 = \omega_{n_0}^2 + (\omega_{n_f}^2 - \omega_{n_0}^2)\hat{f}$ and \hat{f} is the fault estimate provided by the observer (3.4).

Clearly, it can be seen that in the fault-free case $k_1 = 1$, then the FTC controller reverts to a baseline controller.

(2) Reconfiguration controller design

The reconfigurable controller component u_f is activated automatically once a fault f occurs and it is designed as

$$u_f = -\frac{F_1(\hat{x})\hat{f}}{\hat{\omega}_n^2},$$

where $F_1(\hat{x}) = (\omega_{n_0}^2 - \omega_{n_f}^2)\hat{x}_1 + 2(\xi_0\omega_{n_0} - \xi_f\omega_{n_f})\hat{x}_2$.

(3) FTC performance analysis

The FTC system performance based on (3.16) is analysed in Theorem 3.2.

Theorem 3.2 (FTC action) With the asymptotic state and fault estimations obtained from the observer (3.4), the controller (3.16) can compensate the fault f and recover the nominal pitch dynamics.

Proof: Substituting (3.16) into (3.15) yields

$$\begin{aligned} \dot{x}_1 &= x_2, \\ \dot{x}_2 &= G_0(x) + B_0\beta_r + \delta(e_{x_1}, e_{x_2}, e_f, t), \end{aligned} \quad (3.18)$$

where $\delta(e_{x_1}, e_{x_2}, e_f, t) = \tilde{F}_1(x)\hat{f} + F_1(x)e_f + (\omega_{n_f}^2 - \omega_{n_0}^2)(\omega_{n_0}^2\beta_r - F_1(\hat{x})\hat{f})e_f/\hat{\omega}_n^2$ and $\tilde{F}_1(x) = F_1(x) - F_1(\hat{x})$.

Note that $\delta(e_{x_1}, e_{x_2}, e_f, t)$ is a function of the estimation errors e_{x_1} , e_{x_2} and e_f . Since it has been proved in Section 3.2.2 that $\lim_{t \rightarrow \infty} e_{x_1}(t) = 0$, $e_{x_2}(t)$ and $e_f(t)$ are bounded, then $\delta(e_{x_1}, e_{x_2}, e_f, t)$ is bounded. In the case of zero initial conditions, i.e., $e_{x_1}(0) = e_{x_2}(0) = e_f(0) = 0$, then $\lim_{t \rightarrow \infty} \delta(e_{x_1}, e_{x_2}, e_f, t) = 0$. Hence, by ensuring satisfaction of the zero initial conditions, the closed-loop system (3.18) becomes

$$\begin{aligned}\dot{x}_1 &= x_2, \\ \dot{x}_2 &= G_0(x) + B_0\beta_r,\end{aligned}$$

which is exactly the fault-free pitch system (3.1).

It is concluded here that the controller (3.16) can compensate the fault in the pitch system (3.15) automatically, using the state and fault estimation from the observer (3.4). This compensation guarantees the faulty pitch system to perform as a healthy one. \square

3.2.4 Simulation results

In this section the effectiveness of the proposed FE-based FTC design is demonstrated by applying it to a 4.8 MW wind turbine benchmark (Odgaard et al., 2013). The rated generator speed is 162 rad/s. Limits of the pitch angle and pitch rate are $[-2^\circ, 90^\circ]$ and $[-9^\circ/s, 9^\circ/s]$, respectively. Suppose that there exists a small measurement noise modelled by a zero mean white Gaussian noise with a variance of $1.0e - 10$.

The three pitch systems use the same PI baseline controller (3.17) with $K_P = 1$ and $K_I = 4$. The observer parameters are given in Table 3.1 and the other configurations of the wind turbine system (e.g., the generator control) follow the benchmark.

Table 3.1 Design parameters of the observers.

	ρ_{v_1}	ϵ_{v_1}	σ_{v_2}	σ_f	ϵ_{v_2}	ϵ_f	τ_1
Pitch 1	0.14	0.01	0.1	0.05	0.01	0.01	0.001
Pitch 2	0.09	0.01	0.15	0.05	0.01	0.01	0.001
Pitch 3	0.14	0.01	0.2	0.01	0.01	0.01	0.001

Simulations are carried out in two cases: 1) only the pitch system 3 has an actuator fault f_3 , and 2) the three pitch systems have faults f_1 , f_2 , and f_3 , respectively. The simulations use the same wind speed given in Fig. 3.7, which covers almost the whole

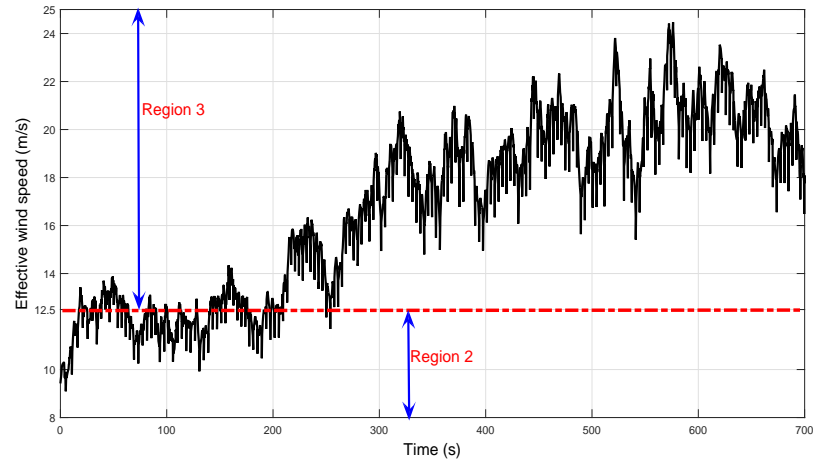


Fig. 3.7 Effective wind speed.

area of Region 3 and part of Region 2. In Region 2 the wind turbine aims at maximizing power capture and the pitch angles are set to be zero. Thus, the pitch angle references are always set to zero in Region 2.

(1) Case 1: single actuator fault

The simulation results are shown in Figs. 3.8 – 3.14. Fig. 3.8 shows that the fault f_3 on the pitch system 3 is estimated with acceptable accuracy. In the time interval $t \in [0, 250]$ s, the effective wind speed changes between Regions 2 and 3. Since the pitch angle reference is always set to be zero in Region 2, the FE observer has zero control input and thus cannot estimate the fault. This is why f_3 is not well estimated in the time period of $t \in [0, 250]$ s.

Figs. 3.9 – 3.14 show that in the presence of f_3 , the pitch actuator 3 has slow pitch rate, which thus causes an undesired pitch angle response in the pitch system 3 and subsequently in the pitch systems 1 and 2. The undesired pitching results in larger fluctuations on the generator speed and power. However, from the results it can be seen that there is no difference between the performances of the fault free and FTC cases. This means that the proposed FTC design can compensate the considered actuator fault f_3 well and recover the pitch actuator 3 to its nominal situation.

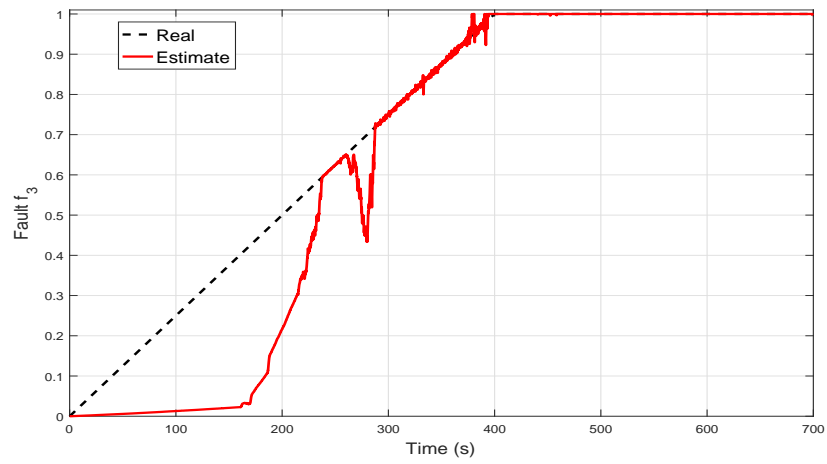


Fig. 3.8 Fault estimation: pitch 3, Case 1.

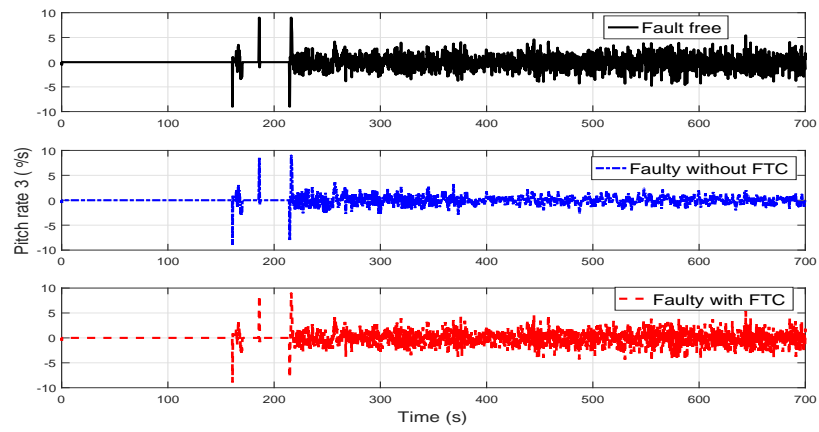


Fig. 3.9 Pitch rate: pitch 3, Case 1.

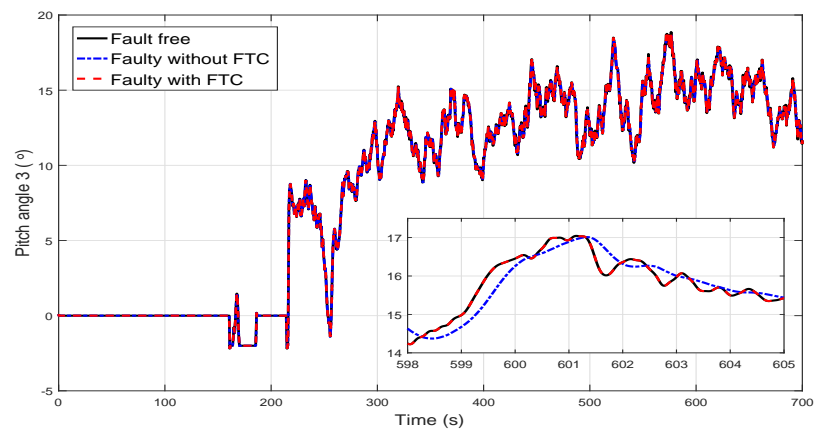


Fig. 3.10 Pitch angle: pitch 3, Case 1.

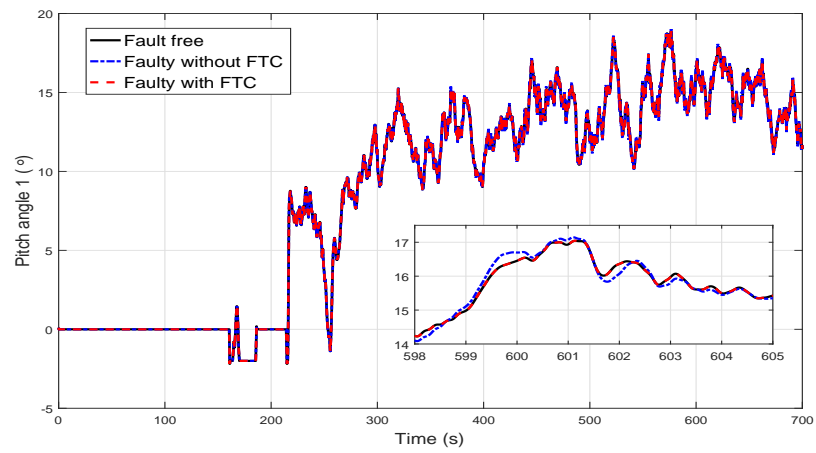


Fig. 3.11 Pitch angle: pitch 1, Case 1.

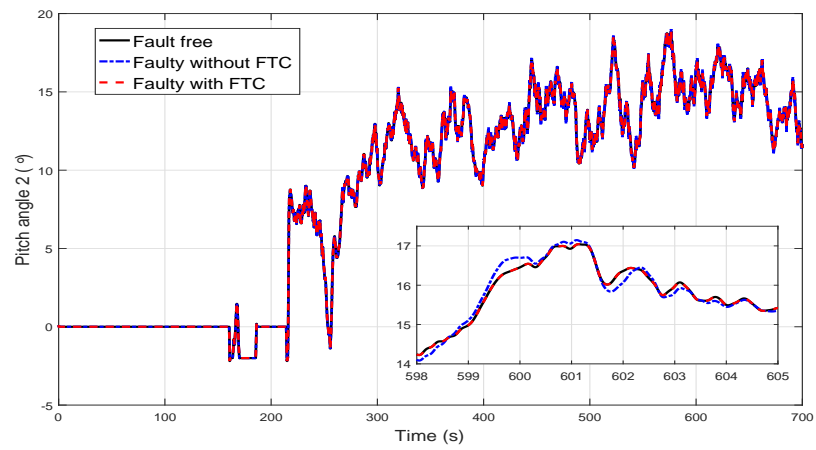


Fig. 3.12 Pitch angle: pitch 2, Case 1.

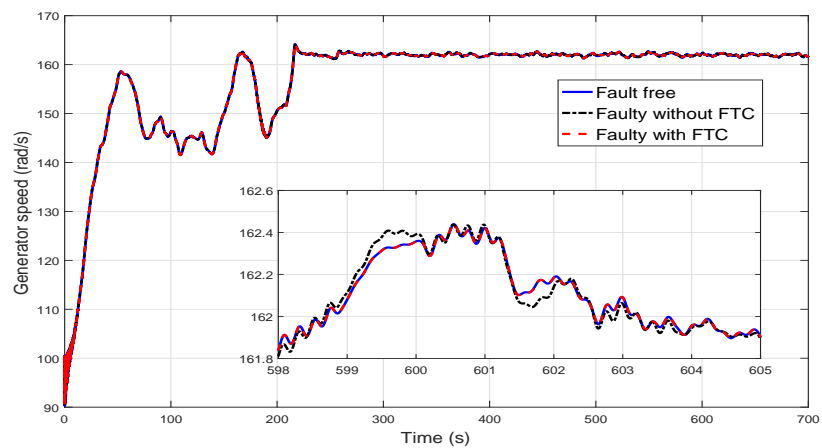


Fig. 3.13 Generator speed: Case 1.

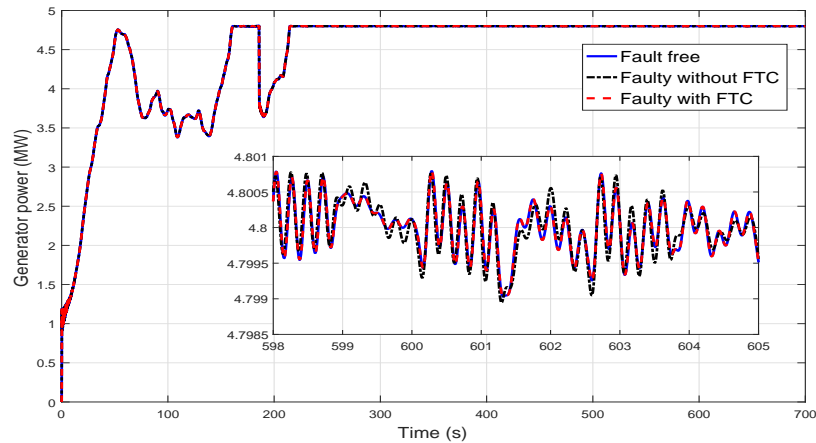


Fig. 3.14 Generator power: Case 1.

(2) Case 2: multiple actuator faults

Figs. 3.15 – 3.17 show that the three faults are estimated with good accuracy except in the time period $t \in [0, 250]$ s as that in Case 1. In Figs. 3.18 – 3.25, the faults slow down the dynamics of the three pitch systems, and thus the generator cannot be kept at rated speed. The fluctuation in generator speed subsequently causes variations in the generator power, leading to pitch angle oscillation and pitch rate saturation. Moreover, the oscillation will unbalance the three pitch systems and increase their blade loads with potential damage to the wind turbine, especially for large turbines (Bossanyi, 2003). However, it can be seen that the proposed FTC design compensates the faults well and recovers the pitch actuator dynamics, ensuring desired pitching action, thus avoiding pitch rate saturation.

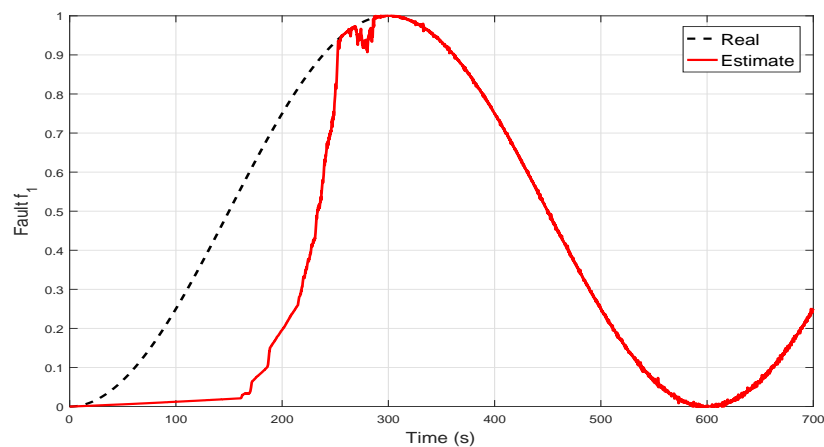


Fig. 3.15 Fault estimation: pitch 1, Case 2.

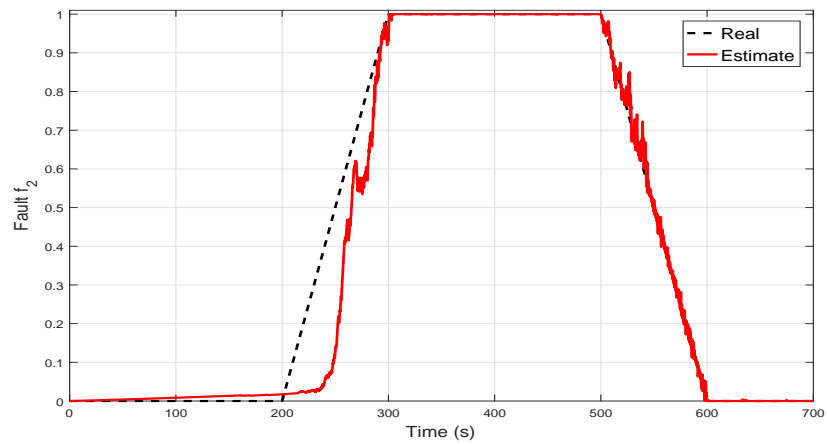


Fig. 3.16 Fault estimation: pitch 2, Case 2.

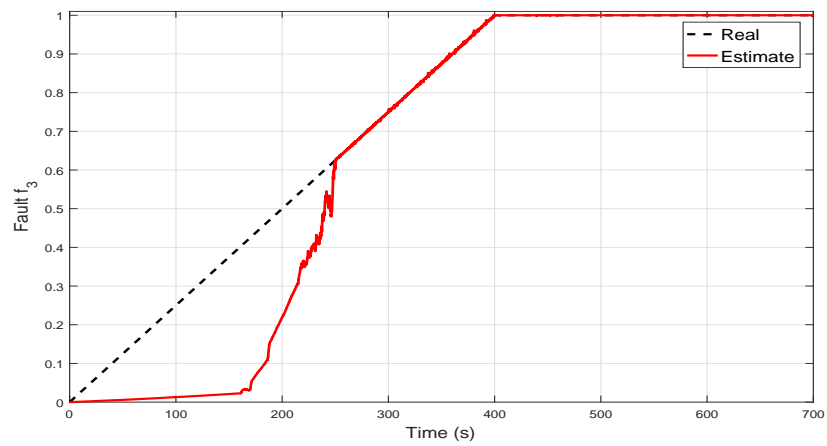


Fig. 3.17 Fault estimation: pitch 3, Case 2.

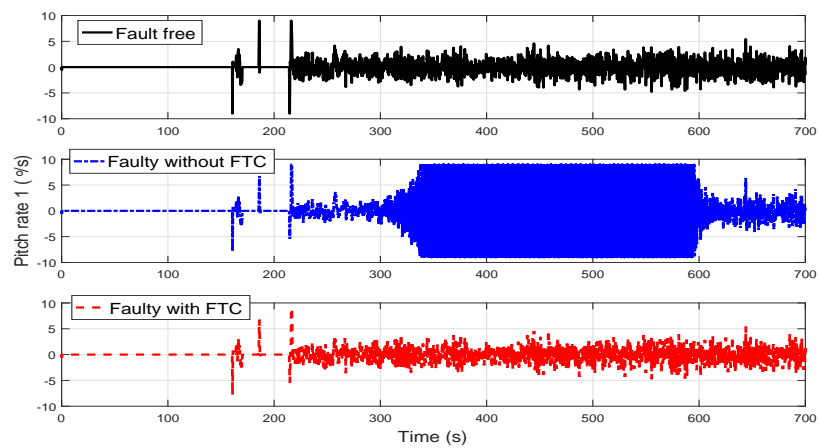


Fig. 3.18 Pitch rate: pitch 1, Case 2.

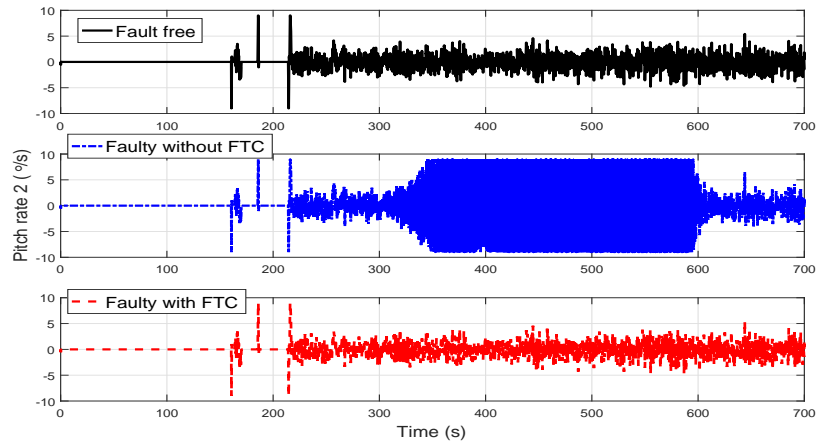


Fig. 3.19 Pitch rate: pitch 2, Case 2.

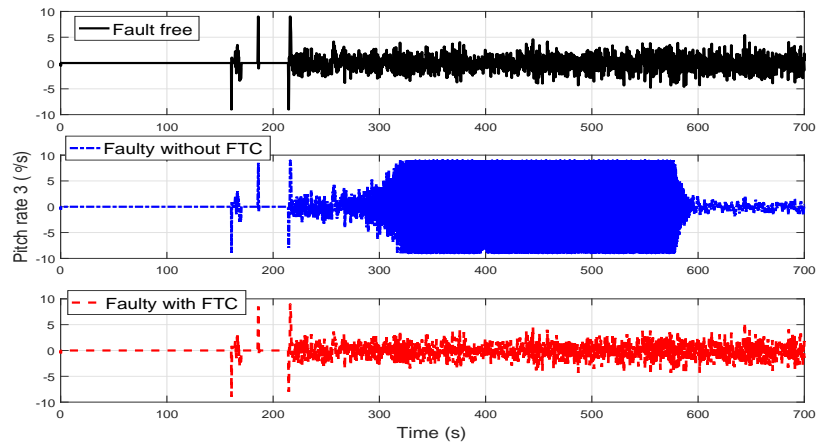


Fig. 3.20 Pitch rate: pitch 3, Case 2.

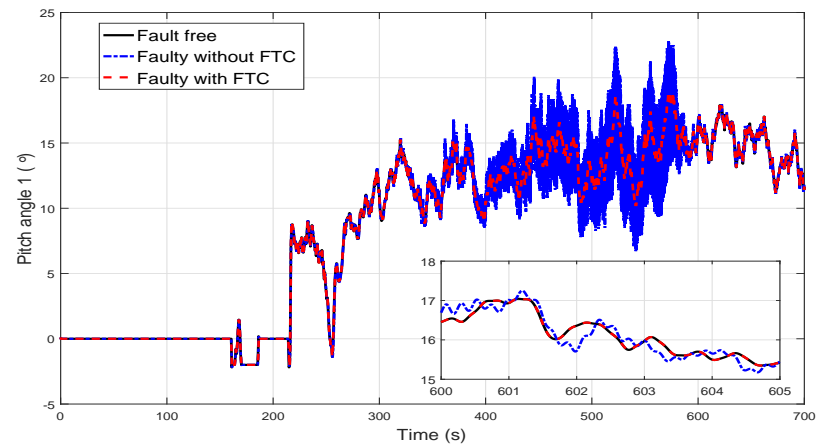


Fig. 3.21 Pitch angle: pitch 1, Case 2.

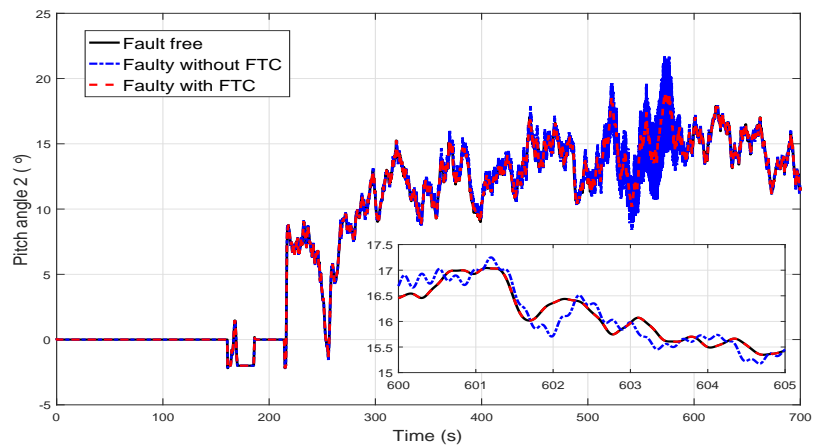


Fig. 3.22 Pitch angle: pitch 2, Case 2.

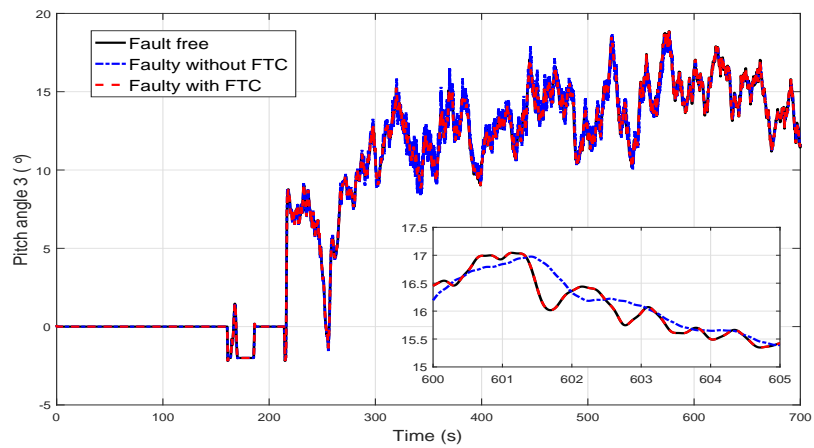


Fig. 3.23 Pitch angle: pitch 3, Case 2.

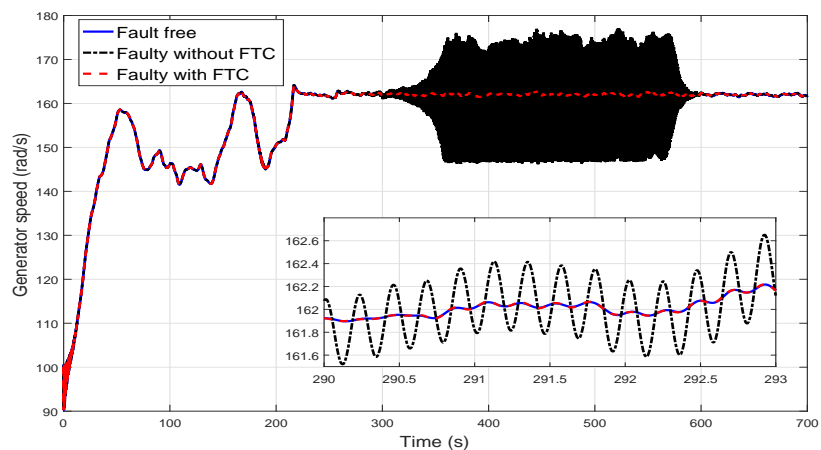


Fig. 3.24 Generator speed: Case 2.

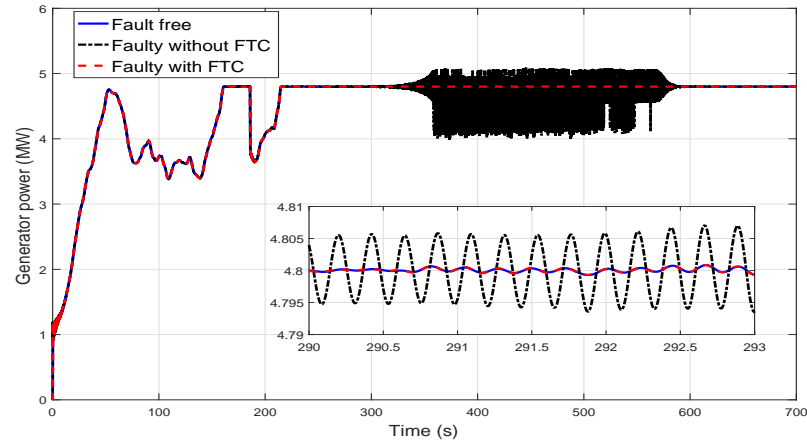


Fig. 3.25 Generator power: Case 2.

(3) Case 3: multiple actuator faults and uncertainties

The proposed FE-based FTC strategy is designed in the absence of pitch actuator system uncertainties. Under such circumstance, the separately designed FE and FTC functions achieve good estimation and control performance in the cases of single and multiple actuator faults, as shown above. This case further investigates the FE/FTC performance in the presence of pitch actuator system uncertainties.

Suppose there exists an uncertainty d associated with each of the actuators of the pitch, then a general model of the dynamics of each pitch system (3.3) can be represented by

$$\begin{aligned}
 \dot{x}_1 &= x_2, \\
 \dot{x}_2 &= G_0(x) + B_0 u + F(x)f + d, \\
 y &= x_1,
 \end{aligned} \tag{3.19}$$

where $d \in \mathbb{R}$ is the unknown sum of moment due to propeller, lift on blade, blade bending, teetering and unbalanced load disturbance (Chichester and Hindmarsh, 1999).

In such a situation, the estimation error system given in (3.6) - (3.8) becomes

$$\begin{aligned}
 \dot{e}_{x_1} &= e_{x_2} - v_1, \\
 \dot{e}_{x_2} &= \tilde{G}_0 + \tilde{F}f + F(\hat{x})e_f + d - v_2, \\
 \dot{e}_f &= \dot{f} - \eta_f \text{sign}(e_f).
 \end{aligned}$$

Following the proof of Theorem 3.1 and Remark 3.1, the equivalent output injection signal of v_2 is

$$v_{eq,2} = F(\hat{x})e_f + d. \quad (3.20)$$

By combining (3.20) and (3.4), the fault estimation \hat{f} is given by

$$\hat{f} = \eta_f \text{sign}(e_f), \quad e_f = \frac{v_{eq,2} - d}{F(\hat{x})}.$$

Clearly, the uncertainty d affects the accuracy of the fault estimation.

In the presence of uncertainty, the FTC pitch control system dynamics (3.19) become

$$\begin{aligned} \dot{x}_1 &= x_2, \\ \dot{x}_2 &= G_0(x) + B_0\beta_r + \delta(e_{x_1}, e_{x_2}, e_f, t) + d, \end{aligned} \quad (3.21)$$

with $\delta(e_{x_1}, e_{x_2}, e_f, t)$ defined in (3.18).

Since $\lim_{t \rightarrow \infty} \delta(e_{x_1}, e_{x_2}, e_f, t) = 0$, in a finite time (3.21) turns into

$$\begin{aligned} \dot{x}_1 &= x_2, \\ \dot{x}_2 &= G_0(x) + B_0\beta_r + d, \end{aligned} \quad (3.22)$$

which still suffer response degradation from the uncertainty d .

Therefore, it can be concluded that the uncertainty d has influence on both the FE and FTC functions, which results in degraded FE/FTC performance, as will be shown in the following simulation results.

Simulations are performed under the same fault scenarios and the same parameters as in Case 2. Suitable uncertainties with physical meaning for the three pitch actuator systems have been taken from Fan and Song (2012) and given as follows: $d_1 = 0.5x_1 \sin(2x_2)$, $d_2 = 0.5x_2x_3 \cos(x_2)$, and $d_3 = x_2x_3 \sin(2x_1x_2)$, respectively. The results in Figs. 3.26 - 3.30 show that in the presence of uncertainties, the proposed FE estimates the faults with degraded accuracy. The FTC cannot recover the pitch actuator dynamics and ensure desired pitching action, which consequently causes fluctuation in generator speed and power output, leading to pitch angle oscillation and pitch rate saturation.

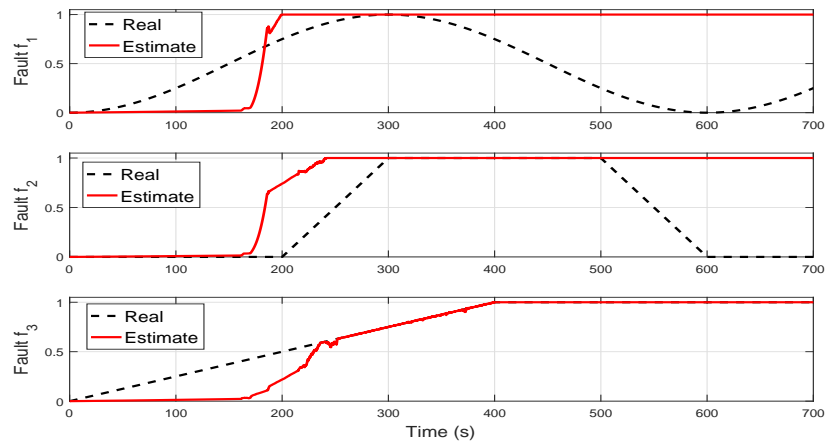


Fig. 3.26 Fault estimation: Case 3.

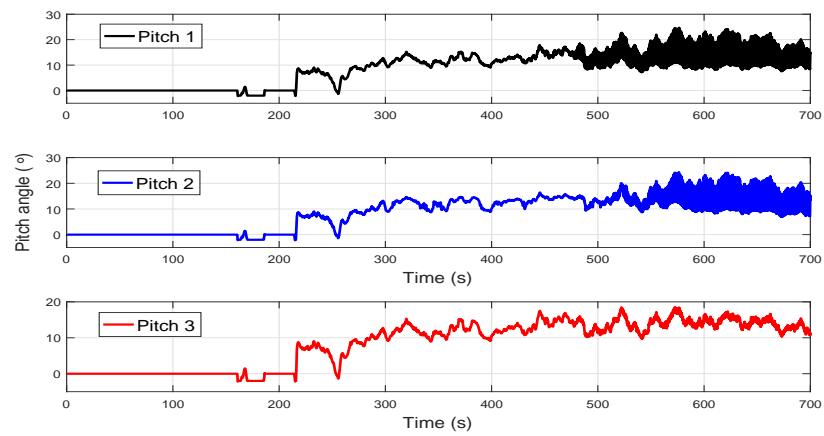


Fig. 3.27 Pitch angle: Case 3.

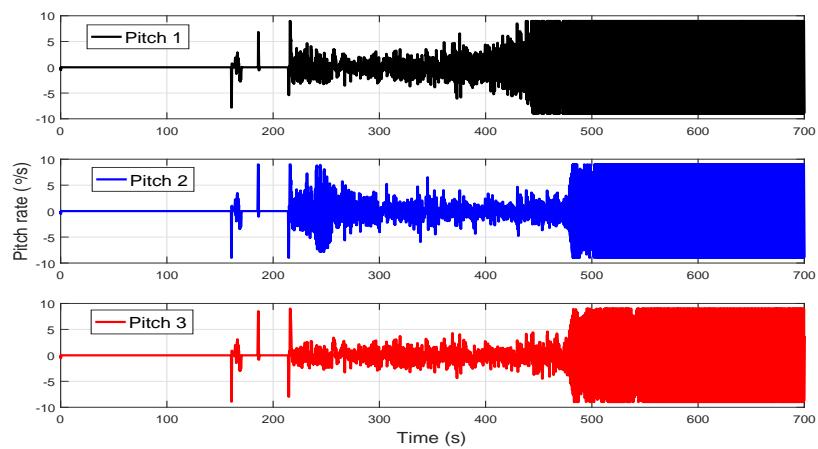


Fig. 3.28 Pitch rate: Case 3.

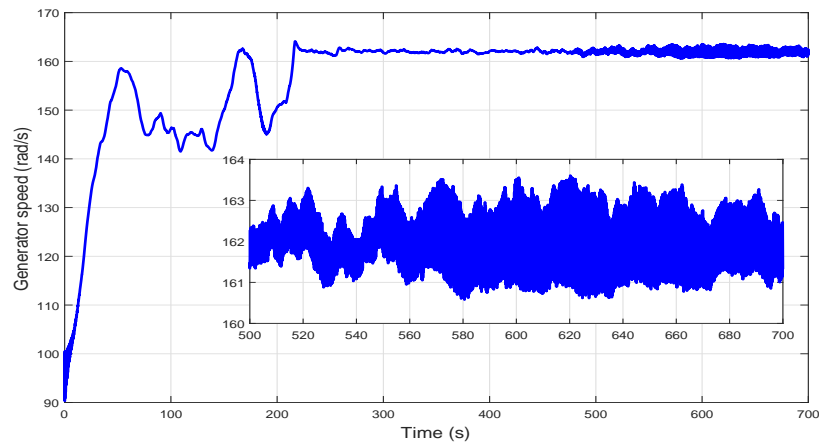


Fig. 3.29 Generator speed: Case 3.

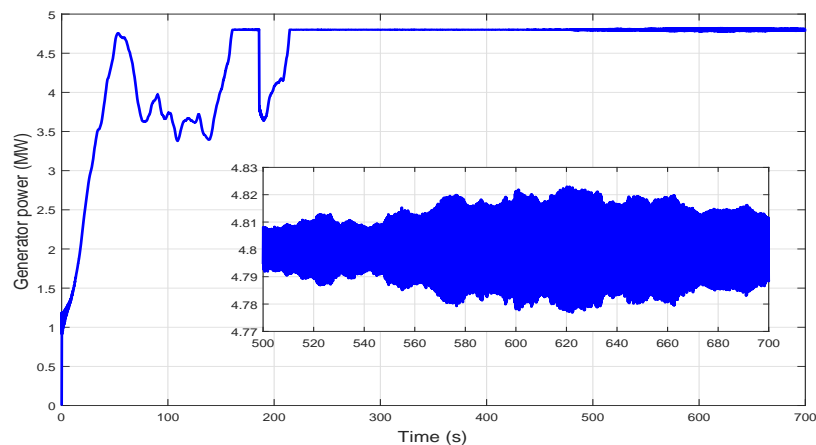


Fig. 3.30 Generator power: Case 3.

Summing the simulations, the proposed FE/FTC can recover the nominal pitch actuator system performance and achieve acceptable wind turbine control performance in the absence of uncertainties. However, the uncertainties d_1 , d_2 , and d_3 affect both the FE and FTC performances. In this situation, the separately designed FE/FTC functions cannot guarantee acceptable system performance, due to the interactions which exist between the uncertainties acting on each of the FE and FTC functions (see Section 3.3 for more discussion). This uncertainty interaction gives rise to a requirement for integrated design of FE/FTC to achieve overall robust FTC system performance, by taking into account the uncertainty effects.

3.3 Mathematical analysis: a theoretical motivation

The fault-tolerant pitch control system described in Section 3.2 shows the power of the FE-based FTC approach. It also provides a way of understanding a significant disadvantage of the separated design paradigm outlined in Fig. 3.31. However, the majority of the existing FE-based FTC systems follow this scheme by assuming satisfaction of the well-known Separation Principle (see Appendix B), e.g., Jiang et al. (2006), Gao and Ding (2007), and de Loza et al. (2015). The challenge of this thesis is that the Separation Principle no longer holds when in addition to modelling uncertainty there is also uncertainty associated with the FE role used in compensating the faults. Errors in the state and fault estimation will cause uncertainty in the FTC function.

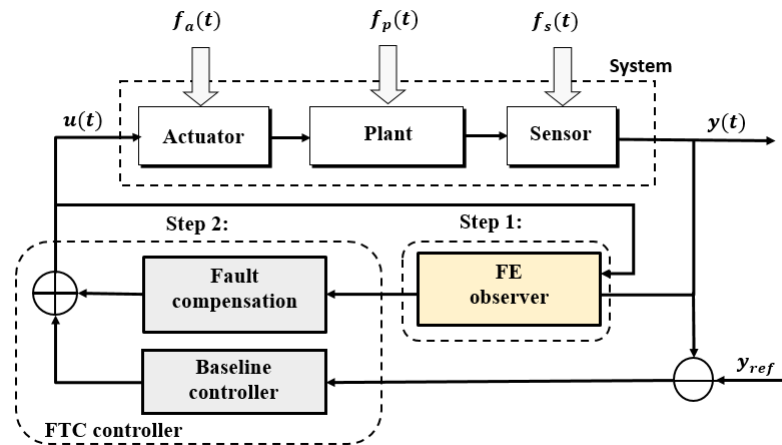


Fig. 3.31 The separated FE/FTC system scheme.

The basic idea of FE-based FTC and design challenges are illustrated below using an adaptive FE observer (Jiang et al., 2006) together with a state-feedback FTC controller (Gao and Ding, 2007).

Consider again the uncertain linear system (2.1) represented by

$$\begin{aligned}\dot{x}(t) &= Ax(t) + Bu(t) + Ff(t) + \Delta(t), \\ y(t) &= Cx(t).\end{aligned}\tag{3.23}$$

In order to design a state observer and controller, the system is assumed to satisfy the following assumptions: 1) The pair (A, B) is controllable and $\text{rank}(B, F) = \text{rank}(B) = m$; 2) The actuator fault $f(t)$ is bounded with bounded first-order time derivative $\dot{f}(t)$.

The state and fault are estimated using an adaptive observer

$$\begin{aligned}\hat{\dot{x}}(t) &= A\hat{x}(t) + Bu(t) + F\hat{f}(t) + L(y(t) - \hat{y}(t)), \\ \hat{\dot{f}}(t) &= M\hat{f}(t) + N(y(t) - \hat{y}(t)), \\ \hat{y}(t) &= C\hat{x}(t),\end{aligned}\tag{3.24}$$

where $\hat{x}(t)$ and $\hat{y}(t)$ are the estimates of $x(t)$ and $y(t)$, respectively. The design matrices L , M , and N are of compatible dimensions and for which more details can be found in Jiang et al. (2006).

Define the estimation errors of the state and fault as $e(t) = x(t) - \hat{x}(t)$ and $e_f(t) = f(t) - \hat{f}(t)$, respectively. It follows from (3.23) and (3.24) that

$$\begin{aligned}\dot{e}(t) &= (A - LC)e(t) + Fe_f(t) + \Delta(t), \\ \dot{e}_f(t) &= Me_f(t) - NCe_x(t) + \dot{f}(t) - Mf(t).\end{aligned}\tag{3.25}$$

It is seen from the above estimation error system that the system uncertainty (including the lumped uncertainty $\Delta(t)$, the fault $f(t)$ and its modelling error $\dot{f}(t)$) affects the state estimation and FE performance.

A general form of an FE-based state-feedback FTC controller is

$$u(t) = -K_x \hat{x}(t) - B^\dagger F \hat{f}(t),\tag{3.26}$$

where K_x is the baseline controller gain and $B^\dagger F$ is the fault compensation gain. B^\dagger is the left pseudo-inverse of B .

Substituting (3.26) into (3.23) gives the closed-loop control system

$$\dot{x}(t) = (A - BK_x)x(t) + BK_x e(t) + Fe_f(t) + \Delta(t).\tag{3.27}$$

The controller gain K_x is determined to ensure that the closed-loop FTC system is robustly stable using the H_∞ optimization approach (Gao and Ding, 2007).

It can be seen from (3.27) that the closed-loop FTC system is affected by both the system uncertainty $\Delta(t)$ and estimation uncertainty (i.e., the estimation errors $e(t)$ and $e_f(t)$).

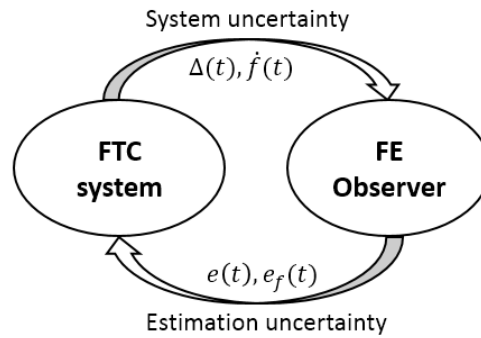


Fig. 3.32 Bi-directional robustness interactions between FE and FTC functions.

It follows from (3.25) and (3.27) that there exist *bi-directional robustness interactions* between the FE observer and FTC system, as summarized in Fig. 3.32. **Since uncertainty and estimation errors inevitably exist in real systems, it is true that all the observer-based FE and FTC systems include the *bi-directional robustness interactions*.** Without taking into account of these mutual interactions, the well designed FE observer and FTC controller may not fit well when assembled together and result in a closed-loop system with degraded performance and robustness.

3.4 Concluding discussion

The separately designed FE/FTC functions can achieve acceptable closed-loop performance in the ideal cases when no system uncertainty exists. However, since uncertainties and estimation errors inevitably exist in real system operations, *bi-directional robustness interactions* inevitably exist in the FE-based FTC systems. It breaks down the well-known Separation Principle (see Appendix B) and gives rise to a necessary and important consideration of integrated FE/FTC design, which thus motivates the research presented in this thesis.

Although few studies consider together the designs of FE and FTC for an overall FTC solution, e.g., Jia et al. (2015b); Rodrigues et al. (2014), the effects of system uncertainty are not taken into account. Therefore, their strategies are not truly integrated FE/FTC designs as defined in this thesis. It is clear that the true integration of FE/FTC, or even more broadly fault diagnosis and FTC, still remain very open problems. In the following chapters, strategies will be developed to achieve the true integration of FE/FTC with applications to a 3-DOF helicopter system and a three-machine power system.

Part I

Integrated FE/FTC design for uncertain linear systems

Chapter 4: Integrated FE/FTC design: H_∞ optimization approach

4.1 Introduction

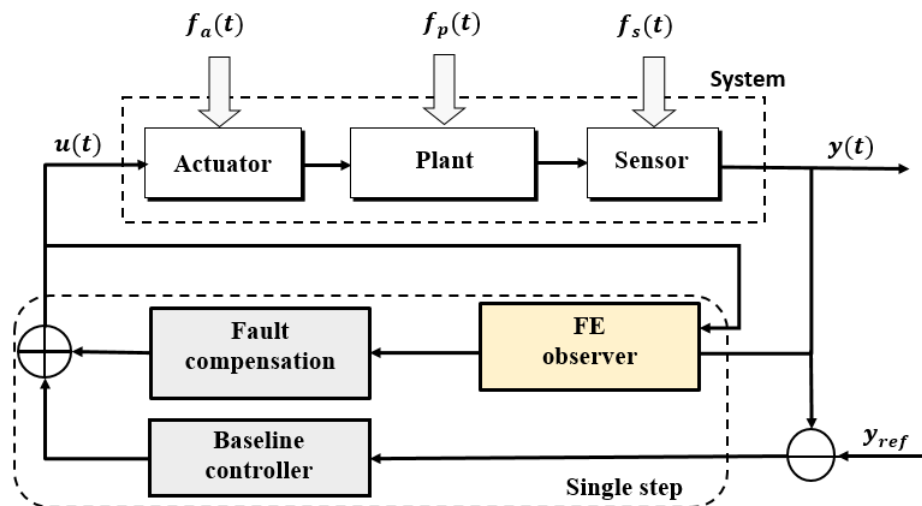


Fig. 4.1 The integrated FE/FTC system scheme.

As discussed in Chapter 3, the FE-based FTC system involves the process of FE used to estimate the fault and FTC to compensate the fault effects. The combination of estimation and control leads to *bi-directional robustness interactions*, which gives rise to a requirement of integrating together the designs of the FE and FTC functions. This chapter aims to develop an integrated FE/FTC design strategy using the scheme in Fig. 4.1, in which the baseline controller is used to maintain nominal system performance and the fault compensation component is automatically activated once a fault is estimated by the FE observer. The elaboration of the strategy is based on the assumption that the system considered is linear with uncertain parameters with potential faults that have

either additive or multiplicative effects on the dynamics. Compared with the existing literature, the main contributions of this chapter are summarized as follows.

- *Reduced-/full-order ASUIOs without rank condition are proposed to achieve FE.* There are many existing FE observers, e.g., adaptive observers (Jiang et al., 2006; Kabore and Wang, 2001), SMO (Edwards and Tan, 2006), ASO (Gao and Ding, 2007), UIO (Odgaard and Stoustrup, 2012), moving horizon estimation (Feng and Patton, 2014), and combined SMO and ASO (Shi et al., 2015). However, in the adaptive observer the faults are estimated with finite errors. Moreover, in order to estimate time-varying faults the observer has a Proportional-Integral (PI) structure with carefully chosen learning rate. The canonical form SMO (Edwards and Tan, 2006) requires several state transformations as well as *a priori* knowledge of the upper bounds of the faults and it is difficult to reconstruct sensor and actuator faults simultaneously. The ASO reconstructs the faults in a polynomial form with *a priori* knowledge of their orders. The moving horizon estimation is a complex on-line optimization problem. The existing UIOs are obtained after satisfying a well-known rank condition (Chen and Patton, 1999). By combining ASO and UIO, a full-order augmented state UIO (ASUIO) without requiring the rank condition is proposed in Tan et al. (2015), but the effect of system uncertainty is not taken into account and FTC is out of its scope.

In this chapter, reduced-/full-order ASUIOs without rank condition are proposed to achieve 1) time-varying fault estimation for the state feedback case and 2) simultaneous estimation of time varying faults and system state for the output feedback case, respectively. The proposed ASUIOs do not require state transformation and fault information (upper bounds and fault characteristics), or on-line computation. Another new property of the reduced-order ASUIO for FE is that the estimation of system state variables is not necessary, leading to the design of an observer with reduced dimension.

- *Both the cases of state/output feedback sliding mode FTC are studied.* Considering its potential robustness to uncertainty and disturbance, sliding mode control (SMC) has recently been used extensively for FTC designs (e.g., Alwi and Edwards (2008); Huang and Patton (2015); Xiao et al. (2012); Zhao et al. (2014)). However, few works consider unmatched norm-bounded system uncertainty and FE design. Here, sliding mode FTC strategies for both state and output feedback cases are developed for systems subject to unmatched norm-bounded uncertainty.

- *An integrated FE/FTC design strategy is proposed.* For systems with additive or multiplicative faults, it is shown that the integrated design can be converted into an

observer-based robust control problem solved via H_∞ optimization with a single-step LMI formulation.

The remainder of this chapter is organized as follows. Section 4.2 gives the problem formulation. Sections 4.3 and 4.4 develop integrated FE/FTC strategies for the additive faults case using state or output feedback, respectively. Section 4.5 describes an integrated design for systems with multiplicative faults. Section 4.6 provides an illustrative example and Section 4.7 summarizes this chapter.

4.2 Problem formulation

Consider a class of linear systems represented by

$$\begin{aligned}\dot{x}(t) &= (A + \Delta A(t))x(t) + Bu(t) + F_a f_a(t) + Dd(t), \\ y(t) &= Cx(t) + F_s f_s(t),\end{aligned}\tag{4.1}$$

where $x \in \mathbb{R}^n$, $u \in \mathbb{R}^m$, and $y \in \mathbb{R}^p$ stand for the state, control input, and system output vectors, respectively. $f_a \in \mathbb{R}^q$ and $f_s \in \mathbb{R}^{q_1}$ denote the actuator and sensor faults, respectively, which might be viewed as actuator or sensor offsets in physical systems (Isermann, 2011). $d \in \mathbb{R}^l$ denotes the external disturbance. $\Delta A(t)$ represents the unknown unmatched system matrix uncertainty. The matrices A , B , F_a , D , C , and F_s are known constant matrices of compatible dimensions. Without loss of generality, it is assumed in this chapter that F_a and F_s are of full-column rank and $q \leq m$ and $q_1 \leq p$.

Assumption 4.1 The pair (A, C) is observable, the pair (A, B) is controllable, and the actuator fault f_a is matched, i.e., $\text{rank}(B, F_a) = \text{rank}(B) = m$.

Assumption 4.2 The trios (A, C, F_a) and (A, C, F_s) are observable, i.e., the following rank conditions are satisfied: $\text{rank} \begin{bmatrix} A & F_a \\ C & 0 \end{bmatrix} = n + q$, $\text{rank} \begin{bmatrix} A & 0 \\ C & F_s \end{bmatrix} = n + q_1$.

Assumption 4.3 The uncertainty matrix $\Delta A(t)$ is norm-bounded (energy bounded) and has the form: $\Delta A(t) = M_0 F_0(t) \text{tr} N_0$, where M_0 and N_0 are known matrices with appropriate dimensions, and $F_0(t) \in \mathbb{R}^{r_1 \times r_2}$ is an unknown matrix satisfying $F_0^\top(t) F_0(t) \leq I_{r_2}$.

Assumption 4.4 The faults and disturbance satisfy $\|f_a\| \leq \bar{f}_a$, $\|f_s\| \leq \bar{f}_s$, and $\|d\| \leq d_0$ with unknown positive scalars \bar{f}_a , \bar{f}_s , and d_0 , respectively. Moreover, f_a and f_s have norm-bounded first-order time derivatives.

Remark 4.1 Assumption 4.1 provides some standard requirements of controlled systems, while $\text{rank}(B, F_a) = \text{rank}(B)$ ensures that f_a lies in the range space spanned by the control u so that the fault effect can be compensated through control actions, as defined in Section 1.2.1. Assumption 4.2 is required to ensure the actuator fault f_a and sensor fault f_s to be observable and can be estimated using the augmented state observer methods proposed in the chapter. Assumption 4.3 gives a general representation of a system unmatched uncertainty matrix used in H_∞ optimization. Assumption 4.4 implies that the faults and disturbance considered are norm-bounded with unknown upper bounds, this is useful for practical application.

The following problem is to be addressed in this chapter.

Problem 4.1 Given the system (4.1) with uncertainty, disturbance, and faults, design together the following FE and FTC functions to guarantee system stability after the fault occurrence: 1) *FE observer*: estimate the faults for the state feedback case, and simultaneously the faults and system state for the output feedback case; 2) *Sliding mode FTC controller*: state/output feedback controller for compensating the fault effect and ensuring closed-loop system stability.

Note that Problem 4.1 is an observer-based robust control problem and the solution for it requires a bilinear matrix inequality (BMI) that cannot be solved directly using the LMI toolbox. To obviate this BMI problem, a two-step method is proposed in Shi and Patton (2015b) for FE/FTC design for linear parameter varying descriptor systems with actuator/sensor faults and disturbance. However, this two-step approach can only obtain a suboptimal solution of the overall system design, and the feasible controller gains obtained in the first step cannot guarantee the solvability of the observer designed in the second step.

A robust observer-based control design was proposed in Lien (2004) for uncertain linear systems with equality constraint solved by a single-step LMI formulation. More recently, a new observer-based control design approach was proposed in Kheloufi et al. (2013) without equality constraint with the help of the Young Inequality (Boyd et al., 1994). However, as commented in Wang and Jiang (2014), this new approach has no superiority over the one in Lien (2004), which is thus used in this chapter.

4.3 Integrated FE/FTC design: state feedback

Provided that all the system state variables are available, then only the fault estimation is needed for the FTC design. In this case, a reduced-order ASUIO is proposed below to estimate the faults.

4.3.1 Reduced-order ASUIO-based FE design

By treating the faults as new system state variables, the system (4.1) can be augmented into

$$\begin{aligned}\dot{\bar{x}} &= \bar{A}\bar{x} + \bar{B}u + \Delta\bar{A}\bar{x} + \bar{D}\bar{d}, \\ y &= \bar{C}\bar{x},\end{aligned}\tag{4.2}$$

where

$$\begin{aligned}\bar{x} &= \begin{bmatrix} x \\ f_a \\ f_s \end{bmatrix}, \bar{d} = \begin{bmatrix} d \\ \dot{f}_a \\ \dot{f}_s \end{bmatrix}, \bar{A} = \begin{bmatrix} A & F_a & 0 \\ 0 & 0 & 0 \\ 0 & 0 & 0 \end{bmatrix}, \Delta\bar{A} = \begin{bmatrix} \Delta A & 0 & 0 \\ 0 & 0 & 0 \\ 0 & 0 & 0 \end{bmatrix}, \\ \bar{B} &= \begin{bmatrix} B \\ 0 \\ 0 \end{bmatrix}, \bar{D} = \begin{bmatrix} D & 0 & 0 \\ 0 & I_q & 0 \\ 0 & 0 & I_{q_1} \end{bmatrix}, \bar{C} = [C \ 0 \ F_s].\end{aligned}$$

According to Assumption 4.2, it can be verified that the augmented system (4.2) is observable. The reduced-order UIO in Xiong and Saif (2003) is modified here to estimate the faults f_a and f_s , i.e., $z = L\bar{x}$, with $L = [0 \ I_{q+q_1}] \in \mathbb{R}^{(q+q_1) \times (n+q+q_1)}$, in the form of

$$\begin{aligned}\dot{\hat{\xi}}_s &= M\hat{\xi}_s + Gu + Ry, \\ \hat{z} &= \hat{\xi}_s + Hy,\end{aligned}\tag{4.3}$$

where $\hat{\xi}_s \in \mathbb{R}^{q+q_1}$ and $\hat{z} \in \mathbb{R}^{q+q_1}$ denote the observer state and the estimate of z , respectively. The design matrices M , G , R , and H are of appropriate dimensions.

Define $\varepsilon = \xi_s - T\bar{x}$, then the estimation error system is

$$\begin{aligned}\dot{\varepsilon} &= M\varepsilon + (MT + R\bar{C} - T\bar{A})\bar{x} + (G - T\bar{B})u - T\Delta\bar{A}\bar{x} - T\bar{D}\bar{d}, \\ e_s &= \varepsilon + (T + H\bar{C} - L)\bar{x}.\end{aligned}\quad (4.4)$$

The existence condition of an asymptotically stable observer (4.3) is given in Theorem 4.1.

Theorem 4.1 There exists an asymptotically stable observer (4.3) for the system (4.2) when $\Delta\bar{A}\bar{x} = 0$ and $\bar{d} = 0$, if it holds that

$$M \text{ is Hurwitz,} \quad (4.5)$$

$$MT + R\bar{C} - T\bar{A} = 0, \quad (4.6)$$

$$T + H\bar{C} - L = 0, \quad (4.7)$$

$$G - T\bar{B} = 0. \quad (4.8)$$

Proof: With (4.6) - (4.8) and $\Delta\bar{A}\bar{x} = 0$ and $\bar{d} = 0$, the error system (4.4) becomes

$$\dot{\varepsilon} = M\varepsilon,$$

$$e_s = \varepsilon.$$

Since M is Hurwitz, then $\lim_{t \rightarrow \infty} e_s(t) = 0$. □

In the following, a parametrization method is used to solve the matrix equations (4.5) - (4.8). Before that, the solvability of these matrix equations are proved in Lemmas 4.1 and 4.2.

Define a full-row rank matrix: $S = [L^\dagger (I_{n+q+q_1} - L^\dagger L)] = [S_1 \ S_2]$, with the property that $S_2 S_1 = 0$ and $\text{rank}(S) = \text{rank}(S_1) + \text{rank}(S_2) = n + q + q_1$.

Lemma 4.1 The matrix equation

$$\Lambda\Omega = \Psi, \quad (4.9)$$

with $\Omega = \begin{bmatrix} \bar{C}S_2 \\ \bar{C}\bar{A}S_2 \end{bmatrix}$, $\Psi = L\bar{A}S_2$, and the determined matrix Λ , is solvable if it holds that

$$\text{rank} \begin{bmatrix} L\bar{A} \\ \bar{C} \\ \bar{C}\bar{A} \\ L \end{bmatrix} = \text{rank} \begin{bmatrix} \bar{C} \\ \bar{C}\bar{A} \\ L \end{bmatrix}. \quad (4.10)$$

Proof: Post-multiplying both sides of (4.10) with the matrix $[S_2 \ S_1]$ gives

$$\text{rank} \begin{bmatrix} L\bar{A}S_2 & L\bar{A}S_1 \\ \bar{C}S_2 & \bar{C}S_1 \\ \bar{C}\bar{A}S_2 & \bar{C}\bar{A}S_1 \\ LS_2 & LS_1 \end{bmatrix} = \text{rank} \begin{bmatrix} \bar{C}S_2 & \bar{C}S_1 \\ \bar{C}\bar{A}S_2 & \bar{C}\bar{A}S_1 \\ LS_2 & LS_1 \end{bmatrix}. \quad (4.11)$$

According to the definitions of S_1 and S_2 given previously, $LS_2 = 0$ and $LS_1 = I_{n+q+q_1}$. Hence, (4.11) becomes

$$\text{rank} \begin{bmatrix} L\bar{A}S_2 & L\bar{A}S_1 \\ \bar{C}S_2 & \bar{C}S_1 \\ \bar{C}\bar{A}S_2 & \bar{C}\bar{A}S_1 \\ 0 & I_{n+q+q_1} \end{bmatrix} = \text{rank} \begin{bmatrix} \bar{C}S_2 & \bar{C}S_1 \\ \bar{C}\bar{A}S_2 & \bar{C}\bar{A}S_1 \\ 0 & I_{n+q+q_1} \end{bmatrix}. \quad (4.12)$$

This leads to

$$\text{rank} \begin{bmatrix} L\bar{A}S_2 \\ \bar{C}S_2 \\ \bar{C}\bar{A}S_2 \end{bmatrix} = \text{rank} \begin{bmatrix} \bar{C}S_2 \\ \bar{C}\bar{A}S_2 \end{bmatrix}. \quad (4.13)$$

Therefore, it holds that

$$\text{rank} \begin{bmatrix} \Psi \\ \Omega \end{bmatrix} = \text{rank}(\Omega).$$

Thus, the matrix equation (4.9) is solvable. \square

Lemma 4.2 The pair (M_2, M_1) , where $M_1 = L\bar{A}S_1 - \Psi\Omega^\dagger\Gamma$, $M_2 = (I_{2p} - \Omega\Omega^\dagger)\Gamma$, and $\Gamma = \begin{bmatrix} \bar{C}S_1 \\ \bar{C}\bar{A}S_1 \end{bmatrix}$, is detectable if it holds that

$$\text{rank} \begin{bmatrix} sL - L\bar{A} \\ \bar{C} \\ \bar{C}\bar{A} \end{bmatrix} = \text{rank} \begin{bmatrix} \bar{C} \\ \bar{C}\bar{A} \\ L \end{bmatrix}, \quad \forall s \in \mathbb{C}, \text{Re}(s) \geq 0. \quad (4.14)$$

Proof: Post-multiplying the left hand side of (4.14) by the full row-rank matrix $[S_1 \ S_2]$ gives

$$\begin{aligned} & \text{rank} \left(\begin{bmatrix} sL - L\bar{A} \\ \bar{C} \\ \bar{C}\bar{A} \end{bmatrix} [S_1 \ S_2] \right) \\ &= \text{rank} \begin{bmatrix} sI_{q+q_1} - L\bar{A}S_1 & -\Psi \\ \Gamma & \Omega \end{bmatrix} \\ &= \text{rank} \left(\begin{bmatrix} I_{q+q_1} & \Psi\Omega^\dagger \\ 0 & (I_{2p} - \Omega\Omega^\dagger) \\ 0 & \Omega\Omega^\dagger \end{bmatrix} \begin{bmatrix} sI_{q+q_1} - L\bar{A}S_1 & -\Psi \\ \Gamma & \Omega \end{bmatrix} \right) \\ &= \text{rank} \begin{bmatrix} sI_{q+q_1} - M_1 & 0 \\ M_2 & 0 \\ \Omega\Omega^\dagger\Gamma & \Omega \end{bmatrix} \\ &= \text{rank} \begin{bmatrix} sI_{q+q_1} - M_1 \\ M_2 \end{bmatrix} + \text{rank}(\Omega). \end{aligned} \quad (4.15)$$

Similarly, the right hand side of (4.14) is

$$\begin{aligned} \text{rank} \left(\begin{bmatrix} \bar{C} \\ \bar{C}\bar{A} \\ L \end{bmatrix} [S_1 \ S_2] \right) &= \text{rank} \begin{bmatrix} \bar{C}S_1 & \bar{C}S_2 \\ \bar{C}\bar{A}S_1 & \bar{C}\bar{A}S_2 \\ I_{q+q_1} & 0 \end{bmatrix} \\ &= q + q_1 + \text{rank}(\Omega). \end{aligned} \quad (4.16)$$

By (4.15) and (4.16), it holds that $\text{rank} \begin{bmatrix} sI_{q+q_1} - M_1 \\ M_2 \end{bmatrix} = q + q_1$. Thus, the pair (M_2, M_1) is detectable. \square

It follows from (4.7) that $T = L - HC\bar{C}$. Substituting this into (4.6) yields

$$M(L - HC\bar{C}) + R\bar{C} - (L - HC\bar{C})\bar{A} = 0.$$

Now denote $T_1 = R - MH$, it follows that

$$L\bar{A} - ML = [T_1 \ H] \begin{bmatrix} \bar{C} \\ \bar{C}\bar{A} \end{bmatrix}. \quad (4.17)$$

Post-multiplying both sides of (4.17) by S yields

$$M = L\bar{A}S_1 - [T_1 \ H] \begin{bmatrix} \bar{C}S_1 \\ \bar{C}\bar{A}S_1 \end{bmatrix}, \quad (4.18)$$

$$L\bar{A}S_2 = [T_1 \ H] \begin{bmatrix} \bar{C}S_2 \\ \bar{C}\bar{A}S_2 \end{bmatrix}. \quad (4.19)$$

Rearranging (4.19) as $[T_1 \ H]\Omega = \Psi$, which is solvable according to Lemma 4.1, with a general solution

$$[T_1 \ H] = \Psi\Omega^\dagger + Z(I_{2p} - \Omega\Omega^\dagger), \quad (4.20)$$

where $Z \in \mathbb{R}^{(q+q_1) \times 2p}$ is an arbitrary matrix.

It follows from (4.18) and (4.20) that

$$M = M_1 - ZM_2, \quad H = H_1 + ZH_2, \quad (4.21)$$

where $H_1 = \Psi\Omega^\dagger\Gamma_1$, $H_2 = (I_{2p} - \Omega\Omega^\dagger)\Gamma_1$, and $\Gamma_1 = [0 \ I_p]^\top$.

The matrices M_1 and M_2 in (4.21) are known from Lemma 4.2. By designing Z to make M Hurwitz, H can be obtained. Further using $T_1 = R - MH$ gives R and using Theorem 4.1 gives G .

However, since there exist uncertainty and disturbance in the system (4.1), i.e., $\Delta\bar{A}\bar{x} \neq 0$ and $\bar{d} \neq 0$, the error system (4.4) should be made robustly stable. Denote $\bar{H}_1 = H_1\bar{C} - L$ and substitute $M = M_1 - ZM_2$ and $T = L - HC\bar{C}$ into (4.9), it follows that

$$\dot{e}_s = (M_1 - ZM_2)e_s + (\bar{H}_1 + ZH_2\bar{C})(\Delta\bar{A}\bar{x} + \bar{D}\bar{d}). \quad (4.22)$$

Thus, by designing the arbitrary matrix Z such that (4.22) is robustly stable, the observer (4.3) for the system (4.1) with uncertainty and disturbance can be obtained.

Remark 4.2 The proposed reduced-order ASUIO (with an order of $(q + q_1)$) is interesting in three respects: 1) The traditional UIOs (Chen and Patton, 1999; Odgaard and Stoustrup, 2012; Xiong and Saif, 2003) decouple the disturbance under the satisfaction of a rank condition, i.e., $\text{rank}(\bar{C}\bar{D}) = \text{rank}(\bar{D})$, which is restrictive and often cannot be satisfied. H_∞ optimization is employed here to attenuate the disturbance and the arbitrary matrix Z is obtained using LMI tools; 2) In contrast to the majority of existing FE approaches (with an order of $(n + q + q_1)$), the fault estimation is achieved without extra effort to estimate the system state variables which are available for FTC design; 3) Note that (4.10) and (4.14) are two sufficient conditions for the existence of a solution to Theorem 4.1 as well as the proposed reduced-order ASUIO. However, since $L\bar{A} = 0$, so if $\text{Re}(s) > 0$, then these two conditions are always satisfied.

4.3.2 State feedback sliding mode FTC design

This section describes the design of an FTC controller with the function of compensating the fault effect and also stabilizing the system state of (4.1), using the concept of SMC. Recall that the general aim of SMC is to achieve robust insensitivity to matched uncertainty acting within the control channels, using a combination of linear and switched feedback. The SMC must be designed to reach a sliding surface and the switching operation designed to keep the system motion in the sliding manifold.

Since it is assumed that all the state variables are available, a switching function for (4.1) using the system state is defined as

$$s_1 = N_1 x - \int_0^t v_1(\tau) d\tau, \quad (4.23)$$

where $s_1 \in \mathbb{R}^m$ and $N_1 = B^\dagger - Y_1(I_n - BB^\dagger)$, with $B^\dagger = (B^\top B)^{-1}B^\top$ and a design matrix $Y_1 \in \mathbb{R}^{m \times n}$. v_1 is a time-varying function to be designed. Differentiating s with respect to time gives

$$\dot{s}_1 = N_1(A + \Delta A)x + u + N_1 F_a f_a + N_1 D d - v_1. \quad (4.24)$$

Design the control input as

$$u = u_{l_1} + u_{n_1}, \quad (4.25)$$

where the linear feedback component is $u_{l_1} = v_1 - E_1 \hat{f}_a$ and $v_1 = -K_s x$, with a design matrix $K_s \in \mathbb{R}^{m \times n}$ and $E_1 = B^\dagger F_a$. The nonlinear component $u_{n_1} = -\rho_{s_1}(t) \text{sign}(s_1)$, with a design parameter $\rho_{s_1}(t)$.

Consider a Lyapunov function for (4.24) given by

$$V_{s_{10}} = \frac{1}{2} s_1^\top s_1.$$

It follows from (4.24) and (4.25) that the time derivative of $V_{s_{10}}$ is

$$\begin{aligned} \dot{V}_{s_{10}} &= s_1^\top [N_1(A + \Delta A)x + u + N_1 F_a f_a + N_1 D d] \\ &= s_1^\top [(N_1 A + N_1 \Delta A)x + E_1 e_{f_a} + N_1 D d] \\ &\leq (\eta_{s_1} - \rho_{s_1}(t)) \|s_1\|, \end{aligned} \quad (4.26)$$

where η_{s_1} is an unknown scalar satisfying $\eta_{s_1} \geq (\|N_1 A\| + \|N_1 M_0\| \|N_0\|) \|x\| + \|E_1\| \|e_{f_a}\| + \|N_1 D\| \|d_0\|$.

Design $\rho_{s_1}(t) = \hat{\eta}_{s_1} + \varepsilon_{s_1}$, where ε_{s_1} is a positive design scalar and the scalar $\hat{\eta}_{s_1}$ is introduced to estimate the unknown scalar η_{s_1} using an update law

$$\dot{\hat{\eta}}_{s_1} = \sigma_1 \|s_1\|, \quad \hat{\eta}_{s_1}(0) = 0, \quad (4.27)$$

with a positive learning rate σ_1 to be designed.

Define the estimation error of η_{s_1} as $\tilde{\eta}_{s_1} = \eta_{s_1} - \hat{\eta}_{s_1}$. Consider a Lyapunov function

$$V_{s_1} = V_{s_{10}} + \frac{1}{2\sigma_1} \tilde{\eta}_{s_1}^2.$$

It follows from (4.26) and (4.25) that

$$\begin{aligned}
\dot{V}_{s_1} &= \dot{V}_{s_{10}} - \frac{1}{\sigma_1} \tilde{\eta}_{s_1} \dot{\hat{\eta}}_{s_1} \\
&\leq [\omega_{s_1} + \eta_{s_1} - \rho_{s_1}(t)] \|s_1\| - \tilde{\eta}_{s_1} \|s_1\| \\
&\leq -\varepsilon_{s_1} \|s_1\| \\
&\leq 0.
\end{aligned} \tag{4.28}$$

Since V_{s_1} is positive definite, it follows from (4.28) and the Barbalat's lemma (Slotine et al., 1991) that $V_{s_1}(t) \leq V_{s_1}(0)$. Therefore, $s_1(t)$ and $\tilde{\eta}_{s_1}(t)$ are bounded. This means that the designed controller (4.25) can maintain the sliding motion around $s_1 = 0$. Moreover, in the case of zero initial condition (i.e. $V_{s_1}(0) = 0$), it holds that $\lim_{t \rightarrow \infty} s_1(t) = 0$. In such case, the sliding surface $s_1 = 0$ is reachable and the idealized sliding motion is maintained.

Consider next the system stability analysis corresponding to the sliding mode. By setting $\dot{s}_1 = 0$, it follows from (4.24) that the equivalent control input (Edwards and Spurgeon, 1998) is

$$u_{eq_1} = -[N_1(A + \Delta A)x + N_1 Dd] + u_{l_1}. \tag{4.29}$$

Substituting (4.29) into (4.1) gives the equivalent closed-loop system

$$\dot{x} = (\Theta_1 A - BK_s)x + \Theta_1 \Delta A x + F_1 e_s + \Theta_1 Dd, \tag{4.30}$$

where $\Theta_1 = I_n - BN_1$ and $F_1 = [F_a \ 0]$.

Therefore, the system (4.1) is maintained on the sliding mode with the equivalent control (4.29) by designing K_x such that (4.30) is stable. The closed-loop system (4.30) contains the uncertainty $\Delta A x$ and disturbance d , which must be minimized to achieve a suitable degree of robustness. This is achieved using H_∞ optimization given in the next section.

4.3.3 Integrated synthesis

The proposed state feedback integrated FE/FTC design is summarized in Fig. 4.2.

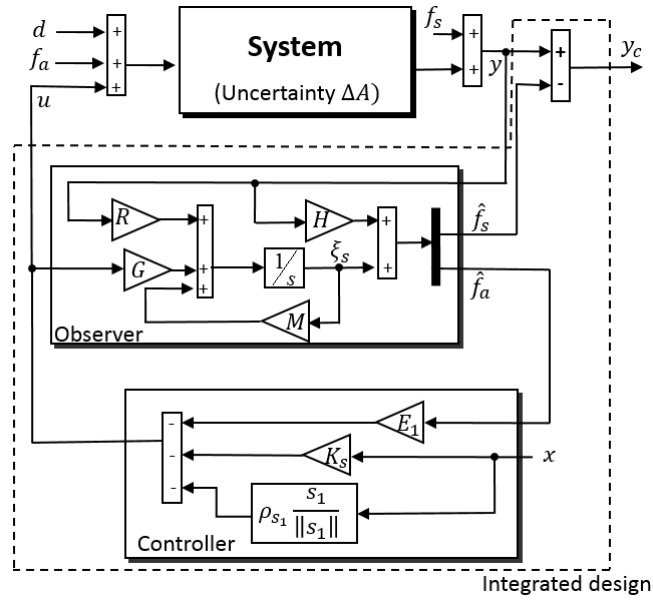


Fig. 4.2 Integrated FE/FTC design: state feedback case.

The augmented closed-loop system consisting of (4.22) and (4.30) is

$$\begin{aligned}
 \dot{x} &= (\Theta_1 A - BK_s)x + \Theta_1 \Delta A x + F_1 e_s + D_1 \bar{d}, \\
 \dot{e}_s &= (M_1 - ZM_2)e_s + (\bar{H}_1 + ZH_2\bar{C})(\Delta\bar{A}\bar{x} + \bar{D}\bar{d}), \\
 y_c &= y - F_s \hat{f}_s, \\
 z_s &= C_{sx}x + C_{se}e_s,
 \end{aligned} \tag{4.31}$$

where $z_s \in \mathbb{R}^r$ is the measured output and $D_1 = [\Theta_1 D \ 0]$.

Theorem 4.2 Under Assumptions 4.1 - 4.4, given a positive scalar γ_s , the augmented closed-loop system (4.31) is stable with H_∞ performance $\|G_{z_s \bar{d}}\|_\infty < \gamma_s$, if there exist symmetric positive definite matrices P and Q , and matrices \hat{P} , R_1 , and R_2 such that

$$PB = B\hat{P}, \tag{4.32}$$

$$\begin{bmatrix}
 \chi_{11} & \chi_{12} & \chi_{13} & \chi_{14} & 0 & C_{sx}^\top \\
 * & \chi_{22} & \chi_{23} & 0 & \chi_{25} & C_{se}^\top \\
 * & * & -\gamma_s^2 I & 0 & 0 & 0 \\
 * & * & * & -I & 0 & 0 \\
 * & * & * & * & -I & 0 \\
 * & * & * & * & * & -I
 \end{bmatrix} < 0, \tag{4.33}$$

where $\chi_{11} = \text{He}(P\Theta_1 A - BR_1) + 2N_0^\top N_0$, $\chi_{12} = PF_1$, $\chi_{13} = PD_1$, $\chi_{14} = P\Theta_1 M_0$, $\chi_{22} = \text{He}(QM_1 - R_2 M_2)$, and $\chi_{23} = (Q\bar{H}_1 + R_2 H_2 \bar{C})\bar{D}$, $\chi_{25} = (Q\bar{H}_1 + R_2 H_2 \bar{C})\bar{M}_0$. Then the gains are given by $K_s = \hat{P}^{-1}R_1$ and $Z = Q^{-1}R_2$.

Proof: Consider a Lyapunov function $V_{e_s} = e_s^\top Q e_s$ with a symmetric positive definite matrix $Q \in \mathbb{R}^{(q+q_1) \times (q+q_1)}$. Define $W_1 = \bar{H}_1 + ZH_2\bar{C}$ and $\chi_{s_1} = \text{He}(e_s^\top QW\Delta\bar{A}\bar{x})$ and $\bar{M}_0 = [M_0^\top 0]^\top$, so that

$$\begin{aligned} \chi_{s_1} &= - \left[\bar{M}_0^\top W_1^\top Q e_s - F_0 N_0 x \right]^\top \left[\bar{M}_0^\top W_1^\top Q e_s - F_0 N_0 x \right] \\ &\quad + e_s^\top Q W_1 \bar{M}_0 \bar{M}_0^\top W_1^\top Q e_s + x^\top N_0^\top F_0^\top F_0 N_0 x \\ &\leq e_s^\top Q W_1 \bar{M}_0 \bar{M}_0^\top W_1^\top Q e_s + x^\top N_0^\top N_0 x. \end{aligned}$$

Then it follows that

$$\begin{aligned} \dot{V}_{e_s} &= e_s^\top \text{He}(Q(M_1 - ZM_2))e_s + \text{He}(e_s^\top QW_1\Delta\bar{A}\bar{x}) + \text{He}(e_s^\top QW_1\bar{D}\bar{d}) \\ &\leq e_s^\top \left[\text{He}(Q(M_1 - ZM_2)) + QW_1\bar{M}_0\bar{M}_0^\top W_1^\top Q \right] e_s + x^\top N_0^\top N_0 x \\ &\quad + \text{He}(e_s^\top QW_1\bar{D}\bar{d}). \end{aligned} \quad (4.34)$$

Further consider $V_x = x^\top P x$ with a positive definite matrix $P \in \mathbb{R}^{n \times n}$. Denote $\chi_{s_2} = \text{He}(x^\top P\Theta_1\Delta A x)$, then

$$\begin{aligned} \chi_{s_2} &= - \left[M_0^\top \Theta_1^\top P x - F_0 N_0 x \right]^\top \left[M_0^\top \Theta_1^\top P x - F_0 N_0 x \right] \\ &\quad + x^\top P \Theta_1 M_0 M_0^\top \Theta_1^\top P x + x^\top N_0^\top F_0^\top F_0 N_0 x \\ &\leq x^\top P \Theta_1 M_0 M_0^\top \Theta_1^\top P x + x^\top N_0^\top N_0 x. \end{aligned}$$

Similarly, it can be shown that

$$\begin{aligned} \dot{V}_x &= x^\top \left[\text{He}(P(\Theta_1 A - BK_s)) + P\Theta_1 M_0 M_0^\top \Theta_1^\top P + N_0^\top N_0 \right] x \\ &\quad + \text{He}(x^\top P F_1 e + x^\top P D_1 \bar{d}). \end{aligned} \quad (4.35)$$

Let $\xi_s = [x^\top e_s^\top]^\top$, the H_∞ performance $\|G_{z_s \bar{d}}\|_\infty < \gamma_s$ can be represented by

$$J = \int_0^\infty \left(z_s^\top z_s - \gamma_s^2 \bar{d}^\top \bar{d} \right) dt < 0. \quad (4.36)$$

Denote $V_s = V_{xs} + V_{es}$, then under zero initial conditions, it follows that

$$\begin{aligned}
J &= \int_0^\infty \left(z_s^\top z_s - \gamma_s^2 \bar{d}^\top \bar{d} + \dot{V}_s \right) dt - \int_0^\infty \dot{V}_s dt \\
&= \int_0^\infty \left(z_s^\top z_s - \gamma_s^2 \bar{d}^\top \bar{d} + \dot{V}_s \right) dt - V_s(\infty) + V_s(0) \\
&\leq \int_0^\infty \left(z_s^\top z_s - \gamma_s^2 \bar{d}^\top \bar{d} + \dot{V}_s \right) dt.
\end{aligned} \tag{4.37}$$

It can be seen from (4.37) that a sufficient condition of (4.36) is

$$J_1 = z_s^\top z_s - \gamma_s^2 \bar{d}^\top \bar{d} + \dot{V}_s < 0. \tag{4.38}$$

It follows from (4.38) with (4.34) and (4.35) that

$$\begin{aligned}
J_1 &\leq \begin{bmatrix} \xi_s \\ \bar{d} \end{bmatrix}^\top \begin{bmatrix} J_{11} & \chi_{12} & \chi_{13} \\ * & J_{22} & \chi_{23} \\ * & * & -\gamma_s^2 I \end{bmatrix} \begin{bmatrix} \xi_s \\ \bar{d} \end{bmatrix} \\
&< 0,
\end{aligned} \tag{4.39}$$

where $J_{11} = \chi_{11} + P\Theta_1 M_0 M_0^\top \Theta_1^\top P + C_{sx}^\top C_{sx}$, $\chi_{11} = \text{He}(P(\Theta_1 A - BK_x)) + 2N_0^\top N_0$, $\chi_{12} = PF_1$, $\chi_{13} = PD_1$, $J_{22} = \chi_{22} + C_{se}^\top C_{se} + QW_1 \bar{M}_0 \bar{M}_0^\top W_1^\top Q$, $\chi_{22} = \text{He}(Q(M_1 - ZM_2))$, and $\chi_{23} = QW_1 \bar{D}$.

By using the Schur complement (see Appendix A.2), (4.39) holds if

$$\begin{bmatrix} \chi_{11} & \chi_{12} & \chi_{13} & P\Theta_1 M_0 & 0 & C_{sx}^\top \\ * & \chi_{22} & \chi_{23} & 0 & QW_1 \bar{M}_0 & C_{se}^\top \\ * & * & -\gamma_s^2 I & 0 & 0 & 0 \\ * & * & * & -I & 0 & 0 \\ * & * & * & * & -I & 0 \\ * & * & * & * & * & -I \end{bmatrix} < 0. \tag{4.40}$$

Note that the constraint (4.40) is nonlinear and cannot be solved directly using the LMI toolbox. However, it can be further modified into linear constraints (4.32) and (4.33) by defining $PB = B\hat{P}$, $R_1 = \hat{P}K_s$, and $R_2 = QZ$. \square

Remark 4.3 Note that the equality constraint (4.32) is difficult to solve using the LMI toolbox. However, by using the method presented in Corless and Tu (1998), for a

positive scalar β_s , it can be converted into the following optimization problem and solved using the Matlab LMI toolbox:

$$\text{subject to (4.33) and } \begin{array}{l} \text{Minimize } \beta_s \\ \left[\begin{array}{cc} \beta_s I & PB - B\hat{P} \\ \star & \beta_s I \end{array} \right] > 0. \end{array}$$

4.4 Integrated FE/FTC design: output feedback

Section 4.3 presents a state feedback based integrated FE/FTC strategy with the assumption that the system variables are fully available. However, this is often not the case in practical applications. This section considers an output feedback based integrated FE/FTC strategy, for which purpose one more assumption is made.

Assumption 4.5 In the system (4.1), $\text{rank}(CB) = \text{rank}(B)$.

4.4.1 Full-order ASUIO-based FE design

The following ASUIO is proposed to estimate the augmented state \bar{x} in (4.2)

$$\begin{aligned} \dot{\xi}_o &= M_o \xi_o + G_o u + L_o y, \\ \hat{x} &= \xi_o + H_o y, \end{aligned} \quad (4.41)$$

where $\xi_o \in \mathbb{R}^{n+q+q_1}$ and $\hat{x} \in \mathbb{R}^{n+q+q_1}$ denote the observer system state and the augmented state estimate, respectively. The design matrices M_o , G_o , L_o , and H_o are of appropriate dimensions.

Define the estimation error as $e_o = \bar{x} - \hat{x}$, then it follows from (4.2) and (4.41) that

$$\begin{aligned} \dot{e}_o &= (\Xi \bar{A} - L_1 \bar{C}) e_o + (\Xi \bar{A} - L_1 \bar{C} - M_o) \xi_o + (\Xi \bar{B} - G_o) u \\ &\quad + [(\Xi \bar{A} - L_1 \bar{C}) H_o - L_2] y + \chi_a, \end{aligned} \quad (4.42)$$

where $\Xi = I_{n+q+q_1} - H_o \bar{C}$, $L_o = L_1 + L_2$, and $\chi_a = \Xi \Delta \bar{A} \bar{x} + \Xi \bar{D} \bar{d}$.

According to Theorem 4.1, the necessary conditions for the asymptotically stability of the error system (4.42) are

$$M_o \text{ is Hurwitz,} \quad (4.43)$$

$$\Xi\bar{A} - L_1\bar{C} - M_o = 0, \quad (4.44)$$

$$\Xi\bar{B} - G_o = 0, \quad (4.45)$$

$$(\Xi\bar{A} - L_1\bar{C})H_o - L_2 = 0. \quad (4.46)$$

With (4.44) - (4.46) the error system (4.42) becomes

$$\dot{e}_o = (\Xi\bar{A} - L_1\bar{C})e_o + \Xi\Delta\bar{A}\bar{x} + \Xi\bar{D}\bar{d}. \quad (4.47)$$

Thus, by designing H_o and L_1 such that the error system (4.47) is robustly stable, the observer (4.41) can be obtained.

4.4.2 Output feedback sliding mode FTC design

A switching function for (4.1) using the system output information is designed as

$$s_2 = N_2 y_c - \int_0^t v_2(\tau) d\tau, \quad (4.48)$$

where $s_2 \in \mathbb{R}^m$, $N_2 = (CB)^\dagger - Y_2(I_p - CB(CB)^\dagger)$ with a design matrix $Y_2 \in \mathbb{R}^{m \times p}$ and $(CB)^\dagger = ((CB)^\top CB)^{-1} (CB)^\top$. $y_c = y - F_s \hat{f}_s = Cx + F_s e_{f_s}$ with the sensor fault estimation error e_{f_s} . v_2 is a time-varying function to be designed.

Differentiating s_2 with respect to time gives

$$\dot{s}_2 = N_2 C [(A + \Delta A)x + F_a f_a + Dd] + N_2 F_s \dot{e}_{f_s} + u - v_2. \quad (4.49)$$

Design the control input as

$$u = u_{l_2} + u_{n_2}, \quad (4.50)$$

where the linear component is $u_{l_2} = v_2 - E_2 \hat{f}_a$ and $v_2 = -K_o \hat{x}$, with a design matrix $K_o \in \mathbb{R}^{m \times n}$ and $E_2 = B^\dagger F_a$. \hat{x} and \hat{f}_a are the estimates of the system state and actuator

fault, respectively. The nonlinear component u_{n_2} is designed as $u_{n_2} = -\rho_{s_2}(t)\text{sign}(s_2)$, with a design parameter $\rho_{s_2}(t)$.

Consider a Lyapunov function for (4.49)

$$V_{s_{20}} = \frac{1}{2}s_2^\top s_2.$$

It follows from (4.49) and (4.50) that the time derivative of $V_{s_{20}}$ is

$$\begin{aligned} \dot{V}_{s_{20}} &= s_2^\top [N_2C((A + \Delta A)x + F_a f_a + Dd) + N_2F_s \dot{e}_{f_s} + u - v_2] \\ &= s_2^\top [(N_2CA + N_2C\Delta A)x + K_o e_x + E_2 e_{f_a} + N_2CDd + N_2F_s \dot{e}_{f_s}] \\ &\leq (\eta_{s_2} - \rho_{s_2}(t))\|s_2\|, \end{aligned} \quad (4.51)$$

where η_{s_2} is an unknown scalar that satisfies $\eta_{s_2} \geq (\|N_2CA\| + \|N_2M_0\|\|N_0\|)\|x\| + \|K_o\|\|e_x\| + \|E_2\|\|e_{f_a}\| + \|N_2CD\|d_0 + \|N_2F_s\|\|\dot{e}_{f_s}\|$.

Define $\rho_{s_2}(t) = \hat{\eta}_{s_2} + \varepsilon_{s_2}$, where ε_{s_2} is a positive design scalar and $\hat{\eta}_{s_2}$ is used to estimate the unknown scalar η_{s_2} with an update law

$$\dot{\hat{\eta}}_{s_2} = \sigma_2\|s_2\|, \quad \hat{\eta}_{s_2}(0) = 0, \quad (4.52)$$

where σ_2 is a positive design scalar.

Define the estimation error of η_{s_2} as $\tilde{\eta}_{s_2} = \eta_{s_2} - \hat{\eta}_{s_2}$. Consider a Lyapunov function

$$V_{s_2} = V_{s_{20}} + \frac{1}{2\sigma_2}\tilde{\eta}_{s_2}^2.$$

It follows from (4.51) and (4.52) that

$$\begin{aligned} \dot{V}_{s_2} &= \dot{V}_{s_{20}} - \frac{1}{\sigma_2}\tilde{\eta}_{s_2}\dot{\hat{\eta}}_{s_2} \\ &\leq [\eta_{s_2} - \rho_{s_2}(t)]\|s_2\| - \tilde{\eta}_{s_2}\|s_2\| \\ &\leq -\varepsilon_{s_2}\|s_2\| \\ &\leq 0, \end{aligned} \quad (4.53)$$

Since V_{s_2} is positive definite, it follows from (4.53) and the Barbalat's lemma (Slotine et al., 1991) that $V_{s_2}(t) \leq V_{s_2}(0)$. Therefore, $s_2(t)$ and $\tilde{\eta}_{s_2}(t)$ are bounded. This means

that the designed controller (4.50) can maintain the sliding motion around $s_2 = 0$. Moreover, in the case of zero initial condition (i.e. $V_{s_2}(0) = 0$), it holds that $\lim_{t \rightarrow \infty} s_2(t) = 0$. In such case, the sliding surface $s_2 = 0$ is reachable and the idealized sliding motion is maintained.

Consider next the system stability analysis corresponding to the sliding mode. By setting $\dot{s}_2 = 0$, it follows from (4.49) that the equivalent control input (Edwards and Spurgeon, 1998) is

$$u_{eq2} = -N_2C[(A + \Delta A)x + Dd] - N_2F_s\dot{e}_{f_s} + u_{l_2}. \quad (4.54)$$

Substituting (4.54) into (4.1) gives the equivalent closed-loop system

$$\dot{x} = (\Theta_2A - BK_o)x + F_2e_o + \Theta_2\Delta Ax + \bar{D}_2\bar{d}_2, \quad (4.55)$$

where $\Theta_2 = I_n - BN_2C$, $F_2 = [BK_o \ F_a \ 0]$, $\bar{D}_2 = [\Theta_2D \ -N_2F_s]$, and $\bar{d}_2 = [d^\top \ \dot{e}_{f_s}^\top]^\top$.

Therefore, the system (4.1) is maintained on the sliding mode with the equivalent control (4.54) by designing K_x such that (4.55) is stable. The closed-loop system (4.55) contains the uncertainty ΔAx and disturbance d , which must be minimized to achieve a suitable degree of robustness. This is achieved using H_∞ optimization given in the next section.

4.4.3 Integrated synthesis

The proposed output-feedback based integrated FE/FTC design scheme is shown in Fig. 4.3. The augmented closed-loop system consisting of (4.47) and (4.55) is

$$\begin{aligned} \dot{x} &= (\Theta_2A - BK_o)x + F_2e_o + \Theta_2\Delta Ax + D_2\bar{d}_2, \\ \dot{e}_o &= (\Xi\bar{A} - L_1\bar{C})e_o + \Xi\Delta\bar{A}\bar{x} + \Xi\bar{D}_1\bar{d}_2, \\ y_c &= y - F_s\hat{f}_s, \\ z_o &= C_{ox}x + C_{oe}e_o, \end{aligned} \quad (4.56)$$

where $z_o \in \mathbb{R}^r$ is the measured output, $\bar{D}_1 = [\bar{D} \ 0]$, and $D_2 = [\Theta_2D \ 0 \ -N_2F_s]$.

Theorem 4.3 Under Assumptions 4.1 - 4.4 and 4.5, given a positive scalar γ_o , the augmented closed-loop system (4.56) is stable with H_∞ performance $\|G_{z_o\bar{d}}\|_\infty < \gamma_o$, if there exist symmetric positive definite matrices P_o , Q_1 , Q_2 , and Q_3 , and matrices \hat{P}_o ,

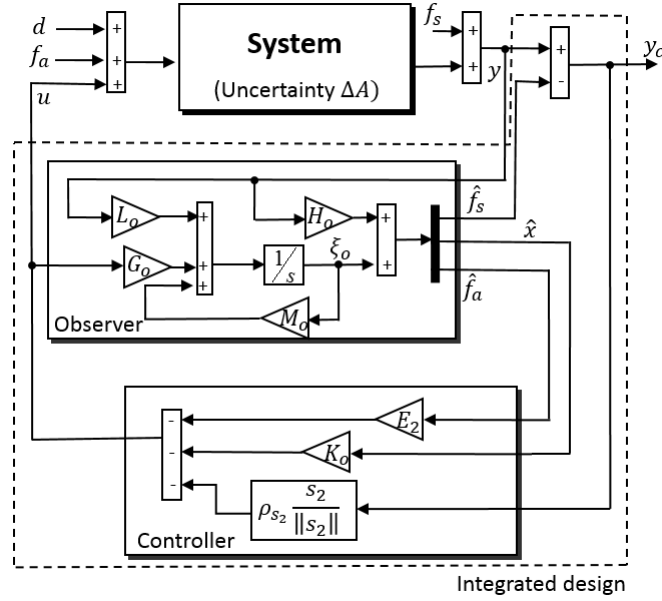


Fig. 4.3 Integrated FE/FTC design: output feedback case.

$X_i, i = 1, 2, \dots, 7$, such that

$$P_o B = B \hat{P}_o, \quad (4.57)$$

$$\bar{\Xi}_{11 \times 11} < 0, \quad (4.58)$$

where $\bar{\Xi}$ is a symmetric block matrix whose (i, j) block element is represented by $\bar{\Xi}_{i,j}$.

For $1 \leq i \leq j \leq 11$,

$$\bar{\Xi}_{1,1} = \text{He}(P_o \Theta_2 A - B X_1) + 2N_0^\top N_0, \quad \bar{\Xi}_{1,2} = B X_1, \quad \bar{\Xi}_{1,3} = P_o F_a, \quad \bar{\Xi}_{1,5} = P_o \Theta_2 D,$$

$$\bar{\Xi}_{1,8} = -P_o N_2 F_s, \quad \bar{\Xi}_{1,9} = P_o \Theta_2 M_0, \quad \bar{\Xi}_{1,11} = C_{ox}^\top, \quad \bar{\Xi}_{2,2} = \text{He}(Q_1 A - X_2 C A - X_3 C),$$

$$\bar{\Xi}_{2,3} = Q_1 F_a - X_2 C F_a - A^\top C^\top X_4^\top - C^\top X_5^\top, \quad \bar{\Xi}_{2,4} = M_3 F_s - A^\top C^\top X_6^\top - C^\top X_7^\top,$$

$$\bar{\Xi}_{2,5} = Q_1 D - X_2 C D, \quad \bar{\Xi}_{2,7} = -X_2 F_s, \quad \bar{\Xi}_{2,10} = (Q_1 - X_2 C) M_0, \quad \bar{\Xi}_{2,11} = C_{ex}^\top,$$

$$\bar{\Xi}_{3,3} = \text{He}(-X_4 C F_a), \quad \bar{\Xi}_{3,4} = -X_5 F_s - F_a^\top C^\top X_6^\top, \quad \bar{\Xi}_{3,5} = -X_4 C D, \quad \bar{\Xi}_{3,6} = Q_2,$$

$$\bar{\Xi}_{3,7} = -X_4 F_s, \quad \bar{\Xi}_{3,10} = -X_4 C M_0, \quad \bar{\Xi}_{3,11} = C_{efa}^\top, \quad \bar{\Xi}_{4,4} = \text{He}(-X_7 F_s), \quad \bar{\Xi}_{4,5} = -X_6 C D,$$

$$\bar{\Xi}_{4,7} = Q_3 - X_6 F_s, \quad \bar{\Xi}_{4,10} = -X_6 C M_0, \quad \bar{\Xi}_{4,11} = C_{efs}^\top, \quad \bar{\Xi}_{5,5} = \bar{\Xi}_{6,6} = \bar{\Xi}_{7,7} = \bar{\Xi}_{8,8} = -\gamma_o^2 I,$$

$$\bar{\Xi}_{9,9} = \bar{\Xi}_{10,10} = \bar{\Xi}_{11,11} = -I, \quad \bar{\Xi}_{i,j} \text{ are zero for all the others.}$$

Then the gains are given by: $K_o = \hat{P}_o^{-1} X_1$, $H_1 = Q_1^{-1} X_2$, $H_2 = Q_2^{-1} X_4$, $H_3 = Q_3^{-1} X_6$,

$L_{11} = Q_1^{-1} X_3$, $L_{12} = Q_2^{-1} X_5$, and $L_{13} = Q_3^{-1} X_7$.

Proof: Denote $C_{oe} = [C_{ex} \ C_{efa} \ C_{efs}]$, $Q_o = \text{diag}(Q_1(n \times n), Q_2(q \times q), Q_3(q_1 \times q_1))$, $L_1 = [L_{11}; L_{12}; L_{13}]$, and $H_o = [H_1; H_2; H_3]$, and consider the Lyapunov functions $V_{x_o} = x^\top P_o x$ and $V_{e_o} = e_o^\top Q_o e_o$. The proof is similar to that of Theorem 4.2 and thus is omitted here. \square

According to Remark 4.3, Theorem 4.3 can be further converted into a similar optimization problem with a positive scalar β_o .

4.5 Integrated FE/FTC design: multiplicative faults

Sections 4.3 and 4.4 focus on the integrated FE/FTC designs for systems with actuator/sensor faults. The considered faults are added to the system state and output, i.e., additive faults, resulting in changes in the mean values of the system state and outputs. Besides additive faults, multiplicative faults which are defined as component faults (even some kinds of actuator and sensor faults are in the form of multiplicative faults, e.g., partial loss of actuator effectiveness) also need to be discussed, since they affect the stability and degrade the performance of the post-fault system. Several works have been published on some topics related to multiplicative faults, e.g., multiplicative fault modelling and diagnosis (Ding, 2008), and multiplicative fault estimation (Gao and Duan, 2012; Tan and Edwards, 2004; Wang and Daley, 1996).

Consider an uncertain linear system in the form of

$$\begin{aligned} \dot{x} &= (A + \Delta A(t))x + Bu + F_m f_m + Dd, \\ y &= Cx, \end{aligned} \quad (4.59)$$

where x , y , u , d , A , B , D , and C are defined in (4.1). $F_m \in \mathbb{R}^{n \times q_m}$ is a constant fault distribution matrix. $f_m \in \mathbb{R}^{q_m}$ is a fictitious fault function of the multiplicative faults $\theta_i \in \mathbb{R}$, $i = 1, 2, \dots, q_m$. It is defined as

$$f_m = B_m \sum_{i=1}^{q_m} \theta_i \phi_i(A, B, x, u), \quad (4.60)$$

where $B_m = F_m^\dagger - (F_m^\dagger F_m - I_{q_m})W$ with an arbitrary matrix $W \in \mathbb{R}^{q_m \times n}$. $\theta_i \in \mathbb{R}$, $i = 1, 2, \dots, q_m$, are time-varying scalar functions denoting the multiplicative faults, and $\phi_i(A, B, x, u) \in \mathbb{R}^{n \times 1}$, $i = 1, 2, \dots, q_m$, are known functions related to A , B , x , and u .

The formulation (4.60) represents a wide class of multiplicative faults, e.g.,

$$\begin{aligned}\sum_{i=1}^{q_A} \theta_{A_i} A_i x &= F_{m_A} \left(B_{m_A} \sum_{i=1}^{q_A} \theta_{A_i} A_i x \right) = F_{m_A} f_{m_A}, \\ \sum_{i=1}^{q_B} \theta_{B_i} B_i u &= F_{m_B} \left(B_{m_B} \sum_{i=1}^{q_B} \theta_{B_i} B_i u \right) = F_{m_B} f_{m_B}, \\ \sum_{i=1}^{q_A} \theta_{A_i} A_i x + \sum_{i=1}^{q_B} \theta_{B_i} B_i u &= F_m \left(B_m \sum_{i=1}^{q_A} \theta_{A_i} A_i x + B_m \sum_{i=1}^{q_B} \theta_{B_i} B_i u \right) = F_m f_m,\end{aligned}$$

where A_i , $i = 1, 2, \dots, q_A$, and B_i , $i = 1, 2, \dots, q_B$, denote the known matrices related to A and B .

In the literature (Ding, 2008; Gao and Duan, 2012; Tan and Edwards, 2004; Wang and Daley, 1996), the effort was put into the estimation of θ_i , $i = 1, 2, \dots, q_m$. However, few works have been published on FTC design for systems with multiplicative faults. Provided that the aim is to achieve acceptable closed-loop system performance, the purpose of FTC design is to compensate for the effect of the multiplicative faults, whatever their sources or size. This can be achieved even if the fictitious multiplicative fault f_m cannot reflect the real fault location and size. In this respect, the integrated FE/FTC design of the system (4.59) along with multiplicative fault can be achieved through the designs proposed in Sections 4.3 - 4.4 with minor modification, by estimating and compensating the fictitious multiplicative fault f_m with the chosen F_m satisfying $\text{rank}(B, F_m) = \text{rank}(B) = m \leq n$.

Remark 4.4 The considered system (4.1) is required to satisfy the matching condition as defined in Section 1.2.1, i.e., $\text{rank}(B, F_a) = \text{rank}(B)$. However, when $\text{rank}(B, F_a) \neq \text{rank}(B)$ but $\text{rank}(B) = m \leq n$, the actuator fault f_a can be handled in the following way: Denote $F_a f_a = (BB^\dagger + B^\perp B^{\perp\dagger}) F_a f_a$ where $B^\perp \in \mathbb{R}^{n \times (n-m)}$ spans the null space of B and $BB^\dagger + B^\perp B^{\perp\dagger} = I_n$. Using the proposed design strategy, the matching part $BB^\dagger F_a f_a$ of the actuator fault can be estimated and compensated, while the unmatched part $B^\perp B^{\perp\dagger} F_a f_a$ can be treated as a disturbance whose effect can be minimized using H_∞ optimization.

Remark 4.5 In this chapter, the existing nonlinear constraints are converted into linear ones by introducing equality constraints. Although this facilitates the solution of the considered optimization problem (Problem 4.1), the equality constraints impose restrictions on the controlled system models. As discussed in Lien (2004) and Kheloufi et al. (2013), necessary conditions for the feasibility of the obtained LMIs are: 1)

The system (4.1) is stabilizable and detectable, and 2) the matrix B is full-column rank. These two conditions are satisfied for most controlled systems. However, more conservativeness might be imposed on the optimization problem in some special cases, e.g., for the DC motor model studied in Section 4.6, the symmetric positive definite matrices P and P_0 are required to be diagonal as the matrix B is of the form $B = [B_1^\top \ 0]^\top$, where B_1 is a non-null matrix of appropriate dimension.

Remark 4.6 Recall that by using an adaptive law in the proposed controller to estimate the unknown scalar related to the faults and disturbance, of which *a priori* knowledge of the upper bounds are not required. This adaptive updating requires some on-line computation. However, except for the adaptive gains all the other controller and observer gains are pre-determined off-line, mainly by solving single-step LMIs. Moreover, the proposed design procedure is quite straightforward and easy to follow. The proposed integrated design strategies are with acceptable computational complexity and can be applicable in practice.

4.6 A tutorial example

Considering the stabilization control for a DC motor with the state-space model

$$\begin{aligned} \dot{x} &= (A + \Delta A)x + Bu + Dd, \\ y &= Cx, \end{aligned} \quad (4.61)$$

with state vector $x = [i_a \ w]^\top$, control input $u = v_a$, disturbance $d = -\frac{T_l}{J_i}$, output y , and

$$A = \begin{bmatrix} -\frac{R_a}{L_a} & -\frac{K_v}{L_a} \\ \frac{K_m}{J_i} & -\frac{B_0}{J_i} \end{bmatrix}, B = \begin{bmatrix} \frac{1}{L_a} \\ 0 \end{bmatrix}, D = \begin{bmatrix} 0 \\ 1 \end{bmatrix}, C = \begin{bmatrix} 1 & 0 \\ 0 & 1 \end{bmatrix}, \Delta A = \begin{bmatrix} 0 & \sigma_v \\ \sigma_m & 0 \end{bmatrix},$$

where i_a , w , and v_a are the armature current, the angular velocity, and the armature voltage, respectively. R_a is the armature resistance and L_a is the inductance. K_v and K_m are the voltage and motor constants which are supposed to have parameter variations $|\sigma_v| \leq 0.06$ and $|\sigma_m| \leq 0.06$, respectively. J_i is the moment of inertia and B_0 is the friction coefficient. T_l is the unknown load torque. The control design purpose is to regulate the output y (the armature current and angular velocity) to zero.

Taken from Bélanger (1995) the nominal parameters of the DC motor: $R_a = 1.2$, $L_a = 0.05$, $K_v = 0.6$, $K_m = 0.6$, $J_i = 0.1352$, and $B_0 = 0.3$. The parameter variations

and disturbance are assumed to be $\sigma_v = \sigma_m = -0.01$ and $d = 0.01 \sin(t)$, respectively. Denote $|\sigma_v| \leq \alpha_v$ and $|\sigma_m| \leq \alpha_m$ with two positive scalars α_v and α_m . According to Assumption 4.3, it is chosen that

$$M_0 = \begin{bmatrix} 1 & 0 \\ 0 & 1 \end{bmatrix}, F_0 = \begin{bmatrix} \frac{\sigma_v}{\alpha_v} & 0 \\ 0 & \frac{\sigma_m}{\alpha_m} \end{bmatrix}, N_0 = \begin{bmatrix} 0 & \alpha_v \\ \alpha_m & 0 \end{bmatrix},$$

where $\alpha_v = 0.01$ and $\alpha_m = 0.01$.

4.6.1 Integrated FE/FTC design with additive faults

As considered by Isermann (2011), there might be additive faults during the operation of the DC motor system (4.61). Consider here an offset fault of the armature current and angular velocity sensors, i.e., sensor fault f_s , and a voltage sensor gain fault of v_a , i.e., actuator fault f_a . It follows from (4.1) that the model (4.61) now becomes

$$\begin{aligned} \dot{x} &= (A + \Delta A)x + Bu + F_a f_a + Dd, \\ y &= Cx + F_s f_s, \end{aligned} \quad (4.62)$$

where

$$F_a = \begin{bmatrix} \frac{1}{10L_a} \\ 0 \end{bmatrix}, f_a = \begin{cases} 0.5, & 0 \text{ s} \leq t \leq 2 \text{ s} \\ 1, & 2 \text{ s} < t \leq 3 \text{ s} \\ 0.2, & 3 \text{ s} < t \leq 3.5 \text{ s} \\ 0.6, & 3.5 \text{ s} < t \leq 4 \text{ s} \\ 1, & t > 4 \text{ s} \end{cases},$$

$$F_s = \begin{bmatrix} -1 \\ 1 \end{bmatrix}, f_s = \begin{cases} 0, & 0 \text{ s} \leq t \leq 1 \text{ s} \\ 0.1 \sin(0.5(t-1)), & t > 1 \text{ s} \end{cases}.$$

Case 1: state feedback

Assumptions 4.1 - 4.4 are satisfied for the system (4.62). Given $C_{sx} = [1 \ 1; 0 \ 1; 0 \ 0; 0 \ 0]$, $C_{se} = [0 \ 0; 0 \ 0; 0.5 \ 0; 0.5 \ 0.5]$ and $Y_1 = 0.5_{2 \times 1}$. Solving Theorem 4.2 with $\beta_s = 0.001$ and $\gamma_s = 1.5$ gives

$$K_x = [25.1814 \ 0.6952], M = \begin{bmatrix} -4.2303 & 9.2831 \\ 0.4752 & -6.2832 \end{bmatrix}, G = \begin{bmatrix} -42.3034 \\ 4.75169 \end{bmatrix},$$

$$R = \begin{bmatrix} 28.8781 & 25.3039 \\ -5.4923 & -3.7974 \end{bmatrix}, H = \begin{bmatrix} 2.1152 & 2.4184 \\ -0.2376 & 0.5156 \end{bmatrix}.$$

For comparison, closed-loop system simulations using the separated design and the proposed integrated design are performed with $\varepsilon_{s_1} = 0.5$, $\sigma_1 = 2$, $x(0) = 0.5_{2 \times 1}$, and $\hat{\eta}_{s_1}(0) = 0$.

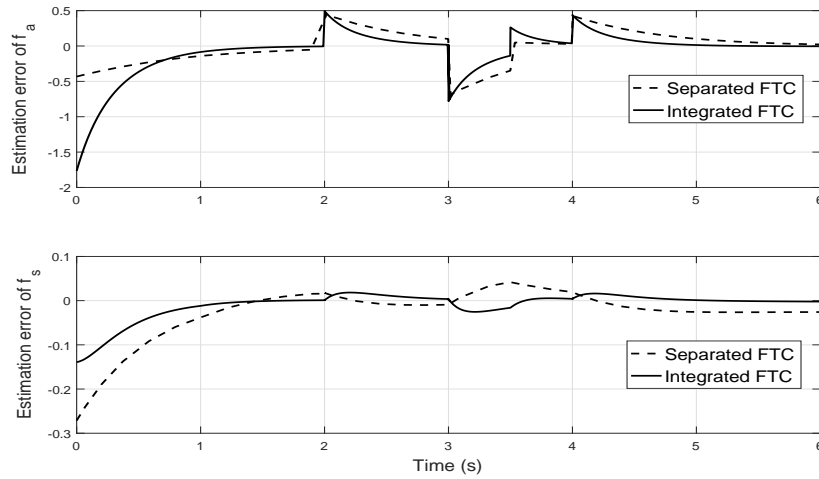


Fig. 4.4 FE performance: state feedback case.

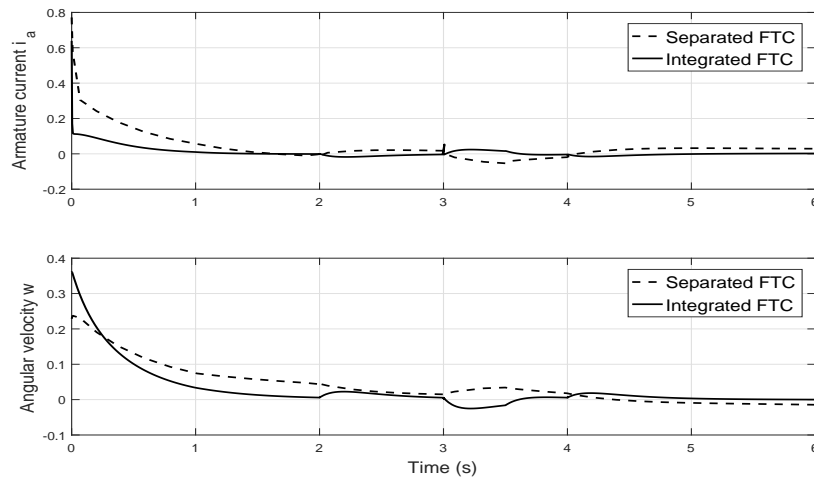


Fig. 4.5 FTC performance: state feedback case.

The simulation results in Figs. 4.4 and 4.5 show the FE performance and the time response of the closed-loop system outputs, respectively. Using the proposed integrated FTC design, the armature current and the angular velocity of the DC motor are regulated to be asymptotically stable. Although the separated design can stabilize the system, it

suffers from worse estimation and control performance, i.e., larger overshoot and much longer settling time. Moreover, the proposed integrated design achieves better fault estimation performance compared with the separated design.

Case 2: output feedback

Assumptions 4.1 - 4.5 are satisfied for the system (4.62). Given $C_{ox} = [I_2; 0_{4 \times 2}]$, $C_{ex} = [0_{2 \times 2}; I_2; 0_{2 \times 2}]$, $C_{efa} = [0_{4 \times 1}; 1; 0]$, $C_{efs} = [0_{5 \times 1}; 1]$, and $Y_2 = 0.1_{2 \times 1}$. Solving Theorem 4.3 with $\beta_o = 0.001$ and $\gamma_o = 0.8$ gives the gains

$$K_x = [3.4029 \ 0.0176], \quad M = \begin{bmatrix} -34.3138 & 23.3121 & 0.2824 & 54.2566 \\ 34.0176 & -24.1150 & -0.2827 & -54.7929 \\ 2.7427 & -13.3834 & -4.3725 & 5.5399 \\ 9.8072 & -15.6594 & 0.6276 & -29.815 \end{bmatrix},$$

$$G = \begin{bmatrix} 2.8236 \\ -2.8268 \\ -43.7253 \\ 6.2756 \end{bmatrix}, \quad L = \begin{bmatrix} -12.7729 & -10.5811 \\ 12.8517 & 10.67 \\ 35.8476 & 29.2368 \\ -0.7900 & 0.5830 \end{bmatrix}, \quad H = \begin{bmatrix} 0.8588 & 0.2516 \\ 0.1413 & 0.7531 \\ 2.1863 & 0.6864 \\ -0.3138 & 0.0876 \end{bmatrix}.$$

Simulations are performed with $\varepsilon_{s_2} = 0.5$, $\sigma_2 = 1$, $x(0) = 0.5_{2 \times 1}$, and $\hat{\eta}_{s_2}(0) = 0$.

The simulation results in Figs.4.6 and 4.7 show the fault estimation and time responses of the closed-loop system outputs, respectively. The phenomena observed from the results are similar to those of the state feedback case.

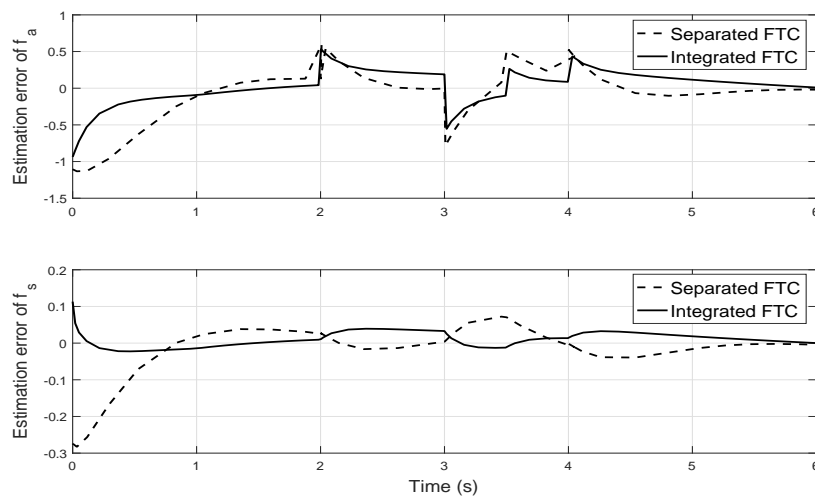


Fig. 4.6 FE performance: output feedback case.

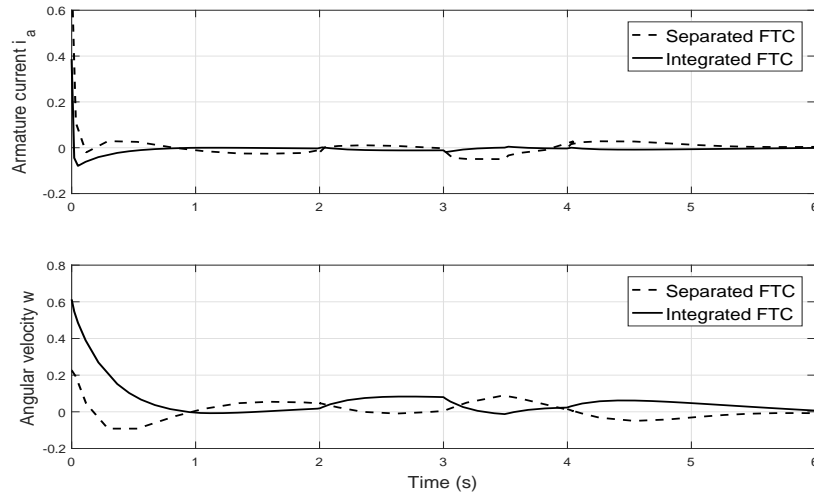


Fig. 4.7 FTC performance: output feedback case.

4.6.2 Integrated FE/FTC design with multiplicative faults

Suppose that there exists partial loss of actuator effectiveness (a multiplicative actuator fault) in the system (4.61), then the faulty model is represented as

$$\begin{aligned} \dot{x} &= (A + \Delta A)x + B(1 - \theta)u + Dd, \\ y &= Cx, \end{aligned} \quad (4.63)$$

where the scalar $\theta \in [0, 1]$ denotes the extent of the loss of actuator effectiveness. If $\theta = 0$, the actuator is healthy. If $\theta = 1$, the actuator has totally lost effectiveness, which cannot be handled by control design and is out of the scope of this study. If $\theta \in (0, 1)$, the actuator effectiveness is reduced by a factor θ . The matrices A , ΔA , B , D , and C are defined the same as those in (4.62) and

$$\theta = \begin{cases} 0, & 0 \text{ s} \leq t \leq 0.1 \text{ s} \\ -0.1(1 - e^{-t}) + 1, & 0.1 \text{ s} < t \leq 1 \text{ s} \\ 0.1, & 1 \text{ s} < t \leq 1.2 \text{ s} \\ 0.99, & 1.2 \text{ s} < t \leq 1.5 \text{ s} \\ 0.2, & 1.5 \text{ s} < t \leq 2 \text{ s} \\ 0.8, & 2 \text{ s} < t \leq 3 \text{ s} \end{cases}.$$

According to (4.59), the partial loss of actuator effectiveness can be represented by a fictitious fault with $B(-\theta)u = F_m f_m$, $F_m = [1/(10L_a); 0]$, and $f_m = -10\theta u$.

The integrated FE/FTC design of (4.63) is similar to that of (4.62) with $f_s = 0$ and by replacing $F_a f_a$ with $F_m f_m$. Thus, the proposed design strategy for the additive fault case is easily amenable to cover this multiplicative case. Without loss of generality and to consider a more practically realizable situation, only the output feedback case is studied, for which the observer/controller gains in the output feedback case can be applied. Simulations are performed with the same initial conditions of the output feedback case.

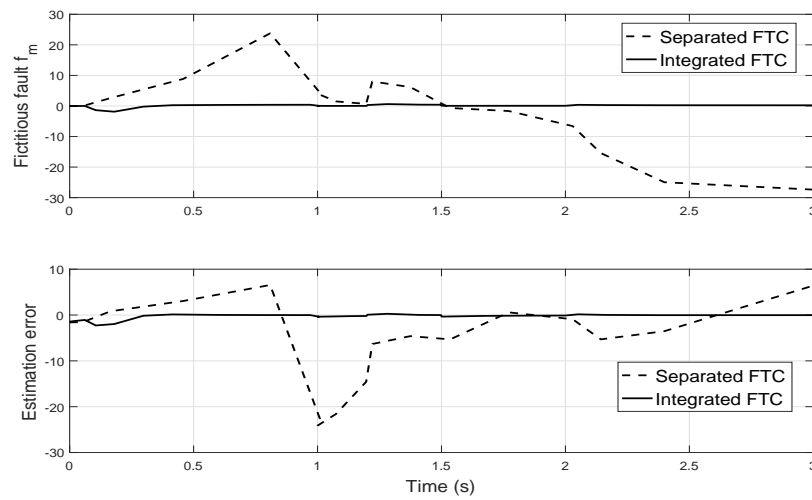


Fig. 4.8 Fictitious fault estimation performance.

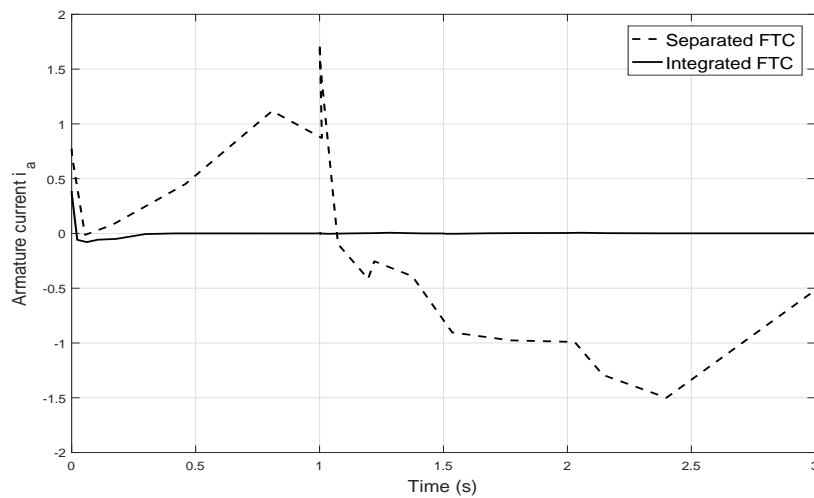


Fig. 4.9 FTC performance of i_a : multiplicative fault case.

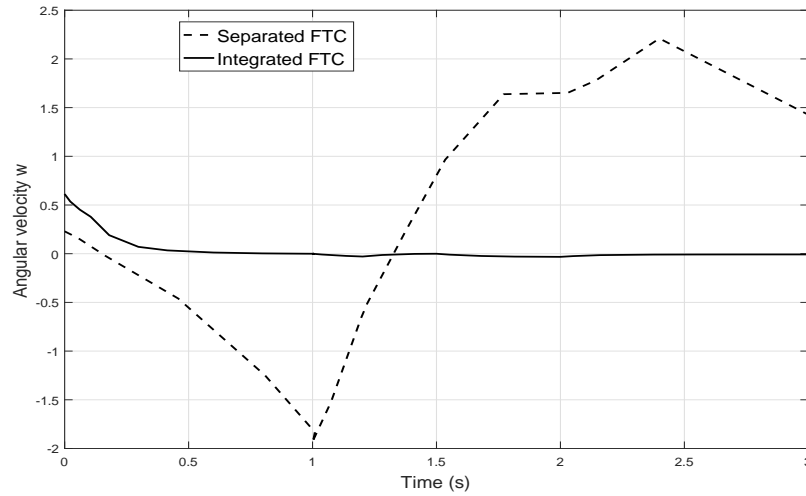


Fig. 4.10 FTC performance of w : multiplicative fault case.

Depending on both the time-varying multiplicative fault θ and the control inputs u , the fictitious faults f_m are different for the separated and integrated FTC designs. However, as observed in Fig. 4.8, the fictitious fault estimation performance of the integrated FTC design is better than that of the separated design. For the FTC performance shown in Figs. 4.9 and 4.10, the integrated FTC design also has quick response and small overshoot, while the separated design leads to an unstable system.

Summing up, the simulation results for the DC model example with system uncertainty, external disturbance, and faults, show that the proposed integrated design successfully demonstrates superior FE/FTC performance compared with the separated design by taking account of the bi-directional robustness interactions between the observer and control system.

4.7 Summary and discussion

This chapter proposes a strategy for integrated FE/FTC design for linear systems with system uncertainty, disturbance, and faults which are additive or multiplicative. The proposed approach designs together the FE and FTC functions following an observer-based robust control framework, achieved by H_∞ optimization with a single-step LMI formulation. Both the cases of state and output feedback FTC are discussed. Comparative simulations of the stabilisation control for a DC model show that the proposed integrated design leads to better FE and FTC performance than the separated design.

Limitations of this H_∞ optimization approach are summarized as follows: 1) The single-step LMI formulation for solving the integrated FE/FTC problem has limited design freedom, since only the robust performance index is adjustable; 2) It considers only continuously differentiable matched faults, which limits its application capability.

To overcome these limitations, Chapter 5 develops a decoupling integrated FE/FTC design strategy with more design freedom and can estimate and compensate non-differentiable unmatched faults.

Chapter 5: Integrated FE/FTC design: decoupling approach

5.1 Introduction

An integrated FE/FTC design strategy (see Fig. 5.1(a)) for linear systems has been proposed in Chapter 4 based on H_∞ optimization. Although this approach effectively obtains all the observer and controller gains through solving LMI constraints in a single-step, it is limited in the following three aspects: 1) The faults considered are assumed to be continuously differentiable and matched, which limits the applicability of the designs; 2) Their LMI formulations have limited design freedom; 3) The perturbation effects on the control system are just minimized, resulting in conservative robust designs.

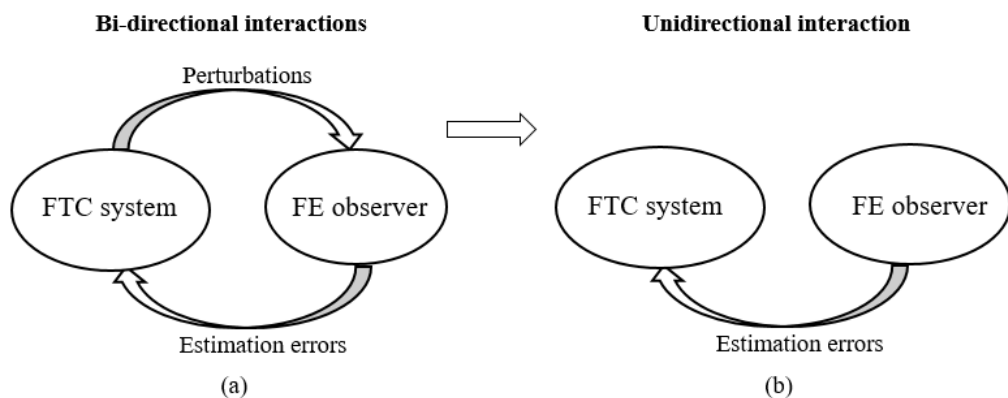


Fig. 5.1 Robustness interactions within (a) integrated and (b) decoupling FE/FTC.

To overcome these limitations, this chapter proposes a decoupling approach for integrated FE/FTC design for linear systems, as shown in Fig. 5.1(b). The main contributions are summarized as follows.

- A novel FE observer is proposed to estimate a more general class of faults. The actuator and sensor faults are assumed to be continuously differentiable in the literature

(de Loza et al., 2015; Gao and Ding, 2007; Jiang et al., 2006) and in Chapter 4. Although there is no such requirement in the SMOs (Edwards et al., 2000; Huang et al., 2016) by using the concept of equivalent output injection, the SMO (Edwards et al., 2000) has a canonical form in which several coordinate transformations are required and the other SMO (Huang et al., 2016) is designed based on H_∞ optimization. In this chapter, an adaptive sliding mode ASUIO is proposed to estimate the system state, actuator fault and perturbation, without requiring coordinate transformation, H_∞ optimization, and *a priori* knowledge of the unknown fault bounds.

- *A decoupling FE/FTC approach is developed to offer more design freedom.* By using a descriptor approach, the system perturbation is augmented as a system state and estimated. Therefore, the proposed observer is unaffected by the control system perturbations. Moreover, with an appropriately designed switched component, the effect of the actuator fault on the estimation error dynamics is removed. By combining the above descriptor augmentation and SMO methods, the FE observer is decoupled from the FTC system, which recovers the Separation Principle and allows more freedom for the FE/FTC design. It should be noted that the proposed decoupling approach is different from the separated designs in the literature in that the *bi-directional robustness interactions* are taken in account. Therefore, it should be discussed under the framework of integrated design.

- *Active perturbation cancellation contributes to a more robust FTC system.* As an alternative methodology to H_∞ robust optimization, disturbance-observer-based control has also been used to achieve robust system design (Chen et al., 2016d). In the current work, instead of being suppressed, the perturbations are compensated actively using adaptive backstepping control to cancel perturbations in all the subsystems (de Loza et al., 2015). A more robust FTC system can then be achieved using this cancellation with an appropriate observer.

The remainder of this chapter is organized as follows. Section 5.2 formulates the problem. Section 5.3 describes the basic idea of the proposed decoupling approach. Section 5.4 proposes the FE design with an adaptive sliding mode ASUIO. Section 5.5 presents the adaptive backstepping FTC design. A tutorial example of a DC motor is provided in Section 5.6. Finally, Section 5.7 draws the conclusion.

5.2 Problem formulation

Consider a linear system in the form of

$$\begin{aligned}\dot{x}(t) &= Ax(t) + Bu(t) + Ff(t) + D_1d(t), \\ y(t) &= Cx(t) + D_2d(t),\end{aligned}\tag{5.1}$$

where $x \in \mathbb{R}^n$, $u \in \mathbb{R}^m$, and $y \in \mathbb{R}^p$ are the state, control input, and measure output, respectively. $f \in \mathbb{R}^l$ is the actuator fault vector. $d \in \mathbb{R}^q$ denotes the perturbation including external disturbance and/or system uncertainty (Chen and Patton, 1999). The constant matrices $A \in \mathbb{R}^{n \times n}$, $B \in \mathbb{R}^{n \times m}$, $F \in \mathbb{R}^{n \times l}$, $D_1 \in \mathbb{R}^{n \times q}$, $C \in \mathbb{R}^{p \times n}$, and $D_2 \in \mathbb{R}^{p \times q}$ are known. To simplify the presentation the time index is omitted in the following study. The system (5.1) is assumed to satisfy the following assumptions.

Assumption 5.1 The pair (A, C) is observable, the pair (A, B) is controllable, and $\text{rank}(D_2) = q$.

Assumption 5.2 There exists an unknown positive constant f_0 such that $\|f\| \leq f_0$. The perturbation d is norm-bounded with a bounded first-order time derivative.

This study uses extensively the matched and unmatched definitions of the fault f and perturbation d given in Section 1.2.1.

Remark 5.1 It is rational to assume the perturbation d to be differentiable. The perturbation includes system uncertainty and/or external disturbance. On the one hand, the system uncertainty is a function of system state variables and it is continuously differentiable. On the other hand, according to the output regulation theory (Isidori, 1995), the external disturbance can be described as a differentiable exogenous system, which represents many disturbances in engineering, e.g., constant and harmonics. Although normally the distribution matrix D_1 of the perturbation cannot be obtained directly, an approximate modelling of it can be determined through several ways described in Chen and Patton (1999).

Remark 5.2 Compared with Chapter 4 and the other works in the literature (e.g. de Loza et al. (2015); Gao and Ding (2007); Jiang et al. (2006)), this chapter considers a more general class of actuator faults, which can be 1) differentiable or non-differentiable, and 2) matched or unmatched. The distribution matrix F represents the influence of faults on the system actuator and it is known if one has defined which faults are to be estimated and compensated.

This work aims to propose an FE-based FTC system for (5.1) to ensure that the system output can track its reference in the presence of actuator faults and perturbation. The FTC system design includes 1) an adaptive sliding mode UIO for estimating the system state, fault, and perturbation, and 2) an adaptive backstepping FTC controller for compensating the fault and perturbation to achieve satisfactory output tracking.

A decoupling approach will be used to achieve the integrated design of the observer and controller. Specifically, the adaptive sliding mode ASUIO will be designed to be decoupled from the control system, which enables the recovery of the well-known Separation Principle (see Appendix B) and thus the estimation and control can be designed separately.

5.3 Basic idea of the decoupling approach

In this section, a ASUIO using the method in Chapter 4 is first described briefly for estimating the state and fault of the system (5.1).

Defining f as a new state and augmenting the system (5.1) into

$$\begin{aligned}\dot{\bar{x}}_o &= \bar{A}_o \bar{x}_o + \bar{B}_o u + \bar{D}_1 \bar{d}, \\ y &= \bar{C}_o \bar{x}_o + D_2 d,\end{aligned}\tag{5.2}$$

where

$$\begin{aligned}\bar{x}_o &= \begin{bmatrix} x \\ f \end{bmatrix}, \bar{d} = \begin{bmatrix} d \\ \dot{f} \end{bmatrix}, \bar{A}_o = \begin{bmatrix} A & F \\ 0 & 0 \end{bmatrix}, \bar{B}_o = \begin{bmatrix} B \\ 0 \end{bmatrix}, \\ \bar{D}_1 &= \begin{bmatrix} D_1 & 0 \\ 0 & I_l \end{bmatrix}, \bar{C}_o = [C \ 0].\end{aligned}$$

The augmented state \bar{x}_o is estimated by a ASUIO with the form of

$$\begin{aligned}\dot{\xi}_o &= M_o \xi_o + G_o u + L_o y, \\ \hat{\bar{x}}_o &= \xi_o + H_o y,\end{aligned}\tag{5.3}$$

where $\xi_o, \hat{\bar{x}}_o \in \mathbb{R}^{n+l}$ are the observer system state and the augmented state estimate, respectively. $M_o, G_o, L_o,$ and H_o are design matrices.

Define the estimation error as $e_o = \bar{x}_o - \hat{x}_o$, then

$$\dot{e}_o = \Xi_2 e_o + \Xi_3 \xi_o + \Xi_4 u + \Xi_5 \bar{C}_o \bar{x}_o + \chi_o \quad (5.4)$$

where $\Xi_1 = I_{n+l} - H_o \bar{C}_o$, $L_o = L_{o1} + L_{o2}$, $\Xi_2 = \Xi_1 \bar{A}_o - L_{o1} \bar{C}$, $\Xi_3 = \Xi_1 \bar{A}_o - L_{o1} \bar{C}_o - M_o$, $\Xi_4 = \Xi_1 \bar{B}_o - G_o$, $\Xi_5 = (\Xi_1 \bar{A}_o - L_{o1} \bar{C}_o) H_o - L_{o2}$, and $\chi_o = \Xi_1 \bar{D}_1 \bar{d} - L_o D_2 d - H_o D_2 \dot{d}$.

By designing $\Xi_i = 0$, $i = 3, 4, 5$, the error system (5.4) becomes

$$\dot{e}_o = \Xi_2 e_o + \chi_o. \quad (5.5)$$

The ASUIO (5.3) described above based on the method in Chapter 4 is restrictive in two aspects: 1) The actuator fault f is required to be differentiable so that it can be augmented as a new system state; 2) The error dynamics (5.5) are affected by the uncertain term χ_o , which is a function of the system perturbations (d and \dot{d}) and fault modelling errors \dot{f} . The estimation errors in turn affect the FTC system performance since the controller uses the state and fault estimates. Therefore, there exist *bi-directional robustness interactions* between the observer (5.3) and the FTC system. In other words, the FE and FTC functions are coupled with each other, as shown in Fig. 5.2(a).

The second aspect implies that if there is neither system perturbations nor fault modelling errors acting on the error dynamics (5.5), then the estimation performance is not affected by the FTC system and the observer is decoupled from the control system. Therefore, one way to achieve the decoupling is to design an observer with error dynamics free from the perturbations (d and \dot{d}) and fault modelling errors \dot{f} , using a combination of the following two methods.

- *Descriptor augmentation.* The system (5.1) can be augmented into a descriptor form (5.6) in Section 5.4 with d as a new system state. In the augmented system, the only unknown input signal is the actuator fault f . Therefore, there will be no perturbation acting on the state estimation error dynamics, as shown in (5.13).
- *SMO.* It can be seen from the ASUIO (5.3) that modelling f as a new system state requires the differentiability assumption and leads to the existence of the fault modelling errors \dot{f} . They can be removed by the SMO method (Edwards et al., 2000) for FE, in which the actuator fault is reconstructed through the *equivalent output injection* signal corresponding to an idealized sliding motion, without a need of modelling the fault, e.g., as a new system state.

Such an SMO exists under the satisfaction of 1) no system perturbation affects the state estimation error dynamics and 2) in the error dynamics the fault is matched with respect to the switched component. The first requirement is fulfilled by the descriptor augmentation described above, while the second one can be met using appropriate design matrices (i.e., T and W in the proposed observer (5.7)), which is discussed in detail in Remark 5.4.

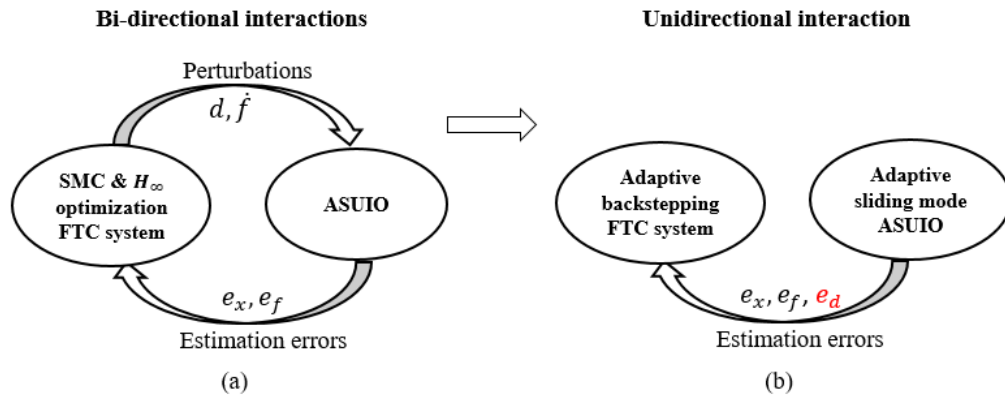


Fig. 5.2 Robustness interactions within (a) integrated and (b) decoupling FE/FTC.

Therefore, the proposed adaptive sliding mode ASUIO (5.7) combines the descriptor augmentation method with SMO and can remove the effect of the perturbations and fault modelling errors. This decouples the FE observer from the FTC system and it leads to the existence of just a *unidirectional robustness interaction* (Fig. 5.2(b)), rather than the bi-directional interactions described in Chapter 4 (Fig. 5.2(a)). The decoupling recovers the Separation Principle for the proposed FE observer and FTC system designs.

Remark 5.3 This chapter follows a new Separation Principle achieved by the use of a novel FE observer design (5.7) that is decoupled from the FTC system. It is different from the classical Separation Principle (see Appendix B) used extensively in the literature (e.g., de Loza et al. (2015); Gao and Ding (2007); Jiang et al. (2006)). Their designs cannot achieve overall robust FTC system performance since they ignore the existing *bi-directional robustness interactions* between the observer and control system. In this chapter, however, the interactions are taken into account and eliminated in the observer and controller designs. Therefore, the Separation Principle used here should be discussed under the integrated design framework.

5.4 Adaptive sliding mode ASUIO design

Following the basic idea of the adaptive sliding mode ASUIO described in Section 5.3, this section presents the design detail.

5.4.1 Observer design

Consider the perturbation d as a new system state and augment the system (5.1) into a descriptor form

$$\begin{aligned} E\dot{\bar{x}} &= \bar{A}\bar{x} + Bu + Ff, \\ y &= \bar{C}\bar{x}, \end{aligned} \quad (5.6)$$

where $\bar{x} = [x^\top \ d^\top]^\top$, $E = [I_n \ 0_{n \times q}]$, $\bar{A} = [A \ D_1]$, and $\bar{C} = [C \ D_2]$.

The augmented state \bar{x} is estimated by the observer

$$\begin{aligned} \dot{z} &= Nz + Ju + Ly + Wv, \\ \hat{x} &= z + Hy, \\ \hat{y} &= \bar{C}\hat{x}, \end{aligned} \quad (5.7)$$

where $z \in \mathbb{R}^{n+q}$ is the observer state, $\hat{x} \in \mathbb{R}^{n+q}$ is the estimate of \bar{x} . $N \in \mathbb{R}^{(n+q) \times (n+q)}$, $J \in \mathbb{R}^{(n+q) \times m}$, $L \in \mathbb{R}^{(n+q) \times p}$, $W \in \mathbb{R}^{(n+q) \times p}$, and $H \in \mathbb{R}^{(n+q) \times p}$ are design matrices.

The discontinuous switched component v is defined as

$$v = \rho_v \text{sign}(Q^\top e_y),$$

where $e_y = y - \hat{y}$, ρ_v is a design scalar, and $Q \in \mathbb{R}^{p \times l}$ is a design matrix.

Define $\varepsilon = TE\bar{x} - z$, where $T \in \mathbb{R}^{(n+q) \times n}$ is a design matrix. It follows from (5.6) and (5.7) that

$$\dot{\varepsilon} = N\varepsilon + (T\bar{A} - NTE - L\bar{C})\bar{x} + (TB - J)u + TFf - Wv. \quad (5.8)$$

Define the estimation error of \bar{x} as $e = \bar{x} - \hat{x}$. According to (5.8), the composite error system is

$$\begin{aligned}\dot{e} &= N\varepsilon + (T\bar{A} - NTE - L\bar{C})\bar{x} + (TB - J)u + TFf - Wv, \\ e &= \varepsilon + (I_{n+q} - H\bar{C} - TE)\bar{x}.\end{aligned}\quad (5.9)$$

Design the following matrix equations,

$$T\bar{A} - NTE - L\bar{C} = 0, \quad (5.10)$$

$$TB - J = 0, \quad (5.11)$$

$$I_{n+q} - H\bar{C} - TE = 0. \quad (5.12)$$

Upon satisfaction of the above matrix equations, it follows from (5.9) that $e = \varepsilon$ and

$$\dot{e} = Ne + TFf - Wv. \quad (5.13)$$

Remark 5.4 If the matrices T and W are designed such that $TF = W\bar{W}$, where \bar{W} is some matrix with compatible dimension, then the error system (5.13) becomes

$$\dot{e} = Ne + W(\bar{W}f - v).$$

Since the fault function $\bar{W}f$ is matched with respect to the switched component v , thus its effect can be totally cancelled by an appropriately designed v in Section 5.4.2. In such a case, the error dynamics are reduced to

$$\dot{e} = Ne,$$

which is asymptotically stable by designing N in (5.14) to be Hurwitz and not affected by the control system. Therefore, the observer (5.7) is decoupled from the FTC system.

5.4.2 Estimation performance analysis

This section provides an analysis of the estimation performance of the observer (5.7), as given in Theorem 5.1.

Theorem 5.1 Under Assumptions 5.1 - 5.2, the observer (5.7) estimates the augmented system state \bar{x} and the actuator fault f accurately in finite time, if there exists a symmetric matrix $P \in \mathbb{R}^{(n+q) \times (n+q)}$, a matrix $Q \in \mathbb{R}^{p \times l}$, and a positive constant ξ , such that

$$PN + N^T P < -\xi I_{n+q}, \quad (5.14)$$

$$PTF = \bar{C}^T Q. \quad (5.15)$$

The fault is estimated by: $\hat{f} = v_{eq}$, where v_{eq} is the equivalent output injection signal.

Proof: 1) Augmented system state estimation

Consider the following Lyapunov function for the error system (5.13),

$$V_{e_0} = e^T P e.$$

The time derivative of V_{e_0} along the error system is

$$\dot{V}_{e_0} = e^T (PN + N^T P) e + 2 (e^T PTF f - e^T P W v). \quad (5.16)$$

Design $W = P^{-1} \bar{C}^T Q$ and $PTF = \bar{C}^T Q$. Note that $TF = WQ$, which leads to the satisfaction of the matching condition as described in Remark 5.4. By using these designs and $e_y^T v = \rho_v \|e_y\|$, (5.16) becomes

$$\begin{aligned} \dot{V}_{e_0} &= e^T (PN + N^T P) e + 2 \left((Q^T e_y)^T f - (Q^T e_y)^T v \right) \\ &\leq e^T (PN + N^T P) e + 2 \|Q^T e_y\| (\rho - \rho_v), \end{aligned} \quad (5.17)$$

where $\rho = \|Q\| f_0$.

In order to cancel the unknown scalar ρ , design $\rho_v = \hat{\rho} + \varepsilon$, where ε is a positive design constant and $\hat{\rho}$ is used to estimate ρ by

$$\hat{\rho} = \sigma_0 \|Q^T e_y\|, \quad (5.18)$$

with a positive design constant σ_0 .

Define the estimation error of ρ as $\tilde{\rho} = \rho - \hat{\rho}$. Consider a Lyapunov function

$$V_e = V_{e_0} + \frac{1}{\sigma_0} \tilde{\rho}^2.$$

According to (5.14), (5.17), and (5.18) and using the fact that $\dot{\rho} = 0$, one has

$$\begin{aligned} \dot{V}_e &= \dot{V}_{e_0} + \frac{2}{\sigma_0} \tilde{\rho} (-\sigma_0 \|e_y\|) \\ &\leq e^\top \left(PN + N^\top P \right) e + 2 \|Q^\top e_y\| (\rho - \hat{\rho} - \varepsilon - \tilde{\rho}) \\ &\leq -\xi \|e\|^2 - 2\varepsilon \|Q^\top e_y\| \\ &\leq 0. \end{aligned} \tag{5.19}$$

It follows from (5.19) and the Barbalat's lemma (Slotine et al., 1991) that $\lim_{t \rightarrow \infty} V_e(t) = 0$. Therefore, $V_e(t) \leq V_e(0)$, and e and $\tilde{\rho}$ are bounded. Furthermore, $|e(t)| \leq \sqrt{2V_e(0)}$. Under zero initial condition $V_e(0) = 0$ (i.e., $e(0) = \tilde{\rho}(0) = 0$), then it holds that $\lim_{t \rightarrow \infty} e(t) = 0$ and $\lim_{t \rightarrow \infty} \tilde{\rho}(t) = 0$. Therefore, under the zero initial condition, the sliding surface $Q^\top e_y = 0$ is reachable and the observer (5.7) estimates the augmented system state \bar{x} accurately.

2) Actuator fault estimation

It follows from $e_y = \bar{C}e$ and (5.13) that

$$\dot{e}_y = \bar{C}Ne + \bar{C}TFf - \bar{C}Wv. \tag{5.20}$$

It is proved in 1) that the sliding surface is reachable. During the sliding motion, $e_y = 0$ and $\dot{e}_y = 0$. Hence, (5.20) becomes

$$0 = \bar{C}Ne + \bar{C}P^{-1}\bar{C}^\top Q(f - v_{eq}), \tag{5.21}$$

where v_{eq} is the so-called *equivalent output injection* signal representing the average behaviour of the switched component v and the effort necessary to maintain the sliding motion (Edwards et al., 2000).

Since e converges to zero in finite time,

$$0 = \bar{C}P^{-1}\bar{C}^\top Q(f - v_{eq}).$$

This means that in finite time $v_{eq} \rightarrow f$. Therefore, the actuator fault estimation can be designed as $\hat{f} = v_{eq}$. \square

Remark 5.5 The equivalent output injection signal v_{eq} can be obtained by passing the switched component v through an appropriately designed low-pass filter (Edwards and Spurgeon, 1998), i.e.,

$$v_{eq} \cong \frac{1}{\tau s + 1} v,$$

with a time constant τ .

5.4.3 Observer parameters determination

In Sections 5.4.1 - 5.4.2 the FE observer (5.7) is described with its finite convergent estimation performance analyzed. This section proposes a way to determine the observer gains using a parametrization approach based on a theorem equivalent to Theorem 5.1.

The matrix equation (5.12) can be rearranged as

$$[T \ H] \begin{bmatrix} E \\ \bar{C} \end{bmatrix} = I_{n+q}. \quad (5.22)$$

Denote $\Omega_1 = \begin{bmatrix} E \\ \bar{C} \end{bmatrix}$ and $\Sigma_1 = I_{n+q}$. Since $\text{rank}(\Omega_1) = \text{rank} \begin{bmatrix} \Omega_1 \\ \Sigma_1 \end{bmatrix} = n + q$, the matrix equation (5.22) is solvable and its general solution is

$$[T \ H] = \Sigma_1 \Omega_1^\dagger - Y_1 \left(I_{n+p} - \Omega_1 \Omega_1^\dagger \right),$$

where Y_1 is any real matrix with the dimension $(n + q) \times (n + p)$. Then T and H can be parametrized as

$$T = T_1 - Y_1 T_2, \quad H = H_1 - Y_1 H_2, \quad (5.23)$$

with

$$\begin{aligned} T_1 &= \Sigma_1 \Omega_1^\dagger \begin{bmatrix} I_n \\ 0 \end{bmatrix}, \quad T_2 = (I_{n+p} - \Omega_1 \Omega_1^\dagger) \begin{bmatrix} I_n \\ 0 \end{bmatrix}, \\ H_1 &= \Sigma_1 \Omega_1^\dagger \begin{bmatrix} 0 \\ I_p \end{bmatrix}, \quad H_2 = (I_{n+p} - \Omega_1 \Omega_1^\dagger) \begin{bmatrix} 0 \\ I_p \end{bmatrix}. \end{aligned}$$

From (5.12), one has $TE = I_{n+q} - H\bar{C}$. Substituting it into (5.10) gives

$$[N \bar{L}] \begin{bmatrix} I_{n+q} \\ \bar{C} \end{bmatrix} = T\bar{A}, \quad (5.24)$$

where $\bar{L} = L - NH$.

Denote $\Omega_2 = \begin{bmatrix} I_{n+q} \\ \bar{C} \end{bmatrix}$ and $\Sigma_2 = T\bar{A}$. Since $\text{rank}(\Omega_2) = \text{rank} \begin{bmatrix} \Omega_2 \\ \Sigma_2 \end{bmatrix} = n+q$, the matrix equation (5.24) is solvable and its general solution is

$$[N \bar{L}] = \Sigma_2 \Omega_2^\dagger - Y_2 (I_{n+q+p} - \Omega_2 \Omega_2^\dagger),$$

where Y_2 is any real matrix with the dimension $(n+q) \times (n+q+p)$. Therefore, the matrices N and \bar{L} are given by

$$N = N_1 - Y_2 N_2, \quad \bar{L} = \bar{L}_1 - Y_2 \bar{L}_2, \quad (5.25)$$

with

$$\begin{aligned} N_1 &= \Sigma_2 \Omega_2^\dagger \begin{bmatrix} I_{n+q} \\ 0 \end{bmatrix}, \quad N_2 = (I_{n+q+p} - \Omega_2 \Omega_2^\dagger) \begin{bmatrix} I_{n+q} \\ 0 \end{bmatrix}, \\ \bar{L}_1 &= \Sigma_2 \Omega_2^\dagger \begin{bmatrix} 0 \\ I_p \end{bmatrix}, \quad \bar{L}_2 = (I_{n+q+p} - \Omega_2 \Omega_2^\dagger) \begin{bmatrix} 0 \\ I_p \end{bmatrix}. \end{aligned}$$

It can be seen that once the matrices Y_1 and Y_2 are determined, by using the parametrizations (5.23) and (5.25), the matrix equations (5.10) - (5.12) can be solved and all the observer design parameters can thus be obtained.

However, do such matrices Y_1 and Y_2 really exist? Before proving their existence by Lemma 5.2, the following lemma is presented.

Lemma 5.1 For all $s \in \mathbb{C}$, $\text{Re}(s) \geq 0$, it holds that

$$\text{rank} \begin{bmatrix} sI_{n+q} & -\Omega_1^\dagger \\ 0 & I_{n+p} - \Omega_1 \Omega_1^\dagger \end{bmatrix} = n + q.$$

Proof: Note that

$$\text{rank} \begin{bmatrix} I_{n+q} & 0 \\ 0 & \Omega_1 \end{bmatrix} = \text{rank} \begin{bmatrix} sI_{n+q} & 0 & \Omega_1^\dagger \Omega_1 \\ 0 & I_{n+p} & \Omega_1 \end{bmatrix}. \quad (5.26)$$

The left hand side of (5.26) is

$$\text{rank} \begin{bmatrix} I_{n+q} & 0 \\ 0 & \Omega_1 \end{bmatrix} = n + q + \text{rank}(\Omega_1). \quad (5.27)$$

The right hand side of (5.26) is

$$\begin{aligned} & \text{rank} \begin{bmatrix} sI_{n+q} & 0 & \Omega_1^\dagger \Omega_1 \\ 0 & I_{n+p} & \Omega_1 \end{bmatrix} \\ &= \text{rank} \left\{ \begin{bmatrix} I_{n+q} & -\Omega_1^\dagger \\ 0 & I_{n+p} - \Omega_1 \Omega_1^\dagger \\ 0 & \Omega_1 \Omega_1^\dagger \end{bmatrix} \begin{bmatrix} sI_{n+q} & 0 & \Omega_1^\dagger \Omega_1 \\ 0 & I_{n+p} & \Omega_1 \end{bmatrix} \right\} \\ &= \text{rank} \begin{bmatrix} sI_{n+q} & -\Omega_1^\dagger & 0 \\ 0 & I_{n+p} - \Omega_1 \Omega_1^\dagger & 0 \\ 0 & \Omega_1 \Omega_1^\dagger & \Omega_1 \end{bmatrix} \\ &= \text{rank} \begin{bmatrix} sI_{n+q} & -\Omega_1^\dagger \\ 0 & I_{n+p} - \Omega_1 \Omega_1^\dagger \end{bmatrix} + \text{rank}(\Omega_1). \end{aligned} \quad (5.28)$$

By comparing (5.27) with (5.28), it can be seen that

$$\text{rank} \begin{bmatrix} sI_{n+q} & -\Omega_1^\dagger \\ 0 & I_{n+p} - \Omega_1 \Omega_1^\dagger \end{bmatrix} = n + q.$$

□

Lemma 5.2 There exist matrices Y_1 and Y_2 such that the matrix equations (5.10) - (5.12) are solvable.

Proof: It follows from (5.23) and (5.25) that

$$\begin{aligned} N &= (T_1 - Y_1 T_2) \bar{A} \Omega_2^\dagger \begin{bmatrix} I_{n+q} \\ 0 \end{bmatrix} - Y_2 N_2 \\ &= T_1 \Phi - Y T_{2N}, \end{aligned}$$

where $\Phi = \bar{A} \Omega_2^\dagger \begin{bmatrix} I_{n+q} \\ 0 \end{bmatrix}$, $T_{2N} = \begin{bmatrix} T_2 \Phi \\ N_2 \end{bmatrix}$, and $Y = [Y_1 \ Y_2]$.

Therefore, the matrix Y exists if the pair $(T_1 \Phi, T_{2N})$ is observable, i.e.,

$$\text{rank} \begin{bmatrix} sI_{n+q} - T_1 \Phi \\ T_2 \Phi \\ N_2 \end{bmatrix} = n + q. \quad (5.29)$$

A sufficient condition for (5.29) is

$$\text{rank} \begin{bmatrix} sI_{n+q} - T_1 \Phi \\ T_2 \Phi \end{bmatrix} = n + q. \quad (5.30)$$

Define $\bar{\Phi} = \begin{bmatrix} I_n \\ 0 \end{bmatrix} \Phi$. Since

$$\Sigma_1 = I_{n+q}, \quad T_1 = \Sigma_1 \Omega_1^\dagger \begin{bmatrix} I_n \\ 0 \end{bmatrix}, \quad T_2 = (I_{n+p} - \Omega_1 \Omega_1^\dagger) \begin{bmatrix} I_n \\ 0 \end{bmatrix},$$

then

$$\begin{bmatrix} sI_{n+q} - T_1 \Phi \\ T_2 \Phi \end{bmatrix} = \begin{bmatrix} sI_{n+q} & -\Omega_1^\dagger \\ 0 & I_{n+p} - \Omega_1 \Omega_1^\dagger \end{bmatrix} \begin{bmatrix} I_{n+q} \\ \bar{\Phi} \end{bmatrix}.$$

It is clear that $\text{rank} \begin{bmatrix} I_{n+q} \\ \bar{\Phi} \end{bmatrix} = n + q$. Thus, (5.30) holds if we can prove that

$$\text{rank} \begin{bmatrix} sI_{n+q} & -\Omega_1^\dagger \\ 0 & I_{n+p} - \Omega_1 \Omega_1^\dagger \end{bmatrix} = n + q. \quad (5.31)$$

Since (5.31) has already been proved in Lemma 5.1, thus the sufficient condition (5.30) holds. This proves that the pair $(T_1 \Phi, T_2 N)$ is observable and the matrices Y_1 and Y_2 exist. \square

According to Lemma 5.2, by substituting the parametrizations of N and T to (5.14) and (5.15) and solving Theorem 5.2, one can obtain the matrices Y_1 and Y_2 and thus all the observer parameters.

Theorem 5.2 Under Assumptions 5.1 - 5.2, the observer (5.7) can estimate the augmented system state \bar{x} and the actuator fault f accurately in finite time, if there exists a symmetric positive definite matrix $P \in \mathbb{R}^{(n+q) \times (n+q)}$, matrices $Q \in \mathbb{R}^{p \times l}$ and $M \in \mathbb{R}^{(n+q) \times (2n+2p+q)}$, and positive constants ξ and β , such that

$$\text{He} \left(PT_1 \Phi - M \begin{bmatrix} T_2 \Phi \\ N_2 \end{bmatrix} \right) < -\xi I_{n+q}, \quad (5.32)$$

$$\begin{bmatrix} \beta I & (PT_1 - MT_2)F - \bar{C}^\top Q \\ * & \beta I \end{bmatrix} > 0. \quad (5.33)$$

Then the matrices Y_1 and Y_2 are given by

$$Y_1 = P^{-1}M \begin{bmatrix} I_{n+p} \\ 0 \end{bmatrix}, Y_2 = P^{-1}M \begin{bmatrix} 0 \\ I_{n+p+q} \end{bmatrix}.$$

Proof: Substituting (5.23) and (5.25) into (5.14) and (5.15) and defining $M = PY$, then the inequality (5.32) is derived from (5.14) directly. Moreover, by using the method described in Corless and Tu (1998), the equality constraint (5.15) can be converted into the inequality (5.33). \square

5.5 FTC design

Since the fault f and perturbation d are unmatched, their effect on the system dynamics cannot be compensated through direct control actions. However, it is known that backstepping control can compensate unmatched perturbations (de Loza et al., 2015). Thus in this section an adaptive backstepping FTC controller is used to compensate f and d .

5.5.1 System reformulation

Suppose the system (5.1) can be represented in a strict-feedback form (de Loza et al., 2015)

$$\begin{aligned}\dot{x}_1 &= A_1x_1 + B_1(x_2 + F_1f + S_1d), \\ \dot{x}_i &= A_i\bar{x}_i + B_i(x_{i+1} + F_if + S_id), \quad i = 2, \dots, r-1, \\ \dot{x}_r &= A_r\bar{x}_r + B_r(u + F_rf + S_rd),\end{aligned}\tag{5.34}$$

where $x_i \in \mathbb{R}^{n_i}$ are the new system state, $x_{r+1} = u$, and x_1 is the system output. $\bar{x}_i = [x_1^\top, \dots, x_i^\top]^\top$, $\text{rank}(B_i) = n_i$ and $\sum_{i=1}^r n_i = n$. The matrices A_i , F_i , and S_i are of compatible dimensions. The original system state is $x = [x_1^\top, \dots, x_r^\top]^\top$

Remark 5.6 Many physical systems can be rearranged into a strict-feedback form required for backstepping control design (Krstic et al., 1995). Moreover, using the decomposition algorithm described in Polyakov (2012), a controllable system (5.1) can always be decomposed into the required block-controllable (triangular) form. Backstepping control is also used in de Loza et al. (2015) for systems in the form of (5.34) for actuator fault and perturbation compensation. However, the estimation error effect on the control system is not taken into account and in their work a separated approach is used to design the FE and FTC functions.

5.5.2 Adaptive backstepping FTC controller design

The backstepping FTC design aims to 1) compensate the actuator fault f and perturbation d , and 2) ensure that the system output x_1 can track a given reference x_d , using the system state estimate \hat{x}_i , fault estimate \hat{f} , and perturbation estimate \hat{d} .

Define the estimation errors as $e_{x_i} = x_i - \hat{x}_i$, $e_{\bar{x}_i} = \bar{x}_i - \hat{\bar{x}}_i$, $i = 1, 2, \dots, r$, $e_f = f - \hat{f}$, and $e_d = d - \hat{d}$. Although Theorem 5.1 shows that all these estimation errors are bounded and converge to zero in finite time, they still have side effect on the transient performance of the FTC system, which should be taken into account in the control design. Therefore, an adaptive method is incorporated with backstepping control to estimate and compensate the estimation error effect automatically.

1) Step i: $1 \leq i \leq r-1$

Define $z_i = \hat{x}_i - \alpha_{i-1}$, where α_{i-1} is a design virtual control and $z_0 = 0$ and $\alpha_0 = x_d$. It follows from (5.34) that

$$\dot{z}_i = A_i \bar{x}_i + B_i (x_{i+1} + F_i f + S_i d) - \dot{e}_{x_i} - \dot{\alpha}_{i-1}.$$

Consider a Lyapunov function

$$V_{z_{i0}} = \frac{1}{2} z_i^\top z_i,$$

then its derivative is

$$\dot{V}_{z_{i0}} = z_i^\top [A_i \bar{x}_i + B_i (\alpha_i + F_i f + S_i d)] + z_i^\top B_i z_{i+1} + z_i^\top (B_i e_{x_{i+1}} - \dot{e}_{x_i} - \dot{\alpha}_{i-1}). \quad (5.35)$$

To ensure satisfactory tracking, compensate the fault and perturbation, and cancel the feed through side effect from the estimation error system (5.13) (i.e., the term $z_i^\top (B_i e_{x_{i+1}} - \dot{e}_{x_i})$ in (5.35)), design α_i as

$$\alpha_i = -B_i^{-1} \left[c_i z_i + \rho_{z_i} \text{sign}(z_i) + B_{i-1}^\top z_{i-1} + A_i \hat{\bar{x}}_i \right] - F_i \hat{f} - S_i \hat{d}, \quad (5.36)$$

where c_i is a positive design constant and ρ_{z_i} is an adaptive parameter to be determined.

Substituting (5.36) into (5.35) gives

$$\dot{V}_{z_{i0}} \leq -c_i \|z_i\|^2 - z_{i-1}^\top B_{i-1} z_i + z_i^\top B_i z_{i+1} + (\rho_i - \rho_{z_i}) \|z_i\|, \quad (5.37)$$

where ρ_i is an unknown constant satisfying $\rho_i \geq \|A_i e_{\bar{x}_i} + B_i F_i e_f + B_i S_i e_d + B_i e_{x_{i+1}} - \dot{e}_{x_i} - \dot{\alpha}_{i-1}\|$, which represents the side effect of the estimation errors on the z_i subsystem.

In order to cancel ρ_i , define $\rho_{z_i} = \hat{\rho}_i + \varepsilon_i$. ε_i is a positive design constant and $\hat{\rho}_i$ is used to estimate ρ_i with

$$\dot{\hat{\rho}}_i = \sigma_i \|z_i\|, \quad (5.38)$$

where σ_i is a positive design constant.

Define the estimation error of ρ_i as $\tilde{\rho}_i = \rho_i - \hat{\rho}_i$. Consider a Lyapunov function

$$V_{z_i} = V_{z_{i0}} + \frac{1}{2\sigma_i} \tilde{\rho}_i^2.$$

According to (5.37) and (5.38),

$$\begin{aligned} \dot{V}_{z_i} &= \dot{V}_{z_{i0}} + \frac{1}{\sigma_i} \tilde{\rho}_i (-\sigma_i \|z_i\|) \\ &\leq -c_i \|z_i\|^2 - z_{i-1}^\top B_{i-1} z_i + z_i^\top B_i z_{i+1}. \end{aligned} \quad (5.39)$$

For the first i steps, consider the Lyapunov function

$$V_i = V_{i-1} + V_{z_i}$$

and define $V_0 = 0$. Then it follows from (5.39) that

$$\dot{V}_i \leq - \sum_{j=1}^i c_j \|z_j\|^2 + z_i^\top B_i z_{i+1}. \quad (5.40)$$

2) Step r:

Note that

$$\dot{z}_r = A_r \bar{x}_r + B_r (u + F_r f + S_r d) - \dot{e}_{x_r} - \dot{\alpha}_{r-1}.$$

Consider the following Lyapunov function for z_r ,

$$V_{z_{r0}} = \frac{1}{2} z_r^\top z_r.$$

The time derivative of $V_{z_{r0}}$ is

$$\dot{V}_{z_{r0}} = z_r^\top [A_r \bar{x}_r + B_r(u + F_r f + S_r d)] - z_r^\top (\dot{e}_{x_r} + \dot{\alpha}_{r-1}). \quad (5.41)$$

The FTC control law u is designed as

$$u = -B_r^{-1} \left[c_r z_r + \rho_{z_r} \text{sign}(z_r) + B_{r-1}^\top z_{r-1} + A_r \hat{x}_r \right] - F_r \hat{f} - S_r \hat{d}, \quad (5.42)$$

where c_r is a design constant and ρ_{z_r} is an adaptive parameter to be designed.

Substituting (5.42) into (5.41) yields

$$\dot{V}_{z_{r0}} \leq -c_r \|z_r\|^2 - z_{r-1}^\top B_{r-1} z_r + (\rho_r - \rho_{z_r}) \|z_r\|, \quad (5.43)$$

where ρ_r is an unknown constant such that $\rho_r \geq \|A_r e_{\bar{x}_r} + B_r F_r e_f + B_r S_r e_d - \dot{e}_{x_r} - \dot{\alpha}_{r-1}\|$.

Define $\rho_{z_r} = \hat{\rho}_r + \varepsilon_r$, where ε_r is a positive design constant and $\hat{\rho}_r$ is the estimate of ρ_r updated by

$$\dot{\hat{\rho}}_r = \sigma_r \|z_r\|, \quad (5.44)$$

with a positive design constant σ_r .

Define the estimation error of ρ_r as $\tilde{\rho}_r = \rho_r - \hat{\rho}_r$. Consider a Lyapunov function

$$V_{z_r} = V_{z_{r0}} + \frac{1}{2\sigma_r} \tilde{\rho}_r^2.$$

According to (5.43) and (5.44),

$$\begin{aligned} \dot{V}_{z_r} &= \dot{V}_{z_{r0}} + \frac{1}{\sigma_r} \tilde{\rho}_r (-\sigma_r \|z_r\|) \\ &\leq -c_r \|z_r\|^2 - z_{r-1}^\top B_{r-1} z_r. \end{aligned} \quad (5.45)$$

Finally, for the overall control system consider the Lyapunov function

$$V_r = V_{r-1} + V_{z_r}.$$

It follows from (5.40) and (5.45) that

$$\dot{V}_r \leq - \sum_{j=1}^r c_j \|z_j\|^2.$$

By designing $c_j \geq 0$, $j = 1, 2, \dots, r$, one has $\dot{V}_r < 0$. Since V_r is positive definite, it follows from the Barbalat's lemma (Slotine et al., 1991) that $V_r(t) \leq V_r(0)$. Hence, $z_j(t)$ and $\tilde{\rho}_j$, $j = 1, 2, \dots, r$, are bounded, and the system output x_1 tracks the reference x_d with bounded error. Moreover, under the zero initial conditions, i.e., $z_j(0) = 0$ and $\tilde{\rho}_j = 0$, $j = 1, 2, \dots, r$, $\lim_{t \rightarrow \infty} V_r(t) = 0$ and thus $\lim_{t \rightarrow \infty} z_j(t) = 0$. This means that, in the presence of actuator fault and perturbation, the system output x_1 tracks the reference x_d accurately.

Remark 5.7 Although the proposed decoupling approach facilitates the FE and FTC designs, the estimation errors inevitably affect the transient performance of the closed-loop FTC system (e.g., with large overshoot). To improve the transient performance the following additional strategies have been incorporated with the proposed design.

- Eigenvalue assignment for the observer. The FTC system performance can be largely recovered if the observer dynamics are (much) faster than the closed-loop dynamics. To reach this, the eigenvalues of the matrix N are located into an acceptable LMI region (see Appendix A.3). Specifically, it is achieved by adding a pole placement constraint (5.46) to the existing constraints (5.32) and (5.33) to place the eigenvalues of N into a strip region (a, b) , where a and b are negative constants.

$$\begin{bmatrix} \Pi - 2bP & 0 \\ * & -\Pi + 2aP \end{bmatrix} < 0, \quad (5.46)$$

where $\Pi = \text{He} \left(PT_1 \Phi - M \begin{bmatrix} T_2 \Phi \\ N_2 \end{bmatrix} \right)$.

- The estimation error effect on the FTC system is taken into account in the controller design through online estimation and compensation using the adaptive gains.

Remark 5.8 In the special cases when the control matching condition (defined in Section 1.2) holds, i.e., $\text{rank}(B, F) = \text{rank}(B, D_1) = \text{rank}(B)$, the perturbation and fault acting on the state dynamics can be compensated directly by introducing their estimates into the control action. Therefore, in such cases it is not necessary to represent the system into the triangular form (5.34). FTC can then be achieved through standard state-feedback control in Chapter 4.

Remark 5.9 The proposed approach can achieve compensation of both perturbations and faults. Although the work (Cao et al., 2011) also considers this kind of compensation problem, it focuses on a part of the disturbances modelled by a known linear exogenous system and requires full system state information. Moreover, the integrated FE/FTC design problem described in this chapter is far beyond the concern of Cao et al. (2011). It is also worth noting that, in the absence of faults, the proposed approach is reduced to be a disturbance-observer-based control method which has been researched extensively and relates to significant potential industrial applications (Chen et al., 2016d).

5.6 A tutorial example

Consider the angular velocity tracking control of a DC motor modelled by

$$\begin{aligned} \dot{x} &= Ax + B(u + f) + D_1 d, \\ y &= Cx + D_2 d, \end{aligned}$$

where $x = [w \ i_a]^\top$ is the state, $u = v_a$ is the control input, y is the output, f is an actuator fault, and d is the perturbation. The system matrices are defined by

$$A = \begin{bmatrix} -\frac{B_0}{J_i} & \frac{K_m}{J_i} \\ -\frac{K_v}{L_a} & -\frac{R_a}{L_a} \end{bmatrix}, \quad B = \begin{bmatrix} 0 \\ \frac{1}{L_a} \end{bmatrix}, \quad D_1 = \begin{bmatrix} 0.1 \\ 0.1 \end{bmatrix}, \quad C = \begin{bmatrix} 1 & 0 \\ 0 & 1 \end{bmatrix}, \quad D_2 = \begin{bmatrix} 1 \\ 0 \end{bmatrix}.$$

The physical parameters of the DC motor are defined as follows. w , i_a , and v_a are the angular velocity, armature current, and armature voltage, respectively. R_a is the armature resistance. L_a is the inductance. K_v and K_m are the voltage and motor constants, respectively. J_i is the moment of inertia. B_0 is the friction coefficient. Compared with the DC motor model in Chapter 4, the perturbation acting on the output y is also considered in this simulation.

The angular velocity tracking reference is $x_d = 1$. The parameters of the DC motor are (Bélanger, 1995): $R_a = 1.2$, $L_a = 0.05$, $K_v = 0.6$, $K_m = 0.6$, $J_i = 0.1352$, and $B_0 = 0.3$.

Given $\gamma = 10$, $\beta = 0.1$, $a = -20$, and $b = -3$. By solving (5.32) and (5.33) in Theorems 5.2 and (5.46) in Remark 5.7, the obtained observer parameters are

$$\begin{aligned}
 P &= \begin{bmatrix} 40.049 & 0 & -13.5837 \\ 0 & 26.4654 & 0 \\ -13.5837 & 0 & 40.049 \end{bmatrix}, J = \begin{bmatrix} 0.8194 \\ 10.8593 \\ 0.8212 \end{bmatrix}, \\
 N &= \begin{bmatrix} -8.3206 & 1.8049 & -5.5059 \\ -3.4689 & -14.0715 & 3.1010 \\ -6.2471 & -1.4370 & -8.0692 \end{bmatrix}, L = \begin{bmatrix} 0.1041 & 3.0416 \\ 0.0543 & -5.3760 \\ -0.0959 & -4.0558 \end{bmatrix}, \\
 H &= \begin{bmatrix} 0 & -0.041 \\ 0 & 0.457 \\ 1 & -0.0411 \end{bmatrix}, Q = \begin{bmatrix} 21.7099 \\ 287.3947 \end{bmatrix}.
 \end{aligned}$$

The adaptive backstepping FTC controller parameters are chosen as: $c_1 = 35$, $\sigma_1 = 0.1$, $\varepsilon_1 = 0.1$, $c_2 = 60$, $\sigma_2 = 0.1$, $\varepsilon_2 = 0.1$, $\sigma_0 = 5$, and $\varepsilon = 1$.

Comparative simulations are performed for the DC motor (5.47) using the following four methods:

- *Nominal design.* It includes a UIO (Chen and Patton, 1999) for state estimation and a state feedback controller, designed separately without FE/FTC.
- *Separated FE/FTC design.* It includes a ASUIO in Chapter 4 for fault and state estimation and a state feedback FTC controller, designed separately by ignoring the perturbation in the observer design and the estimation errors in the control system.
- *Integrated FE/FTC design* in Chapter 4. It includes a ASUIO for fault and state estimation and a state feedback FTC controller, designed together using a single-step LMI formulation by taking into account the effect of the perturbation and estimation errors.
- *Proposed decoupling FE/FTC design.*

In the separated and integrated designs, the perturbation d is treated as a sensor fault. Two cases of simulations are carried out with differentiable and non-differentiable actuator faults, respectively, using the same observer and controller gains given above and the same zero initial conditions.

5.6.1 Differentiable fault case

Suppose the DC motor suffers from a differentiable actuator fault f and a perturbation d characterized by

$$d(t) = \begin{cases} 0.05 \sin(\pi t), & 0 \text{ s} \leq t \leq 10 \text{ s} \\ 3 \sin(4\pi t) + [0.1 \ 0.5]x, & 10 \text{ s} < t \leq 15 \text{ s} \end{cases},$$

$$f(t) = \begin{cases} 0, & 0 \text{ s} \leq t \leq 2 \text{ s} \\ 0.04(t-2)^2 + \sin(\pi(t-2)), & 2 \text{ s} < t \leq 7 \text{ s} \\ 1, & 7 \text{ s} < t \leq 10 \text{ s} \\ 2 \sin(3\pi(t-10)) + 1, & 10 \text{ s} < t \leq 15 \text{ s} \end{cases}.$$

The above f and d have different characteristics in different time periods, which are used to test the system performance under different fault and perturbation scenarios. Moreover, a Gaussian noise w with zero-mean and variance 0.001^2 is added to the measure outputs in the time interval $t \in (10, 15]$ s.

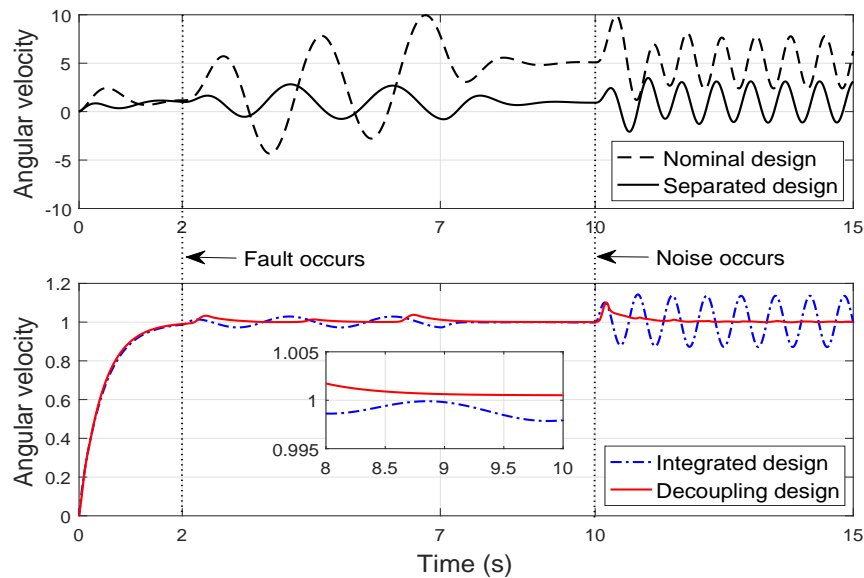


Fig. 5.3 Angular velocity: differentiable fault case.

It is seen in Fig. 5.3 that among the four methods simulated only the decoupling method achieves good tracking performance in the presence of the actuator fault. Fig. 5.4 shows that the control efforts of the decoupling and integrated approaches are similar but much smaller than those of the other two methods. As shown in Figs. 5.5 - 5.6, the decoupling

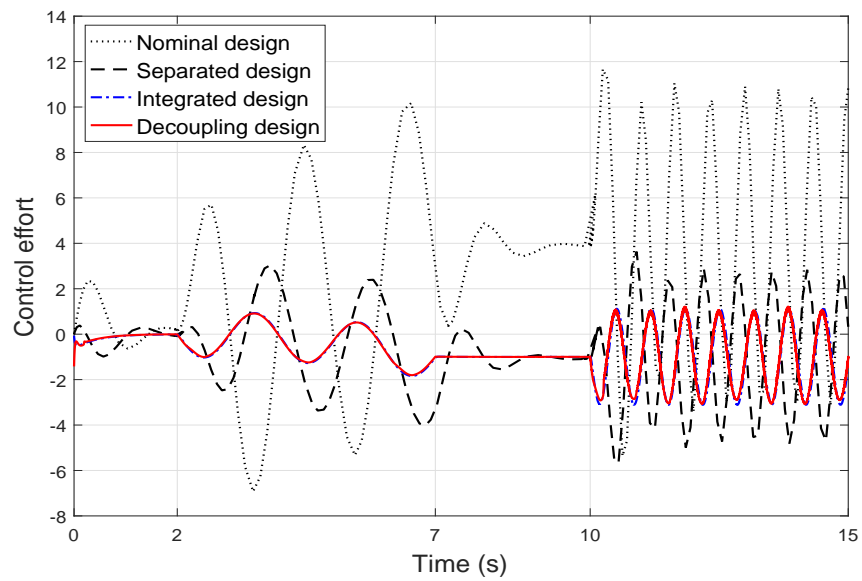


Fig. 5.4 Control effort: differentiable fault case.

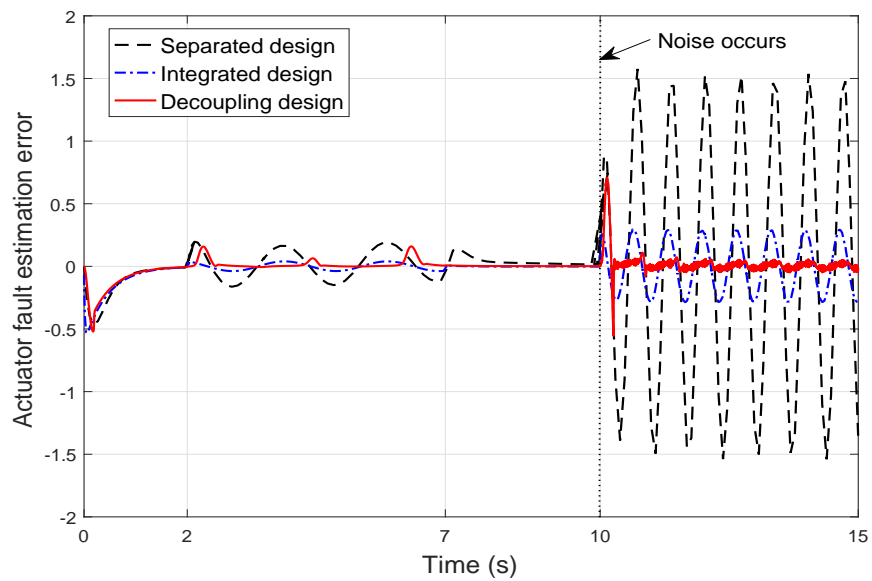


Fig. 5.5 Fault estimation: differentiable fault case.

method has better fault and perturbation estimation performance than the separated and integrated methods, even in the presence of measurement noise.

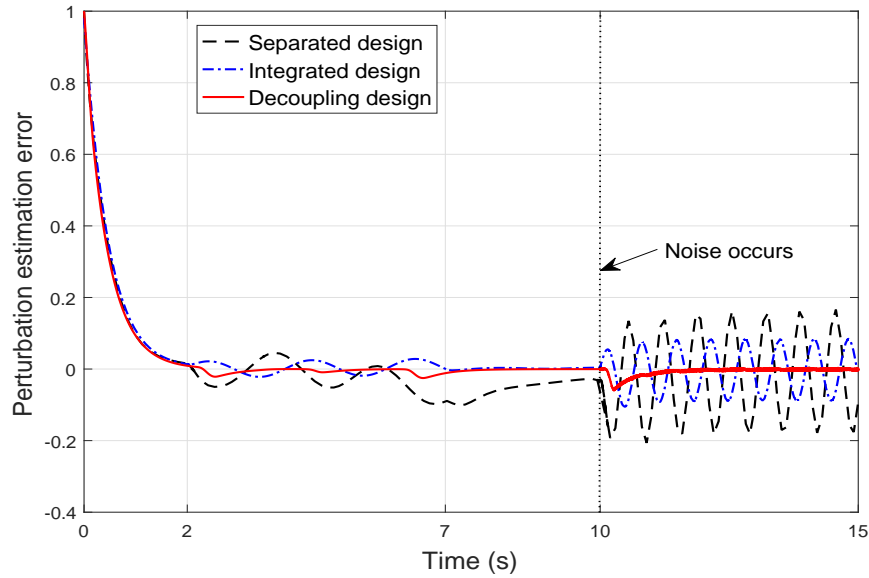


Fig. 5.6 Perturbation estimation: differentiable fault case.

5.6.2 Non-differentiable fault case

Consider the case in which the DC motor is subject to a perturbation d and a non-differentiable fault f (a Weierstrass function that is smooth but nowhere differentiable (Hardy, 1916)) in the forms of

$$d(t) = 2 \sin(2\pi t), 0 \text{ s} \leq t \leq 5 \text{ s},$$

$$f(t) = \sum_{k=0}^{50} 0.5^k \cos(3^k \pi t), 0 \text{ s} \leq t \leq 5 \text{ s}.$$

It is seen from Fig. 5.7 that neither of the nominal and separated FE/FTC designs achieves angular velocity tracking. Although the angular velocity of the integrated design tracks the reference with small error, it has oscillatory dynamic response. Only the decoupling approach has good tracking performance. As shown in Fig. 5.8, the control efforts of the decoupling and integrated designs are similar but much smaller than those of the other two designs. Figs. 5.9 and 5.10 show that the decoupling approach has much better fault and perturbation estimation performance than the separated and integrated methods.

Summarizing the above two simulation cases for the DC motor (5.47) subject to actuator faults (differentiable or non-differentiable) and perturbations, the superiority ranking of the four control designs from low to high, in terms of robust FE/FTC performance, is

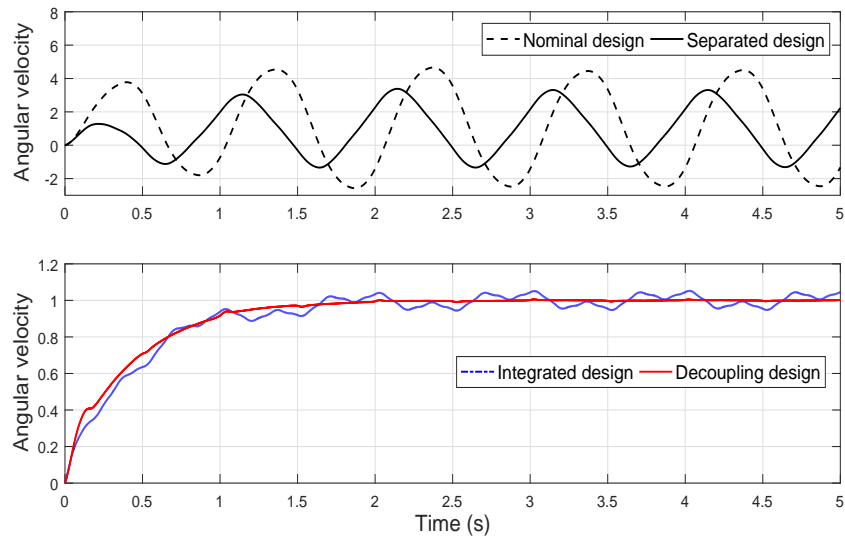


Fig. 5.7 Angular velocity: non-differentiable fault case.

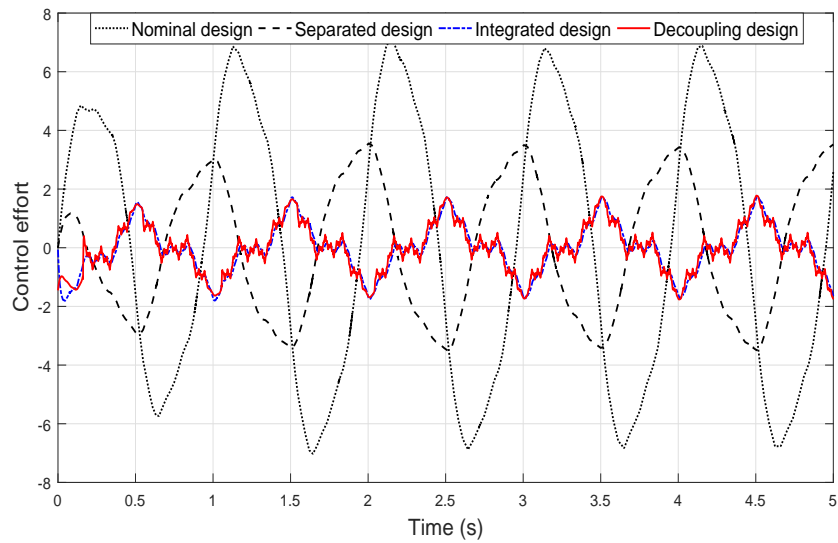


Fig. 5.8 Control effort: non-differentiable fault case.

that 1) the nominal approach, 2) the separated approach, 3) the integrated approach, and 4) the proposed decoupling approach.

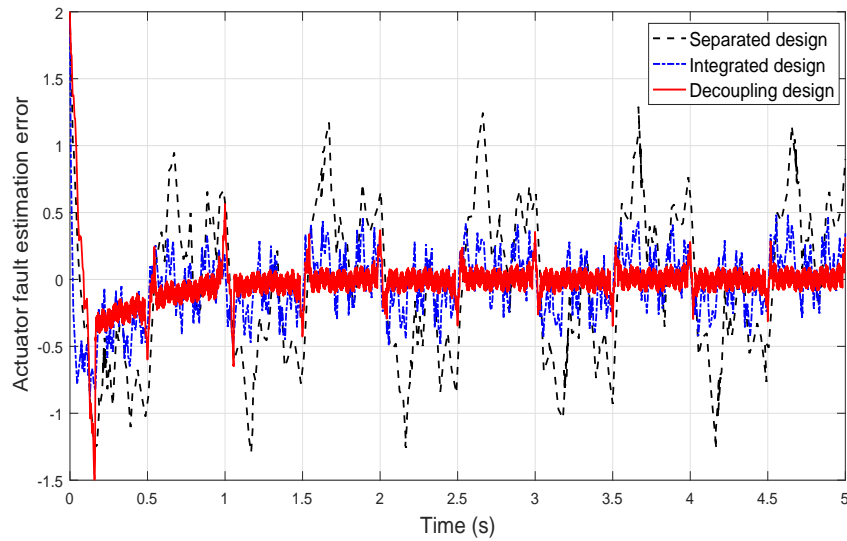


Fig. 5.9 Fault estimation: non-differentiable fault case.

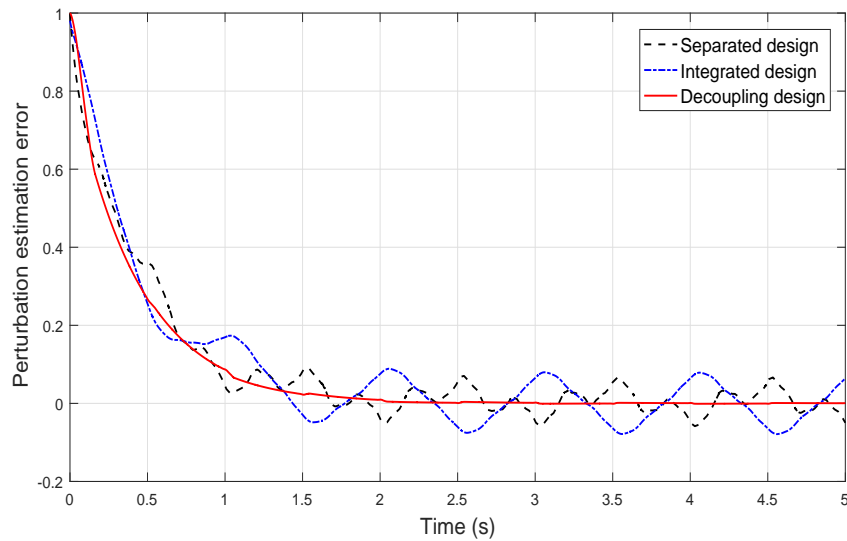


Fig. 5.10 Perturbation estimation: non-differentiable fault case.

5.7 Summary and discussion

An effective single-step integrated FE/FTC design strategy is proposed in Chapter 4 using H_∞ optimization. However, this approach is conservative with low freedom and can only be applied for differentiable matched faults.

This chapter further develops a decoupling approach for integrated FE/FTC design for linear systems with actuator faults and perturbations. An adaptive sliding mode

ASUIO is used to estimate the system state, fault and perturbation. With the estimates an adaptive backstepping FTC controller is then designed to compensate for the fault and perturbation to ensure output tracking.

The proposed approach is advantageous in that the FE function is decoupled from the FTC system which allows great FE/FTC design freedom and it can handle actuator faults which are differentiable or non-differentiable, and matched or unmatched. The DC motor comparative simulations demonstrate that the proposed decoupling approach has superiority over the approaches of nominal control, separated FE/FTC, and H_∞ optimization integrated FE/FTC in Chapter 4, in the sense of acceptable robust FE and FTC performances.

Part II

Integrated FE/FTC design for uncertain nonlinear systems

Chapter 6: Integrated FE/FTC for non-linear systems using T-S fuzzy modelling

6.1 Introduction

Integrated FE/FTC designs for linear systems are proposed in Chapters 4 and 5 based on the H_∞ optimization and decoupling approaches, respectively. This chapter extends the H_∞ optimization approach for nonlinear systems. The nonlinear nature of dynamic systems means that methods such as T-S fuzzy (Takagi and Sugeno, 1985) inference reasoning can be combined with the appropriate FTC theory as an extension to the linear strategies. Using this approach a continuous nonlinear system can be modelled as a multiple-model representation corresponding to a number of regions of state space behaviour. Each of the multiple T-S models is represented by an IF-THEN rule corresponding to a linear system. Based on this the existing robust FTC theory can be applied to each of the local linear models, so that the T-S system can then have both local and global robust FTC properties (including good fault-tolerance, etc.) (Benzaouia et al., 2015; Liu et al., 2013a; Mendonça et al., 2012; Tong et al., 2014b; Witczak et al., 2008; Xu et al., 2015).

Existing FTC approaches based on T-S approaches are either PFTC or AFTC. Although PFTC might achieve acceptable control performance (Huo et al., 2012; Tong et al., 2014a,b; Xu et al., 2015), it cannot obtain local fault magnitude information and this approach is not suitable for online system repair in the presence of faults.

Traditional AFTC approaches make use of FDI have been proposed in Benzaouia et al. (2015); Mendonça et al. (2012). Considering the design complexity of the FDI approach, many observer-based FE/FTC strategies for T-S fuzzy systems have also

been developed. A UIO-based FE and FTC design is proposed in Witczak et al. (2008) for systems with actuator faults. Adaptive observer (AO) based reconfigurable FTC designs are developed in Ichalal et al. (2012). An AO-based dynamic output feedback FTC design, focusing on actuator faults and external disturbance is presented in Zhang et al. (2010a). Liu et al. (2013a) and Liu et al. (2013b) describe FE/FTC designs for stochastic systems with actuator/sensor faults and disturbance using sliding mode ASOs. Huang and Yang (2014) propose an extended state observer FE/FTC design for time-delay systems in the presence of actuator faults and external disturbance. Shaker and Patton (2014) propose an extended state observer fault tolerant tracking control problem application to an offshore wind turbine system with sensor faults and external disturbance. Yang et al. (2014) develop an AO-based FTC strategy for systems with actuator fault using a delta operator approach. Jia et al. (2015a) propose an AO-based FTC scheme for descriptor systems subject to actuator faults and disturbance.

However, in these works the FE and FTC functions are designed separately without taking into account the effect of system and estimation uncertainties and the resulting *bi-directional robustness interactions* described in Chapter 3.

These backgrounds inspire the proposal in this chapter to integrate the FE and FTC designs for application to a class of nonlinear systems subjected to actuator/sensor faults. This work extends the *bi-directional robustness interactions* concept described in Chapter 3 to take into account properly the robustness interactions between the FE and FTC functions for nonlinear systems using T-S fuzzy modelling approach. Compared with the literature, the contributions of this chapter are summarized as follows.

- *A novel ASUIO is proposed for simultaneous state and fault estimation.* In this study, an ASUIO is proposed to estimate the T-S fuzzy system state variables and faults using a continuous linear observer with no requirements for fault bounds or rank conditions. The faults are assumed to be in polynomial form with bounded ν -th (highest) derivatives corresponding to known positive constants ν . This approach is non-conservative in the robustness sense and it can estimate time-varying or even unbounded faults (Gao and Ding, 2007). The difference between this new ASUIO and the one in Chapter 4 is that it estimates not only the faults themselves but also their $(\nu - 1)$ -th derivatives. This reduces the effects that the fault modelling errors have on the estimation performance.
- *A systematic strategy for integrated FE/FTC design is developed.* In this chapter an FTC strategy is proposed for the considered nonlinear systems in the presence of modelling uncertainty, faults, and external disturbance. The FE and FTC designs are re-formulated into an observer-based robust control problem solved using a single-step

LMI procedure, as a nonlinear extension of the integrated FE/FTC design for linear systems in Chapter 4.

The remainder of this chapter is organized as follows. Section 6.2 formulates the problem. Sections 6.3 - 6.5 present the designs of an ASUIO-based FE and an FTC controller. Section 6.6 provides a tutorial example of a nonlinear inverted pendulum and cart system, followed by the conclusions in Section 6.7.

6.2 Problem statement

Consider a class of nonlinear systems described by

$$\begin{aligned} \dot{x} &= f_x(x, u, f_a, d), \\ y &= f_y(x, f_s), \end{aligned} \quad (6.1)$$

where $x \in \mathbb{R}^n$, $u \in \mathbb{R}^m$, and $y \in \mathbb{R}^p$ stand for the state, control input, and output vectors, respectively. $f_a \in \mathbb{R}^q$ and $f_s \in \mathbb{R}^{q_1}$ denote the actuator and sensor faults, respectively. $d \in \mathbb{R}^l$ denotes the external disturbance. It is assumed that the nonlinear functions $f_x(\cdot)$ and $f_y(\cdot)$ are continuous and bounded in the sectors $x_i \in [a_i, b_i]$, where x_i is the i th system state variable and some constants a_i and b_i . It should be noted that, without loss of generality, the system properties studied in this chapter, including controllability, observability, and stability, are all local properties.

Considering modelling uncertainty, the system (6.1) can be modelled by the following T-S fuzzy system using sector nonlinearity (Takagi and Sugeno, 1985):

$$\begin{aligned} \dot{x} &= \sum_{i=1}^h \rho_i(\theta(t)) \left[(A_i + \Delta A_i)x + B_i u + F_i f_a + D_i d \right], \\ y &= Cx + F_s f_s, \end{aligned} \quad (6.2)$$

where $A_i \in \mathbb{R}^{n \times n}$, $B_i \in \mathbb{R}^{n \times m}$, $F_i \in \mathbb{R}^{n \times q}$, $D_i \in \mathbb{R}^{n \times l}$, $C_i \in \mathbb{R}^{p \times n}$, and $F_s \in \mathbb{R}^{p \times q_1}$ are known constant matrices. $\Delta A_i \in \mathbb{R}^{n \times n}$ are perturbed matrices with structures $\Delta A_i = M_{0i} F_{0i} N_{0i}$, where $F_{0i} \in \mathbb{R}^{r_{i1} \times r_{i2}}$ are known Lebesgue measurable matrices satisfying $F_{0i}^\top(t) F_{0i}(t) \leq \mu_i I_{r_{i2}}$ for some known scalars μ_i and matrices M_{0i} and N_{0i} of appropriate dimensions. h is the number of sub-models, and $\rho_i(\theta(t))$ are the membership functions and $\theta(t) = [\theta_1, \dots, \theta_s]$ is premise variable vector depending on the measurable state

variables, where s is the number of the premise variables. The premise variables are some measurable variables of the system state.

Define η_{ij} ($i = 1, \dots, h$ and $j = 1, \dots, s$) as the fuzzy sets characterized by the membership functions. Further define $\eta_{ij}(\theta_j)$ as the grades of the membership of θ_j in the fuzzy sets η_{ij} , then the membership functions can be defined as

$$\rho_i(\theta) = \frac{\sigma_i(\theta)}{\sum_{i=1}^h \sigma_i(\theta)}, \quad \sigma_i(\theta) = \prod_{j=1}^s \eta_{ij}(\theta_j),$$

which satisfy $0 \leq \rho_i(\theta) \leq 1$ and $\sum_{i=1}^h \rho_i(\theta) = 1$.

Throughout this study, the following assumptions are made.

Assumption 6.1 All the sub-models of (6.2) are observable and controllable in the fuzzy sets which they are defined, i.e., the pairs (A_i, C) are observable and the pairs (A_i, B_i) are controllable. Moreover, the fuzzy system (6.2) is observable and controllable in the sectors $x_i \in [a_i, b_i]$.

Assumption 6.2 The trios (A, C, F_i) and (A, C, F_s) are observable, i.e., the following rank conditions are satisfied: $\text{rank} \begin{bmatrix} A & F_i \\ C & 0 \end{bmatrix} = n + q$, $\text{rank} \begin{bmatrix} A & 0 \\ C & F_s \end{bmatrix} = n + q_1$.

Assumption 6.3 The actuator fault f_a is matched (see Section 1.2.1), i.e., $\text{rank}(B_i, F_i) = \text{rank}(B_i)$, $i = 1, 2, \dots, h$.

Assumption 6.4 The k -th derivative of f_a and the k_1 -th derivative of f_s with respect to time are bounded for some given scalars k and k_1 .

Remark 6.1 Assumption 6.1 implies that the i -th ($i = 1, 2, \dots, h$) sub-models are locally observable/controllable, and the whole fuzzy system (6.2) is globally observable and controllable within the entire sectors $x_i \in [a_i, b_i]$. Assumption 6.2 is required to ensure the actuator fault f_a and sensor fault f_s to be observable and can be estimated using the augmented state observer methods proposed in the chapter. The local observability and controllability together with Assumption 6.3 allow the existence of observers and controllers for each of the fuzzy models to achieve FE/FTC functions. The satisfaction of global observability/controllability guarantees the existence of an observer and a controller to achieve FE/FTC performance for the whole fuzzy system. Hence, a global fuzzy observer and fuzzy controller system is obtained by combining the local observers and controllers of each sub-model through appropriate membership functions.

The local observability and controllability properties can be verified using the following criteria: the i -th sub-model of (6.2) is 1) observable if $\text{rank}[C; CA_i; CA_i^2; \dots; CA_i^{n-1}] = n$, and 2) controllable if $\text{rank}[B_i, A_i B_i, A_i^2 B_i, \dots, A_i^{n-1} B_i] = n$. Sufficient criteria of robust observability and controllability for fuzzy systems are given in Ho et al. (2013) and Chen et al. (2009). This work considers only the observability and controllability of each triple (A_i, B_i, C) of the fuzzy system (6.2), which are special cases of the work of Ho et al. (2013) and Chen et al. (2009). Therefore, the sufficient criteria in Ho et al. (2013) and Chen et al. (2009) can be directly modified to verify the global observability and controllability of the considered fuzzy system (6.2).

6.3 ASUIO-based FE

Define $\omega_s = f_a^{(s)}$ and $v_t = f_s^{(\sigma)}$, where $s = 0, 1, \dots, k-1$ and $\sigma = 0, 1, \dots, k_1-1$, then the system (6.2) is augmented into

$$\begin{aligned} \dot{\bar{x}} &= \sum_{i=1}^h \rho_i \left(\bar{A}_i \bar{x} + \bar{B}_i u + \Delta \bar{A}_i \bar{x} + \bar{D}_i \bar{d} \right), \\ y &= \bar{C} \bar{x}, \end{aligned} \quad (6.3)$$

where

$$\begin{aligned} \bar{x} &= \begin{bmatrix} x \\ \omega \\ v \end{bmatrix}, \quad \omega = \begin{bmatrix} \omega_0 \\ \omega_1 \\ \vdots \\ \omega_{k-1} \end{bmatrix}, \quad v = \begin{bmatrix} v_0 \\ v_1 \\ \vdots \\ v_{k_1-1} \end{bmatrix}, \quad \bar{d} = \begin{bmatrix} d \\ \omega_{k-1} \\ v_{k_1-1} \end{bmatrix}, \\ \bar{A}_i &= \begin{bmatrix} A_i & F_i & 0 & 0 & 0 \\ 0 & 0 & I_{(k-1)q} & 0 & 0 \\ 0 & 0 & 0 & 0 & 0 \\ 0 & 0 & 0 & 0 & I_{(k_1-1)q_1} \\ 0 & 0 & 0 & 0 & 0 \end{bmatrix}, \quad \Delta \bar{A}_i = \begin{bmatrix} \Delta A_i & 0 & \dots & 0 & 0 \\ 0 & 0 & \dots & 0 & 0 \\ 0 & 0 & \dots & 0 & 0 \\ \vdots & \vdots & \ddots & \vdots & \vdots \\ 0 & 0 & \dots & 0 & 0 \end{bmatrix}, \end{aligned}$$

$$\bar{B}_i = \begin{bmatrix} B_i \\ 0_{(kq+k_1q_1) \times m} \end{bmatrix}, \bar{D}_i = \begin{bmatrix} D_i & 0 & 0 \\ 0 & 0_{(k-1)q \times q} & 0 \\ 0 & I_q & 0 \\ 0 & 0 & 0_{(k_1-1)q_1 \times q_1} \\ 0 & 0 & I_{q_1} \end{bmatrix},$$

$$\bar{C} = [C \ 0_{p \times kq} \ F_s \ 0_{p \times (k_1-1)q_1}].$$

Remark 6.2 It follows from Assumptions 6.1 and 6.2 that

$$\text{rank} \begin{bmatrix} sI_{n+kq+k_1q_1} - \bar{A}_i \\ \bar{C} \end{bmatrix} = \text{rank} \begin{bmatrix} sI_n - A_i & [-F_i \ 0] & 0 \\ 0 & J_s(I_q) & 0 \\ 0 & [0 \ sI_q] & 0 \\ 0 & 0 & J_s(I_{q_1}) \\ 0 & 0 & [0 \ sI_{q_1}] \\ C & 0 & [F_s \ 0] \end{bmatrix}$$

$$= n + kq + k_1q_1 \text{ (i.e., full rank)}$$

$$\text{with } J_s(I_\kappa) = \begin{bmatrix} sI_\kappa & -I_\kappa & & \\ & sI_\kappa & \ddots & \\ & & \ddots & -I_\kappa \\ & & & sI_\kappa \end{bmatrix}.$$

Thus, all the sub-models of the augmented system (6.3) are observable so that the overall augmented system is observable.

The augmented state vector \bar{x} of (6.3) is estimated by an ASUIO in the form of

$$\begin{aligned} \dot{z} &= \sum_{i=1}^h \rho_i (M_i z + G_i u + L_i y), \\ \hat{x} &= z + Hy, \end{aligned} \tag{6.4}$$

where $z, \hat{x} \in \mathbb{R}^{n+kq+k_1q_1}$ are the observer state and the estimate of \bar{x} , respectively. The design matrices M_i, G_i, L_i , and H are of compatible dimensions.

Define the estimation error as $e = \bar{x} - \hat{x}$, then from (6.3) and (6.4)

$$\dot{e} = \sum_{i=1}^h \rho_i [(\Xi \bar{A}_i - L_{1i} \bar{C})e + \Theta_1 z + \Theta_2 u + \Theta_3 y + \Xi \Delta \bar{A}_i \bar{x} + \Xi \bar{D}_i \bar{d}], \tag{6.5}$$

where $\Xi = I_{n+kq+k_1q_1} - H\bar{C}$, $L_i = L_{1i} + L_{2i}$, $\Theta_1 = \Xi\bar{A}_i - L_{1i}\bar{C} - M_i$, $\Theta_2 = \Xi\bar{B}_i - G_i$ and $\Theta_3 = (\Xi\bar{A}_i - L_{1i}\bar{C})H - L_{2i}$.

Design the following matrix equations ($i = 1, \dots, h$):

$$\Xi\bar{A}_i - L_{1i}\bar{C} - M_i = 0, \quad (6.6)$$

$$\Xi\bar{B}_i - G_i = 0, \quad (6.7)$$

$$(\Xi\bar{A}_i - L_{1i}\bar{C})H - L_{2i} = 0. \quad (6.8)$$

Upon the satisfaction of the conditions (6.6) - (6.8) and considering the uncertainty and disturbance, (6.5) can be rearranged into

$$\dot{e} = \sum_{i=1}^h \rho_i [(\Xi\bar{A}_i - L_{1i}\bar{C})e + \Xi\Delta\bar{A}_i\bar{x} + \Xi\bar{D}_i\bar{d}]. \quad (6.9)$$

Remark 6.3 It should be noted that $G_i = \Xi B_i$, and the remaining matrices L_{2i} and M_i can be derived immediately from (6.6) - (6.8) once the matrices L_{1i} and H are designed to ensure the robust stability of (6.9) in the sequel. Thus, the design of the observer (6.4) is reduced to a comparatively simple design of L_{1i} and H , which facilitates the FE/FTC design procedure.

6.4 FTC controller

Design an FTC controller for the system (6.2) as

$$u = \sum_{i=1}^h \rho_i K_i \hat{x}, \quad (6.10)$$

where $K_i = [K_{xi} \ K_{fi} \ 0_{m \times ((k-1)q+k_1q_1)}]$ with the state-feedback control gains $K_{xi} \in \mathbb{R}^{m \times n}$ and the actuator fault compensation gains $K_{fi} \in \mathbb{R}^{m \times q}$, respectively. According to Assumption 6.3, K_{fi} are chosen as $K_{fi} = -B_i^\dagger F_i$, where B_i^\dagger is the left pseudo-inverse of B_i .

Substituting (6.10) into (6.2) gives the closed-loop system

$$\dot{x} = \sum_{i=1}^h \sum_{j=1}^h \rho_i \rho_j [(A_i + B_i K_{xj})x + E_{ij}e + \Delta A_i x + D_i d], \quad (6.11)$$

where $E_{ij} = [-B_i K_{xj} \ F_i \ 0]$.

6.5 FE and FTC synthesis

6.5.1 Separated designs of FE/FTC

As summarized in Chapter 3, the state-of-art way to synthesize the FE and FTC gains is the separated design approach, by designing first the FE observer and then the FTC controller. This separated FE/FTC design idea is achieved based on the satisfaction of the Separation Principle and it neglects the *bi-directional robustness interactions* resulting from the disturbance and uncertainty. In this respect, the error dynamics are rearranged into

$$\begin{aligned} \dot{e} &= \sum_{i=1}^h \rho_i [(\Xi \bar{A}_i - L_{1i} \bar{C})e + \Xi \bar{D}_i \bar{d}], \\ z_e &= C_{e_1} e, \end{aligned} \quad (6.12)$$

where $z_e \in \mathbb{R}^{z_1}$ is the measured output and C_{e_1} is a constant matrix of appropriate dimension. Suppose that the observer has already been made stable, i.e., $e = 0$, then the feedback control system becomes

$$\begin{aligned} \dot{x} &= \sum_{i=1}^h \sum_{j=1}^h \rho_i \rho_j [(A_i + B_i K_{xj})x + \Delta A_i x + D_i d], \\ y_c &= y - F_s \hat{f}_s, \\ z_x &= C_{x_1} x, \end{aligned} \quad (6.13)$$

where y_c is the compensated system output, \hat{f}_s is the sensor fault estimate, $z_x \in \mathbb{R}^{z_2}$ is the measured output, and the constant matrix C_{x_1} is of appropriate dimension.

Theorems 6.1 and 6.2 are sufficient pre-requisites for the determination of the observer and controller gains, respectively.

Theorem 6.1 Given a positive scalar γ_1 , the error dynamics (6.12) are stable with H_∞ performance $\|G_{z_e \bar{d}}\|_\infty < \gamma_1$, if there exists a symmetric positive definite matrix Y_1 , and

matrices W_1 and W_{2i} , such that for all $i = 1, 2, \dots, h$,

$$\begin{bmatrix} \Psi_1 & Y_1 \bar{D}_i - W_1 \bar{C} \bar{D}_i & C_{e_1}^\top \\ \star & -\gamma_1^2 I & 0 \\ \star & \star & -I \end{bmatrix} < 0,$$

where $\Psi_1 = \text{He}(Y_1 \bar{A}_i - W_1 \bar{C} \bar{A}_i - W_{2i} \bar{C})$. Then the matrix gains are given by $H = Y_1^{-1} W_1$ and $L_{1i} = Y_1^{-1} W_{2i}$.

Proof: The proof of Theorem 6.1 directly follows from the Bounded Real Lemma (see Appendix A.1) with $W_1 = Y_1 H$ and $W_{2i} = Y_1 L_{1i}$, $i = 1, 2, \dots, h$. \square

Theorem 6.2 Given positive scalars γ_2 and ε_{0i} , the control system (6.13) is stable with H_∞ performance $\|G_{z,d}\|_\infty < \gamma_2$, if there exists a symmetric positive definite matrix X_1 and matrices W_{3j} , $j = 1, 2, \dots, h$, such that for all $i = 1, 2, \dots, h$ and $j = 1, 2, \dots, h$,

$$\begin{bmatrix} \Psi_2 & D_i & X_1 C_{x_1}^\top & M_{0i} & X_1 N_{0i}^\top \\ \star & -\gamma_2^2 I & 0 & 0 & 0 \\ \star & \star & -I & 0 & 0 \\ \star & \star & \star & -\varepsilon_{0i} I & 0 \\ \star & \star & \star & \star & -(\varepsilon_{0i} \mu_i)^{-1} I \end{bmatrix} < 0, \quad (6.14)$$

where $\Psi_2 = \text{He}(A_i X_1 + B_i W_{3j})$. Then the control gains are given by $K_{xj} = W_{3j} X_1^{-1}$.

Proof: Denote $\chi_{0i} = x^\top \Delta A_i^\top X_0 x + x^\top X_0 \Delta A_i x$, then for some positive scalars ε_{0i} ,

$$\begin{aligned} \chi_{0i} &= -\left[\sqrt{\varepsilon_{0i}}^{-1} M_{0i}^\top X_0 x - \sqrt{\varepsilon_{0i}} F_{0i} N_{0i} x \right]^\top \times \left[\sqrt{\varepsilon_{0i}}^{-1} M_{0i}^\top X_0 x - \sqrt{\varepsilon_{0i}} F_{0i} N_{0i} x \right] \\ &\quad + \varepsilon_{0i}^{-1} x^\top X_0 M_{0i} M_{0i}^\top X_0 x + \varepsilon_{0i} x^\top N_{0i}^\top F_{0i}^\top F_{0i} N_{0i} x \\ &\leq \varepsilon_{0i}^{-1} x^\top X_0 M_{0i} M_{0i}^\top X_0 x + \varepsilon_{0i} \mu_i x^\top N_{0i}^\top N_{0i} x. \end{aligned}$$

Consider a Lyapunov function $V_{x0} = x^\top X_0 x$, then

$$\begin{aligned} \dot{V}_{x0} &= \sum_{i=1}^h \sum_{j=1}^h \rho_i \rho_j \left[x^\top \text{He}(X_0 (A_i + B_i K_{xj})) x + \chi_{0i} + \text{He}(x^\top X_0 D_i d) \right] \\ &\leq \sum_{i=1}^h \sum_{j=1}^h \rho_i \rho_j \left[x^\top \Theta x + \text{He}(x^\top X_0 D_i d) \right], \end{aligned}$$

where $\Theta = \text{He}(X_0(A_i + B_i K_{xj})) + \varepsilon_{0i}^{-1} X_0 M_{0i} M_{0i}^\top X_0 + \varepsilon_{0i} \mu_i N_{0i}^\top N_{0i}$.

According to the Bounded Real Lemma (see Appendix A.1), the system (6.13) is stable with H_∞ performance $\|G_{z_x d}\|_\infty < \gamma_2$, if it holds that

$$\begin{bmatrix} \Theta & X_0 D_i & C_{x_1}^\top \\ * & -\gamma_2^2 I & 0 \\ * & * & -I \end{bmatrix} < 0. \quad (6.15)$$

Note that the inequality (6.15) is nonlinear. Define $X_1 = X_0^{-1}$. Multiplying both sides of (6.15) by $\text{diag}(X_1, I, I)$ and its transpose and using the Schur complement (see Appendix A.2), then (6.15) becomes

$$\begin{bmatrix} \Psi_2 & D_i & X_1 C_{x_1}^\top & M_{0i} & X_1 N_{0i}^\top \\ * & -\gamma_2^2 I & 0 & 0 & 0 \\ * & * & -I & 0 & 0 \\ * & * & * & -\varepsilon_{0i} I & 0 \\ * & * & * & * & -(\varepsilon_{0i} \mu_i)^{-1} I \end{bmatrix} < 0, \quad (6.16)$$

where $\Psi_2 = \text{He}(A_i X_1 + B_i K_{xj} X_1)$. Further define $W_{3j} = K_{xj} X_1$, then (6.16) directly leads to (6.14). \square

Recalling here the error system (6.9) and the closed-loop control system (6.11)

$$\begin{aligned} \dot{e} &= \sum_{i=1}^h \rho_i [(\Xi \bar{A}_i - L_{1i} \bar{C})e + \Xi \Delta \bar{A}_i \bar{x} + \Xi \bar{D}_i \bar{d}], \\ \dot{x} &= \sum_{i=1}^h \sum_{j=1}^h \rho_i \rho_j [(A_i + B_i K_{xj})x + E_{ij}e + \Delta A_i x + D_i d]. \end{aligned} \quad (6.17)$$

Define $H = [H_1; H_2; H_3; H_4; H_5]$, it follows that

$$\Xi \Delta \bar{A}_i \bar{x} = \begin{bmatrix} (I_n - H_1 C) \Delta A_i x \\ -H_2 C \Delta A_i x \\ -H_3 C \Delta A_i x \\ -H_4 C \Delta A_i x \\ -H_5 C \Delta A_i x \end{bmatrix}, \quad \Xi \bar{D}_i \bar{d} = \begin{bmatrix} (I_n - H_1 C) D_i d \\ -H_2 C D_i d \\ -H_3 C D_i d + \omega_{k-1} \\ -H_4 C D_i d \\ -H_5 C D_i d + v_{k_1-1} \end{bmatrix}. \quad (6.18)$$

It can be seen from (6.17) and (6.18) that: 1) The state estimation and FE are affected by the disturbance d and the uncertainty $\Delta A_i x$, whilst the FE is also affected by the fault modelling errors ω_{k-1} and v_{k-1} ; 2) The feedback control system is affected by the uncertainty, disturbance, and estimation errors. This important phenomenon of *bi-directional robustness interactions* between the FE and FTC function has been defined in Chapter 3. This chapter extends the notion of this robustness interaction into the framework of a T-S fuzzy system representation of a nonlinear system.

Usually when controllers and state observers are designed for nonlinear systems it is assumed that in a state space region close to the system operation a locally linear dynamical system can be used for design. Hence, for such systems it is well known that the Separation Principle (see Appendix B) cannot apply in general. In this work we consider the application of a T-S fuzzy approach to a nonlinear system problem and hence a form of specially integrated design must be used to achieve the robustness in the estimator and controller designs. From the statement above for the considered FE-based FTC system *bi-directional robustness interactions* exist between the FE observer and FTC controller and hence a true integration of these module designs must be achieved to obtain satisfactory robust FTC performance.

So, although the separated design in Section 6.5.1 can avoid the design complexity resulting from the coupling between the observer and controller, it only permits a sub-optimal solution of the overall FTC system design to be achieved, leading to degraded FE/FTC performance. To overcome this, Section 6.5.2 describes an integrated FE/FTC design strategy for the system (6.2) by taking into account the bi-directional interaction.

6.5.2 Integrated design of FE/FTC

Combining (6.9) and (6.11) gives the following composite closed-loop system including estimation with control, based on the T-S formulation given in (6.2),

$$\begin{aligned}
 \dot{x} &= \sum_{i=1}^h \sum_{j=1}^h \rho_i \rho_j [(A_i + B_i K_{xj})x + E_{ij}e + \Delta A_i x + \hat{D}_i \bar{d}], \\
 \dot{e} &= \sum_{i=1}^h \rho_i [(\Xi \bar{A}_i - L_{1i} \bar{C})e + \Xi \Delta \bar{A}_i \bar{x} + \Xi \bar{D}_i \bar{d}], \\
 y_c &= y - F_s \hat{f}_s, \\
 z_r &= C_x x + C_e e,
 \end{aligned} \tag{6.19}$$

where y_c is the compensated system output, \hat{f}_s is the sensor fault estimate, and $z_r \in \mathbb{R}^r$ is the measured output. The matrices C_x and C_e are of compatible dimensions. $\hat{D}_i = [D_i \ 0]$.

Note that the integrated FE/FTC design for the T-S fuzzy system (6.2) is now reformulated into an observer-based robust control problem of the composite closed-loop system (6.19), which will be solved in the sequel using H_∞ optimization with a single-step LMI formulation.

The strategy for solving the integrated FE/FTC robust design is in general a BMI problem as outlined in Lemma 6.1 below. However, Lemma 6.1 leads to a statement that Lemma 6.2 will transform the integrated design into a single-step LMI problem, which facilitates the solution strategy. Lemma 6.1 is inspired by Liu and Zhang (2003) and described as follows.

Lemma 6.1 Given positive scalars γ , ε_{1i} , and ε_{2i} , the closed-loop system (6.19) is stable with H_∞ performance $\|G_{z,r,d}\|_\infty < \gamma$, if there exist two symmetric positive definite matrices X and Y , and matrices K_{xi} , L_{1i} , X_{ii} , $X_{ij} = X_{ji}$, $i \neq j$, $i, j = 1, 2, \dots, h$, such that

$$\begin{bmatrix} \text{He}(X\Lambda_{ii}) & XE_{ii} \\ \star & \text{He}(Y\Gamma_{ii}) \end{bmatrix} < X_{ii}, \quad (6.20)$$

$$\begin{bmatrix} \text{He}(X\Lambda_{ij}) & X(E_{ij} + E_{ji}) \\ \star & \text{He}(Y\Gamma_{ij}) \end{bmatrix} < X_{ij} + X_{ij}^\top, \quad (6.21)$$

$$\begin{bmatrix} X_{11} & \cdots & X_{1h} & \Pi_1 \\ \vdots & \ddots & \vdots & \vdots \\ X_{1h}^\top & \cdots & X_{hh} & \Pi_h \\ \Pi_1^\top & \cdots & \Pi_h^\top & -I \end{bmatrix} < 0, \quad (6.22)$$

where $\Lambda_{ii} = A_i + B_i K_{xi}$, $E_{ii} = [-B_i K_{xi} \ F_i \ 0]$, $\Gamma_{ii} = \Xi \bar{A}_i - L_{1i} \bar{C}$, $\Lambda_{ij} = A_i + A_j + B_i K_{xj} + B_j K_{xi}$, $\Gamma_{ij} = 2(\Xi \bar{A}_i - L_{1i} \bar{C})$, $E_{ij} = [-B_i K_{xj} \ F_i \ 0]$, $E_{ji} = [-B_j K_{xi} \ F_j \ 0]$, $\Pi_i = \text{diag}(\Pi_{1i}, \Pi_{2i})$, $\Pi_{1i} = [\lambda_{1i} X M_{0i} \ \lambda_{2i} N_{0i}^\top \ 0 \ \lambda_{4i} X \hat{D}_i \ C_x^\top]$, $\Pi_{2i} = [0 \ 0 \ \lambda_{3i} Y \Xi \bar{M}_{0i} \ \lambda_{4i} Y \Xi \bar{D}_i \ C_e^\top]$, $\lambda_{1i} = \sqrt{\varepsilon_{2i}^{-1}}$, $\lambda_{2i} = \sqrt{\mu \varepsilon}$, $\lambda_{3i} = \sqrt{\varepsilon_{1i}^{-1}}$, and $\lambda_{4i} = \gamma^{-1}$.

Proof: Consider a Lyapunov function $V_e = e^\top Y e$. Define $\bar{M}_{0i} = [M_{0i}^\top \ 0]^\top$ and $\chi_{1i} = \bar{x}^\top \Delta \bar{A}_i^\top \Xi^\top Y e + e^\top Y \Xi \Delta \bar{A}_i \bar{x}$, then for some positive scalars ε_{1i} ,

$$\begin{aligned} \chi_{1i} &= - \left[\sqrt{\varepsilon_{1i}^{-1}} \bar{M}_{0i}^\top \Xi^\top Y e - \sqrt{\varepsilon_{1i}} F_{0i} N_{0i} x \right]^\top \times \left[\sqrt{\varepsilon_{1i}^{-1}} \bar{M}_{0i}^\top \Xi^\top Y e - \sqrt{\varepsilon_{1i}} F_{0i} N_{0i} x \right] \\ &\quad + \varepsilon_{1i}^{-1} e^\top Y \Xi \bar{M}_{0i} \bar{M}_{0i}^\top \Xi^\top Y e + \varepsilon_{1i} x^\top N_{0i}^\top F_{0i}^\top F_{0i} N_{0i} x \\ &\leq \varepsilon_{1i}^{-1} e^\top Y \Xi \bar{M}_{0i} \bar{M}_{0i}^\top \Xi^\top Y e + \varepsilon_{1i} \mu_i x^\top N_{0i}^\top N_{0i} x. \end{aligned}$$

Thus the time derivative of V_e is

$$\begin{aligned}
\dot{V}_e &= \sum_{i=1}^h \rho_i \left[e^\top \text{He}(Y(\Xi \bar{A}_i - L_{1i} \bar{C}))e + \text{He}(e^\top Y \Xi \bar{D}_i \bar{d}) + \chi_{1i} \right] \\
&\leq \sum_{i=1}^h \rho_i \left\{ e^\top \left[\text{He}(Y(\Xi \bar{A}_i - L_{1i} \bar{C})) + \varepsilon_{1i}^{-1} Y \Xi \bar{M}_{0i} \bar{M}_{0i}^\top \Xi^\top Y \right] e \right. \\
&\quad \left. + \text{He}(e^\top Y \Xi \bar{D}_i \bar{d}) + \varepsilon_{1i} \mu_i x^\top N_{0i}^\top N_{0i} x \right\}. \tag{6.23}
\end{aligned}$$

Consider a Lyapunov function $V_x = x^\top X x$ for the control system. Define $\chi_{2i} = x^\top \Delta A_i^\top X x + x^\top X \Delta A_i x$, it follows that for some positive scalars ε_{2i} ,

$$\begin{aligned}
\chi_{2i} &= - \left[\sqrt{\varepsilon_{2i}}^{-1} M_{0i}^\top X x - \sqrt{\varepsilon_{2i}} F_{0i} N_{0i} x \right]^\top \times \left[\sqrt{\varepsilon_{2i}}^{-1} M_{0i}^\top X x - \sqrt{\varepsilon_{2i}} F_{0i} N_{0i} x \right] \\
&\quad + \varepsilon_{2i}^{-1} x^\top X M_{0i} M_{0i}^\top X x + \varepsilon_{2i} x^\top N_{0i}^\top F_{0i}^\top F_{0i} N_{0i} x \\
&\leq \varepsilon_{2i}^{-1} x^\top X M_{0i} M_{0i}^\top X x + \varepsilon_{2i} \mu_i x^\top N_{0i}^\top N_{0i} x.
\end{aligned}$$

Similarly, the time derivative of V_x is

$$\begin{aligned}
\dot{V}_x &= \sum_{i=1}^h \sum_{j=1}^h \rho_i \rho_j \left[x^\top \text{He}(X(A_i + B_i K_{xj}))x + \text{He}(x^\top X \bar{F}_{ij} e) + \chi_{2i} + \text{He}(x^\top X \hat{D}_i \bar{d}) \right] \\
&\leq \sum_{i=1}^h \sum_{j=1}^h \rho_i \rho_j \left\{ x^\top \left[\text{He}(X(A_i + B_i K_{xj})) + \varepsilon_{2i}^{-1} X M_{0i} M_{0i}^\top X + \varepsilon_{2i} \mu_i N_{0i}^\top N_{0i} \right] x \right. \\
&\quad \left. + \text{He}(x^\top X E_{ij} e) + \text{He}(x^\top X \hat{D}_i \bar{d}) \right\}. \tag{6.24}
\end{aligned}$$

Define $\xi = [x^\top \ e^\top]^\top$ and $V = V_e + V_x$. By (6.23) and (6.24),

$$\begin{aligned}
\dot{V} &\leq \sum_{i=1}^h \sum_{j=1}^h \rho_i \rho_j \xi^\top \begin{bmatrix} J_{1ij} & X E_{ij} \\ \star & J_{2ij} \end{bmatrix} \xi - \sum_{i=1}^h \sum_{j=1}^h \rho_i \rho_j \frac{1}{\gamma^2} \xi^\top P \tilde{D}_i \tilde{D}_i^\top P \xi \\
&\quad + \sum_{i=1}^h \rho_i \left(\bar{d}^\top \tilde{D}_i^\top P \xi + \xi^\top P \tilde{D}_i \bar{d} \right) - z_r^\top z_r, \tag{6.25}
\end{aligned}$$

where γ is a design parameter, $\tilde{D}_i = [\hat{D}_i \ \bar{D}_i]$, $P = \text{diag}(X, Y)$, $\mu_\varepsilon = (\varepsilon_{1i} + \varepsilon_{2i}) \mu_i$,
 $J_{1ij} = \text{He} \left[X(A_i + B_i K_{xj}) \right] + \varepsilon_{2i}^{-1} X M_{0i} M_{0i}^\top X + \mu_\varepsilon N_{0i}^\top N_{0i} + \frac{1}{\gamma^2} X \hat{D}_i \hat{D}_i^\top X + C_x^\top C_x$,
 $J_{2ij} = \text{He} \left[Y(\Xi \bar{A}_i - L_{1i} \bar{C}) \right] + \frac{1}{\gamma^2} Y \Xi \bar{D}_i \bar{D}_i^\top \Xi^\top Y + \varepsilon_{1i}^{-1} Y \Xi \bar{M}_{0i} \bar{M}_{0i}^\top \Xi^\top Y + C_e^\top C_e$.

The H_∞ performance $\|G_{z_r \bar{d}}\|_\infty < \gamma$ can be represented by

$$J = \int_0^\infty \left(z_r^\top z_r - \gamma^2 \bar{d}^\top \bar{d} \right) dt < 0. \quad (6.26)$$

Under zero initial conditions,

$$\begin{aligned} J &= \int_0^\infty \left(z_r^\top z_r - \gamma^2 \bar{d}^\top \bar{d} + \dot{V} \right) dt - \int_0^\infty \dot{V} dt \\ &= \int_0^\infty \left(z_r^\top z_r - \gamma^2 \bar{d}^\top \bar{d} + \dot{V} \right) dt - (V(\infty) + V(0)) \\ &\leq \int_0^\infty \left(z_r^\top z_r - \gamma^2 \bar{d}^\top \bar{d} + \dot{V} \right) dt. \end{aligned}$$

Subsequently, a sufficient condition for (6.26) is

$$J_1 = z_r^\top z_r - \gamma^2 \bar{d}^\top \bar{d} + \dot{V} < 0.$$

Define $\bar{\xi} = [\xi^\top \bar{d}^\top]^\top$ and use (6.25), then equivalently

$$\begin{aligned} J_1 &= \sum_{i=1}^h \sum_{j=1}^h \rho_i \rho_j \bar{\xi}^\top \begin{bmatrix} J_{1ij} & XE_{ij} \\ \star & J_{2ii} \end{bmatrix} \bar{\xi} \\ &\quad - \left(\gamma \bar{d} - \frac{1}{\gamma} \sum_{i=1}^h \rho_i \tilde{D}_i^\top P \bar{\xi} \right)^\top \times \left(\gamma \bar{d} - \frac{1}{\gamma} \sum_{i=1}^h \rho_i \tilde{D}_i^\top P \bar{\xi} \right) \\ &= \sum_{i=1}^h \sum_{j=1}^h \rho_i \rho_j \bar{\xi}^\top \begin{bmatrix} J_{1ij} & XE_{ij} \\ \star & J_{2ii} \end{bmatrix} \bar{\xi} \\ &< 0. \end{aligned} \quad (6.27)$$

By applying the Schur complement (see Appendix A.2) to (6.27), it follows that

$$\sum_{i=1}^h \sum_{j=1}^h \rho_i \rho_j \left(\Phi_{ij} + \Pi_i \Pi_i^\top \right) < 0, \quad (6.28)$$

where $\Pi_i = \text{diag}(\Pi_{1i}, \Pi_{2i})$, $\Phi_{ij} = \begin{bmatrix} \text{He} [X(A_i + B_i K_{xj})] & XE_{ij} \\ \star & \text{He} [Y(\Xi \bar{A}_i - L_{1i} \bar{C})] \end{bmatrix}$,
 $\Pi_{1i} = [\lambda_{1i} X M_{0i} \ \lambda_{2i} N_{0i}^\top \ 0 \ \lambda_{4i} X \hat{D}_i \ C_x^\top]$, $\Pi_{2i} = [0 \ 0 \ \lambda_{3i} Y \Xi \bar{M}_{0i} \ \lambda_{4i} Y \Xi \bar{D}_i \ C_e^\top]$.

If (6.20) - (6.21) hold, then it follows from (6.28) that

$$\sum_{i=1}^h \sum_{j=1}^h \rho_i \rho_j \left(X_{ij} + \Pi_i \Pi_i^\top \right) < 0,$$

which can be ensured by (6.22). \square

Since (6.20) - (6.21) are nonlinear inequalities and cannot be solved by LMI tools directly, Lemma 6.1 is further converted into an equivalent Lemma 6.2 with LMIs.

Lemma 6.2 There exist two symmetric positive definite matrices X and Y , and matrices K_{xi} , L_{1i} , X_{ii} , $X_{ij} = X_{ji}$, $i \neq j$, $i, j = 1, 2, \dots, h$, such that (6.20) - (6.22) hold, if and only if there exist two symmetric positive definite matrices \bar{X} and Y , and matrices K_{xi} , L_{1i} , P_{ij} , and Q_{ij} with P_{ii} and Q_{ii} symmetric, $i < j$, $i, j = 1, 2, \dots, h$, such that

$$\begin{aligned} \text{He}(\Lambda_{ii} \bar{X}) &< P_{ii}, \\ \text{He}(Y \Gamma_{ii}) &< Q_{ii}, \\ \text{He}(\Lambda_{ij} \bar{X}) &< P_{ij} + P_{ij}^\top, \\ \text{He}(Y \Gamma_{ij}) &< Q_{ij} + Q_{ij}^\top, \quad i < j, \\ \begin{bmatrix} P_{11} & \cdots & P_{1h} & \hat{\Pi}_{11} \\ \vdots & \ddots & \vdots & \vdots \\ P_{1h}^\top & \cdots & P_{hh} & \hat{\Pi}_{1h} \\ \hat{\Pi}_{11}^\top & \cdots & \hat{\Pi}_{1h}^\top & -I \end{bmatrix} &< 0, \\ \begin{bmatrix} Q_{11} & \cdots & Q_{1h} \\ \vdots & \ddots & \vdots \\ Q_{1h}^\top & \cdots & Q_{hh} \end{bmatrix} &< 0, \end{aligned}$$

where $\hat{\Pi}_{1i} = [\lambda_{1i} M_{0i} \quad \lambda_{2i} \bar{X} N_{0i}^\top \quad 0 \quad \lambda_{4i} D_i \quad \bar{X} C_x^\top]$.

Proof: The proof of Lemma 6.2 is achieved with minor modification according to the proof of Lemma 2 in Lin et al. (2005), and thus is omitted here. \square

Now Theorem 6.3 based on Lemma 6.2 is given to solve the integrated design problem for the composite closed-loop system (6.19).

Theorem 6.3 Given positive scalars γ , ε_{1i} , and ε_{2i} , the system (6.19) is stable with the H_∞ performance $\|G_{z,d}\|_\infty < \gamma$, if there exist two symmetric positive definite matrices

\bar{X} and Y , and matrices \hat{K}_i , \hat{H} , \hat{L}_i , P_{ij} , and Q_{ij} with P_{ii} and Q_{ii} symmetric, $i < j$, $i, j = 1, 2, \dots, h$, such that

$$\begin{aligned} \text{He}(A_i\bar{X} + B_i\hat{K}_i) &< P_{ii}, \\ \text{He}[(Y - \hat{H}\bar{C})\bar{A}_i - \hat{L}_i\bar{C}] &< Q_{ii}, \\ \text{He}(A_i\bar{X} + A_j\bar{X} + B_i\hat{K}_j + B_j\hat{K}_i) &< P_{ij} + P_{ij}^\top, \\ \text{He}[2((Y - \hat{H}\bar{C})\bar{A}_i - \hat{L}_i\bar{C})] &< Q_{ij} + Q_{ij}^\top, \\ \begin{bmatrix} P_{11} & \cdots & P_{1h} & \hat{\Pi}_{11} \\ \vdots & \ddots & \vdots & \vdots \\ P_{1h}^\top & \cdots & P_{hh} & \hat{\Pi}_{1h} \\ \hat{\Pi}_{11}^\top & \cdots & \hat{\Pi}_{1h}^\top & -I \end{bmatrix} &< 0, \\ \begin{bmatrix} Q_{11} & \cdots & Q_{1h} \\ \vdots & \ddots & \vdots \\ Q_{1h}^\top & \cdots & Q_{hh} \end{bmatrix} &< 0, \end{aligned}$$

where $\hat{\Pi}_{1i} = [\lambda_{1i}M_{0i} \ \lambda_{2i}\bar{X}N_{0i}^\top \ 0 \ \lambda_{4i}D_i \ \bar{X}C_x^\top]$. Then the gains are given by: $K_{xi} = \hat{K}_i\bar{X}^{-1}$, $H = Y^{-1}\hat{H}$, and $L_{1i} = Y^{-1}\hat{L}_i$, $i = 1, 2, \dots, h$.

Proof: Denote $\hat{K}_i = K_{xi}\bar{X}$, $\hat{H} = YH$, and $\hat{L}_i = YL_{1i}$, $i = 1, 2, \dots, h$, then the proof of Theorem 6.3 follows directly from Lemma 6.2. \square

6.5.3 Computational complexity analysis

The design parameters of the observer (6.4) and the controller (6.10) are obtained by solving the LMIs in Theorem 6.3 using the Matlab LMI toolbox (Gahinet et al., 1995). For the LMIs in Theorem 6.3, define R_0 and S_0 as the total row size and the total number of scalar variables, respectively. According to Gahinet et al. (1995), the computational complexity (or number of flops) $N(\varepsilon)$ needed to get an ε -accurate solution of the LMIs in Theorem 6.3 is $N(\varepsilon) = R_0S_0^3 \log(V/\varepsilon)$, where V is a data-dependent scaling factor.

For the proposed integrated FE/FTC approach: $R_0 = (h^2 + 3h + 1)n + (h^2 + 3h)(kq + k_1q_1)/2$ and $S_0 = hnm + p(n + kq + k_1q_1) + (h^2 + h + 2)[n(n + 1) + (n + kq + k_1q_1)(n + kq + k_1q_1 + 1)]/4$. Similarly, it can be calculated for the separated FE/FTC approach that: $R_0 = h[4n + (k + 2)q + (k_1 + 2)q + 2l + z_1 + p]$, $S_0 = hnm + (1 + h)p(n + kq + k_1q_1) + [n(n + 1) + (n + kq + k_1q_1)(n + kq + k_1q_1 + 1)]/2$.

Compared with the separated approach, the proposed integrated approach has higher computational complexity. The computational complexity of the integrated design mainly depends on: 1) dimensions of the system and faults, 2) the sub-model numbers of the fuzzy system, and 3) the fault orders. Among the above three factors, 2) and 3) can be tuned. Although increasing 2) and 3) can provide more accurate approximation of the nonlinear system and fault modelling, it leads to higher computational complexity. Therefore, a trade-off needs to be made for choosing the numbers of fuzzy rules and fault modelling orders.

Furthermore, since the combined observer and controller structures of the integrated and separately designed FTC systems are the same, it also follows that their online computational loads are identical. As the design parameters of the observer/controller are obtained from the LMIs off-line the resulting online computational burden is expected to be low.

Remark 6.4 Two more sets of scalars ε_{1i} and ε_{2i} , $i = 1, 2, \dots, h$, need to be chosen to solve Theorem 6.3, due to the consideration of the presence of the uncertainty. Note that although the T-S fuzzy system control systems (Lin et al., 2005; Liu and Zhang, 2003) use observer-based state feedback, the presence of faults is not considered. In the light of this the current work faces a bigger challenge since both the robust fault estimation and fault tolerant compensation are included. However, by taking into account *a priori* the presence of uncertainty and disturbance and the subsequent *bi-directional robustness interactions* between the FE observer and the FTC control system, the proposed integrated approach is applicable to systems with faults, uncertainty, and external disturbance.

Remark 6.5 As reviewed in Chapter 3, there is no such systematic integrated FE/FTC design strategy for T-S fuzzy systems. The existing works mostly follow the separated FE/FTC design idea, although using different FE observers and control designs. Thus, without loss of generality, a brief presentation of the separated design idea and its conservativeness are provided in Section 6.5.1 for the proposed ASUIO and FTC controller. This motivates the research on the integrated FE/FTC design in this chapter. Comparisons of the performances of these two design methods are provided based on the simulation results shown in Section 6.6, which then help to illustrate the importance and advantages of the integrated design idea.

6.6 A tutorial example

In this section the effectiveness of the proposed integrated design is demonstrated by applying it to the stabilization of an inverted pendulum on a cart. The pendulum used has a nonlinear model (Wang et al., 1996) in the form of

$$\begin{aligned}\dot{x}_1 &= x_2, \\ \dot{x}_2 &= \frac{g \sin(x_1) - amlx_2^2 \sin(2x_1)/2 - a \cos(x_1)u}{4l/3 - aml \cos^2(x_1)}, \\ y &= [x_1 \ x_2]^\top,\end{aligned}$$

where x_1 and x_2 represent the angle of the pendulum from the vertical and the angular velocity, respectively. g is the gravity constant, m is the pendulum mass, M is the cart mass, $2l$ is the pendulum length, u is the force applied to the cart, and $a = 1/(m + M)$. The model parameters used in this study are $m = 2.0$ kg, $M = 8.0$ kg, and $2l = 1.0$ m.

The balancing problem for the pendulum with actuator faults and disturbance is studied in Zhang et al. (2010a) using separately designed adaptive observer and dynamic output feedback controller. The pendulum system (6.29) is nonlinear but two points in (x_1, x_2) are considered to derive the two-rule T-S fuzzy pendulum model. Moreover, the pendulum system model is assumed to have uncertainty, disturbance, and actuator/sensor faults. According to Wang et al. (1996), the following two-rule pendulum system model is valid in the controllable region $x_1 \in (-90, 90)$ deg,

$$\begin{aligned}\dot{x} &= \sum_{i=1}^2 \rho_i(x_1) [(A_i + \Delta A_i)x + B_i(u + f_a) + D_i d], \\ y &= Cx + F_s f_s,\end{aligned}\tag{6.29}$$

where

$$\begin{aligned}\rho_1(x_1) &= 1 - \frac{2}{\pi}|x_1|, \rho_2(x_1) = \frac{2}{\pi}|x_1|, A_1 = \begin{bmatrix} 0 & 1 \\ \frac{g}{4l/3 - aml} & 0 \end{bmatrix}, B_1 = \begin{bmatrix} 0 \\ -\frac{a}{4l/3 - aml} \end{bmatrix}, \\ A_2 &= \begin{bmatrix} 0 & 1 \\ \frac{2g}{\pi(4l/3 - aml\beta^2)} & 0 \end{bmatrix}, B_2 = \begin{bmatrix} 0 \\ -\frac{a\beta}{4l/3 - aml\beta^2} \end{bmatrix}, C = I_2, \\ D_1 = D_2 &= \begin{bmatrix} 0 \\ 0.01 \end{bmatrix}, F_s = \begin{bmatrix} 0.1 \\ 0.3 \end{bmatrix}, \beta = \cos(88^\circ), \Delta A_1 = \Delta A_2 = \begin{bmatrix} 0 & \sigma_1 \\ \sigma_2 & 0 \end{bmatrix},\end{aligned}$$

and $\sigma_1 = 0.1 \cos(t)$, $\sigma_2 = 0.1 \sin(t)$, $d = 0.01 \sin(10t)$, and the faults are

$$f_a = \begin{cases} 1, & 0 \text{ s} \leq t \leq 5 \text{ s} \\ \sin(t), & 5 \text{ s} < t \leq 20 \text{ s} \\ 1, & 20 \text{ s} < t \leq 30 \text{ s} \end{cases}, f_s = \begin{cases} 0.1, & 0 \text{ s} \leq t \leq 14 \text{ s} \\ 0.2, & 14 \text{ s} < t \leq 23 \text{ s} \\ 0.1, & 23 \text{ s} < t \leq 30 \text{ s} \end{cases}.$$

The two sub-models of fuzzy system (6.29) are verified to be locally observable and controllable, whilst the whole fuzzy system is also verified to be globally observable and controllable using the methods proposed in Ho et al. (2013) and Chen et al. (2009).

The integrated FE/FTC design for the pendulum system is solved with parameters: $k = 3$, $k_1 = 2$, $C_x = [I_2; 0_{7 \times 2}]$, $C_e = [0_{2 \times 7}; I_7]$, $\alpha_s = 0.1$, $\beta_s = 0.1$, $\mu = 1$, $\varepsilon_1 = 100$, $\varepsilon_2 = 15$, and $\gamma = 1$. For comparison, the separated FE/FTC design is also simulated with the same system parameters and $\gamma_1 = 0.86$ and $\gamma_2 = 0.5$.

The H_∞ attenuation levels together with computational complexity (see Section 6.5.3) of the integrated and separated designs are listed in Table 6.1. Compared with the separated FE/FTC approach, the proposed integrated approach loses a certain degree of FTC robustness resulting from the sharing of the common Lyapunov matrices in the observer and controller designs. The proposed integrated design also has higher design computational complexity. However, it is shown in the table that for these two approaches the solutions for the gains are not time consuming (performed on a PC computer with a 3.10 GHz 4 cores Intel i5-2400 CPU).

Table 6.1 H_∞ attenuation level and consuming time.

	Integrated design	Separated design	
		Observer	Controller
γ_{\min}	0.10	0.77	0.01
R_0, S_0	47, 142	34, 70	22, 7
CPU time (s)	0.156	0.0468	0.0312

Solving Theorem 6.3 with the chosen parameters gives the following observer and controller gains:

$$K_{x_1} = [1062 \ 309.2], K_{x_2} = [2379.1 \ 672.7],$$

$$\begin{aligned}
M_1 &= \begin{bmatrix} -0.4482 & -14.1330 & -0.0878 & 0 & 0 & -0.1698 & -1.5424 \\ 14.3939 & -0.7661 & -1.0144 & 0 & 0 & -0.4324 & -0.5709 \\ 7.2944 & 69.8885 & -64.1764 & 1 & 0 & -125.1272 & -2.8279 \\ 2.8023 & 27.7887 & -25.4464 & 0 & 1 & -49.7641 & -1.0664 \\ 0.5608 & 6.2677 & -5.6391 & 0 & 0 & -11.1597 & -0.1835 \\ -0.8619 & 1.3328 & 1.9833 & 0 & 0 & -1.2495 & 3.1209 \\ -2.0198 & 1.9634 & 0.9344 & 0 & 0 & 2.0623 & 1.5702 \end{bmatrix}, \\
M_2 &= \begin{bmatrix} -0.9877 & -9.5573 & -0.0019 & 0 & 0 & 1.3561 & -1.5424 \\ 9.5774 & -1.5836 & -0.0221 & 0 & 0 & 1.2341 & -0.5709 \\ 2.9603 & -1.6618 & -1.4005 & 1 & 0 & 4.4030 & -2.8279 \\ 1.0841 & -0.5824 & -0.5553 & 0 & 1 & 1.5952 & -1.0664 \\ 0.1947 & -0.0669 & -0.1231 & 0 & 0 & 0.2092 & -0.1835 \\ -1.5368 & 1.9598 & 0.0433 & 0 & 0 & -5.8085 & 3.1209 \\ -1.6108 & 1.8959 & 0.0204 & 0 & 0 & -4.2464 & 1.5702 \end{bmatrix}, \\
L_1 &= \begin{bmatrix} -107 & 16 \\ -81 & 98 \\ -15150 & 5936 \\ -6029 & 2361 \\ -1340 & 525 \\ 588 & -182 \\ 307 & -87 \end{bmatrix}, \quad L_2 = \begin{bmatrix} -99.1268 & 3.7239 \\ 111.3488 & -0.9468 \\ 601.9768 & -229.2507 \\ 216.8746 & -83.4618 \\ 44.6287 & -16.3783 \\ 93.7791 & 9.0680 \\ 83.5292 & 3.6323 \end{bmatrix}, \\
G_1 &= \begin{bmatrix} -0.0878 \\ -1.0144 \\ -64.1764 \\ -25.4464 \\ -5.6391 \\ 1.9833 \\ 0.9344 \end{bmatrix}, \quad G_2 = \begin{bmatrix} -0.0019 \\ -0.0221 \\ -1.4005 \\ -0.5553 \\ -0.1231 \\ 0.0433 \\ 0.0204 \end{bmatrix}, \quad H = \begin{bmatrix} 15.8632 & -0.1463 \\ 7.7810 & -0.6906 \\ 349.1615 & -106.9607 \\ 137.8961 & -42.4106 \\ 30.0311 & -9.3986 \\ -31.1252 & 3.3054 \\ -20.3739 & 1.5573 \end{bmatrix}.
\end{aligned}$$

6.6.1 Comparison of linear FTC and T-S fuzzy integrated FTC

This section demonstrates the superiority of the proposed T-S fuzzy integrated FTC design to the linear FTC design (with the pendulum model linearized around the stable point, i.e., $\rho_2(x_1) = 0$). The ranges of the balancing initial angle considered for each of the methods are examined here with $z(0) = 0.17 \times 1$ and $x_2(0) = 0$, along with different initial angles.

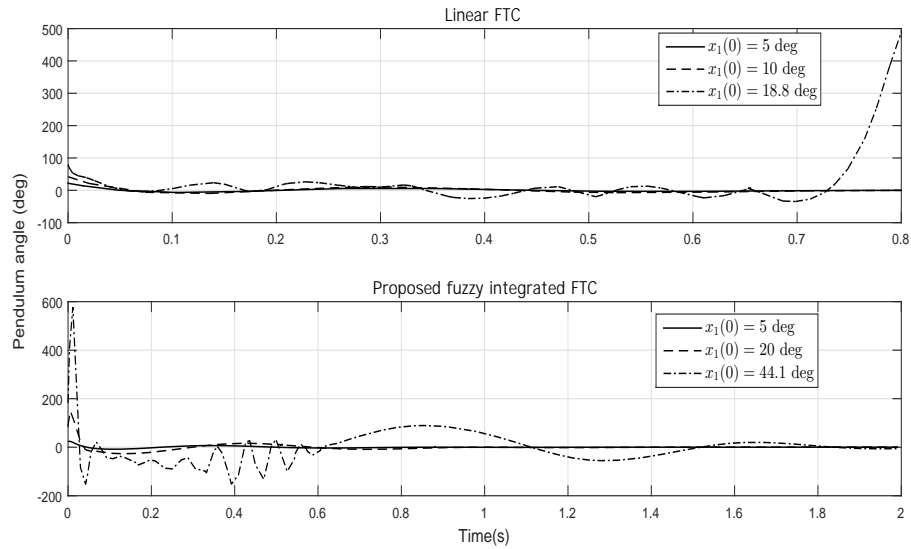


Fig. 6.1 Angle response using linear and T-S fuzzy integrated FTC.

Table 6.2 Maximum initial angle $|x_1(0)|$ of the pendulum.

Cases	T-S fuzzy design	linear design
Actuator fault case	45 deg	19.5 deg
Sensor fault case	44.1 deg	18.8 deg
Actuator/sensor faults case	44.1 deg	18.8 deg

In the presence of both actuator and sensor faults, simulation results in Fig. 6.1 indicate that the proposed T-S fuzzy integrated FTC can balance the pendulum for initial angles $|x_1(0)| \leq 44.1$ deg ($x_2(0) = 0$). In contrast, the linear control fails to balance the pendulum for initial angles $|x_1(0)| \geq 18.8$ deg. Similar simulations are performed for the cases when the pendulum has either an actuator fault or a sensor fault. The maximum initial angles of the pendulum for all the three cases are summarized in Table 6.2, from which it is concluded that the proposed T-S fuzzy integrated FTC design balances the pendulum for much larger initial angles than the linear FTC.

6.6.2 Comparison of integrated and separated FE/FTC designs

In order to demonstrate well the effectiveness of the proposed integrated FE/FTC design and its superior FE/FTC performance compared with the separated design, two sets of simulations are carried out for the pendulum with different initial angles and different uncertainties, respectively.

(1) Performance with different initial angles

Simulations are performed with uncertainties $\sigma_1 = 0.1 \cos(t)$ and $\sigma_2 = 0.1 \sin(t)$ in three cases. *Case 1*: The pendulum has only actuator fault; *Case 2*: The pendulum has only sensor fault; *Case 3*: The pendulum has both actuator and sensor faults.

From Figs. 6.2 - 6.8, it is observed that in the whole range of the balancing initial angles listed in Table 6.2, the proposed integrated FE/FTC design achieves better FE/FTC performance than the separated design in all the three cases simulated. Except for *Case 2* when the pendulum has only actuator fault, the separated design cannot balance the pendulum.

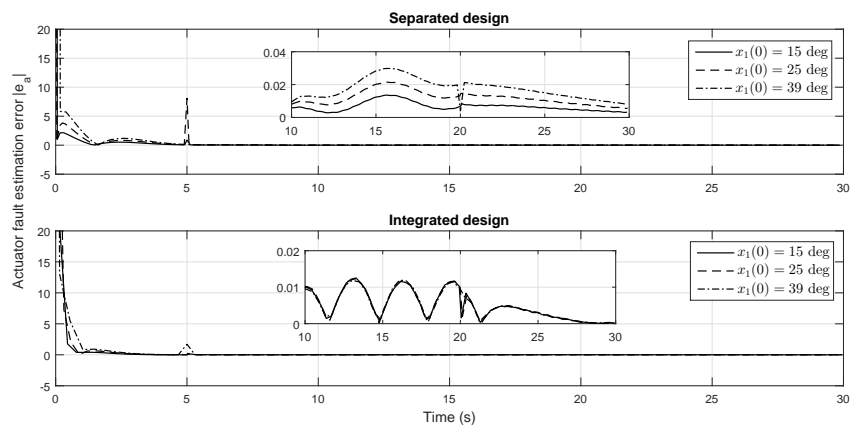


Fig. 6.2 Actuator fault estimation with different initial angles: *Case 1*.

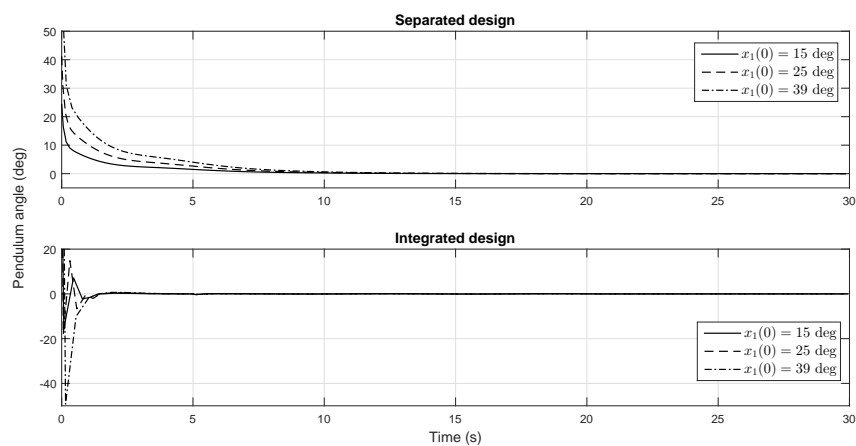
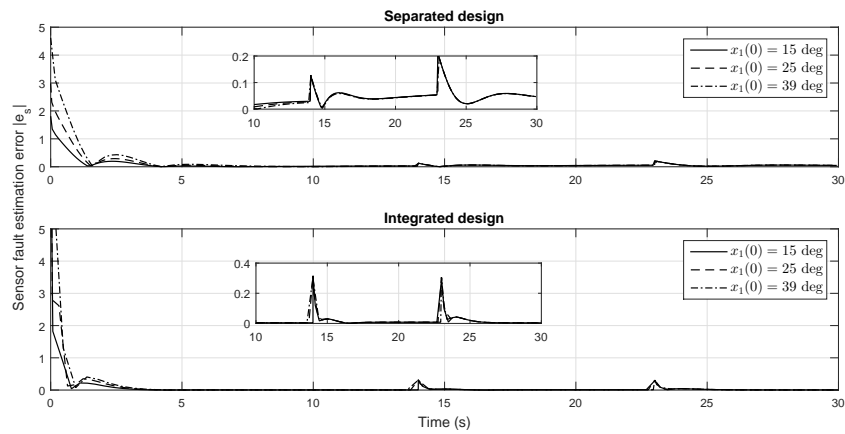
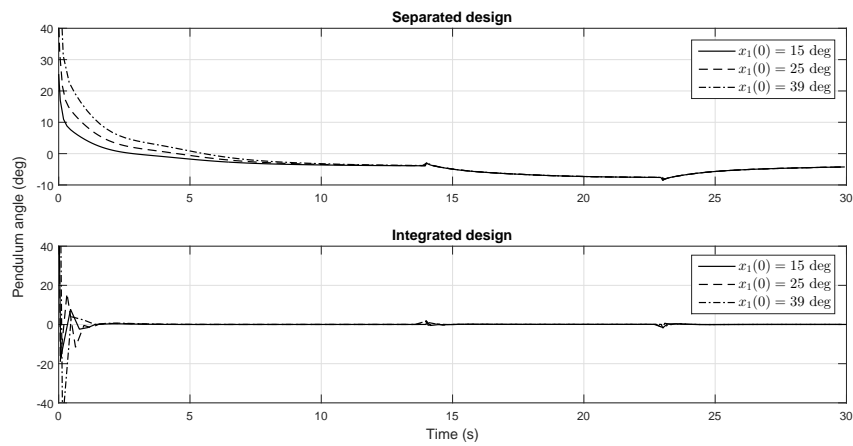
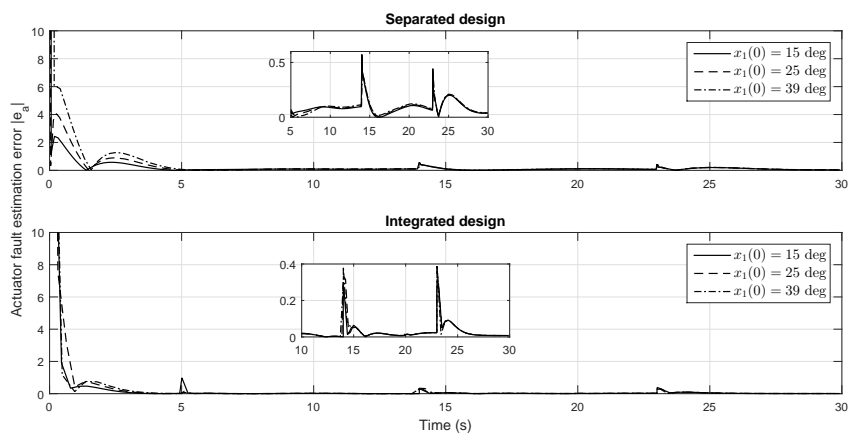


Fig. 6.3 Angle response with different initial angles: *Case 1*.

Fig. 6.4 Sensor fault estimation with different initial angles: *Case 2*.Fig. 6.5 Angle response with different initial angles: *Case 2*.Fig. 6.6 Actuator fault estimation with different initial angles: *Case 3*.

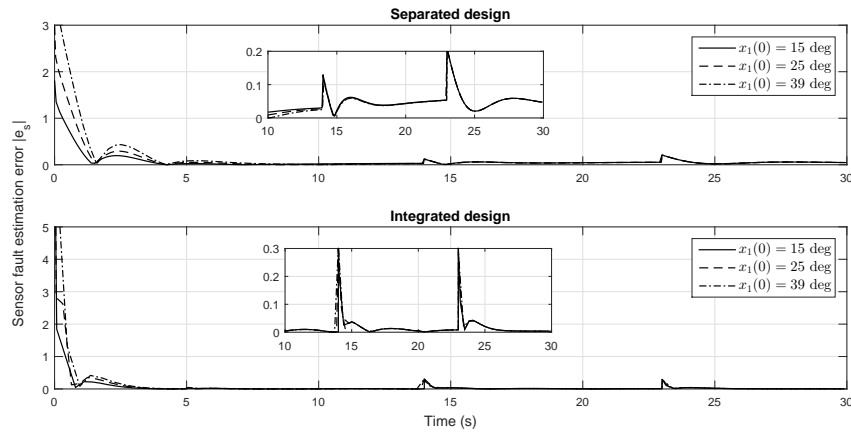


Fig. 6.7 Sensor fault estimation with different initial angles: *Case 3*.

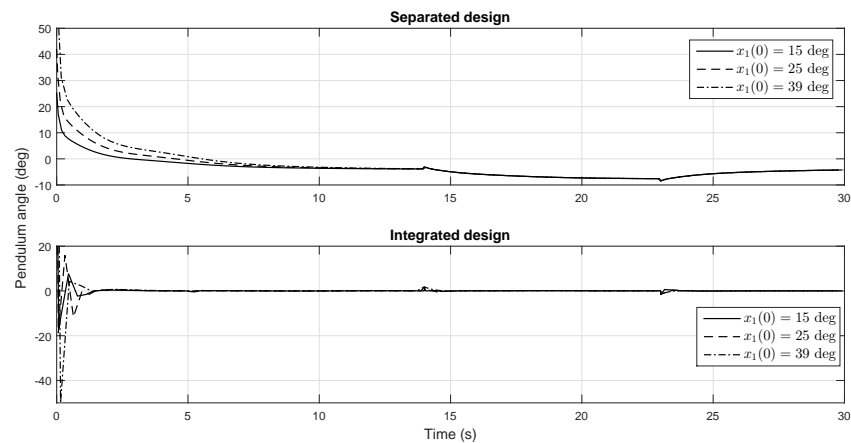
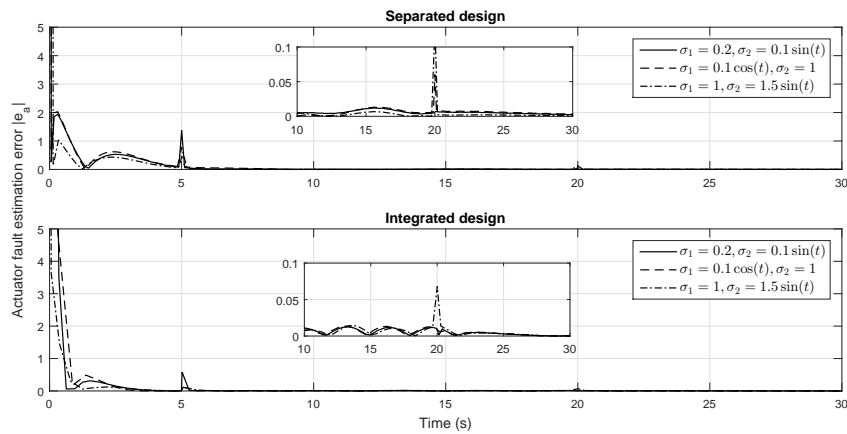
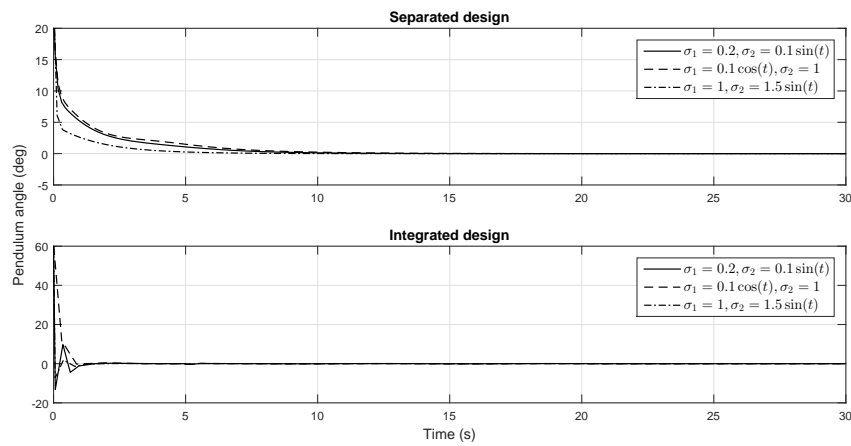
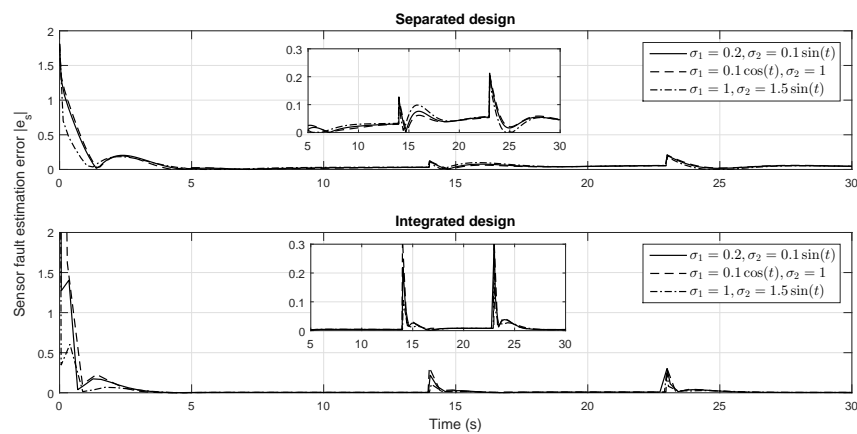


Fig. 6.8 Angle response with different initial angles: *Case 3*.

(2) Performance with different uncertainties

To test the robustness of the proposed design, comparative simulations are performed with initial conditions $z(0) = 0.17 \times 1$ and $x_2(0) = 0$ under different uncertainties. The initial angle is set as $x_1(0) = 15$ deg. Three cases of simulations are carried out. *Case 1*: The pendulum has one actuator fault (with no sensor faults); *Case 2*: The pendulum has only a single sensor fault (with no actuator faults); *Case 3*: The pendulum has one actuator fault and one sensor fault.

In the presence of different uncertainties, it is observed from Figs. 6.9 - 6.15 that the proposed integrated design performs well with better FE/FTC robustness to the uncertainties than the separated design for all the three fault cases considered.

Fig. 6.9 Actuator fault estimation with different uncertainties: *Case 1*.Fig. 6.10 Angle response with different uncertainties: *Case 1*.Fig. 6.11 Sensor fault estimation with different uncertainties: *Case 2*.

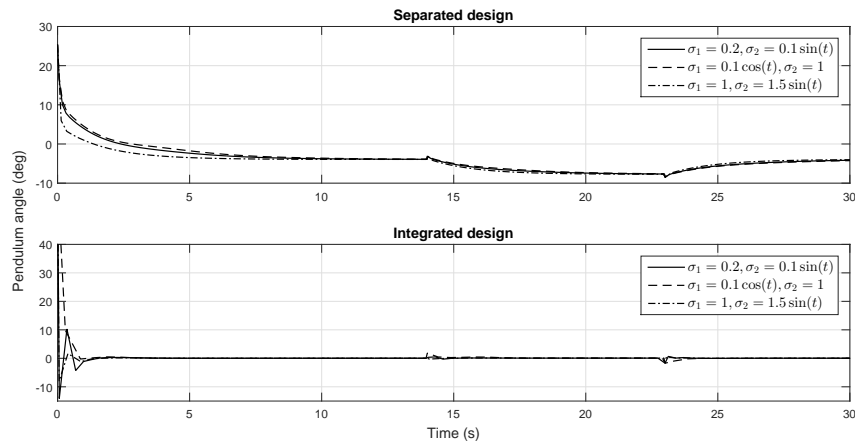


Fig. 6.12 Angle response with different uncertainties: *Case 2*.

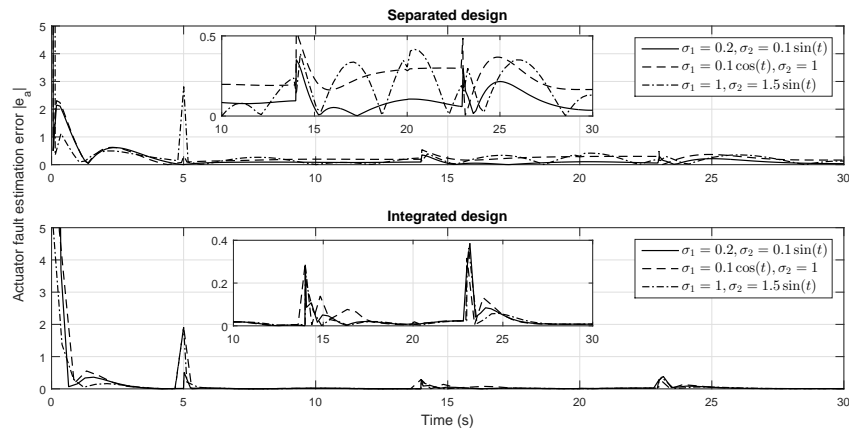


Fig. 6.13 Actuator fault estimation with different uncertainties: *Case 3*.

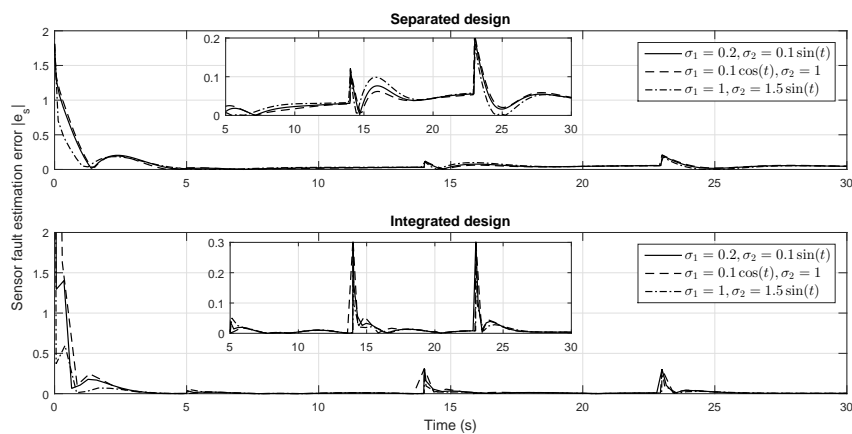


Fig. 6.14 Sensor fault estimation with different uncertainties: *Case 3*.

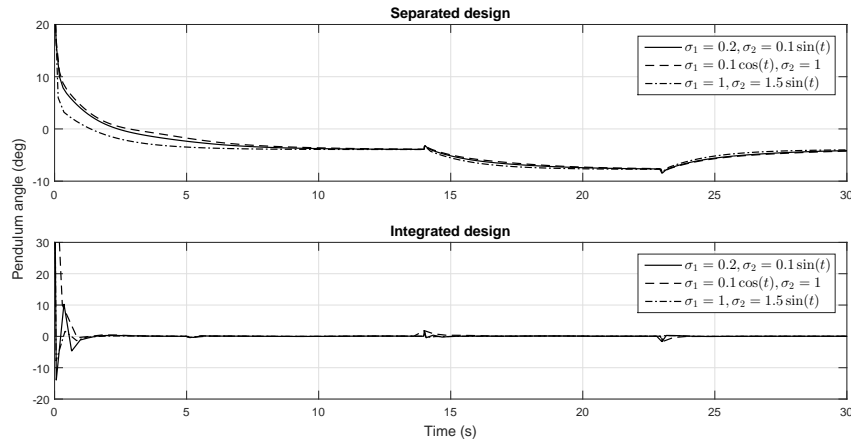


Fig. 6.15 Angle response with different uncertainties: *Case 3*.

Summarizing the results, in the presence of uncertainty, disturbance and faults, the proposed integrated design achieves better FE/FTC performance with higher robustness to the uncertainty than the separated design. Moreover, the separated design is unable to balance the pendulum when sensor faults exist.

6.7 Conclusion

In this chapter a new integrated FE/FTC design strategy is proposed for nonlinear systems subject to actuator and sensor faults along with uncertainty and disturbance using T-S fuzzy modelling. An ASUIO is proposed to estimate the system state variables and faults simultaneously, and then the obtained estimates are used to construct a fuzzy FTC controller. Compared to the FDI-based FTC system design which requires an optimal residual threshold setting and a robust stable reconfigurable mechanism, the direct use of the observer-based FE within the FTC system design framework is proposed to enable the integrated design to be an observer-based robust control problem with a single-step LMI formulation. The simulation example corresponds to a physical system illustrating the effectiveness of the proposed integrated FTC design and its practical potential. By considering in advance the *bi-directional robustness interactions* between the FE and FTC, the proposed integrated design can achieve much better overall FTC system performance than the separated design.

Chapter 7: Integrated FE/FTC for a Lipschitz nonlinear 3-DOF helicopter system with actuator faults and saturation

7.1 Introduction

It is described in Chapter 3 that the occurrence of inevitable system modelling uncertainty and estimation uncertainty lead to an existence of *bi-directional robustness interactions* between the FE and FTC functions within a closed-loop system scheme, which gives rise to a requirement of an integration of FE and FTC to achieve robust FTC performance. Chapter 4 proposes an effective integrated FE/FTC strategy for uncertain linear systems using a single-step LMI formulation and it is extended to T-S fuzzy modelling nonlinear systems in Chapter 6. However, Chapters 4 and 6 do not consider the effects of actuator saturation. Actuator saturation has the effect of paralysing the action of the control system, and hence in order to achieve the full control performance it is necessary to take the saturation into account as a form of malfunction of the system. An integrated FE/FTC design strategy for systems taking into account the actuator saturation becomes the focus of this chapter. The chapter uses as an important application the problem of FTC design of a Lipschitz nonlinear 3-DOF (degree-of-freedom) helicopter system with actuator actuation.

Reliability is critical for flight control systems, since aircraft may suffer from certain system faults (e.g., actuator, sensor and component faults) that prevent them from achieving manoeuvre tasks, degrade system performance and stability, and hence safety. In order to achieve reliable and safe flight, it is necessary to operate the aircraft with redundant systems with either hardware or software redundancy. So that in the presence

of faults, a redundant component or subsystem can be used to return the aircraft to healthy operation. For manned aircraft systems it is usual to use hardware redundancy (i.e., duplicate copies of actuators and sensors). However, for unmanned aircraft the possibility of using hardware redundancy is rather limited due to size and weight restrictions. For such aircraft, analytic forms of redundancy become essential. FTC provides a way for recovering the acceptable aircraft performance and stability in the presence of certain faults.

One way to achieve FTC is to have an FDI unit to detect and isolate the presence of faults with an additional system for managing the switching of different feedback controllers to maintain acceptable aircraft system performance, see for example, Ducard (2009); Edwards et al. (2010); Zolghadri et al. (2014). Instead of using FDI, the work in this thesis focuses on FE (see Chapters 1, 2, and 3 for more discussion).

Unmanned aerial vehicles (UAVs) have numerous applications in military and civilian domains, due to their small size and features of long air hovering, vertical take-off and landing capability, low-speed/-altitude and flexible flight (Hua et al., 2013). The control designs for unmanned helicopters have been researched extensively, see for example, Alexis et al. (2012); Chen et al. (2010); Izaguirre-Espinosa et al. (2016); Li et al. (2015). Considering reliability and safety, FE and FTC designs for helicopter control systems have also attracted much attention, see Ducard (2009); Qi et al. (2014, 2013); Vachtsevanos et al. (2005); Valavanis and Vachtsevanos (2014) and the references therein.

The implementation of FTC of most UAVs becomes very challenging due to the lack of actuator or sensor (hardware) redundancy in these systems. An exception to this for UAVs is the actuator redundancy that exists in hexrotor and octorotor systems. However, in this study all forms of hardware redundancy are excluded as a deliberate exercise to test the potential of FE-based FTC.

The Quanser 3-DOF helicopter model with twin rotors (Apkarian, 2006) is considered in this chapter. This model has been used by many researchers as a benchmark case study which is representative of the rigid body dynamics of a full-size tandem rotor transport and rescue helicopter. Many studies focus on the use of this system to verify control designs (Li et al., 2015; Meza-Sánchez et al., 2015; Shan et al., 2005; Zheng and Zhong, 2011). It is interesting to note that this system can also be representative of a rigid body UAV system. There is no hardware redundancy and the FTC must be based fully on the analytical or functional redundancy concept, e.g., using FE with combined fault and state estimation.

Many FE/FTC designs for the Quanser 3-DOF helicopter model have also been published (Afonso and Galvão, 2010; Chen et al., 2013a, 2016a,c; de Loza et al., 2015; Zheng et al., 2014). Chen et al. (2016a) propose a sliding mode observer (SMO) for actuator fault estimation for a Lipschitz nonlinear helicopter model without uncertainty and external disturbance. In their work the faults are estimated with bounded errors and FTC is not considered. Afonso and Galvão (2010) present a robust model predictive FTC design considering a linear 3-DOF helicopter system with uncertainty, disturbance and an actuator fault. However, model predictive control involves online optimization and their work does not include FE. Chen et al. (2013a, 2016c); Zheng et al. (2014) describe a number of adaptive FTC schemes for uncertain nonlinear 3-DOF helicopter systems, however they also exclude FE in their studies. On the other hand, an FE-based FTC output tracking strategy is developed in de Loza et al. (2015) for a linearized 3-DOF helicopter with perturbations and oscillatory and drift actuator faults. In their work FE is obtained by a high order SMO and FTC is achieved by backstepping SMC based on triangular system decomposition. The main limitations of their work are: 1) the FE requires system output derivatives which are difficult to obtain in real implementation, and 2) the FE observer and FTC controller are designed separately without considering the mutual influences between the estimation and control.

Consideration of actuator saturation is important in flight system design and for full-size aircraft it is always taken into account. It is thus necessary to include a study of the effect of actuator saturation on the performance of an FTC scheme for a UAV. Actuator saturation problems for 3-DOF helicopters have been considered in Kiefer et al. (2010) using an inversion-based control approach, and in Zheng et al. (2015) using an anti-windup compensator. However, neither of these studies pays attention to actuator faults. Qi et al. (2016) considers the self-healing control for a single-rotor UAV with actuator fault and constraints using an anti-windup compensator (not FTC).

This chapter aims to further extend the integrated FE/FTC strategy in Chapter 4 with application to the stabilization of the elevation and pitch motions of an uncertain Lipschitz nonlinear 3-DOF helicopter system with both actuator faults and saturation. Compared with the existing works, the main contributions of this chapter are summarized as follows.

- An uncertain Lipschitz nonlinear 3-DOF helicopter with both actuator faults and saturation is considered. The actuator faults and the saturation are combined into a composite fault function which are non-differentiable. The composite fault function is further approximated by a differentiable function with a sufficiently small error and treated as a new system state that is estimated by a nonlinear ASUIO. Unlike the

adaptive SMO (Chen et al., 2016a) and high order SMO (de Loza et al., 2015) FE methods, the proposed nonlinear ASUIO can achieve asymptotic estimation of the faults with no need for system output derivatives.

- An adaptive sliding mode FTC controller is proposed to compensate the effects of the actuator faults and saturation and stabilize the elevation and pitch motions of the 3-DOF helicopter. SMC is known as a robust control method, since once sliding motion is reached the system is insensitive to any matched perturbation (within the range space spanned by the control input) (Edwards and Spurgeon, 1998). Moreover, the adaptive method is incorporated with the SMC to avoid the requirement of *a priori* knowledge of the perturbation bounds. Compared with model predictive FTC (Afonso and Galvão, 2010), adaptive FTC schemes (Chen et al., 2013a, 2016c; Zheng et al., 2014), and backstepping sliding mode FTC (de Loza et al., 2015), the proposed FTC is easier to design and implement without requiring online optimization and system decomposition. Moreover, the FE observer and FTC controller gains are obtained using a new single-step LMI formulation without involving the equality constraints encountered by the design in Chapter 4.
- In the absence of actuator faults, the proposed integrated FTC design reverts to a new anti-windup control method for compensating the input saturation effect to recover the non-saturated system performance.

The remainder of this chapter is organized as follows. Section 7.2 describes the mathematical model of the 3-DOF helicopter system and formulates the control problem. Section 7.3 proposes a nonlinear ASUIO for FE and Section 7.4 develops an adaptive sliding mode FTC controller. The synthesis of the observer and controller is presented in Section 7.5. Simulation results are provided in Section 7.6 and conclusions are made in Section 7.7.

7.2 Problem formulation

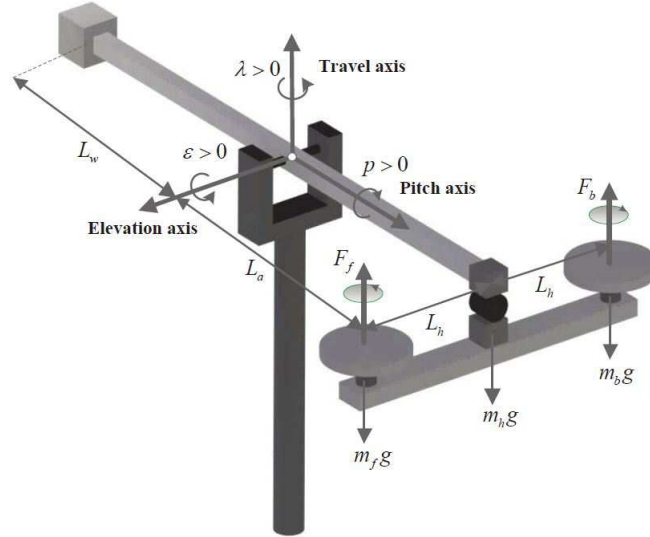


Fig. 7.1 The Quanser 3-DOF helicopter free body diagram (Zheng and Zhong, 2011).

Table 7.1 Definitions of the physical parameters.

Parameter	Physical meaning
ε, p	Elevation angle, pitch angle
F_f, F_b	Control voltages of the front and back motors
J_ε, J_p	Moments of inertia of elevation and pitch axes
K_f	Propeller force-thrust constant
m_h	Mass of the helicopter
L_a	Distance between the travel axis and the helicopter body
L_h	Distance between the pitch axis and each motor
g	Gravity constant
w_ε, w_p	Unknown bounded external disturbances belong to $L_2[0, \infty)$

This work considers the elevation and pitch motions of the Quanser 3-DOF helicopter in Fig. 7.1 with the mathematical model (Zheng and Zhong, 2011)

$$\begin{aligned} J_\varepsilon \ddot{\varepsilon} &= K_f L_a \cos(p) (F_f + F_b) - m_h g L_a \sin(\varepsilon) + w_\varepsilon, \\ J_p \ddot{p} &= K_f L_h (F_f - F_b) + w_p, \end{aligned} \quad (7.1)$$

where the physical parameters are defined in Table 7.1.

Define the system state vector as $x = [x_1 \ x_2 \ x_3 \ x_4]^\top = [\varepsilon \ p \ \dot{\varepsilon} \ \dot{p}]^\top$, the input vector as $u = [u_1 \ u_2]^\top = [F_f \ F_b]^\top$, and the output vector as $y = [\varepsilon \ p \ \dot{\varepsilon} \ \dot{p}]^\top$. Assume that the front and back motors suffer from saturation and unknown bounded actuator faults f_{a1} and f_{a2} , respectively. The actuator faults can be oscillatory faults (Goupil, 2010) or drift faults (de Loza et al., 2015) acting on flight or helicopter control systems. Without loss of generality, f_{a1} and f_{a2} are assumed to have first-order time derivatives \dot{f}_{a1} and \dot{f}_{a2} , respectively. Moreover, f_{a1} , f_{a2} , \dot{f}_{a1} , and \dot{f}_{a2} are bounded and belong to $L_2[0, \infty)$. Thus, the control inputs applied to the helicopter (see Fig. 7.2) can be represented as

$$u_i = \text{sat}(u_{0i} + f_{ai}), \quad i = 1, 2,$$

where u_{0i} is the designed control input and $\text{sat}(\cdot)$ is a saturation function defined by

$$\text{sat}(v) = \begin{cases} \text{sign}(v)\bar{u}, & |v| \geq \bar{u} \\ v, & |v| < \bar{u} \end{cases},$$

with v the input to the actuator and \bar{u} the maximum control magnitude allowed by the actuator.

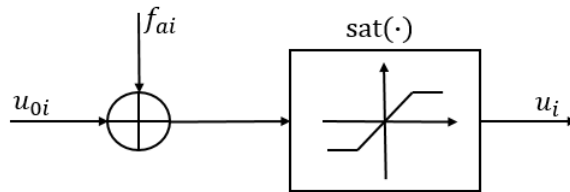


Fig. 7.2 The actuator model with both fault and saturation.

The control input u of the system (7.1) can then be rearranged into

$$u = u_0 + f_0, \tag{7.2}$$

where $u_0 = [u_{01} \ u_{02}]^\top$ is the designed control input vector and $f_0 = [f_{01} \ f_{02}]^\top$ is the composite actuator fault vector with $f_{0i} = \text{sat}(u_{0i} + f_{ai}) - u_{0i}$, $i = 1, 2$.

Remark 7.1 In real operations, the helicopter actuators may suffer from both stuck and partial loss of effectiveness faults (Li and Yang, 2016, 2017). For this case, the control

inputs applied to the helicopter are represented by

$$u_i = \text{sat}(\theta_i u_{0i} + u_{si}), \quad i = 1, 2, \quad (7.3)$$

where θ_i is the partial loss of effectiveness fault taking values within the sector $(0, 1]$ and u_{si} is the stuck fault. Assume that both θ_i and u_{si} are unknown bounded and differentiable time-varying functions. The actuator model (7.3) can be rearranged into

$$u = u_0 + f_0, \quad (7.4)$$

where $u_0 = [u_{01} \ u_{02}]^\top$ is the designed control input vector and $f_0 = [f_{01} \ f_{02}]^\top$ is the composite actuator fault vector with $f_{0i} = \text{sat}(\theta_i u_{0i} + u_{si}) - u_{0i}$, $i = 1, 2$. Since (7.4) and (7.2) are in the same form, the FE and FTC strategies proposed in this chapter can be directly applied to the estimation and compensation of the total effect of saturation and stuck and partial loss of effectiveness faults.

According to the aforementioned definitions a state-space model of (7.1) is given as

$$\begin{aligned} \dot{x} &= Ax + B(u_0 + f_0) + g(x) + Dd, \\ y &= Cx, \end{aligned} \quad (7.5)$$

with $d = [d_1 \ d_2]^\top$ and

$$A = \begin{bmatrix} 0 & 0 & 1 & 0 \\ 0 & 0 & 0 & 1 \\ 0 & 0 & 0 & 0 \\ 0 & 0 & 0 & 0 \end{bmatrix}, \quad B = \begin{bmatrix} 0 & 0 \\ 0 & 0 \\ b_1 & b_1 \\ b_2 & -b_2 \end{bmatrix}, \quad D = \begin{bmatrix} 0 & 0 \\ 0 & 0 \\ 1 & 0 \\ 0 & 1 \end{bmatrix}, \quad g(x) = \begin{bmatrix} 0 \\ 0 \\ g_1(x) \\ 0 \end{bmatrix}, \quad C = I_4,$$

$$b_1 = K_f L_a / J_\varepsilon, \quad b_2 = K_f L_h / J_p, \quad g_1(x) = -m_h g L_a \sin(x_1) / J_\varepsilon,$$

$$d_1 = w_\varepsilon / J_\varepsilon + b_1 (\cos(x_2) - 1) (u_{01} + f_{01} + u_{02} + f_{02}), \quad d_2 = w_p / J_p,$$

where d is a bounded lumped uncertainty including external disturbances (w_ε and w_p) and the system uncertainty $b_1 (\cos(x_2) - 1) (u_{01} + f_{01} + u_{02} + f_{02})$. It is verified that the system (7.5) is observable and controllable. The following assumption is made throughout the chapter.

Assumption 7.1 The nonlinear function $g(x)$ satisfies the Lipschitz constraint

$$\|g(x_t) - g(x)\| \leq L_f \|x_t - x\|, \quad \forall x, x_t \in \mathbb{R}^4,$$

where L_f is the Lipschitz constant independent of x and x_t .

Remark 7.2 It is seen from (7.5) that the nonlinear function $g(x)$ satisfies the Lipschitz constraint in Assumption 7.1 with $L_f = m_h g L_a / J_\varepsilon$.

The present actuator faults and saturation can affect the stability of the helicopter system and prevents it from performing prescribed tasks. This chapter aims to stabilize the elevation and pitch motions of the system (7.5) through an FTC strategy, involving 1) the design of an observer to estimate the system state and the composite actuator fault, and 2) the design of an FTC controller based on the estimate to compensate the faults and saturation effect to ensure system stability.

7.3 FE observer design

This section describes an observer design for estimating the system state x and the composite actuator fault f_0 . A nonlinear ASUIO is used to achieve the estimation, in which f_0 is extended as a new system state and must be differentiable.

It can be seen from (7.2) that f_0 is a function of the designed control input u_0 and the saturation function $\text{sat}(v)$. In this chapter u_0 is designed in Section 7.4 as a state-feedback controller that is differentiable. However, the saturation function $\text{sat}(v)$ is known to be non-differentiable. Therefore, f_0 is non-differentiable which cannot be treated as a new system state. To overcome this, a differentiable approximation of f_0 needs to be attained before designing the nonlinear ASUIO.

7.3.1 Differentiable approximation of the composite actuator fault

The above analysis implies that if the saturation function $\text{sat}(v)$ can be approximated by a differentiable function $\overline{\text{sat}}(v)$, then f_0 is modelled as a new function consisting of a differentiable function of u_0 and $\overline{\text{sat}}(v)$ and the approximation error which can be combined into the uncertainty term. In this way, a differentiable approximation of f_0 is attained.

The saturation function $\text{sat}(v)$ is approximated by a differentiable function $\overline{\text{sat}}(v)$ modified from Freidovich and Khalil (2008) with the form of

$$\overline{\text{sat}}(v) = \begin{cases} v, & 0 \leq |v| \leq \bar{u} \\ v - [v - \bar{u}\text{sign}(v)]^2 \text{sign}(v)/(2\varepsilon_0), & \bar{u} \leq |v| \leq \bar{u} + \varepsilon_0 \\ (\bar{u} + \frac{\varepsilon_0}{2})\text{sign}(v), & |v| \geq \bar{u} + \varepsilon_0 \end{cases}, \quad (7.6)$$

where ε_0 is a positive constant.

It can be shown that the function $\overline{\text{sat}}(v)$ satisfies continuity across $|v| = \bar{u}$ as well as $|v| = \bar{u} + \varepsilon_0$. Furthermore, the left and right derivatives of $\overline{\text{sat}}(v)$ with respect to v at the above boundaries are equal. It follows that $\overline{\text{sat}}(v)$ is differentiable. Moreover, it is bounded uniformly in ε_0 on any bounded interval of ε_0 , and $|\overline{\text{sat}}(v) - \text{sat}(v)| \leq \varepsilon_0/2$ and $0 \leq d\overline{\text{sat}}(v)/dv \leq 1$ for all $v \in \mathbb{R}$. Hence, the approximation error of $\text{sat}(v)$ is small as long as ε_0 is selected to be sufficiently small.

According to (7.6), the control input (7.2) can be further modelled as

$$u = u_0 + f + \Delta u, \quad (7.7)$$

where $f = [f_1 \ f_2]^\top$ and $\Delta u = [\Delta u_1 \ \Delta u_2]^\top$, with $f_i = \overline{\text{sat}}(u_{0i} + f_{ai}) - u_{0i}$ and $\Delta u_i = \text{sat}(u_{0i} + f_{ai}) - \overline{\text{sat}}(u_{0i} + f_{ai})$, $i = 1, 2$.

Now the composite actuator fault f is differentiable, which can then be augmented as a new system state vector of the system (7.5) with input (7.7).

7.3.2 Observer design

The augmented system of (7.5) takes the form

$$\begin{aligned} \dot{\bar{x}} &= \bar{A}\bar{x} + \bar{g}(A_0\bar{x}) + \bar{B}u_0 + \bar{D}\bar{d}, \\ y &= \bar{C}\bar{x}, \end{aligned} \quad (7.8)$$

where $\bar{x} = [x^\top \ f^\top]^\top$, $\bar{d} = [\tilde{d}^\top \ f^\top]^\top$, $\tilde{d} = d + B_2\Delta u$, $B_2 = [0 \ I_2]B$, $A_0 = [I_4 \ 0]$, and

$$\bar{A} = \begin{bmatrix} A & B \\ 0 & 0 \end{bmatrix}, \bar{B} = \begin{bmatrix} B \\ 0 \end{bmatrix}, \bar{D} = \begin{bmatrix} D & 0 \\ 0 & I_2 \end{bmatrix}, \bar{C} = [C \ 0], \bar{g}(A_0\bar{x}) = \begin{bmatrix} g(A_0\bar{x}) \\ 0 \end{bmatrix}.$$

It can be verified that the system (7.8) is observable since the pair (A, C) is observable and B is full rank for the helicopter system (7.5).

A nonlinear ASUIO is designed to estimate the augmented state \bar{x} with the form of

$$\begin{aligned}\dot{z} &= Mz + Gu_0 + N\bar{g}(A_0\hat{x}) + Ly, \\ \hat{x} &= z + Hy,\end{aligned}\tag{7.9}$$

where $z \in \mathbb{R}^6$ is the observer system state and $\hat{x} \in \mathbb{R}^6$ is the estimate of \bar{x} . The matrices $M \in \mathbb{R}^{6 \times 6}$, $G \in \mathbb{R}^{6 \times 2}$, $N \in \mathbb{R}^{6 \times 6}$, $L \in \mathbb{R}^{6 \times 4}$, and $H \in \mathbb{R}^{6 \times 4}$ are to be designed. The estimates of x and f are $\hat{x} = [I_4 \ 0]\hat{x}$ and $[0 \ I_2]\hat{x}$, respectively.

Define the estimation error as $e = \bar{x} - \hat{x}$, then

$$\begin{aligned}\dot{e} &= (\Xi\bar{A} - L_1\bar{C})e + (\Xi\bar{A} - L_1\bar{C} - M)z + (\Xi\bar{B} - G)u_0 + [(\Xi\bar{A} - L_1\bar{C})H - L_2]y \\ &\quad + \Xi\bar{g}(A_0\bar{x}) - N\bar{g}(A_0\hat{x}, t) + \Xi\bar{D}\bar{d},\end{aligned}\tag{7.10}$$

where $\Xi = I_6 - H\bar{C}$ and $L = L_1 + L_2$. The matrices M , N , G , and L_2 are defined as

$$M = \Xi\bar{A} - L_1\bar{C}, \quad N = \Xi, \quad G = \Xi\bar{B}, \quad L_2 = (\Xi\bar{A} - L_1\bar{C})H.\tag{7.11}$$

Note that the design matrices M , N , G , and L_2 can be calculated directly from (7.11) by substituting the matrices L_1 and H attained later through the LMIs in Theorems 7.2 - 7.4 in Section 7.5.

Substituting (7.11) into (7.10) gives

$$\dot{e} = (\Xi\bar{A} - L_1\bar{C})e + \Xi\Delta\bar{g} + \Xi\bar{D}\bar{d},\tag{7.12}$$

where $\Delta\bar{g} = \bar{g}(A_0\bar{x}) - \bar{g}(A_0\hat{x})$.

A sufficient condition for the existence of a robust nonlinear ASUIO (7.9) is given in Theorem 7.1.

Theorem 7.1 There exists a robust nonlinear ASUIO (7.9) if the error system (7.12) is robustly asymptotically stable.

Proof: If (7.12) is robustly asymptotically stable, then by (7.11), the error system (7.10) is also robustly asymptotically stable. Therefore, it holds that $\lim_{t \rightarrow \infty} e(t) = 0$ in the presence of uncertainty and disturbance. \square

According to Theorem 7.1, the solvability of (7.9) now becomes a problem of designing the matrices L_1 and H such that (7.12) is robustly asymptotically stable.

7.4 FTC controller design

This section outlines the design of an adaptive system for FTC based on state and fault estimation. The FTC function is to compensate the estimated effects of the actuator faults and saturation and also stabilize the system state of (7.5). Since in the system (7.5) the measured output vector y may have noise, thus it is appropriate to use the concept of SMC with adaption based on the combined state and fault estimation.

Recall that the general aim of SMC is to achieve robust insensitivity to matched uncertainty acting within the control channels, using a combination of linear and switched feedback. The SMC must be designed to reach a sliding surface and the switching operation designed to keep the system motion in the sliding manifold.

So in this SMC, the sliding surface for the system (7.5) is a function of the system state estimates given as follows:

$$s = N_1 \hat{x} - \int_0^t v(\tau) d\tau = 0, \quad (7.13)$$

where $s \in \mathbb{R}^{2 \times 1}$, \hat{x} is the system state estimate obtained through the observer (7.9) (i.e., $\hat{x} = [I_4 \ 0] \hat{x}$), and $N_1 = B^\dagger - Y_1(I_4 - BB^\dagger)$ with $B^\dagger = (B^\top B)^{-1} B^\top$ and a design matrix $Y_1 \in \mathbb{R}^{2 \times 4}$. v is a time-varying design function.

The first step of the SMC design is to establish the reachability of \hat{x} to the sliding surface (7.13). Differentiating s with respect to time gives

$$\dot{s} = N_1 Ax + u_0 + f + N_1 g(x) + N_1 D \tilde{d} - N_1 \dot{e}_x - v, \quad (7.14)$$

where e_x is the estimation error of x defined as $e_x = x - \hat{x}$.

An FTC controller for the system (7.5) with (7.7) is designed as

$$u_0 = u_l + u_n, \quad (7.15)$$

where u_l is the linear feedback component given by $u_l = v$ and $v = -K\hat{x}$, with a design matrix $K = [K_x \ K_f]$. $K_x \in \mathbb{R}^{2 \times 4}$ is to be determined while K_f is chosen as

$K_f = I_2$. The nonlinear component u_n is $u_n = -\rho \overline{\text{sign}}(s, \theta_0)$, where ρ is a design scalar function. The smooth function $\overline{\text{sign}}(s, \theta_0)$ is defined as $\overline{\text{sign}}(s, \theta_0) = \frac{s}{\|s\| + \theta_0}$ (Edwards and Spurgeon, 1998), with a sufficiently small positive constant θ_0 . It is a differentiable approximation of $\text{sign}(s)$ ensuring that the control function u_0 is also differentiable. Define the approximation error as $\Delta_{\text{sign}} = \text{sign}(s) - \overline{\text{sign}}(s, \theta_0)$, then it can be verified that $\|\Delta_{\text{sign}}\| \leq \frac{1}{\|s\|/\theta_0 + 1} \leq 1$ and for $\|s\| \neq 0$, $\|\Delta_{\text{sign}}\|$ is small by selecting a sufficiently small θ_0 .

Consider the following Lyapunov function

$$V_s = \frac{1}{2} s^\top s.$$

The time derivative of V_s along (7.14) is

$$\begin{aligned} \dot{V}_s &= s^\top [N_1 A x + \Delta_e - \rho \overline{\text{sign}}(s, \theta_0)] \\ &= s^\top [N_1 A x + \Delta_e + \rho \Delta_{\text{sign}} - \rho \text{sign}(s)] \\ &\leq (\eta - \rho) \|s\|, \end{aligned} \quad (7.16)$$

where $\Delta_e = \|N_1 A\| \|x\| + K_x e_x + e_f + N_1 g(x) + N_1 D \tilde{d} + N_1 \dot{e}_x$ and $e_f = f - \hat{f}$. η is an unknown positive constant satisfying $\eta \geq \|\Delta_e\| + \|\rho \Delta_{\text{sign}}\|$.

Define $\rho = \hat{\eta} + \varepsilon$, where ε is a positive design constant. The scalar $\hat{\eta}$ is the estimate of η defined by

$$\dot{\hat{\eta}} = \sigma \|s\|, \quad \hat{\eta}(0) \geq 0, \quad (7.17)$$

with a positive design constant σ .

Define the estimation error of η as $\tilde{\eta} = \eta - \hat{\eta}$. Consider a Lyapunov function

$$V = V_s + \frac{1}{2\sigma} \tilde{\eta}^2.$$

It follows from (7.16) and (7.17) that

$$\begin{aligned} \dot{V} &= s^\top \dot{s} - \frac{1}{\sigma} \tilde{\eta} \dot{\hat{\eta}} \\ &\leq (\eta - \rho) \|s\| - \tilde{\eta} \|s\| \\ &= -\varepsilon \|s\|. \end{aligned} \quad (7.18)$$

Since V_s is positive definite, it follows from (7.18) and the Barbalat's lemma (Slotine et al., 1991) that $V_s(t) \leq V_s(0)$. Therefore, $s(t)$ and $\tilde{\eta}(t)$ are bounded. This means that the designed controller (7.15) can maintain the sliding motion around $s = 0$. Moreover, in the case of zero initial condition (i.e. $V_s(0) = 0$), $\lim_{t \rightarrow \infty} s(t) = 0$ and thus the idealized sliding motion can be maintained.

Consider next the system stability analysis corresponding to the sliding motion. By setting $\dot{s}_2 = 0$, it follows from (7.14) that the equivalent control input (Edwards and Spurgeon, 1998) is

$$u_{eq} = -N_1 [Ax + N_1 g(x) + N_1 D\tilde{d}] + u_l. \quad (7.19)$$

Substituting (7.19) into (7.5) gives the equivalent closed-loop system

$$\dot{x} = (\Theta A - BK_x)x + BKe + \Theta g(x) + \Theta D\tilde{d}, \quad (7.20)$$

where $\Theta = I_4 - BN_1$.

Therefore, the system (7.5) is maintained on the sliding mode with the equivalent control (7.19) by designing K_x such that (7.20) is stable. The closed-loop system (7.20) contains the uncertainty \tilde{d} and nonlinearity $g(x)$, which must be minimized to achieve a suitable degree of robustness. This is achieved using H_∞ optimization given in the next section.

7.5 Synthesis of the FE observer and FTC controller

The 3-DOF helicopter FTC system in Fig. 7.3 includes the designs of the FE observer (7.9) and FTC controller (7.15). To obtain their parameters, a way widely used in the literature is the separated FE/FTC design approach (de Loza et al., 2015), in which the FE observer and FTC controller are designed separately. This approach follows the Separation Principle (see Appendix B) by neglecting of the effects of system uncertainty and nonlinearity on the FE performance and the effect of the estimation error on the FTC system. This section first presents the traditional separated synthesis approach with an analysis of its reservation and drawbacks, and then describes an approach based on the integrated FE/FTC strategy in Chapter 4.

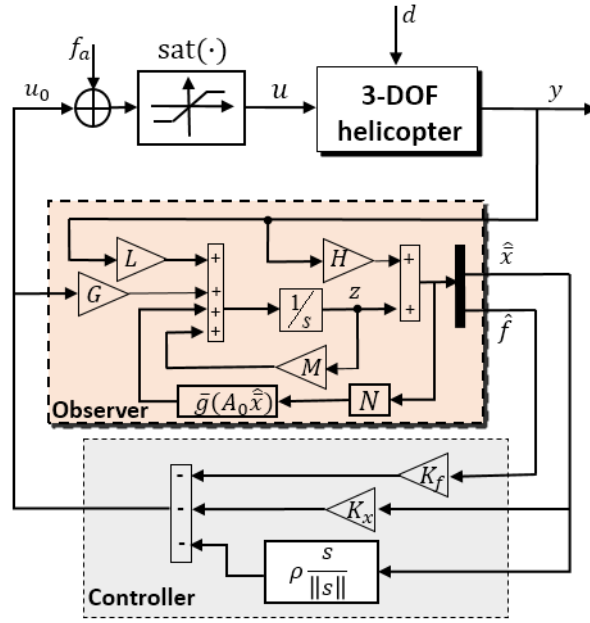


Fig. 7.3 The proposed FE-based FTC 3-DOF helicopter system.

7.5.1 Traditional separated approach

By neglecting the effects of the system uncertainty and nonlinearity on the FE observer, the error system (7.12) is reduced to be

$$\begin{aligned} \dot{e} &= (\Xi\bar{A} - L_1\bar{C})e + \Xi\bar{D}\bar{d}_s, \\ z_{s_1} &= C_{s_1}e, \end{aligned} \quad (7.21)$$

where $\bar{d}_s = [d_s^\top \hat{f}^\top]^\top$ and $d_s = [w_\varepsilon \ w_p]^\top$. $z_{s_1} \in \mathbb{R}^6$ is the measured output with a given coefficient matrix $C_{s_1} \in \mathbb{R}^{6 \times 6}$.

The following theorem is given to design the matrices H and L_1 to make the error system (7.21) robustly stable.

Theorem 7.2 Given a positive scalar γ_{s_1} , the error system (7.21) is stable with H_∞ performance $\|G_{z_{s_1}\bar{d}_s}\|_\infty < \gamma_{s_1}$, if there exists a symmetric positive definite matrix $Q_s \in \mathbb{R}^{6 \times 6}$, and matrices $M_{s_1} \in \mathbb{R}^{6 \times 4}$ and $M_{s_2} \in \mathbb{R}^{6 \times 4}$ such that

$$\begin{bmatrix} \Omega_{1,1} & (Q_s - M_{s_1}\bar{C})\bar{D} & C_{s_1}^\top \\ * & -\gamma_{s_1}^2 I_4 & 0 \\ * & * & -I_6 \end{bmatrix} < 0,$$

where $\Omega_{1,1} = \text{He}(Q_s\bar{A} - M_{s1}\bar{C}\bar{A} - M_{s2}\bar{C})$. Then the gains are given by $H = Q_s^{-1}M_{s1}$ and $L_1 = Q_s^{-1}M_{s2}$.

Proof: By using the Bounded Real Lemma (see Appendix A.1) and defining $M_{s1} = Q_sH$ and $M_{s2} = Q_sL_1$, the proof is trivial and thus is omitted here. \square

Similarly, in the separated approach the FTC system is assumed to be not affected by the estimation error, thus the closed-loop control system (7.20) becomes

$$\begin{aligned}\dot{x} &= (\Theta A - BK_x)x + \Theta g(x) + \Theta D\tilde{d}, \\ z_{s2} &= C_{s2}x,\end{aligned}\tag{7.22}$$

where $z_{s2} \in \mathbb{R}^6$ is the measured output with a given coefficient matrix $C_{s2} \in \mathbb{R}^{4 \times 4}$.

The following theorem is given to design K_x to ensure that (7.22) is robustly stable.

Theorem 7.3 Given positive scalars γ_{s2} and ε_s , the closed-loop system (7.22) is stable with H_∞ performance $\|G_{z_{s2}\tilde{d}}\|_\infty < \gamma_{s2}$, if there exists a symmetric positive definite matrix $P_s \in \mathbb{R}^{4 \times 4}$ and a matrix $M_{s3} \in \mathbb{R}^{2 \times 4}$ such that

$$\begin{bmatrix} \Pi_{1,1} & D & P_s C_{s2}^\top & P_s \\ \star & -\gamma_{s2}^2 I_2 & 0 & 0 \\ \star & \star & -I_4 & 0 \\ \star & \star & \star & -1/(\varepsilon_s L_f^2) I_4 \end{bmatrix} < 0,$$

where $\Pi_{1,1} = \text{He}(\Theta A P_s - B M_{s3}) + \varepsilon_s^{-1} \Theta \Theta^\top$. Then the control gain is given by $K_x = M_{s3} P_s^{-1}$.

Proof: Given a symmetric positive definite matrix $Z_s \in \mathbb{R}^{4 \times 4}$. Assume $g(0) = 0$, then $\|g(x)\| \leq L_f \|x\|, \forall x \in \mathbb{R}^4$. Thus for some positive scalar ε_s ,

$$2x^\top Z_s \Theta g(x) \leq \varepsilon_s^{-1} x^\top Z_s \Theta \Theta^\top Z_s x + \varepsilon_s L_f^2 \|x\|^2.$$

Using the Bounded Real Lemma (see Appendix A.1), the closed-loop system (7.22) is stable with H_∞ performance $\|G_{z_{s2}\tilde{d}}\|_\infty < \gamma_{s2}$, if

$$\begin{bmatrix} \Pi_{1,1} & Z_s D & C_{s2}^\top \\ \star & -\gamma_{s2}^2 I_2 & 0 \\ \star & \star & -I_4 \end{bmatrix} < 0,\tag{7.23}$$

where $\Pi_{1,1} = \text{He}[Z_s(\Theta A - BK_x)] + \varepsilon_s^{-1}Z_s\Theta\Theta^\top Z_s + \varepsilon_s L_f^2 I_4$.

Define $P_s = Z_s^{-1}$ and $M_{s3} = K_x P_s$. Pre- and post-multiplying both sides of (7.23) with $\text{diag}(P_s, I_2)$ and using the Schur Complement (see Appendix A.2), then (7.23) becomes

$$\begin{bmatrix} \Pi_{1,1} & D & P_s C_{s2}^\top & P_s \\ \star & -\gamma_{s2}^2 I_2 & 0 & 0 \\ \star & \star & -I_4 & 0 \\ \star & \star & \star & -1/(\varepsilon_s L_f^2) I_4 \end{bmatrix} < 0,$$

where $\Pi_{1,1} = \text{He}(\Theta A P_s - B M_{s3}) + \varepsilon_s^{-1} \Theta \Theta^\top$. □

The separated approach outlined in Theorems 7.2 and 7.3 allows great design freedom for the FE/FTC design for the 3-DOF helicopter, in which the observer and controller can be optimized independently. However, it can be seen from the error system (7.12) and the control system (7.20) that the system uncertainty, nonlinearity and disturbance affect the estimation, and in turn the estimation error has effect on the closed-loop control system. This leads to the fact that *bi-directional robustness interactions* exist between the FE and FTC functions, which breaks down the Separation Principle (see Appendix B) on which the separated approach based. Therefore, it is necessary to introduce an integrated FE/FTC approach to achieve robust design of the overall FTC system, taking into account the *bi-directional robustness interactions*.

7.5.2 Integrated approach

The composite closed-loop system encompassing (7.12) and (7.20) is

$$\begin{aligned} \dot{x} &= (\Theta_1 A - BK_x)x + BKe + \Theta g(x) + D_1 \bar{d}, \\ \dot{e} &= (\Xi \bar{A} - L_1 \bar{C})e + \Xi \Delta \bar{g} + \Xi \bar{D} \bar{d}, \\ z_c &= C_x x + C_e e, \end{aligned} \tag{7.24}$$

where $z_c \in \mathbb{R}^4$ is the measured output used to verify the closed-loop system performance with matrices $C_x \in \mathbb{R}^{4 \times 4}$ and $C_e \in \mathbb{R}^{4 \times 6}$, and $D_1 = [\Theta D \ 0]$.

Theorem 7.4 provides an integrated strategy to design the observer and controller gains simultaneously using a single-step LMI formulation.

Theorem 7.4 Given positive scalars γ , ε_1 , ε_2 , and ε_3 , the closed-loop system (7.24) is stable with H_∞ performance $\|G_{z_c\bar{d}}\|_\infty < \gamma$, if there exist three symmetric positive definite matrices $Z \in \mathbb{R}^{4 \times 4}$, $Q \in \mathbb{R}^{4 \times 4}$, and $R \in \mathbb{R}^{2 \times 2}$, and matrices $M_1 \in \mathbb{R}^{2 \times 4}$, $M_2 \in \mathbb{R}^{4 \times 2}$, $M_3 \in \mathbb{R}^{4 \times 2}$, $M_4 \in \mathbb{R}^{2 \times 4}$, and $M_5 \in \mathbb{R}^{2 \times 4}$ such that

$$\begin{bmatrix} \Pi_1 & \Pi_2 \\ \star & \Pi_3 \end{bmatrix} < 0, \quad (7.25)$$

with

$$\Pi_1 = \begin{bmatrix} \Xi_{1,1} & \Xi_{1,2} \\ \star & J_{2,2} \end{bmatrix}, \quad \Pi_2 = \begin{bmatrix} \Xi_{1,3} & \Xi_{1,4} & \Xi_{1,5} & 0 & 0 & \Xi_{1,8} \\ J_{2,3} & J_{2,4} & 0 & I_4 & J_{2,7} & 0 \end{bmatrix},$$

$$\Pi_3 = -\text{diag} \left\{ \gamma^2 I_4, I_4, \varepsilon_3^{-1} Z, \varepsilon_3 Z, \varepsilon_1 I_4, (\varepsilon_2 L_f^2)^{-1} I_4 \right\},$$

$$J_{2,2} = \begin{bmatrix} \Xi_{2,2} & \Xi_{2,3} \\ \star & \Xi_{3,3} \end{bmatrix}, \quad J_{2,3} = \begin{bmatrix} QD - M_2CD & 0 \\ -M_4CD & R \end{bmatrix},$$

$$J_{2,4} = C_e^\top = \begin{bmatrix} C_{ex}^\top \\ C_{ef}^\top \end{bmatrix}, \quad J_{2,7} = \begin{bmatrix} Q - M_2C & 0 \\ -M_4C & R \end{bmatrix},$$

$$\Xi_{1,1} = \text{He}(\Theta AZ - BM_1) + \varepsilon_2^{-1} \Theta \Theta^\top, \quad \Xi_{1,2} = [0 \ B], \quad \Xi_{1,3} = [\Theta D \ 0], \quad \Xi_{1,4} = ZC_x^\top,$$

$$\Xi_{1,5} = BM_1, \quad \Xi_{1,8} = Z, \quad \Xi_{2,2} = \text{He}(QA - M_2CA - M_3C) + \varepsilon_1 L_f^2 I_4,$$

$$\Xi_{2,3} = QB - M_2CB - A^\top C^\top M_4^\top - C^\top M_5^\top, \quad \Xi_{3,3} = \text{He}(-M_4CB).$$

Then the controller gains are given by: $K_x = M_1 Z^{-1}$, $H_1 = Q^{-1} M_2$, $H_2 = R^{-1} M_4$, $L_{11} = Q^{-1} M_3$, $L_{12} = R^{-1} M_5$.

Proof: Define a symmetric positive definite matrix $P_1 \in \mathbb{R}^{6 \times 6}$. Since the nonlinear function $g(x)$ is Lipschitz, for some positive scalar ε_1 ,

$$2e^\top P_1 \Xi \Delta \bar{g} \leq \varepsilon_1^{-1} e^\top P_1 \Xi \Xi^\top P_1 e + \varepsilon_1 L_f^2 \|A_0 e\|^2.$$

Define another symmetric positive definite matrix $P \in \mathbb{R}^{4 \times 4}$. Assume $g(0) = 0$, then $\|g(x)\| \leq L_f \|x\|$, $\forall x \in \mathbb{R}^4$. Thus, it holds that, for some positive scalar ε_2 ,

$$2x^\top P \Theta g(x) \leq \varepsilon_2^{-1} x^\top P \Theta \Theta^\top P x + \varepsilon_2 L_f^2 \|x\|^2.$$

Using the Bounded Real Lemma (see Appendix A.1), the closed-loop system (7.20) is stable with H_∞ performance $\|G_{z_c\bar{d}}\|_\infty < \gamma$ if

$$\begin{bmatrix} J_{1,1} & PBK & PD_1 & C_x^\top \\ \star & J_{2,2} & P_1 \Xi \bar{D} & C_e^\top \\ \star & \star & -\gamma^2 I_4 & 0 \\ \star & \star & \star & -I_4 \end{bmatrix} < 0, \quad (7.26)$$

where $J_{1,1} = \text{He}[P(\Theta A - BK_x)] + \varepsilon_2^{-1} P \Theta \Theta^\top P + \varepsilon_2 L_f^2 I_4$ and $J_{2,2} = \text{He}[P_1(\Xi \bar{A} - L_1 \bar{C})] + \varepsilon_1^{-1} P_1 \Xi \Xi^\top P_1 + \varepsilon_1 L_f^2 A_0^\top A_0 I_6$.

Define $Z = P^{-1}$. Pre- and post-multiplying both sides of (7.26) with $\text{diag}(Z, I_6, I_4)$ gives

$$\begin{bmatrix} J_{1,1} & BK & D_1 & ZC_x^\top \\ \star & J_{22} & P_1 \Xi \bar{D} & C_e^\top \\ \star & \star & -\gamma^2 I_4 & 0 \\ \star & \star & \star & -I_4 \end{bmatrix} < 0, \quad (7.27)$$

where $J_{1,1} = \text{He}[(\Theta A - BK_x)Z] + \varepsilon_2^{-1} \Theta \Theta^\top + \varepsilon_2 L_f^2 Z Z$ and $J_{2,2} = \text{He}[P_1(\Xi \bar{A} - L_1 \bar{C})] + \varepsilon_1^{-1} P_1 \Xi \Xi^\top P_1 + \varepsilon_1 L_f^2 A_0^\top A_0 I_6$.

By Young inequality (see Appendix A.4), for some positive scalar ε_3 ,

$$\text{He} \left\{ \begin{bmatrix} BK_x \\ 0 \\ 0 \end{bmatrix} \begin{bmatrix} 0 \\ I_4 \\ 0 \end{bmatrix}^\top \right\} \leq \varepsilon_3 \begin{bmatrix} BK_x Z \\ 0 \\ 0 \end{bmatrix} Z^{-1} \begin{bmatrix} BK_x Z \\ 0 \\ 0 \end{bmatrix}^\top + \frac{1}{\varepsilon_3} \begin{bmatrix} 0 \\ I_4 \\ 0 \end{bmatrix} Z^{-1} \begin{bmatrix} 0 \\ I_4 \\ 0 \end{bmatrix}^\top.$$

Further define $P_1 = \text{diag}(Q_{4 \times 4}, R_{2 \times 2})$, $L_1 = [L_{11}; L_{12}]$, $H = [H_1; H_2]$, $M_1 = K_x Z$, $M_2 = QH_1$, $M_3 = QL_{11}$, $M_4 = RH_2$, and $M_5 = RL_{12}$. Using the Schur complement (see Appendix A.2) repeatedly, (7.27) can be finally reformulated into (7.25). \square

Remark 7.3 In the presence of actuator faults, the proposed strategy estimates and compensates the total effect of the actuator faults and saturation and robustly recover the nominal non-saturated system performance. In the fault-free cases, it can be used as a novel anti-windup control framework to recover non-saturated system performance. Adaptive anti-windup controls have been described in many works, e.g., He et al. (2016), by incorporating an auxiliary system. Nevertheless, this adaptive framework involves a switched designed control through appropriately chosen bounds of the auxiliary system state. Other mainstream anti-windup methods incorporate anti-windup compensators as a part of the normal control function, as summarized in the review Tarbouriech and

Turner (2009). However, the above anti-windup designs are implemented with the measurement of the actuator output, which is not the case in reality and is not even desirable, especially if the actuator has any fast, un-modelled dynamics. Compared with the existing approaches, the proposed design for anti-windup control is convenient in the sense that 1) the proposed observer can achieve simultaneous estimation of the system state and saturation effect without requiring the actuator output measurement, and 2) all the observer and controller gains are obtained by solving the LMI (7.25) in a single-step.

7.6 Simulation results

This section outlines comparative simulations for the elevation and pitch motions of the Quanser 3-DOF helicopter system (7.5) with single or multiple actuator faults, using 1) the nominal control design (without FE/FTC and the state observer and controller are designed separately), 2) the separated FE/FTC approach, and 3) the proposed integrated FE/FTC approach.

Table 7.2 3-DOF helicopter parameters.

Parameter	Value
J_ϵ	0.91 kg·m ²
J_p	0.0364 kg·m ²
K_f	0.5 N/V
m_h	1.01 kg
L_a	0.66 m
L_h	0.177 m
g	9.81 m/s ²

The 3-DOF helicopter system parameters are given in Table 7.2. Due to mechanical limits, the elevation angle is constrained within the range of ± 31.75 deg and the pitch angle is within ± 32.0 deg. The voltage limits of the front and back motors are ± 12 V. The external disturbances acting on the helicopter are supposed to be $w_\epsilon = 0.01 \sin(10t)$ and $w_p = 0.01 \sin(5t)$. To test the system performance, a Gaussian noise with zero-mean and variance 0.001^2 is added to the output measurement.

Choosing $Y_1 = 0.1_{2 \times 4}$, $C_x = [I_4; 0_{6 \times 4}]$, $C_{ex} = [0_{4 \times 4}; I_4; 0_{2 \times 4}]$, $C_{ef} = [0_{8 \times 2}; I_2]$ and solving Theorem 7.4 with $\epsilon_1 = 50$, $\epsilon_2 = 5$, $\epsilon_3 = 0.015$ and $\gamma = 1$, then the observer and

controller gains are

$$\begin{aligned}
 N_1 &= \begin{bmatrix} -0.1 & -0.1 & 1.3788 & 0.2056 \\ -0.1 & -0.1 & 1.3788 & -0.2056 \end{bmatrix}, \\
 K_x &= \begin{bmatrix} 9.2603 & 1.2848 & 9.2833 & 1.3508 \\ 9.2706 & -1.4815 & 9.2857 & -1.3629 \end{bmatrix}, \\
 M &= \begin{bmatrix} -1.4142 & 0 & 0 & 0 & 0 & 0 \\ 0 & -1.4142 & 0 & 0 & 0 & 0 \\ 0 & 0 & -1.4142 & 0 & 0 & 0 \\ 0 & 0 & 0 & -1.4142 & 0 & 0 \\ -0.0003 & 0.0009 & 0.0094 & -0.0021 & -21.6334 & 15.9875 \\ -0.0003 & -0.0009 & 0.0094 & 0.0021 & 15.9870 & -21.6328 \end{bmatrix}, \\
 N &= \begin{bmatrix} 0 & 0 & 0 & 0 & 0 & 0 \\ 0 & 0 & 0 & 0 & 0 & 0 \\ 0 & 0 & 0 & 0 & 0 & 0 \\ 0 & 0 & 0 & 0 & 0 & 0 \\ 0.0001 & -0.0017 & -7.7845 & -7.7367 & 1 & 0 \\ 0.0001 & 0.0017 & -7.7844 & 7.7365 & 0 & 1 \end{bmatrix}, \\
 G &= \begin{bmatrix} 0 & 0 \\ 0 & 0 \\ 0 & 0 \\ 0 & 0 \\ -21.6334 & 15.9875 \\ 15.9870 & -21.6328 \end{bmatrix}, \\
 L &= \begin{bmatrix} 0 & 0 & 0 & 0 \\ 0 & 0 & 0 & 0 \\ 0 & 0 & 0 & 0 \\ 0 & 0 & 0 & 0 \\ 0.0004 & -0.0624 & -43.9508 & -291.0610 \\ 0.0004 & 0.0624 & -43.9493 & 291.0509 \end{bmatrix}, \\
 H &= \begin{bmatrix} 1 & 0 & 0 & 0 \\ 0 & 1 & 0 & 0 \\ 0 & 0 & 1 & 0 \\ 0 & 0 & 0 & 1 \\ -0.0001 & 0.0017 & 7.7845 & 7.7367 \\ -0.0001 & -0.0017 & 7.7844 & -7.7365 \end{bmatrix}.
 \end{aligned}$$

The other control parameters are chosen as: $\varepsilon = 0.1$, $\sigma = 0.01$, and $\theta_0 = 0.001$. For the

separated design, the observer and controller gains are obtained by solving the LMIs in Theorems 7.2 and 7.3 with $\gamma_{s1} = 1$, $\gamma_{s2} = 0.06$, and $\epsilon_s = 0.01$.

All cases are simulated with $\epsilon(0) = 30$ deg and $p(0) = 18$ deg, and the initial values of other parameters are set zero. A first-order low pass filter, whose transfer function is $1/(2\pi f_0 s + 1)$ with a frequency $f_0 = 7$ Hz, is used to filter each of the measure outputs.

7.6.1 Case 1: fault-free

In this case the separated and integrated FE/FTC designs revert to nominal observer-based state feedback robust controls. It is seen from Figs. 7.4 - 7.5 that only the proposed integrated design can stabilize the elevation and pitch angles without suffering from actuator saturation.

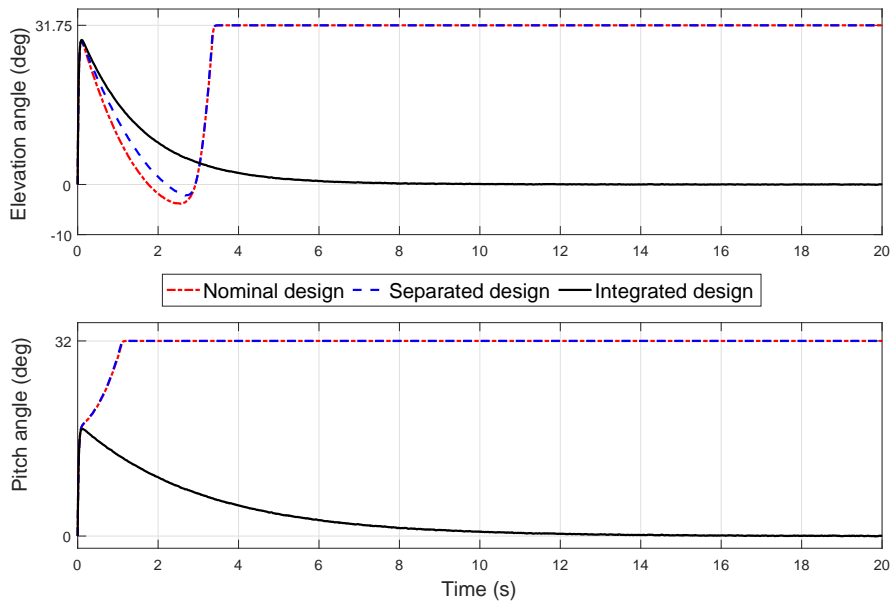


Fig. 7.4 Angle response: Case 1.

7.6.2 Case 2: single actuator fault

In this case the back actuator of the helicopter is healthy, while the front actuator has an actuator fault characterized by

$$f_{a1}(t) = \begin{cases} 0.1t + 0.08t^2, & 0 \text{ s} \leq t \leq 10 \text{ s} \\ 2 \cos(0.5\pi(t - 10)) + 7, & 10 \text{ s} < t \leq 20 \text{ s} \end{cases}.$$

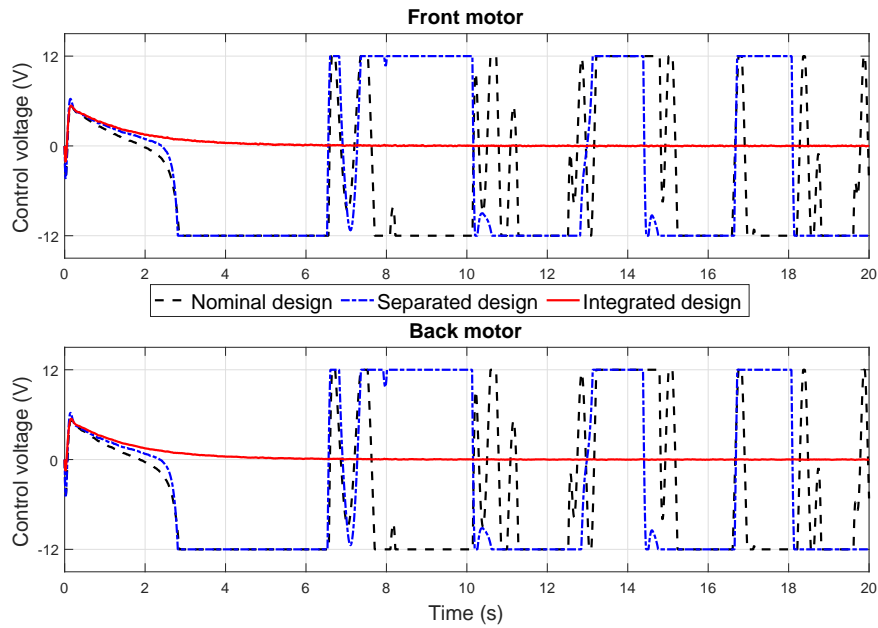


Fig. 7.5 Control effort: Case 1.

It is shown in Fig. 7.6 that the proposed integrated design has better FE performance than the separated design. The angle responses and control efforts in Figs. 7.7 - 7.8 show that only the proposed integrated design can stabilize both the elevation and pitch angles in the presence of a single actuator fault. The nominal and separated designs suffer from saturations in the angles and control inputs.

7.6.3 Case 3: multiple actuator faults

In this case the front and back actuators have oscillatory faults f_{a1} and f_{a2} , respectively. The faults are characterized by

$$f_{a1}(t) = \begin{cases} 0.1t + 0.08t^2, & 0 \leq t \leq 10 \text{ s} \\ 2\cos(0.5\pi(t-10)) + 7, & 10 \text{ s} < t \leq 20 \text{ s} \end{cases},$$

$$f_{a2}(t) = \sin(0.5t) + 0.5\sin(t), \quad 0 \leq t \leq 20 \text{ s}.$$

Similar to Case 2, the results in Figs. 7.9 - 7.11 show that compared with the other two approaches, the proposed integrated approach achieves better performances of FE and output stabilization. Moreover, both the nominal and separated designs have saturations in the angles and control inputs.

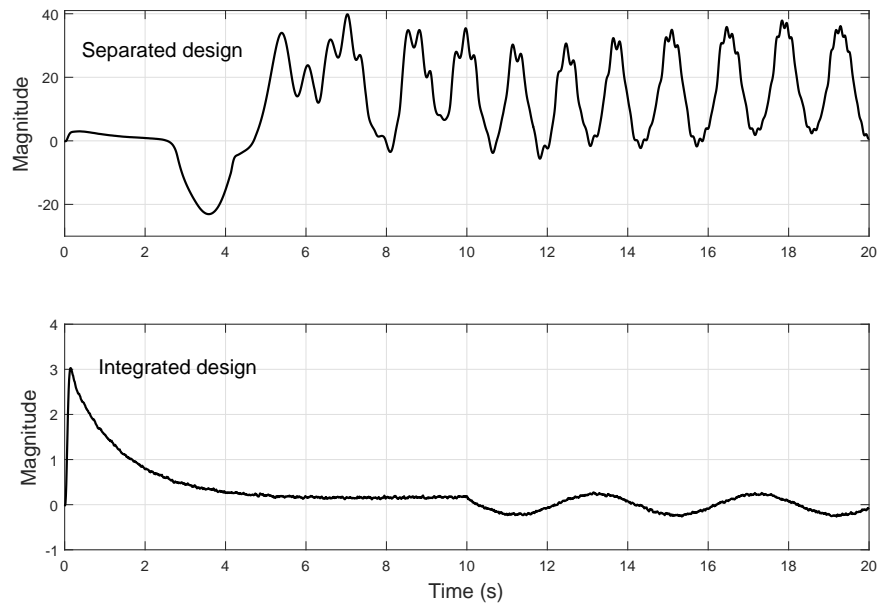


Fig. 7.6 Fault estimation performance: Case 2.

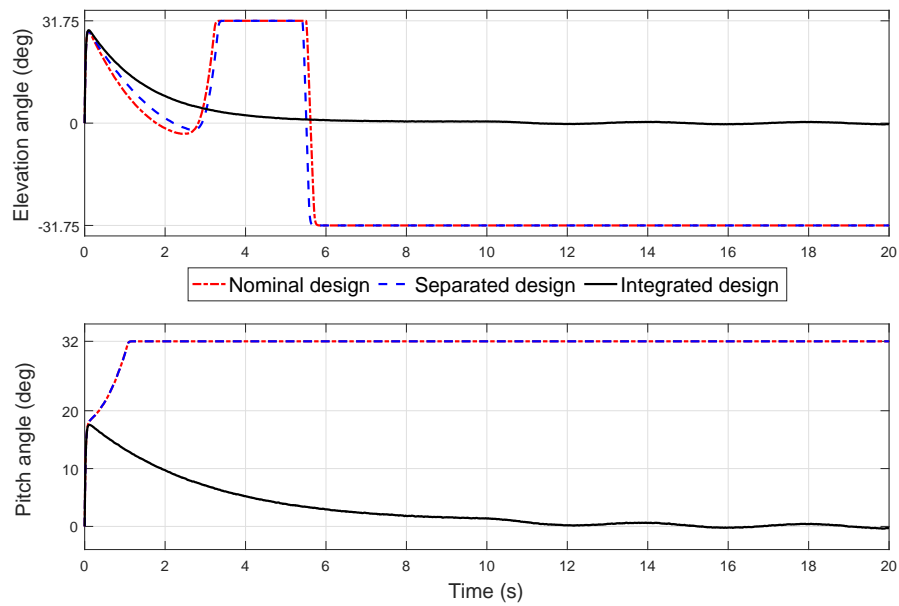


Fig. 7.7 Angle response: Case 2.

Summarizing the results of the three simulation cases: 1) Compared with the nominal and separated designs, the proposed integrated design stabilizes the elevation and pitch motions of the 3-DOF helicopter system with the best transient performance and meanwhile avoids actuator saturation, no matter if actuator faults exist or not. Although

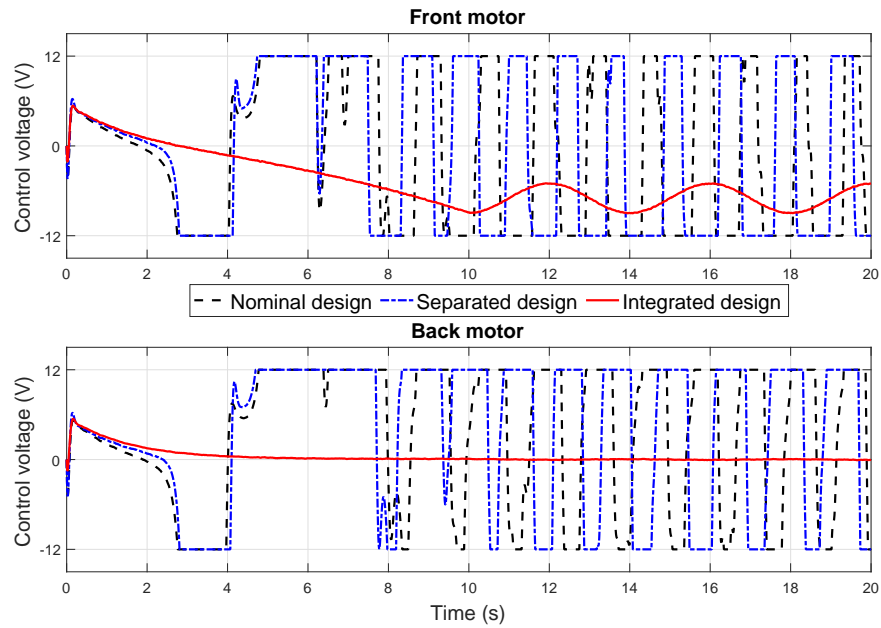


Fig. 7.8 Control effort: Case 2.

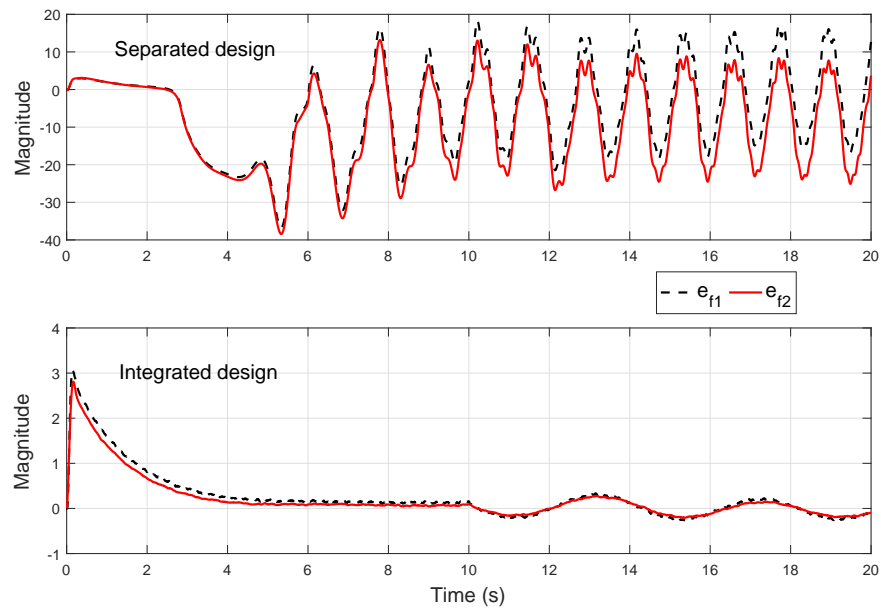


Fig. 7.9 Fault estimation performance: Case 3.

the separated design can also avoid actuator saturation in the presence of actuator faults, it suffers from pitch angle oscillation. 2) The proposed integrated design approach achieves more accurate fault estimation than the separated design.

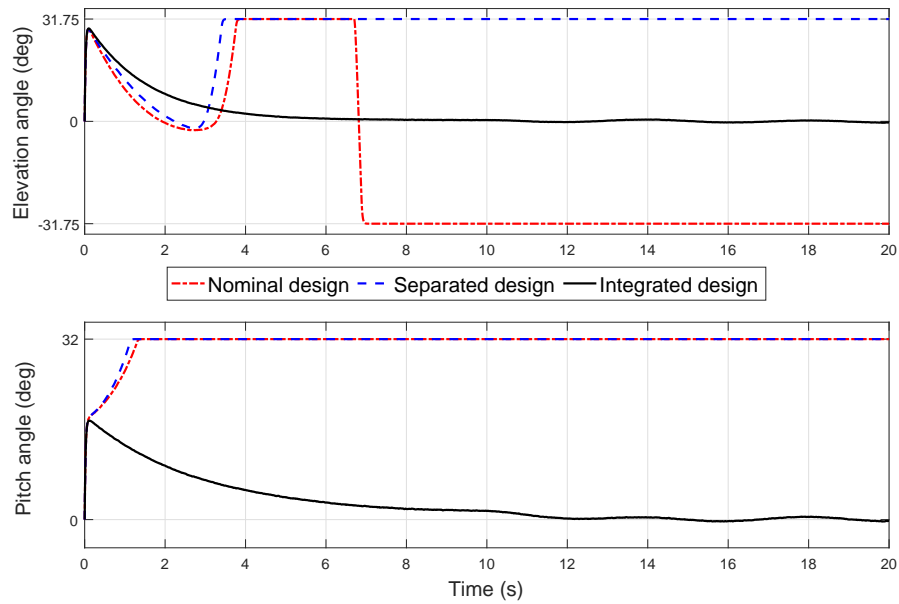


Fig. 7.10 Angle response: Case 3.

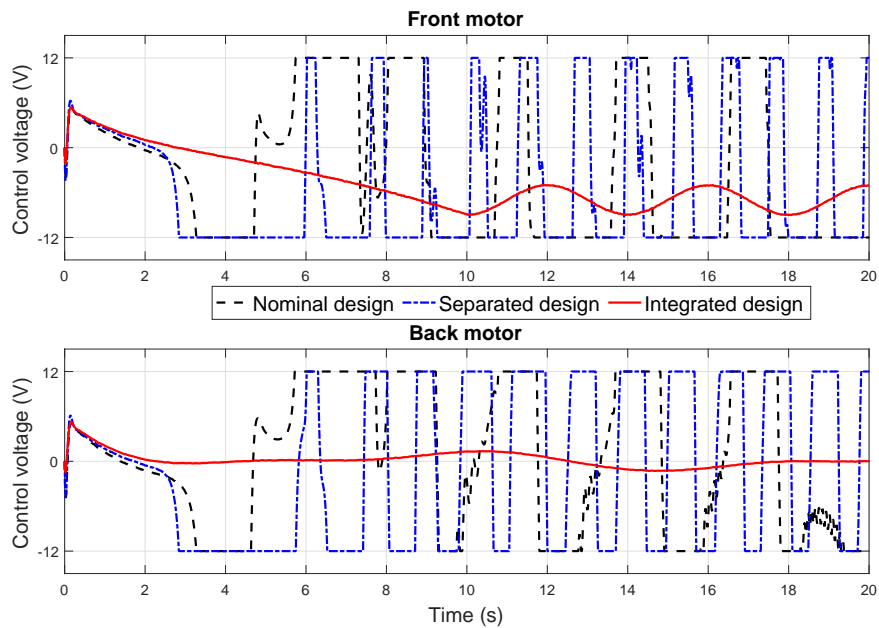


Fig. 7.11 Control effort: Case 3.

The results represent well the expected behaviour of the FTC cases, since 1) the nominal design does not include FE and FTC modules, and 2) the separated design neglects the *bi-directional robustness interactions* between the FE observer and FTC system, resulting from inaccurate estimation as well as system performance with low robustness.

7.7 Conclusion

This chapter demonstrates the capability of the H_∞ optimization approach proposed in Chapter 4 to address the FTC problem for a nonlinear 3-DOF helicopter system subject to actuator faults and saturation, system uncertainty, and external disturbance. A nonlinear ASUIO is used to estimate the system state and faults and an adaptive sliding mode FTC controller using the fault/state estimates is designed to compensate the fault and saturation effects and robustly stabilize the elevation and pitch motions. An integrated design approach with a new single-step LMI formulation without equality constraints is used to solve the observer and controller gains. Compared with the nominal control and separated FE/FTC designs, the integrated approach is shown to be more effective for achieving robust FTC performance (stabilization and fault compensation).

Part III

Integrated FE/FTC design for large-scale interconnected systems

Chapter 8: Integrated FE/FTC for large-scale interconnected systems with application to a 3-machine power system

8.1 Introduction

Chapters 4 - 7 deal with integrated FE/FTC designs for small-scale linear or nonlinear systems. However, the complexity of industrial, process, banking and IT systems increases rapidly as modern technology makes more and more use of interconnected, embedded, networked and distributed architectures (Bakule and Rossel, 2008; Ikeda, 1989; Sandell Jr et al., 1978; Šiljak, 1991, 1996; Šiljak and Zečević, 2005). It is stated in Šiljak (1991) that the complexity of real systems might not be well organized, whilst for control to be effective a good structural system organization is required. This can be achieved using a decentralized system structure in which local interconnected subsystems are well defined. A general diagram of decentralized large-scale control system with n subsystems is outlined in Fig. 8.1, where S_i and C_i are the i -th subsystem and its controller, respectively.

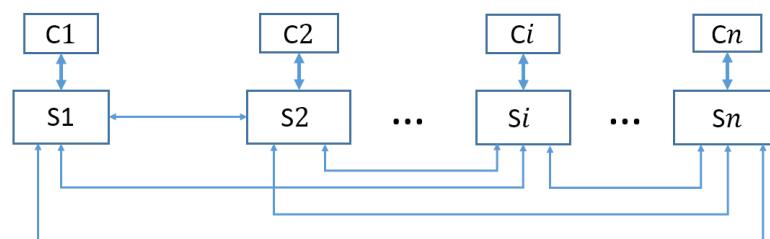


Fig. 8.1 Decentralized large-scale control systems.

Decentralized control is economical and can be reliable. However, the disturbance from interactions should be handled by combined use of state estimation and control. Some researchers use decentralized observer-based control to achieve stability and robustness control goals, e.g., Bakule and Rodellar (1996); Benigni et al. (2010); Kalsi et al. (2009, 2010); Pagilla and Zhu (2004); Shafai et al. (2011); Tili and Braiek (2009a). A further challenge arises when there exist actuator, sensor or process faults. The design problem is further complicated by the combined presence of faults and uncertainties. This challenge goes far beyond the usual design requirements of robust control, since the faults have to be considered as new forms of uncertainty/disturbance acting on the system (Huang et al., 2016).

There are several powerful approaches in the literature for robust FE using specialized observers, e.g., Chung et al. (2001); Hassan et al. (1992); Shankar et al. (2002); Yan and Edwards (2008). If a fault signal can be reconstructed robustly then there is also a possibility of making direct use of the fault estimate in a robust control scheme to compensate the fault effect, providing an opportunity for good FTC performance (Huang et al., 2016). Existing works on FTC for large-scale interconnected systems are classified as follows.

- *PFTC (without fault detection/estimation)*. Jin and Yang (2009) propose an adaptive model matching control for interconnected systems with actuator faults. Panagi and Polycarpou (2011a,b) address the decentralized FTC problems for interconnected nonlinear systems subject to connection faults (faults on interaction functions). Amani et al. (2014) describe a large-scale cooperative FTC system design considering actuator faults. Naghavi et al. (2014) propose a decentralized fault tolerant predictive control for discrete-time interconnected nonlinear systems with connection faults. Huang and Patton (2015) develop an output feedback sliding mode FTC design for interconnected systems with actuator faults. Yang et al. (2015) develop a fault recovery and FTC strategy for interconnected nonlinear systems with both actuator and sensor faults. Adaptive decentralized FTC designs are proposed in Chen et al. (2016a) and Hashemi et al. (2016) for large-scale interconnected nonlinear systems with actuator faults.

- *AFTC (with FDI)*. In Sauter et al. (2006) a decentralized FDI/FTC system is designed for networked systems considering actuator faults. Patton et al. (2007) propose a FTC design with a distributed hierarchical structure for network control systems. Patton and Klinkhieo (2009) provide a two-level sliding mode FTC scheme for distributed and interconnected systems. Khalili et al. (2015) deal with the decentralized fault accommodation problem for multi-agents systems using FDI.

However, few works have considered decentralized FTC system designs via FE, instead of using the FDI approach. FE directly estimates the fault signal, avoiding complex procedures of the threshold setting and fault isolation required in FDI, which can significantly facilitate the FTC system design.

This background motivates the work in this chapter of a decentralized FTC design for large-scale linear systems subject to uncertain nonlinear interactions and actuator or sensor faults, using a decentralized ASUIO for simultaneous estimation of the system state variables and faults. Compared with the existing observers for FE, comparatively simpler implemented decentralized UIOs are developed in Hou and Müller (1994) and Saif and Guan (1992) for state estimation. However, these UIOs require rank condition on the system matrices and FE is out of their scope.

Moreover, there exist *bi-directional robustness interactions* between the FE observer and FTC system for each subsystem, since 1) the uncertain nonlinear interactions affect the state/fault estimation performance and 2) the estimation errors affect the FTC system performance. A concept of integrated design is described in Chapter 3 and strategies are developed in Chapters 4 - 7 for small scale systems to handle these bi-directional interactions to achieve robust FE/FTC design. The main contribution of this chapter is an extension of the integrated design concept to the considered large-scale interconnected systems, and for which an integrated decentralized FE/FTC design is proposed based on H_∞ optimization with a single-step LMI formulation.

The remainder of this chapter is organized as follows. Section 8.2 formulates the problem. Section 8.3 proposes an integrated design for the decentralized ASUIO-based FE and FTC controller for the large-scale systems with actuator fault. This strategy is extended in Section 8.4 for the sensor fault case. Section 8.5 applies the proposed designs to a 3-machine power system. Section 8.6 draws the conclusions.

8.2 Problem statement and preliminaries

Consider a large-scale system consisting of n subsystems and the i -th ($i = 1, 2, \dots, n$) subsystem is represented by

$$\begin{aligned}\dot{x}_i &= A_i x_i + B_i u_i + F_i f_i + h_i(x, t), \\ y_i &= C_i x_i,\end{aligned}\tag{8.1}$$

where $x_i \in \mathbb{R}^{n_i}$, $u_i \in \mathbb{R}^{m_i}$, and $y_i \in \mathbb{R}^{p_i}$ are the state, control input, and system output, respectively. $f_i \in \mathbb{R}^{q_i}$ denote the actuator fault. $A_i \in \mathbb{R}^{n_i \times n_i}$, $B_i \in \mathbb{R}^{n_i \times m_i}$, $C_i \in \mathbb{R}^{p_i \times n_i}$, and $F_i \in \mathbb{R}^{n_i \times q_i}$ are constant matrices. $h_i(x, t) \in \mathbb{R}^{n_i}$ is the uncertain nonlinear interaction term with $x = [x_1^\top, \dots, x_n^\top]^\top$. The following assumptions are made on the system (8.1).

Assumption 8.1 The pairs (A_i, B_i) and (A_i, C_i) are controllable and observable, respectively.

Assumption 8.2 The trios (A_i, C_i, F_i) are observable, i.e., the following rank conditions are satisfied: $\text{rank} \begin{bmatrix} A_i & F_i \\ C_i & 0 \end{bmatrix} = n_i + q_i$.

Assumption 8.3 The fault f_i as well as its first-order derivative are norm-bounded, and the fault is matched, i.e., $\text{rank}(B_i, F_i) = \text{rank}(B_i)$.

Assumption 8.4 The interaction function $h_i(x, t)$ satisfies

$$h_i^\top(x, t)h_i(x, t) \leq \alpha_i x^\top H_{0i}^\top H_{0i} x,$$

where H_{0i} is a known constant matrix and α_i is some positive scalar defined as the uncertain interaction bound.

Remark 8.1 Defining $h(x, t) = [h_1^\top(x, t), \dots, h_n^\top(x, t)]^\top$ as the interaction term of the overall large-scale system, then

$$h^\top(x, t)h(x, t) \leq x^\top H_0^\top H_0 x,$$

where $H_0 = [\sqrt{\alpha_1}H_{01}^\top, \dots, \sqrt{\alpha_n}H_{0n}^\top]^\top$.

This chapter aims to address the following problem.

Problem 8.1 For the large-scale interconnected system (8.1) with uncertain nonlinear interactions and actuator faults, design a decentralized ASUIO to estimate the system states/faults together with a decentralized FTC controller to guarantee the robust stability of the overall closed-loop system.

8.3 Integration of decentralized FE/FTC with actuator faults

The diagram of the proposed decentralized ASUIO-based FTC large-scale system is outlined in Fig. 8.2, where S_i , O_i , and C_i are the i -th subsystems and its observer and controller, respectively.

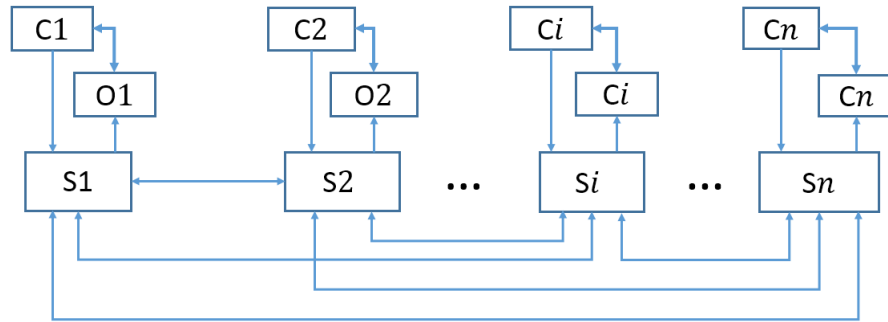


Fig. 8.2 Decentralized integrated FE/FTC design for large-scale systems.

8.3.1 Decentralized FE observer design

Augmenting the i -th subsystem (8.1) into

$$\begin{aligned}\dot{\hat{x}}_i &= \bar{A}_i \bar{x}_i + \bar{h}_i(x, t) + \bar{B}_i u_i + \bar{D}_i \bar{d}_i, \\ y_i &= \bar{C}_i \bar{x}_i,\end{aligned}\quad (8.2)$$

where $\bar{x}_i = \begin{bmatrix} x_i \\ f_i \end{bmatrix}$, $\bar{d}_i = \dot{f}_i$, $\bar{A}_i = \begin{bmatrix} A_i & F_i \\ 0 & 0 \end{bmatrix}$, $\bar{B}_i = \begin{bmatrix} B_i \\ 0 \end{bmatrix}$, $\bar{D}_i = \begin{bmatrix} 0 \\ I_{q_i} \end{bmatrix}$, $\bar{C}_i = [C_i \ 0]$, $\bar{h}_i(x, t) = \begin{bmatrix} h_i(x, t) \\ 0 \end{bmatrix}$. According to Assumption 8.2, it can be verified that the augmented system (8.2) is observable.

The augmented state vector \bar{x}_i is estimated by the ASUIO in the form of

$$\begin{aligned}\dot{z}_i &= M_i z_i + G_i u_i + L_i y_i, \\ \hat{x}_i &= z_i + H_i y_i,\end{aligned}\quad (8.3)$$

where $z_i \in \mathbb{R}^{n_i+q_i}$ is the observer system state vector, and $\hat{x}_i \in \mathbb{R}^{n_i+q_i}$ is the estimate of \bar{x}_i . The design matrices M_i , G_i , N_i , L_i and H_i are of appropriate dimensions.

Define the estimation error as $e_i = \bar{x}_i - \hat{x}_i$, then it follows from (8.2) and (8.3) that

$$\begin{aligned} \dot{e}_i = & (\Xi_i \bar{A}_i - L_{i1} \bar{C}_i) e_i + (\Xi_i \bar{A}_i - L_{i1} \bar{C}_i - M_i) z_i + (\Xi_i \bar{B}_i - G_i) u_i \\ & + [(\Xi_i \bar{A}_i - L_{i1} \bar{C}_i) H_i - L_{i2}] y_i + \Xi_i \bar{h}_i(x, t) + \Xi_i \bar{D}_i \bar{d}_i, \end{aligned} \quad (8.4)$$

where $\Xi_i = I_{n_i+q_i} - H_i \bar{C}_i$ and $L_i = L_{i1} + L_{i2}$.

Necessary conditions for the asymptotic stability of the error system (8.4) are

$$M_i \text{ is Hurwitz,} \quad (8.5)$$

$$\Xi_i \bar{A}_i - L_{i1} \bar{C}_i - M_i = 0, \quad (8.6)$$

$$\Xi_i \bar{B}_i - G_i = 0, \quad (8.7)$$

$$(\Xi_i \bar{A}_i - L_{i1} \bar{C}_i) H_i - L_{i2} = 0. \quad (8.8)$$

Note that the design matrices M_i , G_i , and L_{i2} can be calculated directly from (8.6) - (8.8) once the matrices L_{i1} and H_i are obtained. Thus, the main task in the following is to design the matrices L_{i1} and H_i . With the satisfaction of (8.6) - (8.8), (8.4) is rearranged into

$$\dot{e}_i = (\Xi_i \bar{A}_i - L_{i1} \bar{C}_i) e_i + \Xi_i \bar{h}_i(x, t) + \Xi_i \bar{D}_i \bar{d}_i. \quad (8.9)$$

8.3.2 Decentralized FTC controller design

An FTC controller for the i -th subsystem (8.1) is given as

$$u_i = -K_i \hat{x}_i, \quad (8.10)$$

where $K_i = [K_{xi} \ K_{fi}]$ and $K_{xi} \in \mathbb{R}^{m_i \times n_i}$ is the nominal controller gain and $K_{fi} \in \mathbb{R}^{m_i \times q_i}$ is the actuator fault compensation gain which is chosen as $K_{fi} = B_i^\dagger F_i$.

Substituting (8.10) into (8.1) gives the closed-loop system

$$\dot{x}_i = (A_i - B_i K_{xi}) x_i + B_i K_{fi} e_i + h_i(x, t). \quad (8.11)$$

8.3.3 Integrated synthesis of FE/FTC

The closed-loop system composed of (8.9) and (8.11) is

$$\begin{aligned}\dot{x}_i &= (A_i - B_i K_{xi})x_i + B_i K_i e_i + h_i(x, t), \\ \dot{e}_i &= (\Xi_i \bar{A}_i - L_{i1} \bar{C}_i)e_i + \Xi_i \bar{h}_i(x, t) + \Xi_i \bar{D}_i \bar{d}_i.\end{aligned}\quad (8.12)$$

Therefore, the augmented closed-loop system of the overall large-scale system is

$$\begin{aligned}\dot{x} &= \tilde{A}x + \tilde{F}e + h(x, t), \\ \dot{e} &= \tilde{A}_e e + \Xi \bar{h}(x, t) + \Xi \bar{D} \bar{d}, \\ z &= C_x x + C_e e,\end{aligned}\quad (8.13)$$

where $z \in \mathbb{R}^r$ is the measured output used to verify the closed-loop system performance with matrices $C_x \in \mathbb{R}^{r \times n}$ and $C_e \in \mathbb{R}^{r \times (n+q_1)}$, and $e = [e_1^\top, \dots, e_n^\top]^\top$, $\bar{d} = [\bar{d}_1^\top, \dots, \bar{d}_n^\top]^\top$, $\bar{h}_i(x, t) = [\bar{h}_1^\top(x, t), \dots, \bar{h}_n^\top(x, t)]^\top$, $\tilde{A} = \text{diag}(A_1 - B_1 K_{x1}, \dots, A_n - B_n K_{xn})$, $\tilde{F} = \text{diag}(B_1 K_1, \dots, B_n K_n)$, $\Xi = \text{diag}(\Xi_1, \dots, \Xi_n)$, $\bar{D} = \text{diag}(\bar{D}_1, \dots, \bar{D}_n)$, $\tilde{A}_e = \text{diag}(\Xi_1 \bar{A}_1 - L_{11} \bar{C}_1, \dots, \Xi_n \bar{A}_n - L_{n1} \bar{C}_n)$.

Now the considered integrated design problem can be stated as follows: design the controller gains K_{xi} ($i = 1, \dots, n$) and observer parameter matrices L_{i1} ($i = 1, \dots, n$) to ensure the robust stability of the overall closed-loop system (8.13). This design problem is solved using Theorem 8.1 with a single-step LMI formulation described as follows.

Theorem 8.1 Under Assumptions 8.1 - 8.4, given positive scalars γ , α_i , ε_{i1} , and ε_{i2} , $i = 1, 2, \dots, n$, the overall closed-loop system (8.13) is stable with H_∞ performance $\|G_{z\bar{d}}\|_\infty < \gamma$, if there exist symmetric positive definite matrices $Z_i \in \mathbb{R}^{n_i \times n_i}$, $Q_{i1} \in \mathbb{R}^{n_i \times n_i}$, $Q_{i2} \in \mathbb{R}^{q_i \times q_i}$, and matrices $M_{1i} \in \mathbb{R}^{m_i \times n_i}$, $M_{2i} \in \mathbb{R}^{n_i \times p_i}$, $M_{3i} \in \mathbb{R}^{q_i \times p_i}$, $M_{4i} \in \mathbb{R}^{n_i \times p_i}$, and

$M_{5i} \in \mathbb{R}^{q_i \times p_i}$, $i = 1, \dots, n$, such that

$$\begin{bmatrix} \Pi_{11} & \Pi_{12} & \Pi_{13} & 0 & \Pi_{15} & 0 & \Pi_{17} & 0 & 0 \\ \star & \Pi_{22} & 0 & \Pi_{24} & 0 & \Pi_{26} & 0 & \Pi_{28} & \Pi_{29} \\ \star & \star & -\varepsilon_1^{-1}Z & 0 & 0 & 0 & 0 & 0 & 0 \\ \star & \star & \star & -\varepsilon_1 Z & 0 & 0 & 0 & 0 & 0 \\ \star & \star & \star & \star & -\varepsilon I & 0 & 0 & 0 & 0 \\ \star & \star & \star & \star & \star & -\varepsilon_1 I & 0 & 0 & 0 \\ \star & \star & \star & \star & \star & 0 & -I & 0 & 0 \\ \star & -I & 0 \\ \star & -\gamma^2 \end{bmatrix} < 0, \quad (8.14)$$

where

$$\begin{aligned} \varepsilon &= \sigma(\varepsilon_1 + \varepsilon_2), \varepsilon_1 = \text{diag}(\varepsilon_{11}, \dots, \varepsilon_{n1}), \\ \sigma &= \text{diag}(\sigma_1, \dots, \sigma_n) = \text{diag}(1/\alpha_1, \dots, 1/\alpha_n), \\ \Pi_{11} &= \text{diag}(\Pi_{111}, \dots, \Pi_{11n}), \Pi_{11i} = \text{He}(A_i Z_i - B_i M_{1i}) + \varepsilon_{i2}^{-1} I, \\ \Pi_{12} &= \text{diag}([0 \ F_1], \dots, [0 \ F_n]), \Pi_{13} = \text{diag}(B_1 M_{1i}, \dots, B_n M_{1n}), \\ \Pi_{15} &= \begin{bmatrix} Z_1 H_{011}^\top & \cdots & Z_1 H_{0n1}^\top \\ \vdots & \vdots & \vdots \\ Z_n H_{01n}^\top & \cdots & Z_n H_{0nn}^\top \end{bmatrix}, \Pi_{17} = \begin{bmatrix} Z_1 C_{x1}^\top \\ \vdots \\ Z_n C_{xn}^\top \end{bmatrix}, \\ \Pi_{22} &= \text{diag}(\Pi_{221}, \dots, \Pi_{22n}), \Pi_{22i} = \begin{bmatrix} \Xi_{22i} & \Xi_{23i} \\ \star & \Xi_{33i} \end{bmatrix}, \\ \Xi_{22i} &= \text{He}(Q_{i1} A_i - M_{4i} C_i A_i - M_{2i} C_i), \\ \Xi_{23i} &= Q_{i1} F_i - M_{4i} C_i F_i - (M_{5i} C_i A_i + M_{3i} C_i)^\top, \\ \Xi_{33i} &= \text{He}(-M_{5i} C_i F_i), \Pi_{24} = [0; I], \Pi_{26} = \text{diag}(Q_1 \Xi_1, \dots, Q_n \Xi_n), \\ Q_i \Xi_i &= \begin{bmatrix} Q_{i1} - M_{4i} C_i & 0 \\ -M_{5i} C_i & Q_{i2} \end{bmatrix}, \Pi_{28} = \begin{bmatrix} C_{e1}^\top \\ \vdots \\ C_{en}^\top \end{bmatrix}, \\ \Pi_{29} &= \text{diag}(\Pi_{291}, \dots, \Pi_{29n}), \Pi_{29i} = \begin{bmatrix} 0 \\ Q_{i2} \end{bmatrix}. \end{aligned}$$

Then the gains are given by:

$$K_{xi} = M_{1i} Z_i^{-1}, L_{i11} = Q_{i1}^{-1} M_{2i}, L_{i12} = Q_{i2}^{-1} M_{3i}, H_{i1} = Q_{i1}^{-1} M_{4i}, H_{i2} = Q_{i2}^{-1} M_{5i}.$$

Proof: Denote $\chi_1 = \bar{h}^\top(x, t)\Xi^\top Qe + e^\top Q\Xi\bar{h}(x, t)$. Consider a Lyapunov function $V_e = e^\top Qe$. It follows that for some positive scalar $\varepsilon_1 = \text{diag}(\varepsilon_{11}, \dots, \varepsilon_{n1})$,

$$\begin{aligned}\chi_1 &= -\left[\sqrt{\varepsilon_1}^{-1}\Xi^\top Qe - \sqrt{\varepsilon_1}\bar{h}(x, t)\right]^\top \times \left[\sqrt{\varepsilon_1}^{-1}\Xi^\top Qe - \sqrt{\varepsilon_1}\bar{h}(x, t)\right] \\ &\quad + \varepsilon_1^{-1}e^\top Q\Xi\Xi^\top Qe + \varepsilon_1\bar{h}^\top(x, t)\bar{h}(x, t) \\ &\leq \varepsilon_1^{-1}e^\top Q\Xi\Xi^\top Qe + \varepsilon_1x^\top H_0^\top H_0x.\end{aligned}$$

The time derivative of V_e along (8.9) is

$$\begin{aligned}\dot{V}_e &= e^\top \text{He}(Q\tilde{A}_e)e + \chi_1 \\ &\leq e^\top [\text{He}(Q\tilde{A}_e) + \varepsilon_1^{-1}Q\Xi\Xi^\top Q]e + \varepsilon_1x^\top H_0^\top H_0x.\end{aligned}\quad (8.15)$$

Consider another Lyapunov function $V_x = x^\top Px$. Denote $\chi_2 = h^\top(x, t)Px + x^\top Ph(x, t)$, it follows that for some positive scalar $\varepsilon_2 = \text{diag}(\varepsilon_{12}, \dots, \varepsilon_{n2})$,

$$\begin{aligned}\chi_2 &= -\left[\sqrt{\varepsilon_2}^{-1}Px - \sqrt{\varepsilon_2}h(x, t)\right]^\top \times \left[\sqrt{\varepsilon_2}^{-1}Px - \sqrt{\varepsilon_2}h(x, t)\right] \\ &\quad + \varepsilon_2^{-1}x^\top PPx + \varepsilon_2h^\top(x, t)h(x, t) \\ &\leq \varepsilon_2^{-1}x^\top PPx + \varepsilon_2x^\top H_0^\top H_0x.\end{aligned}$$

Then the time derivative of V_x along (8.11) is

$$\begin{aligned}\dot{V}_x &= x^\top \text{He}(P\tilde{A})x - \text{He}(x^\top P\tilde{F}e) + \chi_2 \\ &\leq x^\top [\text{He}(P\tilde{A}) + \varepsilon_2^{-1}PP]x + \varepsilon_2x^\top H_0^\top H_0x - \text{He}(x^\top P\tilde{F}e).\end{aligned}\quad (8.16)$$

Let $\xi = [x^\top e^\top]^\top$, the H_∞ performance $\|G_{zd}\|_\infty < \gamma$ can be represented as

$$J = \int_0^\infty \left(z^\top z - \gamma^2 d^\top d\right) dt < 0.\quad (8.17)$$

Under zero initial conditions

$$\begin{aligned}
J &= \int_0^\infty \left(z^\top z - \gamma^2 \bar{d}^\top \bar{d} + \dot{V}_x + \dot{V}_e \right) dt - \int_0^\infty (\dot{V}_x + \dot{V}_e) dt \\
&= \int_0^\infty \left(z^\top z - \gamma^2 \bar{d}^\top \bar{d} + \dot{V}_x + \dot{V}_e \right) dt - (V_x(\infty) + V_e(\infty)) + (V_x(0) + V_e(0)) \\
&\leq \int_0^\infty \left(z^\top z - \gamma^2 \bar{d}^\top \bar{d} + \dot{V}_x + \dot{V}_e \right) dt.
\end{aligned}$$

Now, a sufficient condition of (8.17) is

$$z^\top z - \gamma^2 \bar{d}^\top \bar{d} + \dot{V}_x + \dot{V}_e < 0. \quad (8.18)$$

Substituting (8.15) and (8.16) into (8.18) yields

$$\begin{bmatrix} x \\ e \\ \bar{d} \end{bmatrix}^\top \begin{bmatrix} J_{11} & J_{12} & 0 \\ \star & J_{22} & J_{23} \\ \star & \star & -\gamma^2 I \end{bmatrix} \begin{bmatrix} x \\ e \\ \bar{d} \end{bmatrix} < 0, \quad (8.19)$$

where $J_{11} = \text{He}(P\tilde{A}) + (\varepsilon_1 + \varepsilon_2)H_0^\top H_0 + \varepsilon_2^{-1}PP + C_x^\top C_x$, $J_{12} = P\tilde{F}$, $J_{22} = \text{He}(Q\tilde{A}_e) + \varepsilon_1^{-1}e^\top Q\Xi\Xi^\top Q + C_e^\top C_e$, and $J_{23} = Q\Xi\bar{D}$.

Define $Z = P^{-1}$. Pre- and post-multiplying both sides of (8.19) with $\text{diag}(Z, I, I)$, then (8.19) is equivalently converted into

$$\begin{bmatrix} J_{11} & J_{12} & 0 \\ \star & J_{22} & J_{23} \\ \star & \star & -\gamma^2 I \end{bmatrix} < 0, \quad (8.20)$$

where $J_{11} = \text{He}(\tilde{A}Z) + (\varepsilon_1 + \varepsilon_2)ZH_0^\top H_0Z + \varepsilon_2^{-1}I + ZC_x^\top C_xZ$, $J_{12} = \tilde{F}$, $J_{22} = \text{He}(Q\tilde{A}_e) + \varepsilon_1^{-1}Q\Xi\Xi^\top Q + C_e^\top C_e$, and $J_{23} = Q\Xi\bar{D}$.

Define $Z = \text{diag}(Z_1, \dots, Z_n)$, $Q = \text{diag}(Q_1, \dots, Q_n)$, and $Q_i = \text{diag}(Q_{i1}, Q_{i2})$. Note that $J_{12} = \text{diag}([0 \ F_1], \dots, [0 \ F_n]) + \text{diag}([B_1 \ K_{x1} \ 0], \dots, [B_n \ K_{xn} \ 0])$. Using the Young inequality (see Appendix A.4), it follows that for some positive scalars ε_{i1} , $i = 1, \dots, n$,

$$\begin{bmatrix} 0 & B_1 K_{x1} & 0 \\ 0 & 0 & 0 \\ 0 & 0 & 0 \end{bmatrix} \leq \varepsilon_{11}^{-1} \begin{bmatrix} 0 \\ I \\ 0 \end{bmatrix} Z_1^{-1} \begin{bmatrix} 0 \\ I \\ 0 \end{bmatrix}^\top + \varepsilon_{11} \begin{bmatrix} B_1 K_{x1} Z_1 \\ 0 \\ 0 \end{bmatrix} Z_1^{-1} \begin{bmatrix} B_1 K_{x1} Z_1 \\ 0 \\ 0 \end{bmatrix}^\top, \\ \begin{bmatrix} 0 & 0 & 0 \\ 0 & B_i K_{xi} & 0 \\ 0 & 0 & 0 \end{bmatrix} \leq \varepsilon_{i1}^{-1} \begin{bmatrix} 0 \\ I \\ 0 \end{bmatrix} Z_i^{-1} \begin{bmatrix} 0 \\ I \\ 0 \end{bmatrix}^\top + \varepsilon_{i1} \begin{bmatrix} 0 \\ B_i K_{xi} Z_i \\ 0 \end{bmatrix} Z_i^{-1} \begin{bmatrix} 0 \\ B_i K_{xi} Z_i \\ 0 \end{bmatrix}^\top.$$

Denote $\Pi_{22} = \text{He}(Q\tilde{A}_e)$ with the structure $\Pi_{22} = \text{diag}(\Pi_{221}, \dots, \Pi_{22n})$. Note that

$$\Pi_{22i} = \begin{bmatrix} \Xi_{22i} & \Xi_{23i} \\ \star & \Xi_{33i} \end{bmatrix}, \quad \Xi_{33i} = \text{He}(-Q_{i2}H_{i2}C_iF_i), \\ \Xi_{22i} = \text{He}(Q_{i1}(A_i - H_{i1}C_iA_i - L_{i11}C_i)), \\ \Xi_{23i} = Q_{i1}F_i - Q_{i1}H_{i1}C_iF_i - (H_{i2}C_iA_i + L_{i12}C_i)^\top Q_{i2}.$$

Define $M_{1i} = K_{xi}Z_i$, $M_{2i} = Q_{i1}L_{i11}$, $M_{3i} = Q_{i2}L_{i12}$, $M_{4i} = Q_{i1}H_{i1}$, $M_{5i} = Q_{i2}H_{i2}$, and $H_{0i}^\top = [H_{0i1}, \dots, H_{0in}]^\top$, $i = 1, \dots, n$. Using the Schur complement repeatedly, (8.20) can be finally formulated into (8.14). \square

8.4 Extension to sensor fault case

Consider a large-scale system consists of n subsystems and the i -th ($i = 1, 2, \dots, n$) subsystem is

$$\begin{aligned} \dot{x}_i &= A_i x_i + B_i u_i + h_i(x, t), \\ y_i &= C_i x_i + F_{si} f_{si}, \end{aligned} \quad (8.21)$$

where $x_i \in \mathbb{R}^{n_i}$, $u_i \in \mathbb{R}^{m_i}$, and $y_i \in \mathbb{R}^{p_i}$ are the state, control input, and system output vectors, respectively. $f_{si} \in \mathbb{R}^{q_i}$ denotes the sensor fault. $A_i \in \mathbb{R}^{n_i \times n_i}$, $B_i \in \mathbb{R}^{n_i \times m_i}$, $C_i \in \mathbb{R}^{p_i \times n_i}$, and $F_{si} \in \mathbb{R}^{p_i \times q_i}$ are constant matrices. $h_i(x, t) \in \mathbb{R}^{n_i}$ is the uncertain nonlinear interaction term with $x = [x_1^\top, \dots, x_n^\top]^\top$. The following Assumption is made for the sensor fault.

Assumption 8.5 The fault f_{si} is norm-bounded and $\text{rank}(F_{si}) = q_i$.

Assumption 8.6 The trios (A_i, C_i, F_{si}) are observable, i.e., the following rank conditions

$$\text{rank} \begin{bmatrix} A_i & 0 \\ C_i & F_{si} \end{bmatrix} = n_i + q_i.$$

For the large-scale interconnected system (8.21) with uncertain nonlinear interactions and sensor faults, design a decentralized observer to estimate the system state and faults and a decentralized FTC controller based on the estimates to guarantee robust stability of the overall closed-loop system.

By treating the sensor fault as a new system state the i -th subsystem (8.21) can be augmented into

$$\begin{aligned}\dot{\bar{x}}_i &= \bar{A}_i \bar{x}_i + \bar{h}_i(x, t) + \bar{B}_i u_i + \bar{D}_i \bar{d}_i, \\ y_i &= \bar{C}_i \bar{x}_i,\end{aligned}\tag{8.22}$$

where $\bar{x}_i = \begin{bmatrix} x_i \\ f_{si} \end{bmatrix}$, $\bar{d}_i = \dot{f}_{si}$, $\bar{A}_i = \begin{bmatrix} A_i & 0 \\ 0 & 0 \end{bmatrix}$, $\bar{B}_i = \begin{bmatrix} B_i \\ 0 \end{bmatrix}$, $\bar{D}_i = \begin{bmatrix} 0 \\ I_{q_i} \end{bmatrix}$, $\bar{C}_i = [C_i \ F_{si}]$, $\bar{h}_i(x, t) = [h_i^\top(x, t) \ 0]^\top$. According to Assumption 8.6, it can be verified that the augmented system (8.22) is observable.

It can be seen that (8.22) is in a similar form of (8.2), thus the following ASUIO is used to estimate the new state \bar{x}_i ,

$$\begin{aligned}\dot{z}_i &= M_i z_i + G_i u_i + L_i y_i, \\ \hat{x}_i &= z_i + H_i y_i,\end{aligned}\tag{8.23}$$

where $z_i \in \mathbb{R}^{n_i+q_i}$ is the observer system state vector and $\hat{x}_i \in \mathbb{R}^{n_i+q_i}$ is the estimate of \bar{x}_i . The matrices $M_i \in \mathbb{R}^{(n_i+q_i) \times (n_i+q_i)}$, $G_i \in \mathbb{R}^{(n_i+q_i) \times m}$, $n_i \in \mathbb{R}^{(n_i+q_i) \times (n_i+q_i)}$, $L_i \in \mathbb{R}^{(n_i+q_i) \times p_i}$, and $H_i \in \mathbb{R}^{(n_i+q_i) \times q_i}$ are to be designed.

Define the estimation error as $e_i = \bar{x}_i - \hat{x}_i$, then it follows from (8.2) and (8.3) that

$$\begin{aligned}\dot{e}_i &= (\Xi_i \bar{A}_i - L_{i1} \bar{C}_i) e_i + (\Xi_i \bar{A}_i - L_{i1} \bar{C}_i - M_i) z_i + (\Xi_i \bar{B}_i - G_i) u_i \\ &\quad + [(\Xi_i \bar{A}_i - L_{i1} \bar{C}_i) H_i - L_{i2}] y_i + \Xi_i \bar{h}_i(x, t) + \Xi_i \bar{D}_i \bar{d}_i,\end{aligned}\tag{8.24}$$

where $\Xi_i = I_{n_i+q_i} - H_i \bar{C}_i$ and $L_i = L_{i1} + L_{i2}$.

Necessary conditions for the asymptotic stability of the error system (8.4) are

$$M_i \text{ is Hurwitz,} \quad (8.25)$$

$$\Xi_i \bar{A}_i - L_{i1} \bar{C}_i - M_i = 0, \quad (8.26)$$

$$\Xi_i \bar{B}_i - G_i = 0, \quad (8.27)$$

$$(\Xi_i \bar{A}_i - L_{i1} \bar{C}_i) H_i - L_{i2} = 0 \quad (8.28)$$

$$\Xi_i \bar{D}_i = 0. \quad (8.29)$$

Since $\bar{C}_i \bar{D}_i = F_{si}$, then $\text{rank}(\bar{C}_i \bar{D}_i) = \text{rank}(\bar{D}_i) = q_i$. Hence, there exists a matrix $H_i = \bar{D}_i F_{si}^\dagger$ such that (8.29) is satisfied. Note that the design matrices M_i , G_i , and L_{i2} can be calculated directly from (8.26) - (8.28) once the matrix L_{i1} is obtained. Thus, the main task in the following is to design the matrix L_{i1} . With the satisfaction of (8.26) - (8.29), (8.24) is rearranged into

$$\dot{e}_i = (\Xi_i \bar{A}_i - L_{i1} \bar{C}_i) e_i + \Xi_i \bar{h}_i(x, t). \quad (8.30)$$

Remark 8.2 The deduction of (8.30) uses the matrix equations defined in (8.26) - (8.28). Moreover, it is different from (8.4) that the disturbance term $\Xi_i \bar{D}_i \bar{d}_i$ ($\Xi_i = I_{n_i+q_i} - H_i \bar{C}_i$) is removed in (8.30). This is because $\text{rank}(\bar{C}_i \bar{D}_i) = \text{rank}(\bar{D}_i) = q_i$, so there always exists a matrix $H_i = \bar{D}_i (\bar{C}_i \bar{D}_i)^\top (\bar{C}_i \bar{D}_i (\bar{C}_i \bar{D}_i)^\top)^\dagger$ such that $\Xi_i \bar{D}_i = 0$. Hence, in the error system dynamics (8.30), only the matrix L_{i1} needs to be determined.

An FTC controller for the i -th subsystem (8.21) is given as

$$u_i = K_i \hat{x}_i, \quad (8.31)$$

where $K_i = [K_{xi} \ 0]$ and $K_{xi} \in \mathbb{R}^{m_i \times n_i}$ is the normal controller gain.

Substituting (8.31) into (8.21) yields the closed-loop system

$$\begin{aligned} \dot{x}_i &= (A_i + B_i K_{xi}) x_i - B_i K_i e_i + h_i(x, t), \\ y_{ci} &= y_i - F_{si} \hat{f}_{si}, \end{aligned} \quad (8.32)$$

where y_{ci} is the system output with sensor fault compensation and $\hat{f}_{si} = [0 \ I_{q_i}] \hat{x}_i$ is the sensor fault estimate.

Combining (8.30) and (8.32) into a composite closed-loop system

$$\begin{aligned}\dot{x}_i &= (A_i + B_i K_{xi})x_i - B_i K_i e_i + h_i(x, t), \\ \dot{e}_i &= (\Xi_i \bar{A}_i - L_{i1} \bar{C}_i)e_i + \Xi_i \bar{h}_i(x, t), \\ y_{ci} &= y_i - F_{si} \hat{f}_{si}.\end{aligned}\quad (8.33)$$

Hence, the composite closed-loop large-scale system is

$$\begin{aligned}\dot{x} &= \tilde{A}x - \tilde{F}e + h(x, t), \\ \dot{e} &= \tilde{A}_e e + \Xi \bar{h}(x, t), \\ y_c &= y - F_s \hat{f}_s,\end{aligned}\quad (8.34)$$

where $e = [e_1^\top, \dots, e_n^\top]^\top$, $y_c = [y_{c1}^\top, \dots, y_{cn}^\top]^\top$, $y = [y_1^\top, \dots, y_n^\top]^\top$, $\hat{f}_s = [\hat{f}_{s1}^\top, \dots, \hat{f}_{sn}^\top]^\top$, $\bar{h}_i(x, t) = [\bar{h}_1^\top(x, t), \dots, \bar{h}_n^\top(x, t)]^\top$, $\tilde{A} = \text{diag}(A_1 + B_1 K_{x1}, \dots, A_n + B_n K_{xn})$, $\tilde{F} = \text{diag}(B_1 K_1, \dots, B_n K_n)$, $\Xi = \text{diag}(\Xi_1, \dots, \Xi_n)$, $F_s = \text{diag}(F_{s1}, \dots, F_{sn})$, $\tilde{A}_e = \text{diag}(\Xi_1 \bar{A}_1 - L_{11} \bar{C}_1, \dots, \Xi_n \bar{A}_n - L_{n1} \bar{C}_n)$.

Now the integrated design problem considered is reformulated as follows: design the controller gains K_{xi} ($i = 1, \dots, n$) and observer parameter matrices L_{1i} ($i = 1, \dots, n$) to ensure the robust stability of the overall closed-loop system (8.34).

This design problem is solved in the sequel using Theorem 8.2 with a single-step LMI formulation.

Theorem 8.2 Under Assumptions 8.1, 8.4 and 8.5, given positive scalars α_i , ε_{i1} , and ε_{i2} , $i = 1, 2, \dots, n$, if there exist symmetric positive definite matrices $Z_i \in \mathbb{R}^{n_i \times n_i}$, $Q_{i1} \in \mathbb{R}^{n_i \times n_i}$, $Q_{i2} \in \mathbb{R}^{q_i \times q_i}$, and the matrices $M_{1i} \in \mathbb{R}^{m_i \times n_i}$, $M_{2i} \in \mathbb{R}^{n_i \times p_i}$, and $M_{3i} \in \mathbb{R}^{q_i \times p_i}$, $i = 1, \dots, n$, such that

$$\begin{bmatrix} \Pi_{11} & 0 & \Pi_{13} & 0 & \Pi_{15} & 0 \\ * & \Pi_{22} & 0 & \Pi_{24} & 0 & \Pi_{26} \\ * & * & -\varepsilon_1^{-1}Z & 0 & 0 & 0 \\ * & * & * & -\varepsilon_1 Z & 0 & 0 \\ * & * & * & * & -\varepsilon I & 0 \\ * & * & * & * & * & -\varepsilon_1 I \end{bmatrix} < 0, \quad (8.35)$$

where

$$\begin{aligned}
\varepsilon &= \sigma(\varepsilon_1 + \varepsilon_2), \quad \varepsilon_1 = \text{diag}(\varepsilon_{11}, \dots, \varepsilon_{n1}), \\
\sigma &= \text{diag}(\sigma_1, \dots, \sigma_n) = \text{diag}(1/\alpha_1, \dots, 1/\alpha_n), \\
\Pi_{11} &= \text{diag}(\Pi_{111}, \dots, \Pi_{11n}), \quad \Pi_{11i} = \text{He}(A_i Z_i + B_i M_{1i}) + \varepsilon_{i2}^{-1} I, \\
\Pi_{13} &= \text{diag}(B_1 M_{1i}, \dots, B_n M_{1n}), \quad \Pi_{15} = \begin{bmatrix} Z_1 H_{011}^\top & \cdots & Z_1 H_{0n1}^\top \\ \vdots & \vdots & \vdots \\ Z_n H_{01n}^\top & \cdots & Z_n H_{0nn}^\top \end{bmatrix}, \\
\Pi_{22} &= \text{diag}(\Pi_{221}, \dots, \Pi_{22n}), \quad \Pi_{22i} = \begin{bmatrix} \Xi_{22i} & \Xi_{23i} \\ \star & \Xi_{33i} \end{bmatrix}, \\
\Xi_{22i} &= \text{He}(Q_{i1} A_i - Q_{i1} H_{i1} C_i A_i - M_{2i} C_i), \\
\Xi_{23i} &= M_{2i} F_{si} - (Q_{i2} H_{i2} C_i A_i + M_{3i} C_i)^\top, \quad \Pi_{24} = \begin{bmatrix} 0 \\ -I \end{bmatrix}, \\
\Xi_{33i} &= \text{He}(-M_{3i} F_{si}), \quad \Pi_{26} = \text{diag}(Q_1 \Xi_1, \dots, Q_n \Xi_n), \\
Q_i \Xi_i &= \begin{bmatrix} Q_{i1} - Q_{i1} H_{i1} C_i & -Q_{i1} H_{i1} F_{si} \\ -Q_{i2} H_{i2} C_i & Q_{i2} - Q_{i2} H_{i2} F_{si} \end{bmatrix}.
\end{aligned}$$

Then the gains are given by: $K_{xi} = M_{1i} Z_i^{-1}$, $L_{i11} = Q_{i1}^{-1} M_{2i}$, and $L_{i12} = Q_{i2}^{-1} M_{3i}$.

Proof: The proof of Theorem 8.2 is similar to that of Theorem 8.1 and it is thus omitted here. \square

8.5 Application to a 3-machine power system

According to Tlili and Braiek (2009b), a 3-machine power system with steam valve control is presented by the interconnection of 3 subsystems (see Fig. 8.3). Denote the state vector of each machine as $x_i = [\Delta\sigma_i(t) \quad \omega_i(t) \quad \Delta P_{mi}(t) \quad \Delta X_{ei}(t)]^\top$, then the dynamics of the i -th machine ($i = 1, 2, 3$) are represented as

$$\begin{aligned}
\dot{x}_i &= A_i x_i + B_i u_i + h_i(x, t), \\
y_i &= C_i x_i,
\end{aligned} \tag{8.36}$$

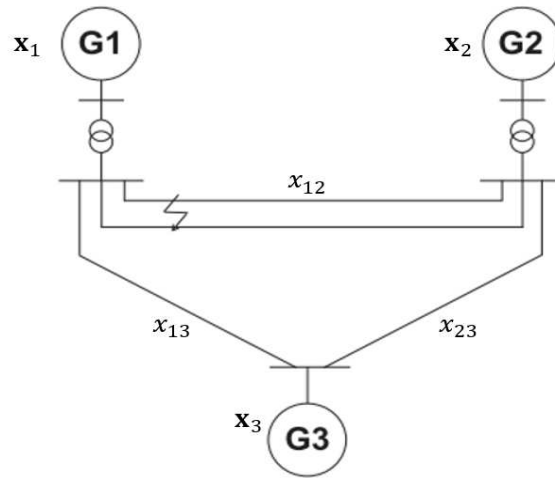


Fig. 8.3 A 3-machine power system.

where $h_i(x, t) = \sum_{j=1, j \neq i}^n p_{ij} G_{ij} g_{ij}(x_i, x_j)$ is the interaction term and $g_{ij}(x_i, x_j) = \sin(\sigma_i - \sigma_j) - \sin(\sigma_{i0} - \sigma_{j0})$,

$$A_i = \begin{bmatrix} 0 & 1 & 0 & 0 \\ 0 & \frac{-D_i}{2H_i} & \frac{\omega_0}{2H_i} & 0 \\ 0 & 0 & \frac{-1}{T_{mi}} & \frac{K_{mi}}{T_{mi}} \\ 0 & \frac{K_{ei}}{T_{ei}R_i\omega_0} & 0 & \frac{-1}{T_{ei}} \end{bmatrix}, \quad B_i = \begin{bmatrix} 0 \\ 0 \\ 0 \\ \frac{1}{T_{ei}} \end{bmatrix}, \quad C_i = I_4, \quad G_{ij} = \begin{bmatrix} 0 \\ -\frac{\omega_0 E'_{qi} E'_{qj} B_{ij}}{2H_i} \\ 0 \\ 0 \end{bmatrix}.$$

The system parameters of the i -th machine (8.36) are defined in Table 8.1. Following the method proposed in Kalsi et al. (2009), it can be determined that the interactions are in the form of a quadratic constraint and obtain the matrices H_{0i} in Assumption 8.4. The parameters of the 3-machine power system can be found in Kalsi et al. (2009).

Table 8.1 Definitions of the physical parameters.

Parameter	Physical meaning
ΔX_{ei}	Control vector u_i
σ_i	Rotor angle
ω_i	Relative speed
P_{mi}	Per unit (pu) mechanical power
X_{ei}	pu steam valve aperture
p_{ij}	Index of connection of the i -th and j -th machines (0: disconnected; 1: connected)
H_i	Inertia constant
D_i	pu damping coefficient
T_{mi}	Time constant for the turbine
K_{mi}	The gain of the turbine
T_{ei}	Time constant for the speed governor
K_{ei}	The gain of the speed governor
R_i	pu regulation constant
B_{ij}	pu Nodal susceptance between the i -th and j -th machines
ω_0	Synchronous machine speed
$\sigma_{i0}, P_{mi0}, X_{ei0}$	Nominal values of σ_i, P_{mi}, X_{ei}
$\Delta\sigma_i$	Deviation of the rotor angle ($\sigma_i - \sigma_{i0}$)
ΔP_{mi}	Deviation of the mechanical power ($P_{mi} - P_{mi0}$)
ΔX_{ei}	Deviation of the steam valve aperture ($X_{ei} - X_{ei0}$)

8.5.1 Actuator fault case

Consider here a serious situation that all of the three machines have actuator faults in the form of (8.1), defined as follows

$$\begin{aligned}
F_1 = B_1, f_1(t) &= \begin{cases} 0, & 0 \text{ s} \leq t \leq 0.1 \text{ s} \\ \sin(3(t-0.1)), & t > 0.1 \text{ s} \end{cases}, \\
F_2 = B_2, f_2(t) &= \begin{cases} 0, & 0 \text{ s} \leq t \leq 0.5 \text{ s} \\ 1, & 0.5 \text{ s} < t \leq 1 \text{ s} \\ 2, & 1 \text{ s} < t \leq 1.5 \text{ s} \\ 0, & 1.5 \text{ s} < t \leq 3 \text{ s} \\ -1, & t > 3 \text{ s} \end{cases}, \\
F_3 = B_3, f_3(t) &= \begin{cases} 0, & 0 \text{ s} \leq t \leq 0.5 \text{ s} \\ -0.5, & 0.5 \text{ s} < t \leq 1.5 \text{ s} \\ 0.5, & 1.5 \text{ s} < t \leq 2 \text{ s} \\ \cos(5t), & t > 2 \text{ s} \end{cases}.
\end{aligned}$$

It is verified that Assumptions 8.1 - 8.4 are satisfied for this 3-machine system in the presence of the previously defined actuator faults. Given $\varepsilon_{11} = 10$, $\varepsilon_{21} = 100$, $\varepsilon_{12} = 10$, $\varepsilon_{22} = 100$, $\varepsilon_{13} = 1000$, $\varepsilon_{23} = 1000$, $\varepsilon_1 = \varepsilon_2 = \varepsilon_3 = 0.1$, solving Theorem 8.1 obtains the upper bounds of the uncertain nonlinear interactions $\alpha_1 = 10$, $\alpha_2 = 10$, and $\alpha_3 = 10$, the H_∞ optimization performance $\gamma_1 = 0.8$, $\gamma_2 = 1$, and $\gamma_3 = 0.8$, and also the following gains:

$$\begin{aligned}
K_{x1} &= \begin{bmatrix} 2.4328 \\ 0.9389 \\ 5.4248 \\ 1.001 \end{bmatrix}, M_1 = \begin{bmatrix} -1.3723 & 0 & 0 & 0 & 0 \\ 0 & -1.3723 & 0 & 0 & 0 \\ 0 & 0 & -1.3724 & 0 & 0 \\ 0 & 0 & 0 & -1.3724 & 0 \\ -0.0019 & -0.0656 & 0 & -0.0018 & -65.6366 \end{bmatrix}, \\
K_{x2} &= \begin{bmatrix} 2.7878 \\ 1.1738 \\ 5.3665 \\ 1.001 \end{bmatrix}, M_2 = \begin{bmatrix} -1.3723 & 0 & 0 & 0 & 0 \\ 0 & -1.3723 & 0 & 0 & 0 \\ 0 & 0 & -1.3724 & 0 & 0 \\ 0 & 0 & 0 & -1.3724 & 0 \\ 0 & -0.0644 & -0.002 & 0.0002 & -64.3886 \end{bmatrix}, \\
K_{x3} &= \begin{bmatrix} 3.3810 \\ 1.2474 \\ 5.4665 \\ 1.001 \end{bmatrix}, M_3 = \begin{bmatrix} -1.3723 & 0 & 0 & 0 & 0 \\ 0 & -1.3724 & 0 & 0 & 0 \\ 0 & 0 & -1.3768 & 0 & 0 \\ 0 & 0 & 0 & -1.3729 & 0.0007 \\ 0.005 & -0.0002 & 0.1642 & -548.4984 & \end{bmatrix},
\end{aligned}$$

$$\begin{aligned}
L_1 &= \begin{bmatrix} 0 & 0 & 0 & 0 \\ 0 & 0 & 0 & 0 \\ 0 & 0 & -0.0001 & 0 \\ 0 & 0 & 0 & 0 \\ 0 & 4.1786 & 0 & -365.18 \end{bmatrix}, \\
L_2 &= \begin{bmatrix} 0 & 0 & 0 & 0 \\ 0 & 0 & 0 & 0 \\ 0 & 0 & -0.0001 & 0 \\ 0 & 0 & 0 & 0 \\ 0 & 4.0991 & 0 & -350.2003 \end{bmatrix}, \quad L_3 = \begin{bmatrix} 0 & 0 & 0 & 0 \\ 0 & 0 & 0 & 0 \\ 0 & 0 & 0 & 0 \\ 0 & 0 & 0 & 0 \\ 0 & 35 & 0 & -29537 \end{bmatrix}, \\
H_1 &= \begin{bmatrix} 1 & 0 & 0 & 0 \\ 0 & 1 & 0 & 0 \\ 0 & 0 & 1 & 0 \\ 0 & 0 & 0 & 1 \\ 0 & 0 & 0 & 6.5637 \end{bmatrix}, \quad G_1 = \begin{bmatrix} 0 \\ 0 \\ 0 \\ 0 \\ -65.6366 \end{bmatrix}, \\
H_2 &= \begin{bmatrix} 1 & 0 & 0 & 0 \\ 0 & 1 & 0 & 0 \\ 0 & 0 & 1 & 0 \\ 0 & 0 & 0 & 1 \\ 0 & 0 & 0 & 6.4389 \end{bmatrix}, \quad G_2 = \begin{bmatrix} 0 \\ 0 \\ 0 \\ 0 \\ -64.3886 \end{bmatrix}, \\
H_3 &= \begin{bmatrix} 1 & 0 & 0 & 0 \\ 0 & 1 & 0 & 0 \\ 0 & 0 & 1 & 0 \\ 0 & 0 & 0 & 0.9999 \\ 0 & 0 & 0 & 54.8498 \end{bmatrix}, \quad G_3 = \begin{bmatrix} 0 \\ 0 \\ 0 \\ 0.0007 \\ -548.4984 \end{bmatrix}.
\end{aligned}$$

Matlab simulations are carried out with initial conditions: $x_1(0) = [0 \ 1 \ 0.5 \ -1]^T$, $x_2(0) = [0.1 \ 0.5 \ -0.1 \ 0.5]^T$, $x_3(0) = [1 \ 0.2 \ 0.5 \ 0]^T$, $z_1(0) = z_2(0) = z_3(0) = 0$.

The results in Figs. 8.4 - 8.7 demonstrate that the proposed integrated FE/FTC design approach achieves good actuator faults estimation performance, and it can compensate the actuator fault in each subsystem and ensure the robust stability of the 3-machine system in the presence of faults and uncertain nonlinear interactions.

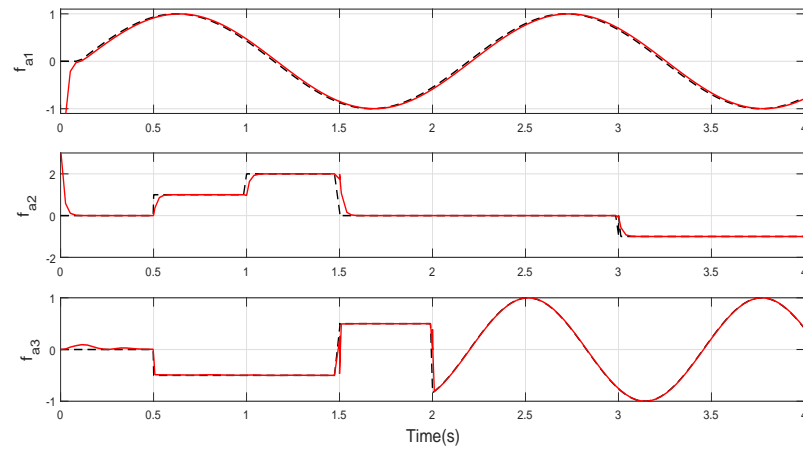


Fig. 8.4 Actuator faults (black dash) and their estimates (red solid).

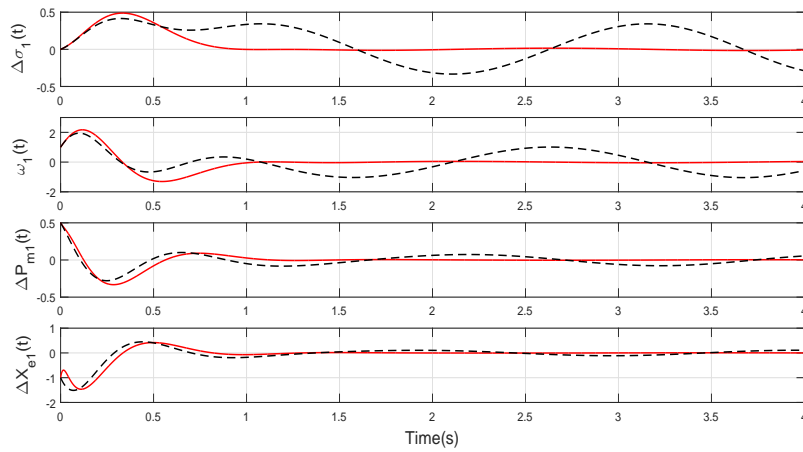


Fig. 8.5 States with (red solid) or without FTC (black dash) for machine 1.

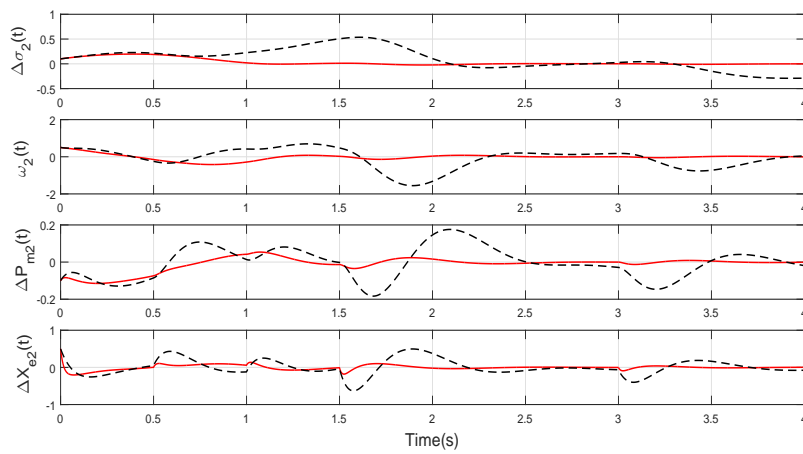


Fig. 8.6 States with (red solid) or without FTC (black dash) for machine 2.

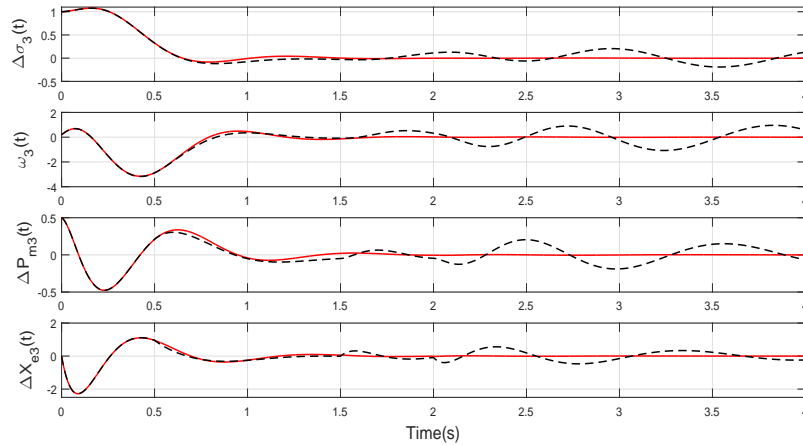


Fig. 8.7 States with (red solid) or without FTC (black dash) for machine 3.

8.5.2 Sensor fault case

Assume that the three machines have the following sensor faults and distribution matrices, respectively,

$$F_{s1} = \begin{bmatrix} 1 \\ 1 \\ 0 \\ -1 \end{bmatrix}, f_{s1}(t) = \begin{cases} 0, & 0 \leq t \leq 1 \text{ s} \\ 0.5 \sin(5(t-1)), & t > 1 \text{ s} \end{cases},$$

$$F_{s2} = \begin{bmatrix} -1 \\ 1 \\ -1 \\ 0 \end{bmatrix}, f_{s2}(t) = \begin{cases} 0, & 0 \leq t \leq 0.5 \text{ s} \\ 0.5, & 0.5 \text{ s} < t \leq 1 \text{ s} \\ 1, & 1 \text{ s} < t \leq 1.5 \text{ s} \\ -0.5, & 1.5 \text{ s} < t \leq 3 \text{ s} \\ 0.5, & t > 3 \text{ s} \end{cases},$$

$$F_{s3} = \begin{bmatrix} 1 \\ -1 \\ 1 \\ -1 \end{bmatrix}, f_{s3}(t) = \begin{cases} 0, & 0 \leq t \leq 0.5 \text{ s} \\ -0.5, & 0.5 \text{ s} < t \leq 1.5 \text{ s} \\ 0.5, & 1.5 \text{ s} < t \leq 2 \text{ s} \\ \cos(2t), & t > 2 \text{ s} \end{cases}.$$

Assumptions 8.1, 8.4 and 8.5 are verified to be satisfied for this 3-machine system with the sensor faults defined above. Given $\epsilon_{11} = 0.1$, $\epsilon_{21} = 10$, $\epsilon_{12} = 0.1$, $\epsilon_{22} = 10$, $\epsilon_{13} = 0.1$, $\epsilon_{23} = 0.1$, $\epsilon_1 = \epsilon_2 = \epsilon_3 = 0.1$, solving Theorem 8.2 obtains the upper bounds of the uncertain nonlinear interactions $\alpha_1 = 10$, $\alpha_2 = 15$, and $\alpha_3 = 10$, and the following

gains:

$$M_1 = \begin{bmatrix} -615.4441 & 21.9319 & 1.5395 & -22.0801 & -572.4321 \\ 20.5299 & -615.3799 & 21.1813 & -21.5835 & -572.6415 \\ -1.2619 & -20.8884 & -636.6549 & 2.6846 & -21.9777 \\ -20.5226 & -21.0616 & -2.9807 & -615.2494 & 564.3018 \\ -126.0678 & -126.2065 & -11.5548 & 121.9984 & -377.2688 \end{bmatrix},$$

$$M_2 = \begin{bmatrix} -615.6669 & -23.8831 & 20.1694 & 0.0134 & 570.6144 \\ -18.7895 & -615.0005 & -2.0824 & 0.3019 & -563.0347 \\ 21.6597 & -40.4695 & -615.7918 & 1.4403 & 550.8054 \\ -0.0146 & -0.3053 & -1.4441 & -636.6365 & 1.7901 \\ 126.4584 & -123.0026 & 116.0965 & 0.9283 & -377.2079 \end{bmatrix},$$

$$M_3 = \begin{bmatrix} -610.7560 & -28.5059 & 25.7146 & -26.6466 & -528.8888 \\ -24.2640 & -609.8096 & -8.1997 & 24.8233 & 521.4286 \\ 25.9215 & -44.4520 & -610.8856 & -25.2598 & -509.5380 \\ -25.3445 & 28.1228 & -26.6054 & -610.5436 & 519.8343 \\ -83.8711 & 81.4057 & -75.6750 & 80.2186 & -333.2816 \end{bmatrix},$$

$$G_1 = \begin{bmatrix} 0 \\ 0 \\ 0 \\ 10 \\ 3.3333 \end{bmatrix}, \quad G_2 = \begin{bmatrix} 0 \\ 0 \\ 0 \\ 10 \\ 0 \end{bmatrix}, \quad G_3 = \begin{bmatrix} 0 \\ 0 \\ 0 \\ 10 \\ 2.5 \end{bmatrix},$$

$$L_1 = \begin{bmatrix} 424.6334 & -211.7426 & -1.5395 & 212.8908 \\ -211.4104 & 423.8744 & 18.0886 & 212.4640 \\ -6.0640 & 13.5625 & 633.7977 & 7.4984 \\ 208.6232 & 208.5255 & 2.9807 & 417.1488 \\ 0.3115 & 0.1131 & -1.5351 & 0.4245 \end{bmatrix},$$

$$L_2 = \begin{bmatrix} 425.4621 & 215.0879 & -210.3742 & -0.0134 \\ 206.4677 & 427.0282 & 220.5605 & -0.3019 \\ -205.2615 & 224.0714 & 429.3328 & 1.4168 \\ -0.5821 & 0.2654 & 0.8474 & 626.6365 \\ -0.7224 & -2.3020 & -1.5795 & 0.0241 \end{bmatrix},$$

$$L_3 = \begin{bmatrix} 478.5338 & 161.7281 & -157.9368 & 158.8688 \\ 154.6212 & 479.1584 & 169.3568 & -155.1804 \\ -153.306 & 171.8365 & 480.644 & 155.5015 \\ 155.303 & -158.7179 & 156.564 & 470.585 \\ 0.5507 & 1.432 & 0.7688 & -0.1125 \end{bmatrix},$$

$$\begin{aligned}
 H_1 &= \begin{bmatrix} 0 & 0 & 0 & 0 \\ 0 & 0 & 0 & 0 \\ 0 & 0 & 0 & 0 \\ 0 & 0 & 0 & 0 \\ 0.3333 & 0.3333 & 0 & -0.3333 \end{bmatrix}, K_{x1} = \begin{bmatrix} -3.3966 \\ -1.0023 \\ -5.4724 \\ -0.9975 \end{bmatrix}, \\
 H_2 &= \begin{bmatrix} 0 & 0 & 0 & 0 \\ 0 & 0 & 0 & 0 \\ 0 & 0 & 0 & 0 \\ 0 & 0 & 0 & 0 \\ -0.3333 & 0.3333 & -0.3333 & 0 \end{bmatrix}, K_{x2} = \begin{bmatrix} -3.9474 \\ -1.2789 \\ -5.4589 \\ -0.9980 \end{bmatrix}, \\
 H_3 &= \begin{bmatrix} 0 & 0 & 0 & 0 \\ 0 & 0 & 0 & 0 \\ 0 & 0 & 0 & 0 \\ 0 & 0 & 0 & 0 \\ 0.25 & -0.25 & 0.25 & -0.25 \end{bmatrix}, K_{x3} = \begin{bmatrix} -3.5927 \\ -1.1992 \\ -5.3466 \\ -1.0054 \end{bmatrix}.
 \end{aligned}$$

Simulations are performed with initial conditions: $x_i(0) = 0.1_{4 \times 1}$ and $z_i(0) = 0.1_{4 \times 1}$, $i = 1, 2, 3$. The results in Figs. 8.8 - 8.11 show that the proposed FTC design achieves good fault estimation and ensures the robust stability of the 3-machine system in the presence of fault and uncertain nonlinear interactions, and the sensor faults effect on the system outputs are well compensated.

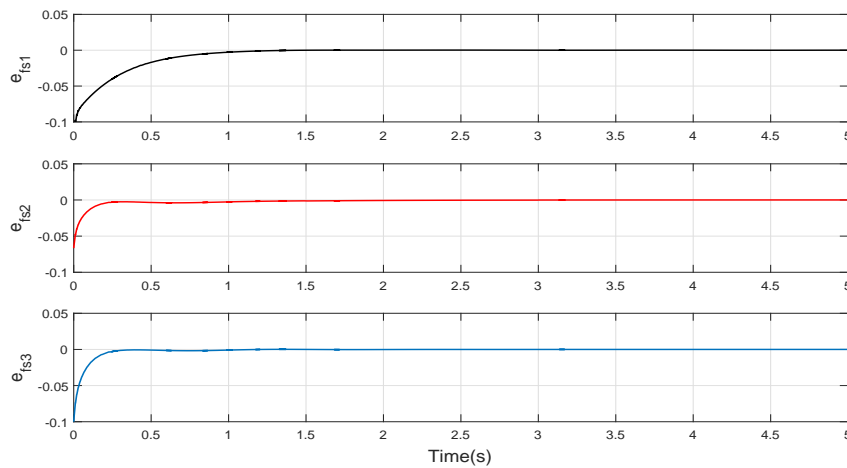


Fig. 8.8 Sensor fault estimation performance.

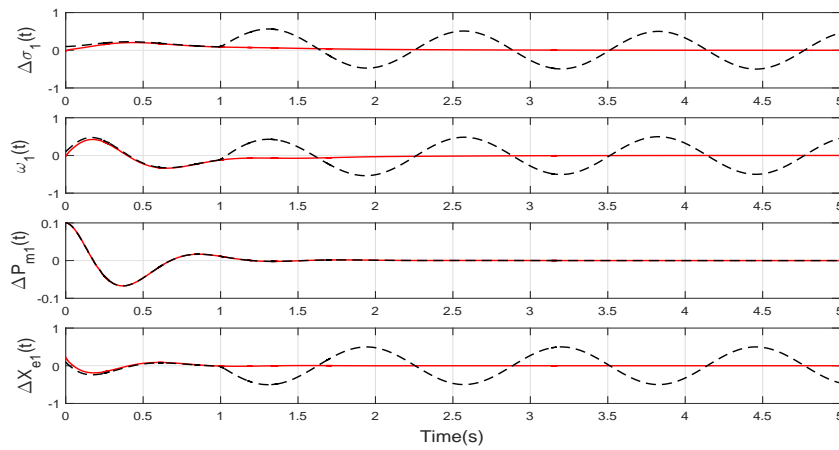


Fig. 8.9 Outputs with (red solid) or without FTC (black dash) for machine 1.

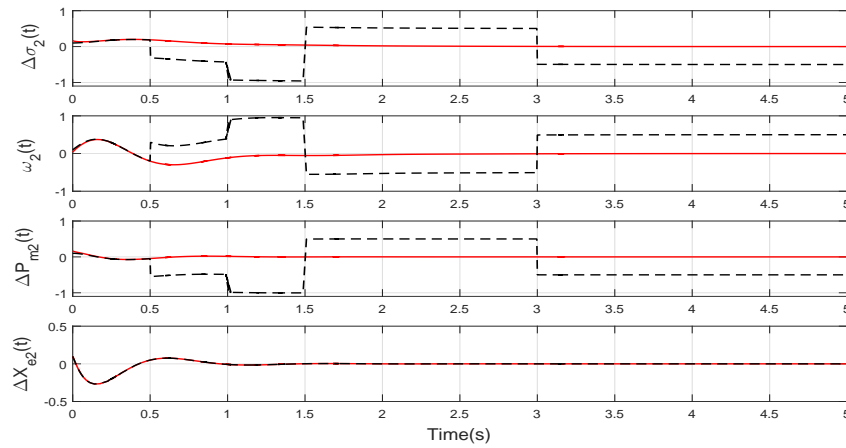


Fig. 8.10 Outputs with (red solid) or without FTC (black dash) for machine 2.

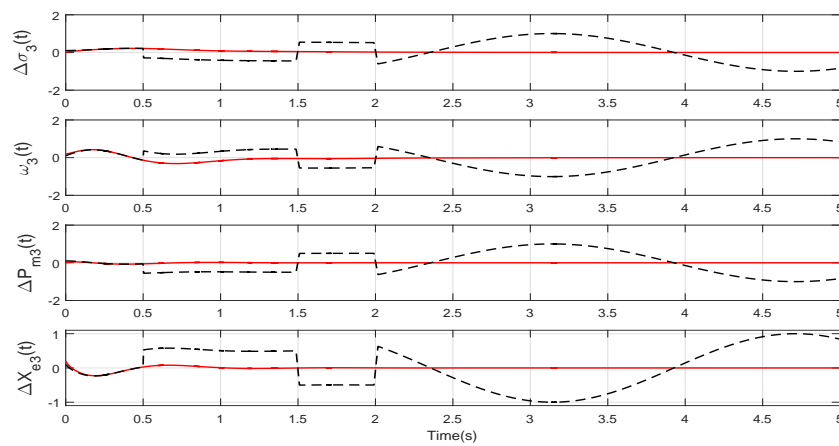


Fig. 8.11 Outputs with (red solid) or without FTC (black dash) for machine 3.

8.6 Conclusion

This chapter extends the H_∞ optimization approach in Chapter 4 to large-scale interconnected systems. An integrated FE/FTC design for large-scale interconnected systems with actuator or sensor faults is proposed, using a decentralized state feedback FTC controller and a decentralized ASUIO for simultaneous estimation of the state variable and faults. A single-step LMI formulation without equality constraints (different from Chapter 4) is proposed to obtain the ASUIO and FTC controller gains. It should be emphasized that although the FE observers and FTC controllers of all the subsystems are designed together, they are decentralized, implemented locally on each subsystem. The local FE/FTC are able to estimate and compensate actuator or sensor faults in each of the subsystems to achieve acceptable robust FTC performance of the whole large-scale systems, which is demonstrated through the study of a 3-machine power system.

Chapter 9: Summary and future research

9.1 Summary

It is shown in this thesis (Chapters 2 and 3) that the presence of uncertainty in state and fault estimation along with the uncertainty associated with control leads to the existence of *bi-directional robustness interactions* between the fault diagnosis and FTC functions. These interactions give rise to a necessary consideration of a joint design of the fault diagnosis and FTC to achieve robust overall system performance. This thesis presents a new concept called **integrated FE and FTC design** to achieve a true integrated FTC system, which is considered to be the fundamental contribution of this work.

To further enhance the need for integrated design, an FE-based FTC wind turbine pitch control system is provided in Chapter 3. This example shows the power of the FE-based FTC scheme to automatically estimate and compensate the faults and maintain nominal robust control system performance. It also demonstrates the limitations of the separated design used considering that *bi-directional robustness interactions* exist. This serves as a practical motivation of the integrated FE/FTC design. Detailed mathematical analysis of the need of integrated design is also provided in Chapter 3.

Following this, a number of strategies are proposed in this thesis to achieve integrated FE/FTC designs for linear, nonlinear, and large-scale interconnected systems, summarized as follows.

(1) Strategies for uncertain linear systems

- Chapter 4 proposes a H_∞ optimization approach for uncertain linear systems, using reduced-/full-order ASUIO observers for FE and sliding mode FTC controllers for fault compensation. The integrated FE/FTC design is reformulated as an observer-based robust control problem solved via a single-step LMI formulation. However, this strategy can only be used to estimate and compensate continuously differentiable matched faults and the LMI formulation leads to a design with limited freedom.

- To overcome the limitations of the above H_∞ optimization approach, a decoupling approach is proposed in Chapter 5 for linear systems. It can estimate and compensate a more general class of faults, which are either matched or unmatched, and differentiable or non-differentiable. It uses an adaptive sliding mode ASUIO and an adaptive backstepping FTC controller. The ASUIO is designed to be decoupled from the FTC system and it recovers the Separation Principle under the framework of integrated FE/FTC design. The decoupling allows greater design freedom when compared with the H_∞ optimization strategy. Moreover, the system perturbation (uncertainty and external disturbance) are also estimated and compensated which helps to attain a more robust FTC system.

(2) Strategies for uncertain nonlinear and large-scale systems

Integrated FE/FTC design strategies are proposed for nonlinear systems with Takagi-Sugeno fuzzy modelling in Chapter 6 and with Lipschitz nonlinearity in Chapter 7, respectively. These integrated FE/FTC strategies are based on extensions of the H_∞ optimization approach proposed in Chapter 4 for linear systems, but use new single-step LMI formulations without requiring the equality constraints that are used in Chapter 4.

Chapter 8 further extends the H_∞ optimization approach for large-scale interconnected systems with unknown nonlinear interactions and actuator/sensor faults.

Besides the above theory contributions, potential industrial applications of the proposed strategies are also evaluated by using physical systems of a 3-DOF helicopter in Chapter 7 and a 3-machine power system in Chapter 8, respectively.

9.2 Future research

Some likely ideas for future research are listed below:

(1) Integrated FE and FTC design with reduced design complexity

- The integrated FE/FTC designs based on the H_∞ optimization approach described in Chapters 4, 6, 7, and 8 using a single-step LMI formulation has considerable design and computational complexity, especially in the case of T-S fuzzy systems (see Section 6.5.3) and large-scale systems. Thus, a simpler way to solve the H_∞ optimization problem with reduced design complexity is of great importance and can be an interesting research direction.

Since the design complexity comes from the existence of *bi-directional robustness interactions*, a way to reduce the design complexity is to decouple the state/fault observer from the FTC system. One possible solution of this is the use of the decoupling approach proposed in Chapter 5, with further extensions to a more general class of systems. Another alternative way is to use combined adaptive state/fault observer and adaptive FTC controller, in which adaptive methods can be employed to automatically estimate and compensate the bi-directional uncertainties.

- It is also important and challenging to extend the proposed integrated FE/FTC strategies for more complex systems, e.g., networked control systems, hybrid systems, stochastic systems, etc.

(2) Integrated FE and FTC design with physical constraints

Due to physical limits, there exist hard constraints (e.g., saturation and rate limits) on the system state and control signals. The presence of faults may make the state and/or inputs reach the constraints, leading to degraded FTC system performance or even unstable FTC systems. Therefore, the effects of hard constraints should be taken into account in FTC system designs.

In the past few years, several works have been published to solve this problem, see for example, FTC designs with input saturation (Hu et al., 2011; Lu and Xia, 2013; Xiao et al., 2012; Zuo et al., 2010), and FTC designs with both state and input constraints (Jin, 2016). An integrated FE/FTC design is proposed in Chapter 7 for a 3-DOF helicopter with actuator faults and only input saturation constraints. Hence, future research can focus on the integrated FE/FTC design for systems subject to a wide range of hard constraints.

Appendix A: Lemmas used frequently in the thesis

A.1 Bounded Real Lemma (Anderson and Vongpanitlerd, 1973)

A linear system

$$\begin{aligned}\dot{x} &= Ax + Dd, \\ z &= Cx,\end{aligned}$$

is stable with H_∞ performance $\|G_{zd}\|_\infty < \gamma$ if and only if there exists a symmetric positive definite matrix P such that

$$\begin{bmatrix} \text{He}(PA) & PD & C^\top \\ * & -\gamma I & 0 \\ * & * & -\gamma I \end{bmatrix} < 0.$$

A.2 Schur complement (Boyd et al., 1994)

For any symmetric matrix \mathcal{S} of the form

$$\mathcal{S} = \begin{bmatrix} \mathcal{S}_{11} & \mathcal{S}_{12} \\ * & \mathcal{S}_{22} \end{bmatrix},$$

if \mathcal{S}_{11} and \mathcal{S}_{22} are invertible, then the following properties hold:

- (1) $\mathcal{S} < 0$ iff $\mathcal{S}_{11} < 0$ and $\mathcal{S}_{22} - \mathcal{S}_{21}\mathcal{S}_{11}^{-1}\mathcal{S}_{12} < 0$;
- (2) $\mathcal{S} < 0$ iff $\mathcal{S}_{22} < 0$ and $\mathcal{S}_{11} - \mathcal{S}_{12}\mathcal{S}_{22}^{-1}\mathcal{S}_{21} < 0$.

A.3 Pole placement lemma (Chilali and Gahinet, 1996)

The system $\dot{x} = Ax$ is \mathcal{D} -stable, if there exists a symmetric positive definite matrix P such that

$$\alpha \otimes P + \text{He}[\beta \otimes (PA)] < 0,$$

where \otimes is the Kronecker product.

Remark A.1 If \mathcal{D} is a strip region: $a < \text{Re}(\lambda) < b$, where λ are the eigenvalues of A and a and b are negative constants, then (A.1) is represented as

$$\begin{bmatrix} \text{He}(PA + A^\top P) - 2bP & 0 \\ * & -\text{He}(PA + A^\top P) + 2aP \end{bmatrix} < 0.$$

A.4 Young inequality (Boyd et al., 1994)

Given matrices X and Y of appropriate dimensions, for any matrix $S > 0$, it holds that

$$X^\top Y + Y^\top X \leq X^\top S X + Y^\top S^{-1} Y.$$

Appendix B: Notes on the Separation Principle

Consider a linear system

$$\begin{aligned}\dot{x} &= Ax + Bu, \\ y &= Cx,\end{aligned}\tag{B.1}$$

where $x(t) \in \mathbb{R}^n$, $u(t) \in \mathbb{R}^m$, and $y(t) \in \mathbb{R}^p$ are the state, control input, and system output vectors, respectively. A , B , and C are known constant matrices of compatible dimensions. It is assumed that the system is observable and controllable.

If the system state vector x is not available for feedback control design, then the following state observer can be designed to estimate x ,

$$\begin{aligned}\dot{\hat{x}} &= A\hat{x} + Bu + L(y - \hat{y}), \\ \hat{y} &= C\hat{x},\end{aligned}\tag{B.2}$$

where $\hat{x} \in \mathbb{R}^n$ and $\hat{y} \in \mathbb{R}^p$ are the estimates of x and y , respectively. $L \in \mathbb{R}^{n \times p}$ is a design matrix.

Define the state estimation error as $e = x - \hat{x}$, then it follows from (B.1) and (B.2) that the error system is

$$\dot{e} = (A - LC)e.\tag{B.3}$$

A controller for stabilizing the system state x using the feedback of the state estimate \hat{x} is designed as

$$u = -K\hat{x}, \quad (\text{B.4})$$

where $K \in \mathbb{R}^{m \times n}$ is the designed controller gain.

Substituting the controller (B.4) into (B.1) gives the closed-loop control system

$$\dot{x} = (A - BK)x + BKe. \quad (\text{B.5})$$

The composite closed-loop system consisting of (B.3) and (B.5) is

$$\begin{bmatrix} \dot{x} \\ \dot{e} \end{bmatrix} = \begin{bmatrix} A - BK & BK \\ 0 & A - LC \end{bmatrix} \begin{bmatrix} x \\ e \end{bmatrix}. \quad (\text{B.6})$$

It can be seen from (B.6) that the system matrix $A_c = \begin{bmatrix} A - BK & BK \\ 0 & A - LC \end{bmatrix}$ is block triangular. Thus, the eigenvalues of the composite system are the union of those of the estimation error system and the control system, i.e., $\lambda(A_c) = \lambda(A - BK) \cup \lambda(A - LC)$. This implies that the state observer (B.2) does not affect the eigenvalues of the original state feedback control system (B.5); nor are the eigenvalues of the observer affected by the connection. Therefore, the design of the state feedback controller (B.4) and the observer (B.2) can be carried out independently. This is called the *Separation Principle* (Chen, 1995).

As analysed below, the Separation Principle is no longer satisfied if there exist system uncertainties in the matrices A , B , and C . Assume that $A_0 = A + \sigma A$, $B_0 = B + \sigma B$, and $C_0 = C + \sigma C$, where σA , σB , and σC are parameter uncertainties. By replacing A , B , and C by A_0 , B_0 , and C_0 in (B.6), the composite closed-loop system in the presence of uncertainties is

$$\begin{bmatrix} \dot{x} \\ \dot{e} \end{bmatrix} = \begin{bmatrix} A + \sigma A - (B + \sigma B)K & (B + \sigma B)K \\ \sigma A + \sigma BK - L\sigma C & A - LC - \sigma BK \end{bmatrix} \begin{bmatrix} x \\ e \end{bmatrix}. \quad (\text{B.7})$$

It is obvious that the system matrix $A_\sigma = \begin{bmatrix} (A + \sigma A) - (B + \sigma B)K & (B + \sigma B)K \\ \sigma A + \sigma BK - L\sigma C & A - LC - \sigma BK \end{bmatrix}$ is not a block triangular. This means that the observer and control system affect each other and cannot be designed independently. Therefore, the existence of uncertainties breaks down the Separation Principle.

Example B.1 Consider a linear system in the form of (B.1) with

$$A = \begin{bmatrix} 0 & 1 \\ 1 & 1 \end{bmatrix}, B = \begin{bmatrix} 0 \\ 1 \end{bmatrix}, C = [1 \ 0], K = [16 \ 9], L = \begin{bmatrix} 18 \\ 89 \end{bmatrix}.$$

According to (B.6),

$$\begin{aligned} \lambda(A_c) &= (-3, -5, -10, -7), \\ \lambda(A - BK) &= (-3, -5), \quad \lambda(A - LC) = (-10, -7). \end{aligned} \quad (\text{B.8})$$

Hence, $\lambda(A_c) = \lambda(A - BK) \cup \lambda(A - LC)$, the Separation Principle holds.

Suppose there exist the following uncertainties in the system: $\sigma A = 0.02A$, $\sigma B = 0.01B$, and $\sigma C = 0.05C$, then according to (B.7),

$$\begin{aligned} \lambda(A_\sigma) &= (-12.1779, -5.3602 \pm j3.5698, -2.2617), \\ \lambda(A + \sigma A - (B + \sigma B)K) &= (-3.1193, -4.9507), \\ \lambda(A - LC - \sigma BK) &= (-9.6572, -7.4328). \end{aligned} \quad (\text{B.9})$$

It can be seen from (B.9) that the Separation Principle is not satisfied in the uncertain case. In the real design procedure, if the system uncertainties (σA , σB , and σC) are ignored, then the Separation Principle is satisfied and the observer and controller are designed separately with desired eigenvalues (B.8). However, when the observer and controller are applied to the real uncertain system, the real eigenvalues of the composite system are (B.9), which are quite different from the desired ones. Therefore, in the presence of the uncertainties, the separated design observer and controller cannot guarantee desired estimation and control performances.

References

- Afonso, R. J. M. and Galvão, R. K. H. (2010). Predictive control of a helicopter model with tolerance to actuator faults. In *Proceedings of the Conference on Control and Fault-Tolerant Systems*, pages 744–751. IEEE.
- Akrad, A., Hilairet, M., and Diallo, D. (2011). Design of a fault-tolerant controller based on observers for a PMSM drive. *IEEE Transactions on Industrial Electronics*, 58(4):1416–1427.
- Alexis, K., Nikolakopoulos, G., and Tzes, A. (2012). Model predictive quadrotor control: attitude, altitude and position experimental studies. *IET Control Theory & Applications*, 6(12):1812–1827.
- Alwi, H. and Edwards, C. (2008). Fault tolerant control using sliding modes with on-line control allocation. *Automatica*, 44(7):1859–1866.
- Amani, A. M., Poorjandaghi, S. S., Afshar, A., and Menhaj, M. B. (2014). Fault tolerant control of large-scale systems subject to actuator fault using a cooperative approach. *Proceedings of the Institution of Mechanical Engineers, Part I: Journal of Systems and Control Engineering*, 228(2):63–77.
- Amirat, Y., Benbouzid, M. E. H., Al-Ahmar, E., Bensaker, B., and Turri, S. (2009). A brief status on condition monitoring and fault diagnosis in wind energy conversion systems. *Renewable and Sustainable Energy Reviews*, 13(9):2629–2636.
- Amoozgar, M. H., Chamseddine, A., and Zhang, Y. (2013). Experimental test of a two-stage kalman filter for actuator fault detection and diagnosis of an unmanned quadrotor helicopter. *Journal of Intelligent & Robotic Systems*, 70(1-4):107–117.
- Anderson, B. and Vongpanitlerd, S. (1973). *Network analysis and synthesis: a modern systems theory approach*. Prentice-Hall, Englewood Cliffs, NJ.
- Apkarian, J. (2006). 3-DOF helicopter reference manual. *Quanser Consulting Inc., Canada*.
- Badihi, H., Zhang, Y., and Hong, H. (2015). Wind turbine fault diagnosis and fault-tolerant torque load control against actuator faults. *IEEE Transactions on Control Systems Technology*, 23(4):1351–1372.
- Bakule, L. and Rodellar, J. (1996). Decentralised control design of uncertain nominally linear symmetric composite systems. *IEE Proceedings-Control Theory and Applications*, 143(6):530–536.

- Bakule, L. and Rossel, J. M. (2008). Overlapping controllers for uncertain delay continuous-time systems. *Kybernetika*, 44(1):17–34.
- Balague, G. T. and Hajiyev, C. (2016). Fault detection, isolation and accommodation in flight control system of A340-Airbus aircraft. In *Sustainable Aviation*, pages 217–232. Springer.
- Bélanger, P. R. (1995). *Control engineering: a modern approach*. Oxford University Press, Inc.
- Bengea, S. C., Li, P., Sarkar, S., Vichik, S., Adetola, V., Kang, K., Lovett, T., Leonardi, F., and Kelman, A. D. (2015). Fault-tolerant optimal control of a building HVAC system. *Science and Technology for the Built Environment*, 21(6):734–751.
- Benigni, A., D’Antona, G., Ghisla, U., Monti, A., and Ponci, F. (2010). A decentralized observer for ship power system applications: Implementation and experimental validation. *IEEE Transactions on Instrumentation and Measurement*, 59(2):440–449.
- Benosman, M. (2009). A survey of some recent results on nonlinear fault tolerant control. *Mathematical Problems in Engineering*, 2010.
- Benzaouia, A., El Hajjaji, A., Hmamed, A., and Oubah, R. (2015). Fault tolerant saturated control for T-S fuzzy discrete-time systems with delays. *Nonlinear Analysis: Hybrid Systems*, 18:60–71.
- Bianchi, F., Mantz, R., and Christiansen, C. (2005). Gain scheduling control of variable-speed wind energy conversion systems using quasi-LPV models. *Control Engineering Practice*, 13(2):247–255.
- Bianchi, F. D., Ocampo-Martinez, C., Kunusch, C., and Sánchez-Pena, R. S. (2015). Fault-tolerant unfalsified control for PEM fuel cell systems. *IEEE Transactions on Energy Conversion*, 30(1):307–315.
- Blanke, M., Kinnaert, M., Lunze, J., Staroswiecki, M., and Schröder, J. (2003). *Diagnosis and fault-tolerant control*. Springer.
- Boem, F., Ferrari, R. M., Keliris, C., Parisini, T., and Polycarpou, M. M. (2017). A distributed networked approach for fault detection of large-scale systems. *IEEE Transactions on Automatic Control*, 62(1):18–33.
- Bossanyi, E. (2003). Individual blade pitch control for load reduction. *Wind energy*, 6(2):119–128.
- Boukhezzar, B., Lupu, L., Siguerdidjane, H., and Hand, M. (2007). Multivariable control strategy for variable speed, variable pitch wind turbines. *Renewable Energy*, 32(8):1273–1287.
- Bourogaoui, M., Sethom, H. B. A., and Belkhodja, I. S. (2016). Speed/position sensor fault tolerant control in adjustable speed drives—A review. *ISA Transactions*, 64:269–284.
- Boyd, S. P., El Ghaoui, L., Feron, E., and Balakrishnan, V. (1994). *Linear matrix inequalities in system and control theory*, volume 15. SIAM.

- Buffington, J., Chandler, P., and Pachter, M. (1999). On-line system identification for aircraft with distributed control effectors. *International Journal of Robust and Nonlinear Control*, 9(14):1033–1049.
- Burton, T., Jenkins, N., Sharpe, D., and Bossanyi, E. (2011). *Wind Energy Handbook*. John Wiley & Sons.
- Campos-Delgado, D., Espinoza-Trejo, D., and Palacios, E. (2008). Fault-tolerant control in variable speed drives: A survey. *IET Electric Power Applications*, 2(2):121–134.
- Cao, S., Guo, L., and Wen, X. (2011). Fault tolerant control with disturbance rejection and attenuation performance for systems with multiple disturbances. *Asian Journal of Control*, 13(6):1056–1064.
- Chadli, M., Abdo, A., and Ding, S. X. (2013). H_-/H_∞ fault detection filter design for discrete-time Takagi–Sugeno fuzzy system. *Automatica*, 49(7):1996–2005.
- Chen, C.-T. (1995). *Linear system theory and design*. Oxford University Press, Inc.
- Chen, F., Hou, R., Jiang, B., and Tao, G. (2013a). Study on fast terminal sliding mode control for a helicopter via quantum information technique and nonlinear fault observer. *International Journal of Innovative Computing, Information and Control*, 9(8):3437–3447.
- Chen, F., Zhang, K., Jiang, B., and Wen, C. (2016a). Adaptive sliding mode observer-based robust fault reconstruction for a helicopter with actuator fault. *Asian Journal of Control*, 18(4):1558–1565.
- Chen, J. and Patton, R. J. (1999). *Robust model-based fault diagnosis for dynamic systems*. Kluwer Academic Publishers, London.
- Chen, L., Patton, R., and Goupil, P. (2016b). Robust fault estimation using an LPV reference model: ADDSAFE benchmark case study. *Control Engineering Practice*, 49:194–203.
- Chen, L., Shi, F., and Patton, R. (2013b). Active FTC for hydraulic pitch system for an off-shore wind turbine. In *Proceedings of International Conference on Control and Fault-Tolerant Systems*, pages 510–515. IEEE.
- Chen, M., Ge, S., and Ren, B. (2010). Robust attitude control of helicopters with actuator dynamics using neural networks. *IET Control Theory & Applications*, 4(12):2837–2854.
- Chen, M., Shi, P., and Lim, C.-C. (2016c). Adaptive neural fault-tolerant control of a 3-DOF model helicopter system. *IEEE Transactions on Systems, Man, and Cybernetics: Systems*, 46(2):260–270.
- Chen, R., Speer, A. P., and Eltoweissy, M. (2011). Adaptive fault-tolerant QoS control algorithms for maximizing system lifetime of query-based wireless sensor networks. *IEEE Transactions on Dependable and Secure Computing*, 8(2):161–176.
- Chen, S.-H., Ho, W.-H., and Chou, J.-H. (2009). Robust controllability of T-S fuzzy-model-based control systems with parametric uncertainties. *IEEE Transactions on Fuzzy Systems*, 17(6):1324–1335.

- Chen, W.-H., Yang, J., Guo, L., and Li, S. (2016d). Disturbance-observer-based control and related methods—an overview. *IEEE Transactions on Industrial Electronics*, 63(2):1083–1095.
- Cheng, M. and Zhu, Y. (2014). The state of the art of wind energy conversion systems and technologies: A review. *Energy Conversion and Management*, 88:332–347.
- Chichester, S. and Hindmarsh, J. (1999). Grid integration of wind energy conversion systems.
- Chilali, M. and Gahinet, P. (1996). H_∞ design with pole placement constraints: an LMI approach. *IEEE Transactions on Automatic Control*, 41(3):358–367.
- Chung, W. H., Speyer, J. L., and Chen, R. H. (2001). A decentralized fault detection filter. *Journal of Dynamic Systems, Measurement, and Control*, 123(2):237–247.
- Cieslak, J., Efimov, D., and Henry, D. (2015). Transient management of a supervisory fault-tolerant control scheme based on dwell-time conditions. *International Journal of Adaptive Control and Signal Processing*, 29(1):123–142.
- Corless, M. and Tu, J. (1998). State and input estimation for a class of uncertain systems. *Automatica*, 34(6):757–764.
- Davoodi, M., Meskin, N., and Khorasani, K. (2014). Integrated fault detection, isolation and control design for continuous-time Markovian jump systems with uncertain transition probabilities. In *Proceedings of the 53rd IEEE Conference on Decision and Control*, pages 5743–5749.
- Davoodi, M., Meskin, N., and Khorasani, K. (2016). Simultaneous fault detection and consensus control design for a network of multi-agent systems. *Automatica*, 66:185–194.
- Davoodi, M. R., Talebi, H., and Momeni, H. R. (2011). A novel simultaneous fault detection and control approach based on dynamic observer. In *Proceedings of the IFAC World Congress*, pages 12036–12041. IEEE.
- de Loza, A. F., Cieslak, J., Henry, D., Zolghadri, A., and Fridman, L. M. (2015). Output tracking of systems subjected to perturbations and a class of actuator faults based on HOSM observation and identification. *Automatica*, 59:200–205.
- Ding, S. X. (2008). *Model-based fault diagnosis techniques: design schemes, algorithms, and tools*. Springer Science & Business Media.
- Ding, S. X. (2009). Integrated design of feedback controllers and fault detectors. *Annual Reviews in Control*, 33(2):124–135.
- Ding, S. X., Zhang, P., Yin, S., and Ding, E. L. (2013). An integrated design framework of fault-tolerant wireless networked control systems for industrial automatic control applications. *IEEE Transactions on Industrial Informatics*, 1(9):462–471.
- Dong, H., Wang, Z., Ding, S. X., and Gao, H. (2014). A survey on distributed filtering and fault detection for sensor networks. *Mathematical Problems in Engineering*, DOI: 10.1155/2014/858624.

- Dong, H., Wang, Z., and Gao, H. (2013). *Filtering, control and fault detection with randomly occurring incomplete information*. John Wiley & Sons.
- Du, Y., Budman, H., and Duever, T. A. (2016). Integration of fault diagnosis and control based on a trade-off between fault detectability and closed loop performance. *Journal of Process Control*, 38:42–53.
- Ducard, G. J. (2009). *Fault-tolerant flight control and guidance systems: practical methods for small unmanned aerial vehicles*. Springer Science & Business Media.
- Dziedkan, Ł., Witczak, M., and Korbicz, J. (2011). Active fault-tolerant control design for takagi-sugeno fuzzy systems. *Bulletin of the Polish Academy of Sciences: Technical Sciences*, 59(1):93–102.
- Edwards, C., Lombaerts, T., and Smaili, H. (2010). Fault tolerant flight control. *Lecture Notes in Control and Information Sciences*, 399.
- Edwards, C. and Spurgeon, S. (1998). *Sliding mode control: theory and applications*. CRC Press.
- Edwards, C., Spurgeon, S. K., and Patton, R. J. (2000). Sliding mode observers for fault detection and isolation. *Automatica*, 36(4):541–553.
- Edwards, C. and Tan, C. P. (2006). Sensor fault tolerant control using sliding mode observers. *Control Engineering Practice*, 14(8):897–908.
- Eliades, D. G. and Polycarpou, M. M. (2010). A fault diagnosis and security framework for water systems. *IEEE Transactions on Control Systems Technology*, 18(6):1254–1265.
- Esbensen, T. and Sloth, C. (2009). *Fault diagnosis and fault-tolerant control of wind turbines*. Master's thesis, Faculty of Engineering, Section for Automation and Control, Aalborg University-Danmark.
- Eterno, J., Weiss, J., Looze, D., and Willsky, A. (1985). Design issues for fault tolerant-restructurable aircraft control. In *Proceedings of the 24th IEEE Conference on Decision and Control*, number 24, pages 900–905.
- Fan, L.-L. and Song, Y.-D. (2012). Neuro-adaptive model-reference fault-tolerant control with application to wind turbines. *IET Control Theory & Applications*, 6(4):475–486.
- Feng, X. and Patton, R. (2014). Active fault tolerant control of a wind turbine via fuzzy MPC and moving horizon estimation. *IFAC Proceedings Volumes*, 47(3):3633–3638.
- Floquet, T., Barbot, J.-P., Perruquetti, W., and Djemai, M. (2004). On the robust fault detection via a sliding mode disturbance observer. *International Journal of control*, 77(7):622–629.
- Freidovich, L. B. and Khalil, H. K. (2008). Performance recovery of feedback-linearization-based designs. *IEEE Transactions on Automatic Control*, 53(10):2324–2334.
- Gahinet, P., Nemirovski, A., Laub, A., and Chilali, M. (1995). Matlab LMI control toolbox. *The MathWorks Inc.*

- Gao, C. and Duan, G. (2012). Robust adaptive fault estimation for a class of nonlinear systems subject to multiplicative faults. *Circuits, Systems, and Signal Processing*, 31(6):2035–2046.
- Gao, R. and Gao, Z. (2016). Pitch control for wind turbine systems using optimization, estimation and compensation. *Renewable Energy*, 91:501–515.
- Gao, Z., Cecati, C., and Ding, S. X. (2015a). A survey of fault diagnosis and fault-tolerant techniques—Part I: Fault diagnosis with model-based and signal-based approaches. *IEEE Transactions on Industrial Electronics*, 62(6):3757–3767.
- Gao, Z., Cecati, C., and Ding, S. X. (2015b). A survey of fault diagnosis and fault-tolerant techniques—Part II: Fault diagnosis with knowledge-based and hybrid/active approaches. *IEEE Transactions on Industrial Electronics*, 62(6):3768–3774.
- Gao, Z. and Ding, S. X. (2007). Actuator fault robust estimation and fault-tolerant control for a class of nonlinear descriptor systems. *Automatica*, 43(5):912–920.
- Geng, H. and Yang, G. (2010). Output power control for variable-speed variable-pitch wind generation systems. *IEEE Transactions on Energy Conversion*, 25(2):494–503.
- Georg, S. and Schulte, H. (2014). Diagnosis of actuator parameter faults in wind turbines using a Takagi-Sugeno sliding mode observer. In *Intelligent Systems in Technical and Medical Diagnostics*, pages 29–40. Springer.
- Gertler, J. (1998). *Fault detection and diagnosis in engineering systems*. CRC press.
- Goupil, P. (2010). Oscillatory failure case detection in the A380 electrical flight control system by analytical redundancy. *Control Engineering Practice*, 18(9):1110–1119.
- Grenaille, S., Henry, D., and Zolghadri, A. (2008). A method for designing fault diagnosis filters for LPV polytopic systems. *Journal of Control Science and Engineering*, 2008:1.
- Gu, Z., Wang, D., and Yue, D. (2010). Fault detection for continuous-time networked control systems with non-ideal QoS. *International Journal of Innovative Computing, Information and Control*, 6(8):3631–3640.
- Hajiyev, C. and Caliskan, F. (2013). *Fault diagnosis and reconfiguration in flight control systems*, volume 2. Springer Science & Business Media.
- Hamayun, M. T., Edwards, C., and Alwi, H. (2012). Design and analysis of an integral sliding mode fault-tolerant control scheme. *IEEE Transactions on Automatic Control*, 57(7):1783–1789.
- Hand, M. M. (1999). Variable-speed wind turbine controller systematic design methodology: a comparison of non-linear and linear model-based designs. Technical report, National Renewable Energy Lab., Golden, CO (US).
- Hardy, G. H. (1916). Weierstrass's non-differentiable function. *Transactions of the American Mathematical Society*, 17(3):301–325.
- Hashemi, M., Askari, J., and Ghaisari, J. (2016). Adaptive decentralised dynamic surface control for non-linear large-scale systems against actuator failures. *IET Control Theory & Applications*, 10(1):44–57.

- Hassan, M. F., Sultan, M. A., and Attia, M. S. (1992). Fault detection in large-scale stochastic dynamic systems. *IEE Proceedings-Control Theory and Applications*, 139(2):119–124.
- He, W., Dong, Y., and Sun, C. (2016). Adaptive neural impedance control of a robotic manipulator with input saturation. *IEEE Transactions on Systems, Man, and Cybernetics: Systems*, 46(3):334–344.
- He, X., Wang, Z., and Zhou, D. (2008). Networked fault detection with random communication delays and packet losses. *International Journal of Systems Science*, 39(11):1045–1054.
- Hespanha, J. P., Naghshtabrizi, P., and Xu, Y. (2007). A survey of recent results in networked control systems. *Proceedings of the IEEE*, 95(1):138–162.
- Ho, W.-H., Chen, S.-H., Chou, J.-H., et al. (2013). Observability robustness of uncertain fuzzy-model-based control systems. *International Journal of Innovative Computing, Information and Control*, 9(2):805–819.
- Hou, M. and Müller, P. (1994). Design of decentralized linear state function observers. *Automatica*, 30(11):1801–1805.
- Hou, M. and Patton, R. (1996). An LMI approach to H_2/H_∞ fault detection observers. In *Proceedings of the UKACC International Conference on Control*, volume 1, pages 305–310. IET.
- Hu, Q., Xiao, B., and Friswell, M. (2011). Robust fault-tolerant control for spacecraft attitude stabilisation subject to input saturation. *IET Control Theory & Applications*, 5(2):271–282.
- Hua, M.-D., Hamel, T., Morin, P., and Samson, C. (2013). Introduction to feedback control of underactuated VTOL vehicles: A review of basic control design ideas and principles. *IEEE Control Systems*, 33(1):61–75.
- Huang, J. and Wu, N. E. (2013). Fault-tolerant placement of phasor measurement units based on control reconfigurability. *Control Engineering Practice*, 21(1):1–11.
- Huang, S.-J. and Yang, G.-H. (2014). Fault tolerant controller design for T-S fuzzy systems with time-varying delay and actuator faults: A k-step fault-estimation approach. *IEEE Transactions on Fuzzy Systems*, 22(6):1526–1540.
- Huang, Z. and Patton, R. J. (2015). Output feedback sliding mode FTC for a class of nonlinear inter-connected systems. *IFAC-PapersOnLine*, 48(21):1140–1145.
- Huang, Z., Patton, R. J., and Lan, J. (2016). Sliding mode state and fault estimation for decentralized systems. In *Variable-Structure Approaches*, pages 243–281. Springer.
- Huo, B., Tong, S., and Li, Y. (2012). Observer-based adaptive fuzzy fault-tolerant output feedback control of uncertain nonlinear systems with actuator faults. *Journal of Control, Automation and Systems*, 10(6):1119–1128.
- Hwang, I., Kim, S., Kim, Y., and Seah, C. E. (2010). A survey of fault detection, isolation, and reconfiguration methods. *IEEE Transactions on Control Systems Technology*, 18(3):636–653.

- Ichalal, D., Marx, B., Ragot, J., and Maquin, D. (2012). New fault tolerant control strategies for nonlinear Takagi-Sugeno systems. *International Journal of Applied Mathematics and Computer Science*, 22(1):197–210.
- Ikeda, M. (1989). Decentralized control of large scale systems. *Three Decades of Mathematical System Theory*, 135:219–242.
- Isermann, R. (2006). *Fault-diagnosis systems: an introduction from fault detection to fault tolerance*. Springer Science & Business Media.
- Isermann, R. (2011). *Fault-diagnosis applications: model-based condition monitoring: actuators, drives, machinery, plants, sensors, and fault-tolerant systems*. Springer Science & Business Media.
- Isermann, R., Schwarz, R., and Stolzl, S. (2002). Fault-tolerant drive-by-wire systems. *IEEE Control Systems*, 22(5):64–81.
- Isidori, A. (1995). *Nonlinear control systems*. Springer-Verlag, London.
- Izaguirre-Espinosa, C., Muñoz-Vázquez, A. J., Sánchez-Orta, A., Parra-Vega, V., and Castillo, P. (2016). Attitude control of quadrotors based on fractional sliding modes: theory and experiments. *IET Control Theory & Applications*, 10(7):825–832.
- Jaimoukha, I. M., Li, Z., and Papakos, V. (2006). A matrix factorization solution to the H_2/H_∞ fault detection problem. *Automatica*, 42(11):1907–1912.
- Jain, T., Yamé, J. J., and Sauter, D. (2013). A novel approach to real-time fault accommodation in NREL's 5-MW wind turbine systems. *IEEE Transactions on Sustainable Energy*, 4(4):1082–1090.
- Jia, Q., Chen, W., Zhang, Y., and Li, H. (2015a). Fault reconstruction and fault-tolerant control via learning observers in Takagi–Sugeno fuzzy descriptor systems with time delays. *IEEE Transactions on Industrial Electronics*, 62(6):3885–3895.
- Jia, Q., Chen, W., Zhang, Y., and Li, H. (2015b). Integrated design of fault reconstruction and fault-tolerant control against actuator faults using learning observers. *International Journal of Systems Science*, pages 1–13.
- Jiang, B., Staroswiecki, M., and Cocquempot, V. (2006). Fault accommodation for nonlinear dynamic systems. *IEEE Transactions on Automatic Control*, 51(9):1578–1583.
- Jiang, S. and Fang, H. (2014). Fault estimation for nonlinear networked systems with time-varying delay and random packet dropout. *Asian Journal of Control*, 16(1):126–137.
- Jiang, Y., Hu, Q., and Ma, G. (2010). Adaptive backstepping fault-tolerant control for flexible spacecraft with unknown bounded disturbances and actuator failures. *ISA transactions*, 49(1):57–69.
- Jin, X. (2016). Adaptive fault tolerant control for a class of input and state constrained MIMO nonlinear systems. *International Journal of Robust and Nonlinear Control*, 26(2):286–302.

- Jin, X.-Z. and Yang, G.-H. (2009). Distributed adaptive robust tracking and model matching control with actuator faults and interconnection failures. *International Journal of Control, Automation and Systems*, 7(5):702–710.
- Kabore, R. and Wang, H. (2001). Design of fault diagnosis filters and fault-tolerant control for a class of nonlinear systems. *IEEE Transactions on Automatic Control*, 46(11):1805–1810.
- Kaldellis, J. K. and Zafirakis, D. (2011). The wind energy (r) evolution: a short review of a long history. *Renewable Energy*, 36(7):1887–1901.
- Kalsi, K., Lian, J., and Zak, S. H. (2009). Decentralized control of multimachine power systems. In *Proceedings of the American Control Conference*, pages 2122–2127. IEEE.
- Kalsi, K., Lian, J., and Zak, S. H. (2010). Decentralized dynamic output feedback control of nonlinear interconnected systems. *IEEE Transactions on Automatic Control*, 55(8):1964–1970.
- Keliris, C., Polycarpou, M. M., and Parisini, T. (2015). A robust nonlinear observer-based approach for distributed fault detection of input–output interconnected systems. *Automatica*, 53:408–415.
- Khalili, M., Zhang, X., Polycarpou, M., Parisini, T., and Cao, Y. (2015). Distributed adaptive fault-tolerant control of uncertain multi-agent systems. *IFAC-PapersOnLine*, 48(21):66–71.
- Kheloufi, H., Zemouche, A., Bedouhene, F., and Boutayeb, M. (2013). On LMI conditions to design observer-based controllers for linear systems with parameter uncertainties. *Automatica*, 49(12):3700–3704.
- Khosrowjerdi, M. J. and Barzegary, S. (2014). Fault tolerant control using virtual actuator for continuous-time Lipschitz nonlinear systems. *International Journal of Robust and Nonlinear Control*, 24(16):2597–2607.
- Kiefer, T., Graichen, K., and Kugi, A. (2010). Trajectory tracking of a 3-DOF laboratory helicopter under input and state constraints. *IEEE Transactions on Control Systems Technology*, 18(4):944–952.
- Korbicz, J., Koscielny, J. M., Kowalczyk, Z., and Cholewa, W. (2012). *Fault diagnosis: models, artificial intelligence, applications*. Springer Science & Business Media.
- Krstic, M., Kokotovic, P. V., and Kanellakopoulos, I. (1995). *Nonlinear and adaptive control design*. John Wiley & Sons, Inc.
- Li, X. and Zhou, K. (2009). A time domain approach to robust fault detection of linear time-varying systems. *Automatica*, 45(1):94–102.
- Li, Y., Liu, S., Wang, Z., and Yan, X. (2014). On H_∞ fault estimator design for linear discrete time-varying systems under unreliable communication link. *Mathematical Problems in Engineering*, 2014.
- Li, Y.-X. and Yang, G.-H. (2016). Robust adaptive fault-tolerant control for a class of uncertain nonlinear time delay systems. *IEEE Transactions on Systems, Man, and Cybernetics: Systems*, DOI: 10.1109/TSMC.2016.2634080.

- Li, Y.-X. and Yang, G.-H. (2017). Adaptive fuzzy decentralized control for a class of large-scale nonlinear systems with actuator faults and unknown dead zones. *IEEE Transactions on Systems, Man, and Cybernetics: Systems*, 47(5):729–740.
- Li, Z., Yu, J., Xing, X., and Gao, H. (2015). Robust output-feedback attitude control of a three-degree-of-freedom helicopter via sliding-mode observation technique. *IET Control Theory & Applications*, 9(11):1637–1643.
- Lien, C.-H. (2004). Robust observer-based control of systems with state perturbations via LMI approach. *IEEE Transactions on Automatic Control*, 49(8):1365–1370.
- Lin, C., Wang, Q.-G., and Lee, T. H. (2005). Improvement on observer-based H_∞ control for T–S fuzzy systems. *Automatica*, 41(9):1651–1656.
- Liu, M., Cao, X., and Shi, P. (2013a). Fault estimation and tolerant control for fuzzy stochastic systems. *IEEE Transactions on Fuzzy Systems*, 21(2):221–229.
- Liu, M., Cao, X., and Shi, P. (2013b). Fuzzy-model-based fault-tolerant design for nonlinear stochastic systems against simultaneous sensor and actuator faults. *IEEE Transactions on Fuzzy Systems*, 21(5):789–799.
- Liu, X. and Zhang, Q. (2003). New approaches to H_∞ controller designs based on fuzzy observers for T–S fuzzy systems via LMI. *Automatica*, 39(9):1571–1582.
- Long, Y. and Yang, G.-H. (2015). Fault detection filter design for stochastic networked control systems. *International Journal of Robust and Nonlinear Control*, 25(3):443–460.
- Lu, K. and Xia, Y. (2013). Finite-time fault-tolerant control for rigid spacecraft with actuator saturations. *IET Control Theory & Applications*, 7(11):1529–1539.
- Lunze, J. and Richter, J. H. (2008). Reconfigurable fault-tolerant control: a tutorial introduction. *European Journal of Control*, 14(5):359–386.
- Maciejowski, J. (1999). Modelling and predictive control: Enabling technologies for reconfiguration. *Annual Reviews in Control*, 23:13–23.
- Maciejowski, J. and Jones, C. (2003). MPC fault-tolerant flight control case study: Flight 1862. In *Proceedings of the International Federation of Automatic Control on Safeprocess Symposium*, number EPFL-CONF-169763, pages 119–124.
- Maybeck, P. S. and Stevens, R. D. (1991). Reconfigurable flight control via multiple model adaptive control methods. *IEEE Transactions on Aerospace and Electronic systems*, 27(3):470–480.
- Mendonça, L. F., Sousa, J., and da Costa, J. S. (2012). Fault tolerant control using a fuzzy predictive approach. *Expert Systems with Applications*, 39(12):10630–10638.
- Menon, P. P. and Edwards, C. (2014). Robust fault estimation using relative information in linear multi-agent networks. *IEEE Transactions on Automatic Control*, 59(2):477–482.
- Meza-Sánchez, M., Aguilar, L. T., and Orlov, Y. (2015). Output sliding mode-based stabilization of underactuated 3-DOF helicopter prototype and its experimental verification. *Journal of the Franklin Institute*, 352(4):1580–1594.

- Mhaskar, P. (2006). Robust model predictive control design for fault-tolerant control of process systems. *Industrial & Engineering Chemistry Research*, 45(25):8565–8574.
- Mhaskar, P., Gani, A., El-Farra, N. H., McFall, C., Christofides, P. D., and Davis, J. F. (2006). Integrated fault-detection and fault-tolerant control of process systems. *AIChE Journal*, 52(6):2129–2148.
- Mohamed, A. Z., Eskander, M. N., and Ghali, F. A. (2001). Fuzzy logic control based maximum power tracking of a wind energy system. *Renewable energy*, 23(2):235–245.
- Molina, M. G. and Alvarez, J. G. (2011). Technical and regulatory exigencies for grid connection of wind generation. In *Wind Farm-Technical Regulations, Potential Estimation and Siting Assessment*. InTech.
- Moor, T. (2016). A discussion of fault-tolerant supervisory control in terms of formal languages. *Annual Reviews in Control*, 41:159–169.
- Muljadi, E. and Butterfield, C. P. (2001). Pitch-controlled variable-speed wind turbine generation. *IEEE Transactions on Industry Applications*, 37(1):240–246.
- Naghavi, S. V., Safavi, A., and Kazerooni, M. (2014). Decentralized fault tolerant model predictive control of discrete-time interconnected nonlinear systems. *Journal of the Franklin Institute*, 351(3):1644–1656.
- Nett, C., Jacobson, C., and Miller, A. (1988). An integrated approach to controls and diagnostics: The 4-parameter controller. In *Proceedings of the American Control Conference*, pages 824–835.
- Niemann, H. and Stoustrup, J. (2003). Controller reconfiguration based on ltr design. In *Proceedings of the 42nd IEEE Conference on Decision and Control*, volume 3, pages 2453–2458. IEEE.
- Nooruldeen, A. and Schmidt, K. W. (2015). State attraction under language specification for the reconfiguration of discrete event systems. *IEEE Transactions on Automatic Control*, 60(6):1630–1634.
- Novak, P., Ekelund, T., Jovik, I., and Schmidtbauer, B. (1995). Modeling and control of variable-speed wind-turbine drive-system dynamics. *IEEE Control Systems*, 15(4):28–38.
- Ocampo-Martinez, C. and Puig Cayuela, V. (2009). Fault-tolerant model predictive control within the hybrid systems framework: Application to sewer networks. *International Journal of Adaptive Control and Signal Processing*, 23(8):757–787.
- Odgaard, P. F. and Stoustrup, J. (2012). Fault tolerant control of wind turbines using unknown input observers. In *Proceedings of IFAC Symposium on Fault Detection, Supervision and Safety of Technical Processes*, pages 313–318.
- Odgaard, P. F., Stoustrup, J., and Kinnaert, M. (2013). Fault-tolerant control of wind turbines: a benchmark model. *IEEE Transactions on Control Systems Technology*, 21(4):1168–1182.

- Pagilla, P. R. and Zhu, Y. (2004). A decentralized output feedback controller for a class of large-scale interconnected nonlinear systems. In *Proceedings of the American Control Conference*, volume 4, pages 3711–3716, Boston, United States. IEEE.
- Panagi, P. and Polycarpou, M. M. (2011a). Decentralized fault tolerant control of a class of interconnected nonlinear systems. *IEEE Transactions on Automatic Control*, 56(1):178–184.
- Panagi, P. and Polycarpou, M. M. (2011b). Distributed fault accommodation for a class of interconnected nonlinear systems with partial communication. *IEEE Transactions on Automatic Control*, 56(12):2962–2967.
- Paoli, A., Sartini, M., and Lafortune, S. (2011). Active fault tolerant control of discrete event systems using online diagnostics. *Automatica*, 47(4):639–649.
- Patton, R. J. (1997). Fault-tolerant control systems: The 1997 situation. In *IFAC symposium on fault detection supervision and safety for technical processes*, volume 3, pages 1033–1054.
- Patton, R. J. (2015). Fault-tolerant control. In *Encyclopedia of Systems and Control*, pages 422–428. Springer.
- Patton, R. J., Frank, P. M., and Clark, R. N. (2013). *Issues of fault diagnosis for dynamic systems*. Springer Science & Business Media.
- Patton, R. J., Kambhampati, C., Casavola, A., Zhang, P., Ding, S., and Sauter, D. (2007). A generic strategy for fault-tolerance in control systems distributed over a network. *European Journal of Control*, 13(2):280–296.
- Patton, R. J. and Klinkhieo, S. (2009). A two-level approach to fault-tolerant control of distributed systems based on the sliding mode. In *Proceedings of the IFAC symposium on Fault Detection, Supervision and Safety of Technical Processes*, pages 1043–1048.
- Patton, R. J., Putra, D., and Klinkhieo, S. (2010). Friction compensation as a fault-tolerant control problem. *International Journal of Systems Science*, 41(8):987–1001.
- Patwardhan, S. C., Manuja, S., Narasimhan, S., and Shah, S. L. (2006). From data to diagnosis and control using generalized orthonormal basis filters. part II: Model predictive and fault tolerant control. *Journal of Process Control*, 16(2):157–175.
- Pedersen, A. S., Richter, J. H., Tabatabaeipour, M., Jóhannsson, H., and Blanke, M. (2016). Fault tolerant emergency control to preserve power system stability. *Control Engineering Practice*, 53:151–159.
- Polyakov, A. (2012). Nonlinear feedback design for fixed-time stabilization of linear control systems. *IEEE Transactions on Automatic Control*, 57(8):2106–2110.
- Polycarpou, M. M. (2001). Fault accommodation of a class of multivariable nonlinear dynamical systems using a learning approach. *IEEE Transactions on Automatic Control*, 46(5):736–742.
- Puig, V. (2016). Admissible model matching fault tolerant control based on LPV fault representation. *Journal of Instrumentation, Automation and Systems*, 2(3):81–90.

- Qi, X., Qi, J., Theilliol, D., Song, D., Zhang, Y., and Han, J. (2016). Self-healing control design under actuator fault occurrence on single-rotor unmanned helicopters. *Journal of Intelligent & Robotic Systems*, 84(1-4):21–35.
- Qi, X., Qi, J., Theilliol, D., Zhang, Y., Han, J., Song, D., and Hua, C. (2014). A review on fault diagnosis and fault tolerant control methods for single-rotor aerial vehicles. *Journal of Intelligent & Robotic Systems*, 73(1-4):535–555.
- Qi, X., Theilliol, D., Qi, J., Zhang, Y., Han, J., Song, D., Wang, L., and Xia, Y. (2013). Fault diagnosis and fault tolerant control methods for manned and unmanned helicopters: A literature review. In *Proceedings of the Conference on Control and Fault-Tolerant Systems*, pages 132–139. IEEE.
- Qin, S. J. (2012). Survey on data-driven industrial process monitoring and diagnosis. *Annual Reviews in Control*, 36(2):220–234.
- Quevedo, J., Puig, V., Cembrano, G., Blanch, J., Aguilar, J., Saporta, D., Benito, G., Hedro, M., and Molina, A. (2010). Validation and reconstruction of flow meter data in the barcelona water distribution network. *Control Engineering Practice*, 18(6):640–651.
- Rauch, H. E. (1995). Autonomous control reconfiguration. *IEEE Control Systems*, 15(6):37–48.
- Ribrant, J. and Bertling, L. (2007). Survey of failures in wind power systems with focus on Swedish wind power plants during 1997-2005. In *Proceedings of the IEEE Power Engineering Society General Meeting*, pages 1–8. IEEE.
- Richter, J. H. (2011). *Reconfigurable control of nonlinear dynamical systems: a fault-hiding approach*, volume 408. Springer.
- Ríos, H., Kamal, S., Fridman, L. M., and Zolghadri, A. (2015). Fault tolerant control allocation via continuous integral sliding-modes: a HOSM-observer approach. *Automatica*, 51:318–325.
- Riverso, S., Boem, F., Ferrari-Trecate, G., and Parisini, T. (2016). Plug-and-play fault detection and control-reconfiguration for a class of nonlinear large-scale constrained systems. *IEEE Transactions on Automatic Control*, DOI: 10.1109/TAC.2016.2535724.
- Robles, D., Puig, V., Ocampo-Martinez, C., and Garza-Castañón, L. E. (2016). Reliable fault-tolerant model predictive control of drinking water transport networks. *Control Engineering Practice*, 55:197–211.
- Rodrigues, M., Hamdi, H., Braiek, N. B., and Theilliol, D. (2014). Observer-based fault tolerant control design for a class of LPV descriptor systems. *Journal of the Franklin Institute*, 351(6):3104–3125.
- Rotondo, D., Nejjari, F., and Puig, V. (2014). A virtual actuator and sensor approach for fault tolerant control of LPV systems. *Journal of Process Control*, 24(3):203–222.
- Rotondo, D., Nejjari, F., Puig, V., and Blesa, J. (2015a). Model reference FTC for LPV systems using virtual actuators and set-membership fault estimation. *International Journal of Robust and Nonlinear Control*, 25(5):735–760.

- Rotondo, D., Ponsart, J.-C., Theilliol, D., Nejjari, F., and Puig, V. (2015b). A virtual actuator approach for the fault tolerant control of unstable linear systems subject to actuator saturation and fault isolation delay. *Annual Reviews in Control*, 39:68–80.
- Saif, M. and Guan, Y. (1992). Decentralized state estimation in large-scale interconnected dynamical systems. *Automatica*, 28(1):215–219.
- Sami, M. and Patton, R. J. (2013). Active fault tolerant control for nonlinear systems with simultaneous actuator and sensor faults. *International Journal of Control, Automation and Systems*, 11(6):1149–1161.
- Sandell Jr, N. R., Varaiya, P., Athans, M., and Safonov, M. G. (1978). Survey of decentralized control methods for large scale systems. *IEEE Transactions on Automatic Control*, 23(2):108–128.
- Sauter, D., Boukhobza, T., and Hamelin, F. (2006). Decentralized and autonomous design for FDI/FTC of networked control systems. *IFAC Proceedings Volumes*, 39(13):138–143.
- Shafai, B., Ghadami, R., and Saif, M. (2011). Robust decentralized PI observer for linear interconnected systems. In *Proceedings of the IEEE International Symposium on Computer-Aided Control System Design*, pages 650–655, Denver, CO, United States. IEEE.
- Shaker, H. R. (2013). Control reconfigurability of bilinear systems. *Journal of Mechanical Science and Technology*, 27(4):1117–1123.
- Shaker, M. S. and Patton, R. J. (2014). Active sensor fault tolerant output feedback tracking control for wind turbine systems via T–S model. *Engineering Applications of Artificial Intelligence*, 34:1–12.
- Shan, J., Liu, H.-T., and Nowotny, S. (2005). Synchronised trajectory-tracking control of multiple 3-DOF experimental helicopters. *IET Control Theory & Applications*, 152(6):683–692.
- Shankar, S., Darbha, S., and Datta, A. (2002). Design of a decentralized detection of interacting LTI systems. *Mathematical Problems in Engineering*, 8(3):233–248.
- Shen, Q., Jiang, B., and Cocquempot, V. (2012). Fault-tolerant control for T–S fuzzy systems with application to near-space hypersonic vehicle with actuator faults. *IEEE Transactions on Fuzzy Systems*, 20(4):652–665.
- Shi, F. and Patton, R. (2015a). An active fault tolerant control approach to an offshore wind turbine model. *Renewable Energy*, 75:788–798.
- Shi, F. and Patton, R. J. (2015b). Fault estimation and active fault tolerant control for linear parameter varying descriptor systems. *International Journal of Robust and Nonlinear Control*, 25(5):689–706.
- Shi, P., Liu, M., and Zhang, L. (2015). Fault-tolerant sliding mode observer synthesis of Markovian jump systems using quantized measurements. *IEEE Transactions on Industrial Electronics*, 62(9):5910–5918.

- Šiljak, D. (1980). Reliable control using multiple control systems. *International Journal of Control*, 31(2):303–329.
- Šiljak, D. D. (1991). *Decentralized control of complex systems*. Academic Press, Boston.
- Šiljak, D. D. (1996). Decentralized control and computations: status and prospects. *Annual Reviews in Control*, 20:131–141.
- Šiljak, D. D. and Zečević, A. I. (2005). Control of large-scale systems: Beyond decentralized feedback. *Annual Reviews in Control*, 29(2):169–179.
- Sloth, C., Esbensen, T., and Stoustrup, J. (2011). Robust and fault-tolerant linear parameter-varying control of wind turbines. *Mechatronics*, 21(4):645–659.
- Slotine, J.-J. E., Li, W., et al. (1991). *Applied nonlinear control*. Englewood Cliffs, NJ, USA: Prentice Hall.
- Song, Y., Hu, J., Chen, D., Ji, D., and Liu, F. (2016). Recursive approach to networked fault estimation with packet dropouts and randomly occurring uncertainties. *Neurocomputing*, 214:340–349.
- Song, Y. and Wang, B. (2013). Survey on reliability of power electronic systems. *IEEE Transactions on Power Electronics*, 28(1):591–604.
- Soylu, S., Buckham, B. J., and Podhorodeski, R. P. (2008). A chattering-free sliding-mode controller for underwater vehicles with fault-tolerant infinity-norm thrust allocation. *Ocean Engineering*, 35(16):1647–1659.
- Staroswiecki, M. (2005). Fault tolerant control: the pseudo-inverse method revisited. *IFAC Proceedings Volumes*, 38(1):418–423.
- Steffen, T. (2005). *Control reconfiguration of dynamical systems: linear approaches and structural tests*, volume 320. Springer Science & Business Media.
- Steinberg, M. (2005). Historical overview of research in reconfigurable flight control. *Proceedings of the Institution of Mechanical Engineers, Part G: Journal of Aerospace Engineering*, 219(4):263–275.
- Stol, K. and Fingersh, L. (2004). Wind turbine field testing of state-space control designs. *National Renewable Energy Laboratory, NREL/SR-500-35061, Golden, Co.*
- Stol, K. A. and Balas, M. J. (2003). Periodic disturbance accommodating control for blade load mitigation in wind turbines. *Journal of Solar Energy Engineering*, 125(4):379–385.
- Takagi, T. and Sugeno, M. (1985). Fuzzy identification of systems and its applications to modelling and control. *IEEE Transactions on Systems, Man, and Cybernetics*, (1):116–132.
- Tan, C. P. and Edwards, C. (2004). Multiplicative fault reconstruction using sliding mode observers. In *Proceedings of the 5th Asian Control Conference*, pages 957–962.
- Tan, D., Patton, R. J., and Wang, X. (2015). A relaxed solution to unknown input observers for state and fault estimation. *IFAC-PapersOnLine*, 48(21):1048–1053.

- Tao, G., Chen, S., Tang, X., and Joshi, S. M. (2013). *Adaptive control of systems with actuator failures*. Springer Science & Business Media.
- Tao, G., Joshi, S. M., and Ma, X. (2001). Adaptive state feedback and tracking control of systems with actuator failures. *IEEE Transactions on Automatic Control*, 46(1):78–95.
- Tarbouriech, S. and Turner, M. (2009). Anti-windup design: an overview of some recent advances and open problems. *IET Control Theory & Applications*, 3(1):1–19.
- Tidriri, K., Chatti, N., Verron, S., and Tiplica, T. (2016). Bridging data-driven and model-based approaches for process fault diagnosis and health monitoring: A review of researches and future challenges. *Annual Reviews in Control*, 42:63–81.
- Tlili, A. S. and Braiek, N. B. (2009a). Decentralized observer based guaranteed cost control for nonlinear interconnected systems. *International Journal of Control and Automation*, 2(2):19–34.
- Tlili, A. S. and Braiek, N. B. (2009b). Decentralized observer based guaranteed cost control for nonlinear interconnected systems. *International Journal of Control and Automation*, 2(2):19–34.
- Tong, S., Huo, B., and Li, Y. (2014a). Observer-based adaptive decentralized fuzzy fault-tolerant control of nonlinear large-scale systems with actuator failures. *IEEE Transactions on Fuzzy Systems*, 22(1):1–15.
- Tong, S., Wang, T., and Li, Y. (2014b). Fuzzy adaptive actuator failure compensation control of uncertain stochastic nonlinear systems with unmodeled dynamics. *IEEE Transactions on Fuzzy Systems*, 22(3):563–574.
- Tornil-Sin, S., Theilliol, D., Ponsart, J.-C., and Puig, V. (2010). Admissible model matching using \mathcal{D}_R -regions: Fault accommodation and robustness against FDD inaccuracies. *International Journal of Adaptive Control and Signal Processing*, 24(11):927–943.
- Vachtsevanos, G., Tang, L., Drozeski, G., and Gutierrez, L. (2005). From mission planning to flight control of unmanned aerial vehicles: strategies and implementation tools. *Annual Review in Control*, 29(1):101–115.
- Valavanis, K. P. and Vachtsevanos, G. J. (2014). *Handbook of unmanned aerial vehicles*. Springer Publishing Company, Incorporated.
- van Schrick, D. (1997). Remarks on terminology in the field of supervision, fault detection and diagnosis. In *Proceedings of the 3rd IFAC Symposium on Fault Detection, Supervision and Safety for Technical Processes*, pages 959–964.
- Veillette, R. J., Medanic, J., and Perkins, W. R. (1992). Design of reliable control systems. *IEEE Transactions on Automatic Control*, 37(3):290–304.
- Venkatasubramanian, V., Rengaswamy, R., and Kavuri, S. N. (2003a). A review of process fault detection and diagnosis: Part II: Qualitative models and search strategies. *Computers & Chemical Engineering*, 27(3):313–326.

- Venkatasubramanian, V., Rengaswamy, R., Kavuri, S. N., and Yin, K. (2003b). A review of process fault detection and diagnosis: Part III: Process history based methods. *Computers & Chemical Engineering*, 27(3):327–346.
- Venkatasubramanian, V., Rengaswamy, R., Yin, K., and Kavuri, S. N. (2003c). A review of process fault detection and diagnosis: Part I: Quantitative model-based methods. *Computers & Chemical Engineering*, 27(3):293–311.
- Wang, H. and Daley, S. (1996). Actuator fault diagnosis: an adaptive observer-based technique. *IEEE Transactions on Automatic Control*, 41(7):1073–1078.
- Wang, H. O., Tanaka, K., and Griffin, M. F. (1996). An approach to fuzzy control of nonlinear systems: stability and design issues. *IEEE Transactions on Fuzzy Systems*, 4(1):14–23.
- Wang, J. L., Yang, G.-H., and Liu, J. (2007). An LMI approach to h -index and mixed H_-/H_∞ fault detection observer design. *Automatica*, 43(9):1656–1665.
- Wang, R. and Wang, J. (2011). Fault-tolerant control with active fault diagnosis for four-wheel independently driven electric ground vehicles. *IEEE Transactions on Vehicular Technology*, 60(9):4276–4287.
- Wang, S. and Jiang, Y. (2014). Comment on “on LMI conditions to design observer-based controllers for linear systems with parameter uncertainties [automatica 49 (2013) 3700–3704]”. *Automatica*, 50(10):2732–2733.
- Wang, W. and Wen, C. (2010). Adaptive actuator failure compensation control of uncertain nonlinear systems with guaranteed transient performance. *Automatica*, 46(12):2082–2091.
- Wang, Y., Wilson, P. A., Liu, X., et al. (2015). Adaptive neural network-based back-stepping fault tolerant control for underwater vehicles with thruster fault. *Ocean Engineering*, 110:15–24.
- Wang, Y.-L. and Xiong, J. (2016). Fault detection filter design for networked control systems with time-varying sampling periods and packet dropouts. *International Journal of Adaptive Control and Signal Processing*, 30:790–806.
- Wen, Q., Kumar, R., Huang, J., and Liu, H. (2008). A framework for fault-tolerant control of discrete event systems. *IEEE Transactions on Automatic Control*, 53(8):1839–1849.
- Weng, Z., Patton, R. J., and Cui, P. (2008). Integrated design of robust controller and fault estimator for linear parameter varying systems. In *Proceedings of the IFAC World Congress*, pages 4535–4539.
- Willsky, A. S. and Jones, H. L. (1974). A generalized likelihood ratio approach to state estimation in linear systems subjects to abrupt changes. In *Proceedings of IEEE Conference on Decision and Control including the 13th Symposium on Adaptive Processes*, volume 13, pages 846–853. IEEE.
- Witczak, M., Dziekan, L., Puig, V., and Korbicz, J. (2008). Design of a fault-tolerant control scheme for Takagi-Sugeno fuzzy systems. In *Proceedings of the 16th Mediterranean Conference on Control and Automation*, pages 280–285. IEEE.

- Wu, N. E. (2004). Coverage in fault-tolerant control. *Automatica*, 40(4):537–548.
- Wu, N. E., Zhou, K., and Salomon, G. (2000). Control reconfigurability of linear time-invariant systems. *Automatica*, 36(11):1767–1771.
- Xiao, B., Hu, Q., and Zhang, Y. (2012). Adaptive sliding mode fault tolerant attitude tracking control for flexible spacecraft under actuator saturation. *IEEE Transactions on Control Systems Technology*, 20(6):1605–1612.
- Xiong, Y. and Saif, M. (2003). Unknown disturbance inputs estimation based on a state functional observer design. *Automatica*, 39(8):1389–1398.
- Xu, D., Ding, S., Wang, Y., and Li, L. (2017). Fault-tolerant control for wireless networked control systems with an integrated scheduler. *International Journal of Adaptive Control and Signal Processing*, 31(1):23–38.
- Xu, Y., Tong, S., and Li, Y. (2015). Adaptive fuzzy decentralised fault-tolerant control for nonlinear large-scale systems with actuator failures and unmodelled dynamics. *International Journal of Systems Science*, 46(12):2195–2209.
- Yan, X. and Edwards, C. (2008). Robust decentralized actuator fault detection and estimation for large-scale systems using a sliding mode observer. *International Journal of control*, 81(4):591–606.
- Yang, G.-H., Wang, J. L., and Soh, Y. C. (2001). Reliable H_∞ controller design for linear systems. *Automatica*, 37(5):717–725.
- Yang, G.-H. and Ye, D. (2010). Reliable control of linear systems with adaptive mechanism. *IEEE Transactions on Automatic Control*, 55(1):242–247.
- Yang, H., Cocquempot, V., and Jiang, B. (2010a). Optimal fault-tolerant path-tracking control for 4WS4WD electric vehicles. *IEEE Transactions on Intelligent Transportation Systems*, 11(1):237–243.
- Yang, H., Jiang, B., and Cocquempot, V. (2010b). Fault tolerant control and hybrid systems. In *Fault Tolerant Control Design for Hybrid Systems*, pages 1–9. Springer.
- Yang, H., Jiang, B., and Staroswiecki, M. (2009). Supervisory fault tolerant control for a class of uncertain nonlinear systems. *Automatica*, 45(10):2319–2324.
- Yang, H., Jiang, B., and Staroswiecki, M. (2012). Fault recoverability analysis of switched systems. *International Journal of Systems Science*, 43(3):535–542.
- Yang, H., Jiang, B., and Staroswiecki, M. (2016). Fault tolerant control for plug-and-play interconnected nonlinear systems. *Journal of the Franklin Institute*, 353(10):2199–2217.
- Yang, H., Jiang, B., Staroswiecki, M., and Zhang, Y. (2015). Fault recoverability and fault tolerant control for a class of interconnected nonlinear systems. *Automatica*, 54:49–55.
- Yang, H., Shi, P., Li, X., and Li, Z. (2014). Fault-tolerant control for a class of T-S fuzzy systems via delta operator approach. *Signal Processing*, 98:166–173.

- Ye, D. and Yang, G.-H. (2006). Adaptive fault-tolerant tracking control against actuator faults with application to flight control. *IEEE Transactions on Control Systems Technology*, 14(6):1088–1096.
- Yetendje, A., Seron, M. M., and De Doná, J. A. (2013). Robust multiactuator fault-tolerant MPC design for constrained systems. *International Journal of Robust and Nonlinear Control*, 23(16):1828–1845.
- Yin, S., Ding, S. X., Xie, X., and Luo, H. (2014a). A review on basic data-driven approaches for industrial process monitoring. *IEEE Transactions on Industrial Electronics*, 61(11):6418–6428.
- Yin, S., Wang, G., and Karimi, H. R. (2014b). Data-driven design of robust fault detection system for wind turbines. *Mechatronics*, 24(4):298–306.
- Yu, X. and Jiang, J. (2015). A survey of fault-tolerant controllers based on safety-related issues. *Annual Reviews in Control*, 39:46–57.
- Zhai, D., Lu, A.-Y., Li, J.-H., and Zhang, Q.-L. (2016). Simultaneous fault detection and control for switched linear systems with mode-dependent average dwell-time. *Applied Mathematics and Computation*, 273:767–792.
- Zhang, K., Jiang, B., and Staroswiecki, M. (2010a). Dynamic output feedback-fault tolerant controller design for Takagi-Sugeno fuzzy systems with actuator faults. *IEEE Transactions on Fuzzy Systems*, 18(1):194–201.
- Zhang, P. and Ding, S. X. (2008). An integrated trade-off design of observer based fault detection systems. *Automatica*, 44(7):1886–1894.
- Zhang, X., Parisini, T., and Polycarpou, M. M. (2004). Adaptive fault-tolerant control of nonlinear uncertain systems: an information-based diagnostic approach. *IEEE Transactions on Automatic Control*, 49(8):1259–1274.
- Zhang, X., Polycarpou, M. M., and Parisini, T. (2010b). Adaptive fault diagnosis and fault-tolerant control of MIMO nonlinear uncertain systems. *International Journal of Control*, 83(5):1054–1080.
- Zhang, Y., Fang, H., and Luo, Z. (2011). H_∞ -based fault detection for nonlinear networked systems with random packet dropout and probabilistic interval delay. *Journal of Systems Engineering and Electronics*, 22(5):825–831.
- Zhang, Y. and Jiang, J. (2001). Integrated active fault-tolerant control using imm approach. *IEEE Transactions on Aerospace and Electronic Systems*, 37(4):1221–1235.
- Zhang, Y. and Jiang, J. (2006). Issues on integration of fault diagnosis and reconfigurable control in active fault-tolerant control systems. *IFAC Proceedings Volumes*, 39(13):1437–1448.
- Zhang, Y. and Jiang, J. (2008). Bibliographical review on reconfigurable fault-tolerant control systems. *Annual Reviews in Control*, 32(2):229–252.
- Zhao, F., Koutsoukos, X., Haussecker, H., Reich, J., and Cheung, P. (2005). Monitoring and fault diagnosis of hybrid systems. *IEEE Transactions on Systems, Man, and Cybernetics, Part B (Cybernetics)*, 35(6):1225–1240.

- Zhao, J., Jiang, B., Shi, P., and He, Z. (2014). Fault tolerant control for damaged aircraft based on sliding mode control scheme. *International Journal of Innovative Computing, Information and Control*, 10(1):293–302.
- Zheng, B. and Zhong, Y. (2011). Robust attitude regulation of a 3-DOF helicopter benchmark: theory and experiments. *IEEE Transactions on Industrial Electronics*, 58(2):660–670.
- Zheng, W., Fuyang, C., and Bin, J. (2014). An improved nonlinear model and adaptive fault-tolerant control for a twin rotor helicopter. In *Proceedings of the 33rd Chinese Control Conference*, pages 3208–3212. IEEE.
- Zheng, Z., Sun, L., and Zou, Y. (2015). Attitude tracking control of a 3-DOF helicopter with actuator saturation and model uncertainties. In *Proceedings of the 34th Chinese Control Conference*, pages 5641–5646. IEEE.
- Zhong, G.-X. and Yang, G.-H. (2015). Robust control and fault detection for continuous-time switched systems subject to a dwell time constraint. *International Journal of Robust and Nonlinear Control*, 25(18):3799–3817.
- Zolghadri, A., Henry, D., Cieslak, J., Efimov, D., and Goupil, P. (2014). *Fault diagnosis and fault-tolerant control and guidance for aerospace vehicles*. Springer.
- Zong, Q., Zeng, F., Liu, W., Ji, Y., and Tao, Y. (2012). Sliding mode observer-based fault detection of distributed networked control systems with time delay. *Circuits, Systems, and Signal Processing*, 31(1):203–222.
- Zuo, Z., Ho, D. W., and Wang, Y. (2010). Fault tolerant control for singular systems with actuator saturation and nonlinear perturbation. *Automatica*, 46(3):569–576.